Regional Risk Assessment for Water Availability and Water-related Energy Sector Impacts in Central Asia

December 2014

Author
J.E. Hunink
A. Lutz
P. Droogers

Client
World Bank /
Industrial Economics

FutureWater Report: 196

FutureWater
Costerweg 1V
6702 AA Wageningen
The Netherlands

+31 (0)317 460050

info@futurewater.nl

www.futurewater.nl

Table of contents

Tables

Figures

Preface

The World Bank is committed to working with the governments of Central Asia to undertake analysis and to identify priorities in adaptation to climate change, including strengthening regional trade through a rigorous, transparent region-scale study. For this purpose, it undertook a regional assessment to identify areas of possible coordination and possible transboundary impact. The overall project objective is to contribute to a better understanding of the challenges and opportunities for effective joint management of climate adaptation, contributing to the objective of the World Bank's Central Asia strategy of energy and water security through enhanced cooperation.

The work presented in this report, was developed by FutureWater and was used as input to the "Central Asia Regional Energy Sector Vulnerability Study" led by the firm Industrial Economics (IEc). The output was the product of intensive collaboration with the IEc expert team, especially Jim Neumann, Alyssa McCluskey and Kenneth Strzepek (MIT, Boston). Also, FutureWater acknowledges the support of the World Bank expert team.

1 Introduction

1.1 Background

The energy sector is sensitive to changes in seasonal weather patterns and extremes that can affect the supply of energy, harm transmission capacity, disrupt oil and gas production, and impact the integrity of transmission pipelines and power distribution. Most infrastructure has been built to design codes based on historic climate data and will require rehabilitation, upgrade or replacement in the coming years. This poses both a challenge and an opportunity for adaptation. Central Asia is one of the most vulnerable regions in Europe and Central Asia. Expected climate impacts range from increased temperature (across the region), changes in precipitation and snow, greater extreme weather events, aridisation and desertification, health, and changes in water resources.

Energy and water are closely interrelated as water is used to generate energy (hydropower, cooling of thermal plants) but energy is also required to fulfil water needs (e.g. pumping, water treatment, desalination). Especially in Central Asia, meeting daily energy needs dependents to a large extent on water. Guaranteeing sufficient water resources for energy production, and appropriately allocating the limited supply, is becoming increasingly difficult. As the region’s population keeps on growing, competing demand for water from other sectors is expected to grow, potentially exacerbating the issue.

The hydrological regimes of the two major rivers in the region, the Syr Darya and the Amu Darya, are complex and vulnerable to climate change. Water diversions to agricultural, industrial and domestic users have reduced flows in downstream regions, resulting in severe ecological damages. The administrative-institutional system is fragmented, with six independent countries sharing control, often with contradicting objectives.

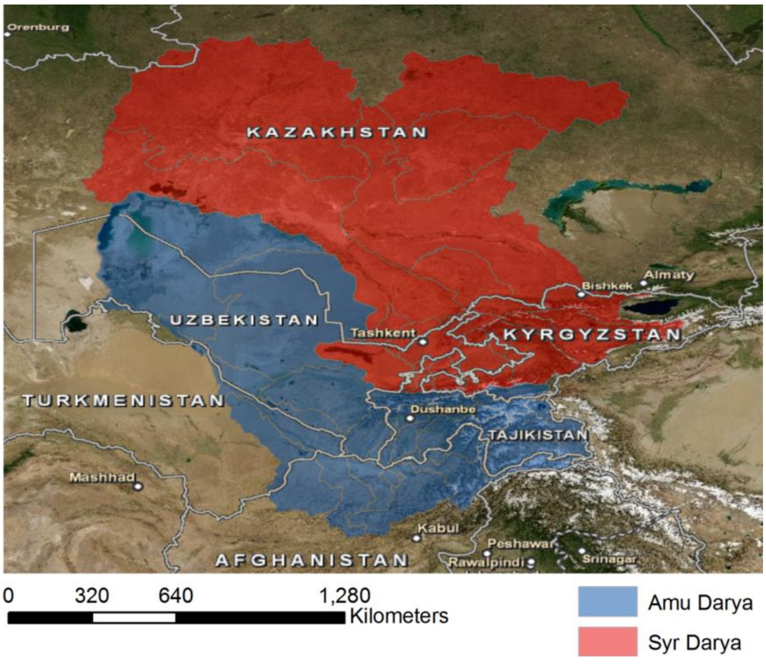

Figure 1-1: Map of the Amu Darya and Syr Darya river basins

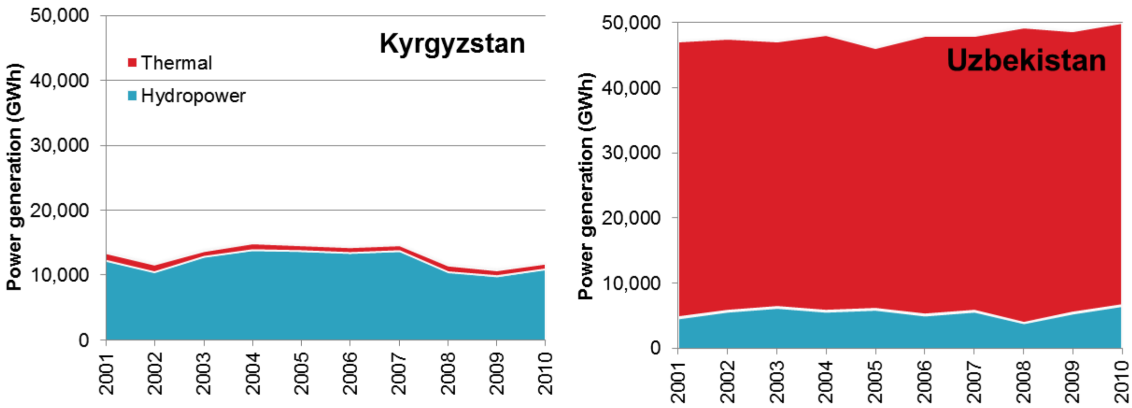

Figure 1-2. Annual hydropower versus thermal energy production for Kyrgyzstan and Uzbekistan. Source: ADB Power Sector Regional Master Plan [*ADB*, 2012]

The upstream states are mostly reliant on hydropower (Figure 1-2). In order to have enough hydropower generating capacity during winter, the upstream states save water during summer in the reservoirs. But this is the period when the downstream countries have the most pressing need for irrigation water, as can be seen in Figure 1-3. In the region, cotton is an important cash crop, and, at the same time, wheat is considered essential in order to meet national food security goals. Especially for Uzbekistan, considerations of self-sufficiency have become more important in recent times where food grain prices have increased considerably on the world market.

As a result, the water resources system is not managed collectively and cooperatively. A mixture of regional, national, and interstate institutions is responsible for allocation decisions. As a result, water and energy allocation among the various sectors and users is not efficient. It is thought that future water resources development in northern Afghanistan will further add fuel to the water and energy conflict in the region.

Future climate change poses additional challenges. The discharge in both the Syr Darya and the Amu Darya rivers is driven mainly by snow and glacial melt. The impact of a warming climate on these key hydrological processes is starting to be understood better [*Lutz et al.*, 2014a] but no mitigation and adaptation strategies are in place. Whereas changes in precipitation levels are hard to predict for the future, there is a solid consensus that average global temperatures are rising. As a result, more precipitation will fall as rain in the upstream and the ice volume in the Tien Shan and Pamir mountain ranges will likely shrink in the long term. Furthermore, changes in sediment loads may pose additional problems.

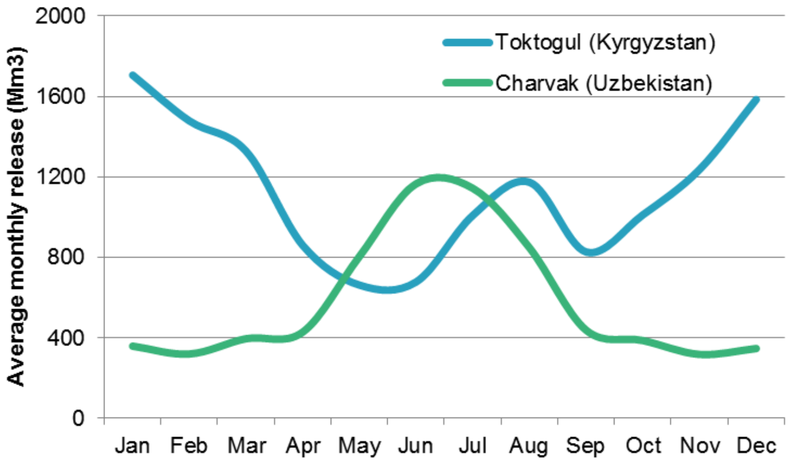

Figure 1-3. Average monthly release from Toktogul dam (Kyrgyzstan) for hydropower and Charvak (Uzbekistan) for irrigation. Source: CAWATER database

The ongoing construction and planning of new dams in Kyrgyzstan and Tajikistan is adding tension to the existing situation. For the downstream countries, these developments have raised concern because this can mean that the upstream states can decouple themselves the necessity to receive energy deliveries in the winter from Kazakhstan, Uzbekistan and Turkmenistan. Regional cross-boundary assessments are critical for decision making in the region to better manage risks and design of mitigation and adaptation strategies.

1.2 Rationale

In 2012, the Asian Development Bank (ADB) study “Water and Adaptation Interventions in Central and West Asia” was carried out by the Finnish Consulting Group (FCG) in collaboration with FutureWater (Netherlands) and the Finnish Meteorological Institute (FMI). The study developed hydrological models for the Amu Darya and Syr Darya and included various climate change impact scenarios. Results were to be used to develop national capacity in each of the participating countries in Central Asia to use these models to prepare climate change impact scenarios and develop adaptation strategies.

The study promoted by the ADB focused principally on water supply and demand issues, with a key focus on agriculture, but did not look into water-related impacts in the energy sector. Climate change impacts were assessed but new climate scenarios and recent new understanding of upstream hydrology requires an update of the hydrological impacts and the downstream impacts on supply and demand with a focus on the energy sector. This requires several improvements in the models used and provides an opportunity to link the model with the economic optimization model BEAM.

The World Bank is committed to working with the governments of Central Asia to undertake analysis and to identify priorities in adaptation to climate change, including strengthening regional trade through a rigorous, transparent region-scale study. Therefore it currently undertakes a regional assessment to identify areas of possible coordination and possible transboundary impact. The overall project objective is to contribute to a better understanding of the challenges and opportunities for effective joint management of climate adaptation, contributing to the objective of the World Bank’s Central Asia strategy of energy and water security through enhanced cooperation. The results of this assessment should guide current and future decision-makers on options for investments in and management of power generation and transmission/distribution assets through enhanced cooperation.

1.3 Objectives

The objective of this study is to support the “Central Asia Regional Energy Sector Vulnerability Study” led by Industrial Economics (IEc) and funded by the World Bank, by carrying out an expanded risk assessment for water availability and water related energy sector impacts in the region, corresponding to Task 3 in the overall project. The work will build on the existing tools developed previously for river and glacial hydrology (SPHY) and water allocation (WEAP), and projections of river runoff under four ”marker” climate scenarios. Various necessary extensions and enhancements of the tools will be made to include the latest understanding of climatological and hydrological processes in the region and to adapt the tool to the project objective.

1.4 Modelling approach

The work described here shows results of three components of the modelling study: (i) the climate downscaling based on the latest IPCC reports and scenarios (ii) the upstream hydrological modelling, and (iii) the downstream river basin system modelling. The basin is divided in an upstream part and a downstream part (Figure 1-4). For the upstream part, the previously an hydrological model called SPHY model, was developed as part of the Asian Development Bank study *Water and Adaptation Interventions in Central and West Asia (TA7532)* [*Immerzeel et al.*, 2012; *Lutz et al.*, 2012]. This model was further updated using the latest insights in high mountain hydrology as detailed in the methodological section. For the upstream part no major human infrastructure influences the hydrological regime. For the downstream part of both basins, a water allocation model was set up including all the main infrastructure, supplies and demands, using the Water Evaluation and Planning (WEAP) tool, also further detailed below.

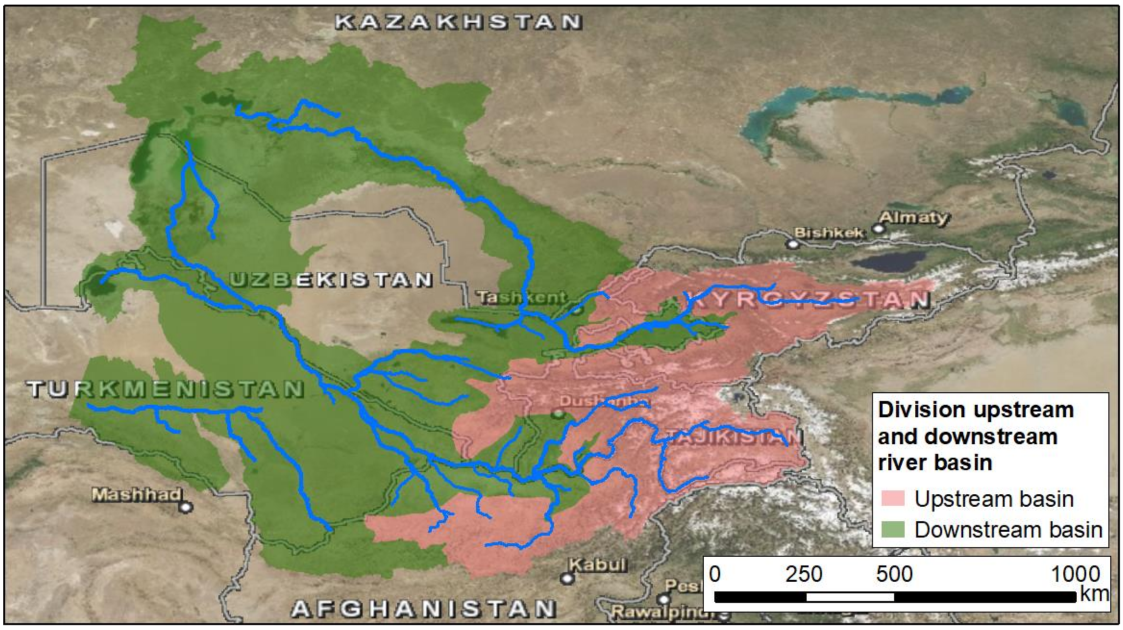

Figure 1-4: Division of the basins in an upstream and downstream domain

1.5 Outline

This Report details the methodological steps and tools that were used, and shows and interprets the results of the modelling assessment (Chapter 3). The climate downscaling methods, the upstream hydrological model specifications and advancements, and the same for the downstream river basin system model WEAP are detailed (Chapter 2). Chapter 3 describes and analyzes the outcomes of these modelling tools. In the Appendix, more details can be found on the Climate change downscaling.

During a recent mission to the region, part of these results was shown to the counterparts and feedback was received. The mission took place from the 10th until the 22nd of November and included meetings and workshops with key stakeholders and decision makers in Turkmenistan, Tadjikistan, Kyrgyzstan, Uzbekistan and Kazakshstan. Based on the feedback received, final modifications were carried out in the modelling tools and in the interpretation of the outcomes.

2 Methodology and tools

2.1 Climate Change scenarios

In 2013/2014 the IPCC published its fifth assessment report (AR5). Working Group 1 published the first part of the report entitled 'The Physical Science Basis' in 2013 [*IPCC*, 2013]. Reports by other working groups discussing the impacts of climate change and mitigation were published in the first half of 2014 and the last part of AR5, the Synthesis Report, is expected to be published at the end of 2014. The Working Group 1's report on 'The Physical Science Basis' discusses the latest climate modeling results which were obtained with the latest GCMs. These models are available from the 5th Climate Model Intercomparison Project (CMIP5) [*Taylor et al.*, 2012].

A study comparing the ensemble of climate models as used for AR4 (CMIP3 ensemble) with the CMIP5 ensemble (all members available in December 2011) for High Central Asia [*Lutz et al.*, 2013] revealed that the CMIP5 ensemble projects greater regional warming and the range in projections for temperature as well as precipitation are wider compared to CMIP3. Besides this observed larger uncertainty, the different ensembles showed significant seasonal differences in the projections (Figure 2-2), which have major implications for the impacts on the cryosphere (glaciers and snow) in the region, where the hydrology is dominated by runoff generated in the cryosphere.

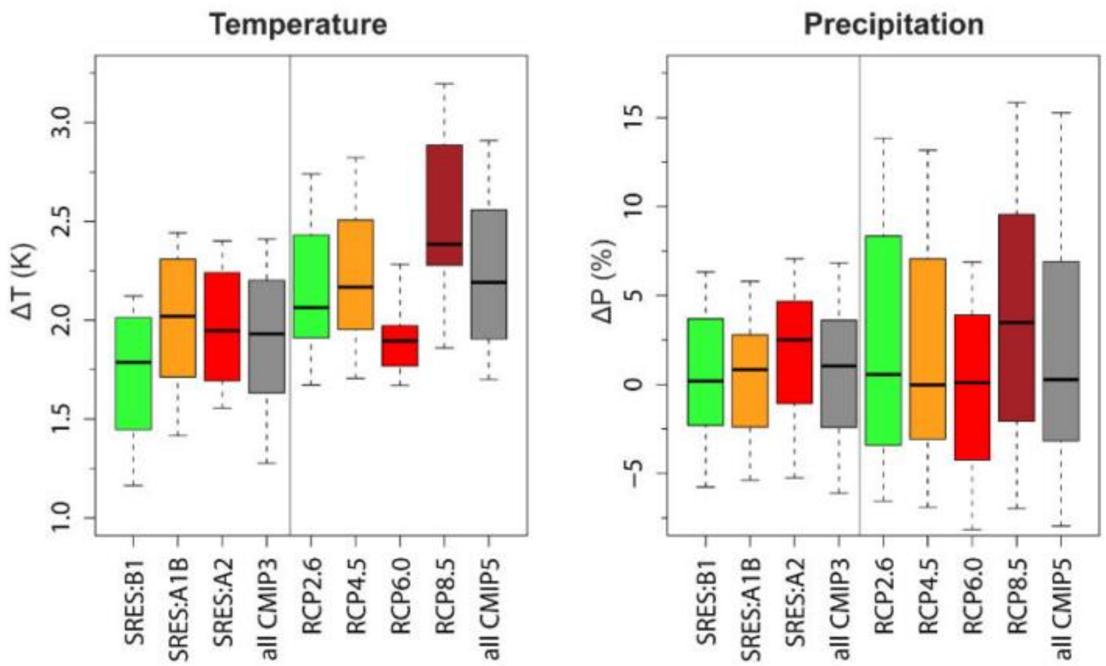

Figure 2-1: Differences in CMIP3 and CMIP5 climate change projections for the High Central Asian region (2031-2060 compared to 1961-1990). From [*Lutz et al.*, 2013]**.**

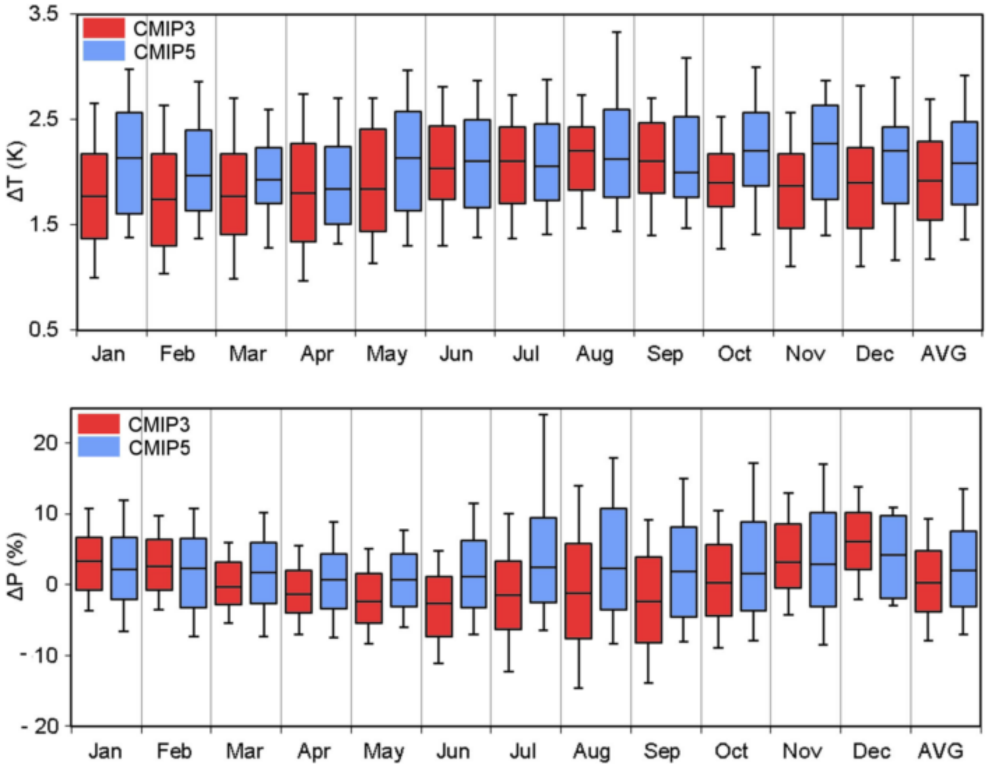

Figure 2-2: Box-whisker plots for projected changed per month in temperature (upper panel) temperature (upper panel) and precipitation (lower panel) for the CMIP3 ensemble (red) and CMIP5 ensemble (blue).

Scenario development for AR4 has been conducted in a mainly sequential form, with socioeconomic and emissions scenarios developed first and climate change projections based on those scenarios carried out next. In contrast with the previous linear process, the parallel approach of AR5 provides better integration, consistency, and consideration of feedbacks, and more time to assess impacts and responses (Figure 2-3). The parallel process is initiated with the identification of the Representative Concentration Pathways (RCPs), which enable the climate modeling (CM) community to proceed with new climate change projections at the same time that new work is carried out in the integrated impact assessment (IAM) and impact and adaptation (IAV) communities (**Figure 2-3**). While the RCPs will enable CM scenario development that explores and characterizes future climate change, they do not constrain future work by the IAM community, which, in its portion of the parallel process, simultaneously develops a range of completely new socioeconomic and emissions scenarios. IAM teams will have complete freedom to develop new scenarios across the full range of possibilities. IAM teams will also explore alternative technological, socioeconomic, and policy futures including both reference (without explicit climate policy intervention) and climate policy scenarios.

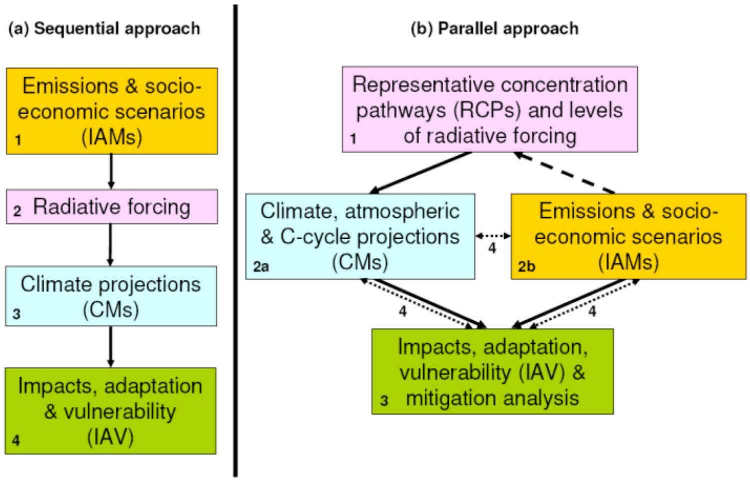

Figure 2-3 Approaches to the development of global scenarios: (a) previous sequential approach used in AR4; (b) parallel approach used in AR5.

Figure 2-4 shows the range of projections in temperature and precipitation change in the upstream parts of the Amu Darya and Syr Darya river basins according to all AR5 GCM runs for RCP4.5 and RCP8.5. From the figure the large uncertainty in future climate over Central Asia is evident. The likely increase in temperature during a period of 100 years ranges from +2.5 °C to +7.5 °C, whereas the likely change in precipitation ranges from -20% to +20%. These values represent the region-averaged changes. At the local scale, the uncertainties may be even larger.

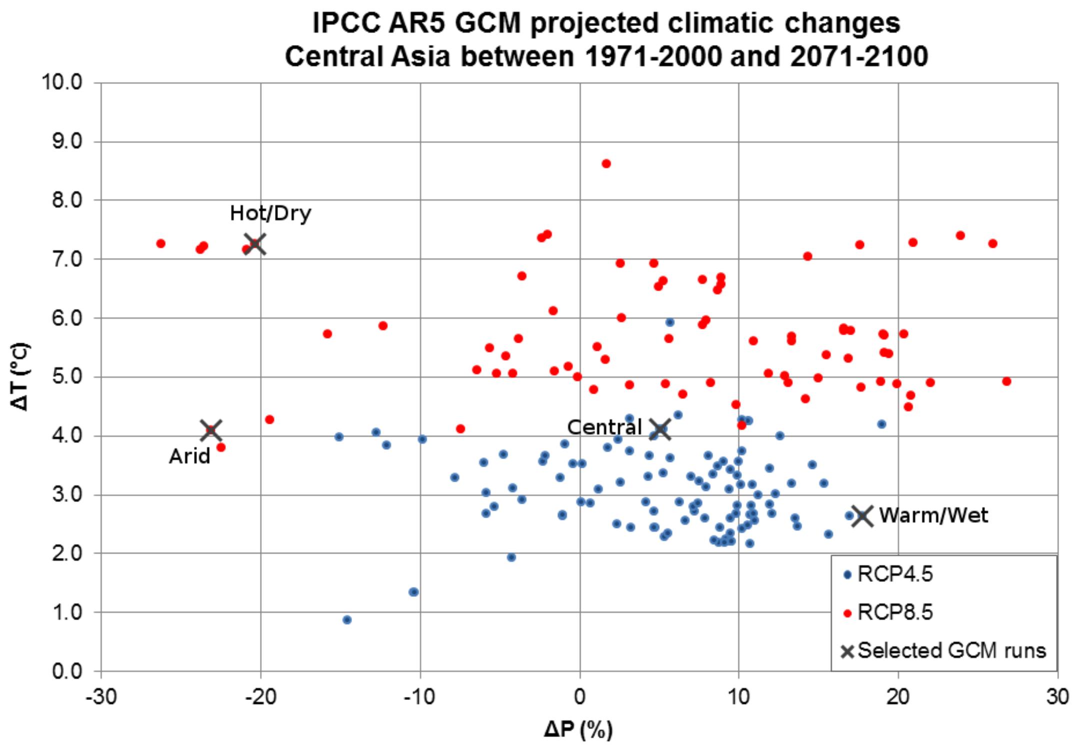

Figure 2-4: Projected changes in temperature and precipitation for the upstream Amu Darya and Syr Darya basins in Central Asia between 1971-2000 and 2071-2100. All AR5 GCM runs for RCP4.5 and RCP8.5 are shown. Values are average for extent shown in Figure 2-5. GCM runs that were selected based on proposed marker scenarios are indicated with black crosses.

Figure 2-5: Area for which GCM analysis was conducted (Figure 2-4).

Four marker scenarios were selected from the corresponding GCM runs from the CMIP5 RCP4.5 and RCP8.5 ensembles (Table 2-1). The selected GCM runs are downscaled using the ‘delta change’ approach to generate model forcing for the upstream SPHY model and downstream WEAP model until 2100. The downscaling process is described with detail in Appendix I.

Table 2-1: Selected GCM runs for each of the four marker scenarios and their projected changes in temperature and precipitation averaged over the Central Asian region between 1971-1990 and 2071-2100.

Marker scenario	GCM run	RCP	ΔT (°C)	ΔP (%)
Arid	FIO-ESM_r2i1p1	RCP8.5	+4.1	-23.1
Hot/dry	IPSL-CM5A-LR_r1i1p1	RCP8.5	+7.3	-20.3
Central	HadGEM2-ES_r2i1p1	RCP4.5	+4.1	+5.0
Warm/Wet	GISS-E2-H_r4i1p2	RCP4.5	+2.6	+17.7

2.2 Modelling of upstream hydrology

2.2.1 SPHY model structure

The SPHY (Spatial Processes in Hydrology) model [*Immerzeel et al.*, 2012; *Lutz and Immerzeel*, 2013] is a raster based highly detailed full distributed cryospheric- hydrological model. The model is based on commonly accepted standards from multiple proven hydrological models. SPHY is created in PCRaster environmental modelling software [*Karssenberg et al.*, 2001]. PCRaster is a spatio-temporal environmental modelling language developed at Utrecht University, the Netherlands. The model runs at 1 x 1 km spatial resolution with daily time steps and incorporates all major hydrological processes as well as cryospheric processes.

The actual runoff which is calculated for each grid cell consists of four contributing factors. These are: runoff originating from rain, runoff originating from snow melt, runoff originating from glacial melt, and base flow, as visualized in Figure 2-6. With the daily air temperature and daily precipitation per grid cell as input the model evaluates how much precipitation falls and it is disaggregated into either snow or rain based on the air temperature distribution. The model evaluates the amount of glacier melt and snow melt or accumulation and which part of snow and glacier melt is directly transformed to runoff and which part refreezes. Rainfall-runoff processes are evaluated in a soil component in the model. The runoff from all contributing components is routed through the system using the DEM.

Each grid cell is divided in fractions. If a cell is (partly) glacierized, the cell has a glacier fraction between 0 and 1 (0: no glacier cover, 1: complete glacier cover). The other fraction of the grid cell can be either ‘snow’ or ‘rain’. This depends on the presence of snow cover, which is determined by the model. As long as snow cover is present, the snow module is active, while the rain module is active when no snow cover is present.

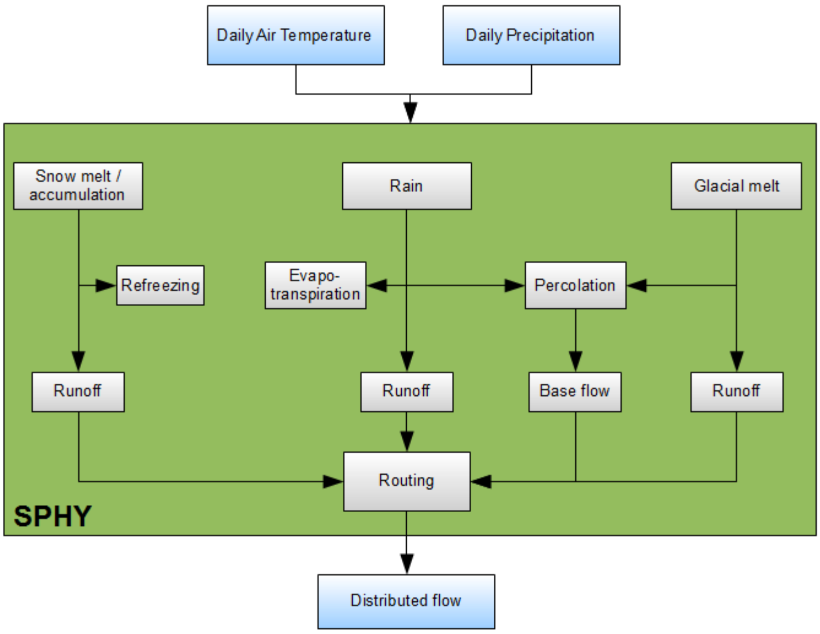

Figure 2-6: Model structure of SPHY model

2.2.2 Cryospheric processes

Since the model is set up for a 1 x 1 km resolution, the ice cover is described as a fraction varying from 0 (no glacial cover) to 1 (100% glacial cover). In this way, 1 x 1 km grid cells which are partly covered with ice can be simulated. A differentiation is made between clean ice glaciers and debris covered glaciers. Glaciers at lower altitude tend to have more debris cover because of the cumulative accumulation of debris from higher grounds and glacier parts with a small slope have more debris cover compared to steep-sloped parts of the glacier. The differentiation between clean ice glaciers and debris covered glaciers is then re-calculated to fractions of the 1 x 1 km grid cells used in the model. Summing the fractions of clean ice glacier and debris covered glacier will always result in a total fraction of one.

Initial conditions for snow cover are obtained directly from the model. A model run is done simulating several years to develop a balanced snow cover. The snow cover at the end of this model run is used as initial snow cover for further model runs. In the model calculations, the amounts of ice and snow are described as millimeters water equivalent. The modelling of processes involving glaciers is described in a schematic way in Figure 2-7. Melt from clean ice glaciers is defined as the air temperature (if above 0 °C) multiplied by the degree day factor for clean ice, multiplied by the clean ice fraction of the glacier cover and the cell fraction with glacier cover.

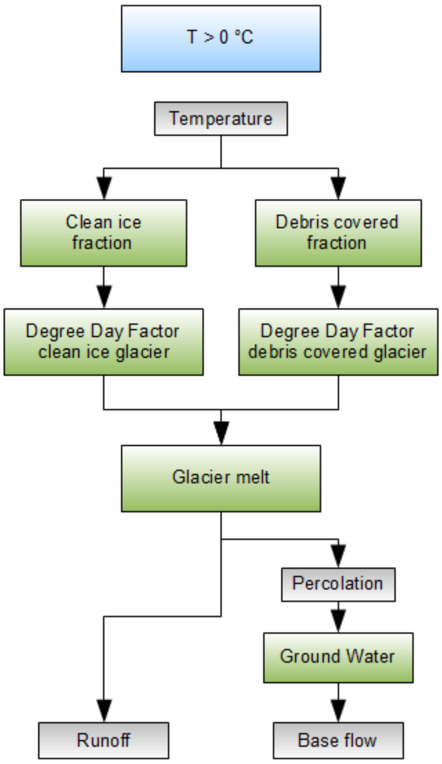

Figure 2-7: Schematic representation glacier related processes in the SPHY model

For the melt from debris covered glaciers the calculation is similar, although a different degree day factor for debris covered glaciers is specified. Melt rates for debris covered glaciers are lower, since the energy fluxes are partly blocked by the (thick) debris cover.

The use of temperature index or degree day models is widespread in cryospheric models to estimate ice and snow melt. In these models an empirical relationship between melt and air temperature based on a frequently observed correlation between the two quantities is assumed [*Hock*, 2005]. Degree-day models are easier to set up compared to energy-balance models, and only require air temperature, which is mostly available and relatively easy to interpolate.

The total glacier melt is then calculated by summing the two components from clean ice glacier melt and debris covered glacier melt. A part of glacial melt comes to runoff, while another part percolates to the ground water. This process is controlled by adjusting the glacial runoff factor.

For each cell the model determines if precipitation falls as snow or rain by comparing the actual air temperature to a critical temperature. When air temperature is below or equal to the critical temperature, precipitation will fall as snow. When air temperature is above the critical temperature, precipitation will fall as rain.

In the model a differentiation is made between the potential snow melt and the actual snow melt (Figure 2-8). The potential snow melt is defined as the air temperature (if above 0 °C) multiplied by a degree day factor for snow multiplied by the cell fraction covered with snow. The actual snow melt however, is limited by the thickness of the snow pack. No more snow can be melted than the amount of snow which is available at the considered time step. The snow storage is then updated, to be used for the next time step. The snow storage is updated by subtracting the melt and/or adding the freshly fallen snow or rain to the water storage in the snow pack. The updated snow storage is the 'old' snow storage with the fresh snow added and the actual snow melt subtracted.

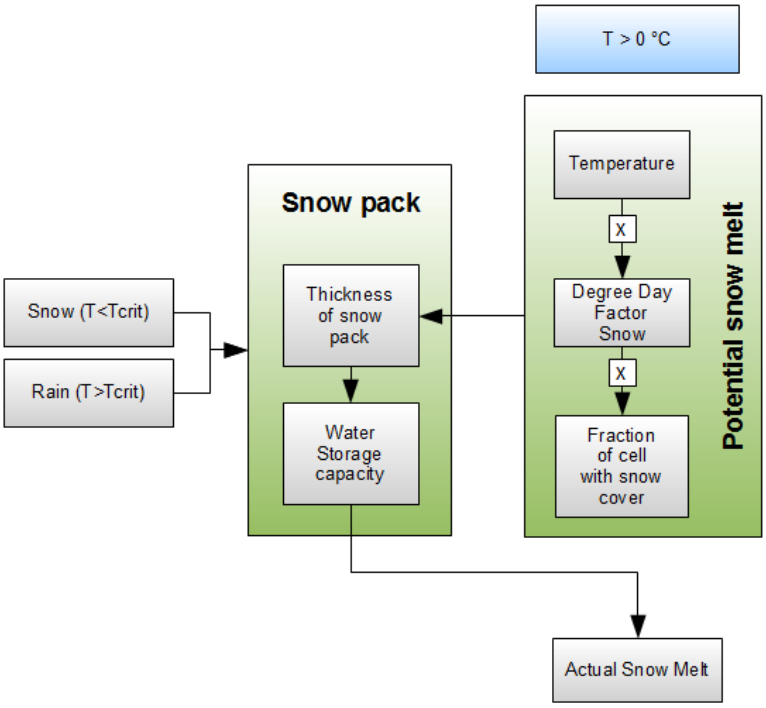

Figure 2-8 Schematic representation of snow related processes in the SPHY model

The water resulting from snow melt will partially refreeze as it infiltrates the underlying snow pack. The maximum amount of water that can refreeze is defined by the water storage capacity of the snow pack which depends on the thickness of the snow pack present and the storage capacity of snow (e.g. the total millimeters of melt water that can refreeze per millimeter of snow). The actual amount of water that is stored in the snow pack is defined as the water stored in the snow pack during the previous time step summed by the actual snow melt. Snow melt will become actual snow melt when the amount of snow melt exceeds the water storage capacity of the snow pack. When all snow in a grid cell has melted, the snow fraction is set to zero. If snow falls on a cell which had no snow during the previous time step the snow fraction is updated to 1.

2.2.3 Rainfall runoff

The modelling steps for rainfall in the SPHY model are represented in Figure 2-9. Precipitation in the model will fall as rain when the air temperature is above a critical temperature.

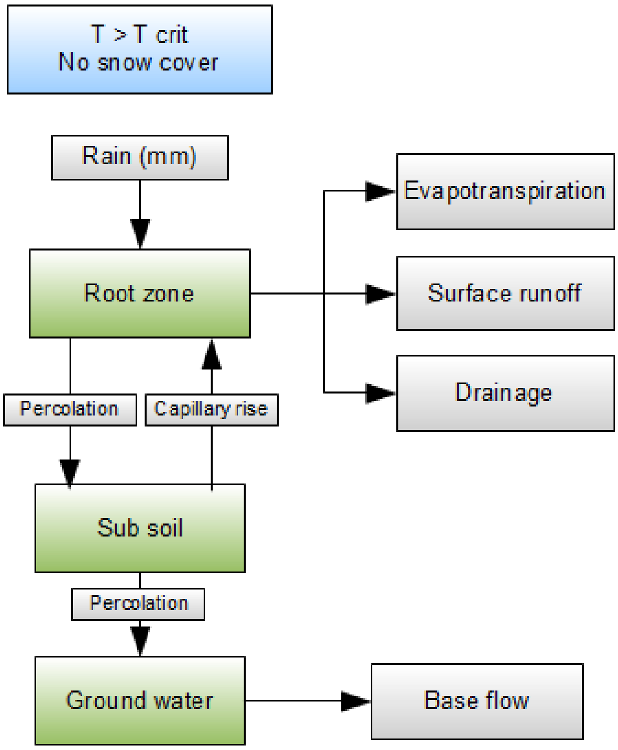

Figure 2-9: Schematic representation of rainfall-runoff modelling in the SPHY model

A soil module based on the saturation excess overland flow (also known as Hewlettian runoff) concept is incorporated in the SPHY model. The soil layer in the model is divided in a root zone and a sub soil. The thickness of the soil is slope dependent in the model. The soil properties are based on pedotransfer functions, to quantify soil properties for different soil types. The soil properties used in the SPHY model are listed in Table 2-2. Using these properties, the model evaluates how much water in the rootzone is available for evapotranspiration, surface runoff, lateral drainage and percolation/capillary rise to/from the subsoil.

Table 2-2: Soil properties used in SPHY model

Rootzone	**Subsoil**
Rooting depth (mm)	Subsoil depth (mm)
Saturated water content (mm/mm)	Saturated water content (mm/mm)
Field capacity (mm/mm)	Field capacity (mm/mm)
Wilting point (mm/mm)	Saturated conductivity (mm/day)
Permanent wilting point (mm/mm)	
Saturated conductivity (mm/day)	

The potential evapotranspiration (ET_{pot}) in the model is calculated using the reference evapotranspiration (ET_{ref}) and a crop coefficient (K_c):

$$ET_{pot} = ET_{ref} \cdot K_c$$

The reference evapotranspiration is calculated according to the Modified Hargreaves method [*Droogers and Allen*, 2002]. This method requires average, maximum and minimum air temperature (T_{avg}, T_{max}, T_{min}), the summed precipitation (P) and incoming extraterrestrial radiation (Ra):

$ET_{ref} = 0.0013 \cdot 0.408Ra \cdot (T_{avg} + 17.0) \cdot ((T_{max}\text{-}T_{min}) - 0.0123P)^{0.76}$

Based on land use type, each grid cell is assigned a K_c factor to calculate the potential evapotranspiration. The actual evapotranspiration (ET_{act}) is the potential evapotranspiration limited by the water available in the rootzone (e.g. the saturation of the root zone).

Excess water is also leaving the rootzone as surface runoff, lateral drainage or percolation to the sub soil. The occurrence of capillary rise from the sub soil to the root zone or percolation from the root zone to the sub soil depends on differences in water saturation of both soil layers. Water percolates from the sub soil to the ground water.

At the moment a 'rain fraction' is covered with snow, it switches to 'snow fraction'. As long as snow cover is present, the snow module (described in section 2.2.2) is active. However, the soil component remains active, although no more precipitation is entering the soil and no more water is leaving the soil as surface runoff or evapotranspiration. Percolation to the subsoil and eventually to the ground water remains active.

2.2.4 Groundwater

A ground water reservoir generating base flow is incorporated in the model. During periods with low runoff the streams are fed by processes such as sustained ground water flow and/or slow throughflow through the deeper soil from earlier precipitation events. This is referred to as base flow. The ground water reservoir is active for each entire grid cell. The ground water is fed by percolation from the sub soil and percolation from the glacier fraction of a cell. These two components provide recharge to the ground water reservoir. The ground water recharge is translated into baseflow released from the reservoir with a certain time lag.

2.2.5 Routing

In the model, the generated runoff is routed through the basin according to a flow direction map based on the DEM. For each cell the local drain direction is defined. The runoff generated per grid cell accumulates with runoff generated in downstream grid cells. Using a linear regression with a regression constant, the time water needs to flow through the reservoir towards the outflow point is simulated.

2.3 High mountain science: latest developments

High Asia's glaciers are a focus of public and scientific debate. Uncertainties in their current and future state are of major concern because they play a major role in the hydrological cycles of many river basins originating in Asia's high mountains. In the IPCC's AR4 an erroneous statement made clear that the knowledge of High Asia's cryosphere and its role in hydrology was insufficient. Since then, numerous scientific studies in this region have been conducted to assess the current and future status of the cryosphere [*Kargel et al.*, 2011; *Bolch et al.*, 2012; *Gardelle et al.*, 2012; *Kääb et al.*, 2012; *Radić et al.*, 2013] A first large scale hydrological modeling assessment using AR4 climate change scenarios indicated decreasing flows around 2050 for most meltwater-dependent river basins in Asia [*Immerzeel et al.*, 2010]. The model and climate change scenarios used for the mentioned study have also been used as basis for ADB's *Water and Adaptation Interventions in Central and West Asia* study.

However, advancing research has led to new insights regarding the future runoff in glacierized basins such as the Amu Darya and Syr Darya. In 2013, a detailed high-resolution study in two glacierized basins in the Indus and Brahmaputra basins was conducted using the latest AR5 climate change scenarios [*Immerzeel et al.*, 2013]. This study showed that glacier melt water is likely to increase until around halfway the 21st century whereafter a decrease is expected (Figure 2-10). This is in contrast to the earlier results, where a decrease was already projected for 2050 [*Immerzeel et al.*, 2010].

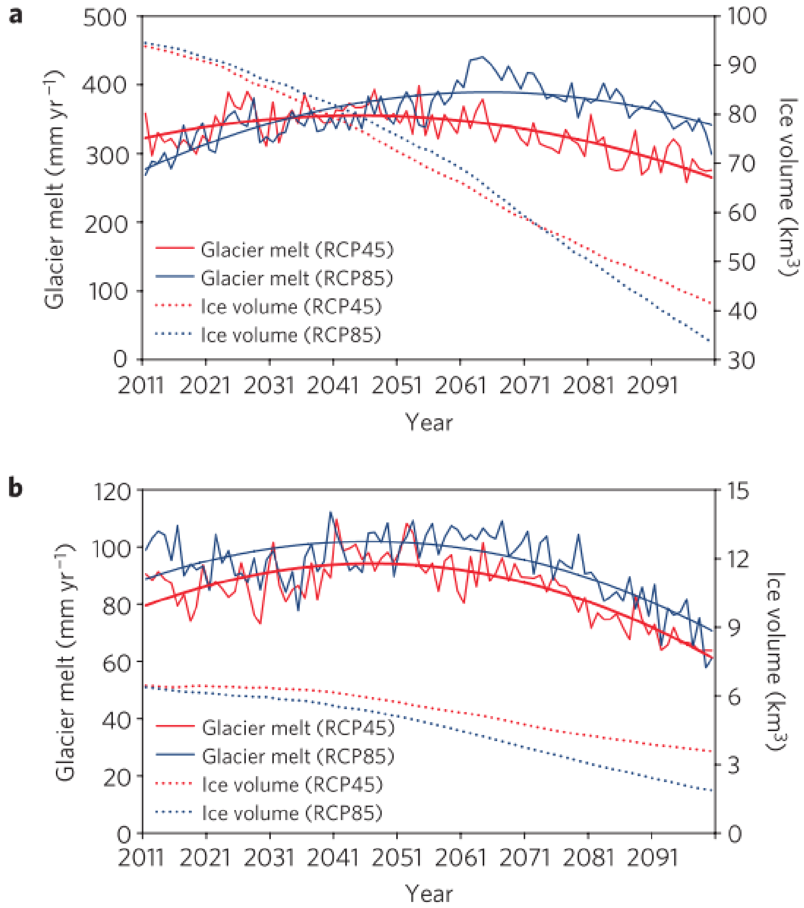

Figure 2-10: Future melt and ice volumes in the Baltoro (a) and Langtang (b) catchments. From [*Immerzeel et al.*, 2013]**.**

There are several reasons for the differences:

- The scale of the model application is different and consequently the physical detail of the model has much improved
- Different time slices are compared and the latest GCMs were used, which project a stronger increase in precipitation.
- The mass balance calculations in the earlier study may have resulted in an overestimation of glacier retreat by 2050 and consequently an underestimation of future glacier melt.

These findings at small scale consequently have led to improvements in the representation of processes in the large scale models such as SPHY. Important changes were made in the parameterization of glacier changes [*Lutz et al.*, 2013] that was used in the ADB study. The improvements in the large scale model and application of this model in five major river basins in the High Asian region recently confirmed that the findings are also valid at the large scale and thus a consistent increase in High Asia's runoff can be expected at least until 2050 [*Lutz et al.*, 2014b]. This study did not include the the Amu Darya and Syr Darya basins)

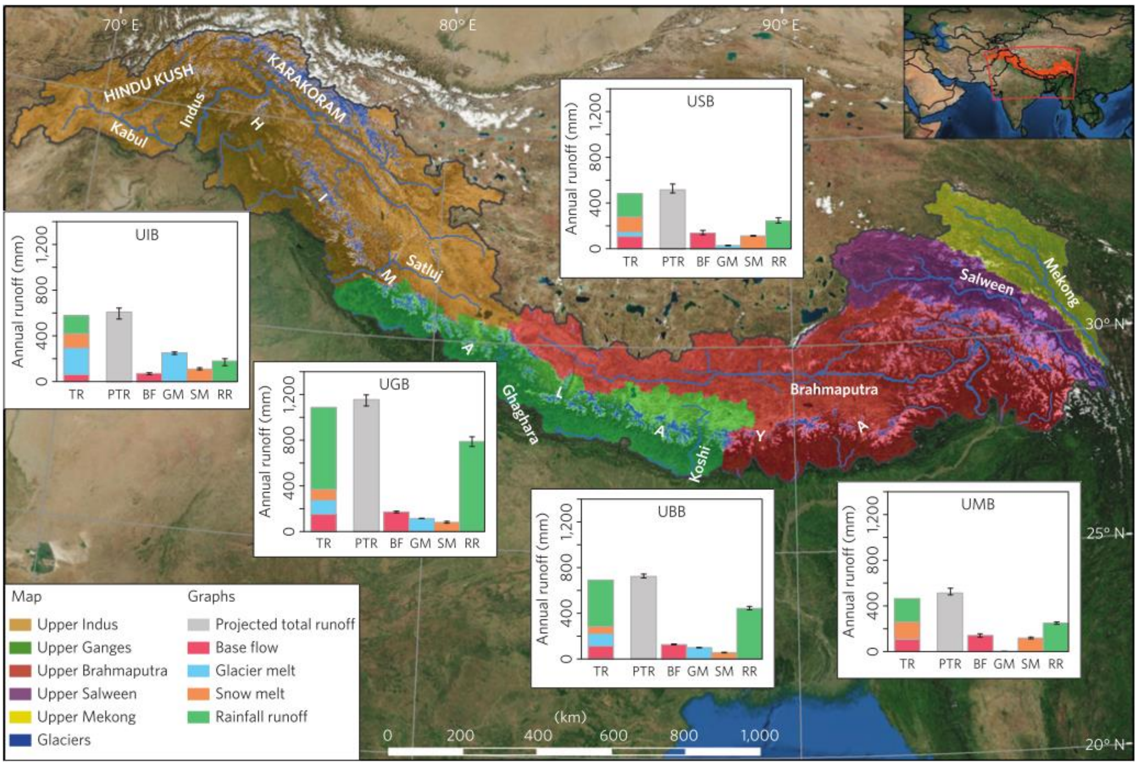

Figure 2-11: The upstream basins of Indus, Ganges, Brahmaputra, Salween and Mekong. Bar plots show increasing runoff until 2050 for each of the five upstream river basins. Error bars indicate the spread in model outputs for the model forced by an ensemble of 4 RCP4.5 GCMs. From [*Lutz et al.*, 2014b]**.**

Another global scale study quantifying the global response of glacier runoff to twenty-first century climate change [*Bliss et al.*, 2014] does include the Central Asian region and shows a slightly different picture for this area, when compared to the western part of South Asia (Figure 2-12). According to this study, the glacier-originated runoff increases until ~2050-2060 for western South Asia, and begins to decrease afterwards. This is consistent with the findings by [*Lutz et al.*, 2014b]. For Central Asia (not included in the study by [*Lutz et al.*, 2014b]) [*Bliss et al.*, 2014] don't find the same increase in glacier-originated runoff during the first half of the 21st century (Figure 2-12). The glacier-originated runoff stays rather constant or decreases slowly during the first half of the 21st century before it decreases more rapidly during the second half of the 21st century.

It is uncertain what causes this difference in response. The current climates of the Central Asian and the South Asian region differ substantially [*Bookhagen and Burbank*, 2010]. The climate in South Asia is dominated by the monsoonal precipitation regime with the bulk of the precipitation falling during June, July, August and September. The climate in the Pamir and Karakoram mountain ranges is much more influenced by westerly streams bringing precipitation during the winter months [*Kapnick et al.*, 2014]. This largely seems to explain the differences in trends in glacier changes during the last decades, with glaciers retreating in South Asia, whereas glaciers are expanding in the Pamir and Karakoram region. This phenomenon is referred to as the "Karakoram anomaly" [*Hewitt*, 2005] or, more recently, the "Pamir-Karakoram anomaly" [*Gardelle et al.*, 2013] . Seasonal differences in future climate change can lead to different responses for regions with different climates. Besides climate, the regions also differ substantially in terms of number of glaciers, glacier size, distribution of glaciers of the elevation. Understanding how the differences between these regions lead to different responses to climate change is one of the current scientific challenges.

- Precipitation

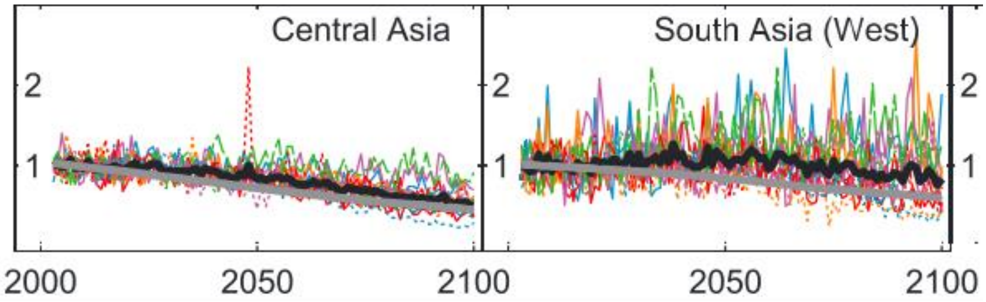

Figure 2-12: Projected annual glacier volume and runoff for 2003-2100 from all glaciers in the Central Asian (left) and western South Asian (right) regions. All lines are normalized to their mean value from 2003-2012. Each colored line represents the projected runoff from one GCM and the black line is the multi-model mean. The grey line is the mean projected ice volume (After [*Bliss et al.*, 2014]**).**

The key enhancements in the SPHY version used for the current study are:

- Improvements were made in the parameterization of glacier changes [Lutz et al., 2013]. Whereas the decrease in glacier extent starts at the lowest part of the glaciers in SPHY 2011 version, the decrease in glacier extent is consistent with elevation in the SPHY 2014 version. This is more realistic as thick glacier tongues, which generate bulk of the glacier melt water, persist longer in the future in the SPHY 2014 version.
- Representation of various other processes have improved. SPHY 2014 version includes a soil layer component, which improves the simulation of process like evapotranspiration, infiltration to ground water and generation of direct rainfall-runoff. The routing scheme has improved with respect to earlier versions.
- CMIP5 climate models instead of CMIP3 climate models were used to force the model for the future. CMIP5 models have a larger range in temperature and precipitation projections compared to CMIP3.

For the reference period, the base input maps, temperature and precipitation forcing data are unchanged with respect to the previous 2011 ADB study. Base input maps include the Digital Elevation Model, local drain direction map, soil and land use maps, initial glacier cover and mask for debris covered and debris free glaciers.

2.4 Modelling of downstream water availability and allocation

2.4.1 The WEAP-ARAL model

WEAP ("Water Evaluation And Planning" system) is a well-known software tool that takes an integrated approach to water resources planning. Allocation of limited water resources between agricultural, municipal and environmental uses requires the consideration of the interdependent nature of supply, demand, water quality and ecological considerations. WEAP aims to incorporate these issues into a practical yet robust tool for integrated water resources planning. WEAP is developed by the Stockholm Environment Institute's U.S. Center. WEAP was originally developed for simulating water balances and evaluating water management strategies in the Aral Sea region [*Raskin et al.*, 1992].

For a recent study carried out for the Asian Development Bank [*Lutz et al.*, 2012] a water allocation model was developed in WEAP for the Amu Darya and the Syr Darya basin incorporating the agricultural and domestic demand sites, catchments, inflow points from upstream, reservoirs and the connections between them. The effects of future changes in temperature and precipitation for the future water availability and demand were simulated until 2050 and the effects of possible adaptation measures were explored. This version of the model will be referred to in this report as ARAL-WEAP2011.

In WEAP, a database maintains water demand and supply information to drive a mass balance model on link-node architecture. Simulations calculate water demand, supply, runoff, infiltration, crop requirements, flows, and storage, and pollution generation, treatment, discharge and instream water quality under varying hydrologic and policy scenarios. Policy scenarios can be analysed to evaluate a full range of water development and management options, taking into account the multiple and competing uses of the different actors and sectors in the basin.

WEAP has a user-friendly GIS-based interface with flexible model output as maps, charts and tables. WEAP is available in also Russian and Farsi languages and it is already at use in the Aral Sea Basin. WEAP license is free of charge to non-profit, governmental or academic organization based in a country receiving development bank support (as all the Central Asian countries).[1]

[1] www.weap21.org

The ARAL-WEAP2011 model runs at a monthly time step for three time intervals: for the reference situation (2001-2010) and for two future time interval (2021-2030 and 2041-2050). The model was calibrated for the reference situation (2001-2010) [*Lutz et al.*, 2012].

The WEAP model used for this Regional Risk Assessment for Water Availability under Climate Change is built upon the ARAL-WEAP2011 model, incorporating a list of modifications and advancements. The following changes and additions were made for this updated version, hereafter called ARAL-WEAP2014:

- Additional hydropower facilities, including several planned upstream run-of-river facilities, planned storage facilities: Rogun and Kambarata-I and refurbishment of existing facilities
- Additional irrigation reservoirs
- Incorporation of thermal power plants to analyze water availability for cooling water
- Transformation of a steady-state approach to a dynamic modelling approach
- Inclusion of reservoir evaporation
- Model performance assessment based on annual and monthly data on hydropower generation and reservoir releases

This methodological section details these updates and advancements carried out for ARAL-WEAP2014. For further details on ARAL-WEAP2011, please refer to the documentation in [*Lutz et al.*, 2012].

2.4.2 Schematic setup

Figure 2-13 and Figure 2-14 show schematic representations of the model setup. The figure includes all the demand sites (agricultural and urban), the reservoirs and the catchments and the links among them. For the upstream reservoirs, the inflow is simulated by the SPHY hydrological model, as indicated by the orange color of the triangle. The upstream catchments that do not drain into a reservoir in the upstream area are indicated with a orange hexagon symbol. In the downstream areas, the hydrology is simulated by a simplified rainfall-runoff model in WEAP.

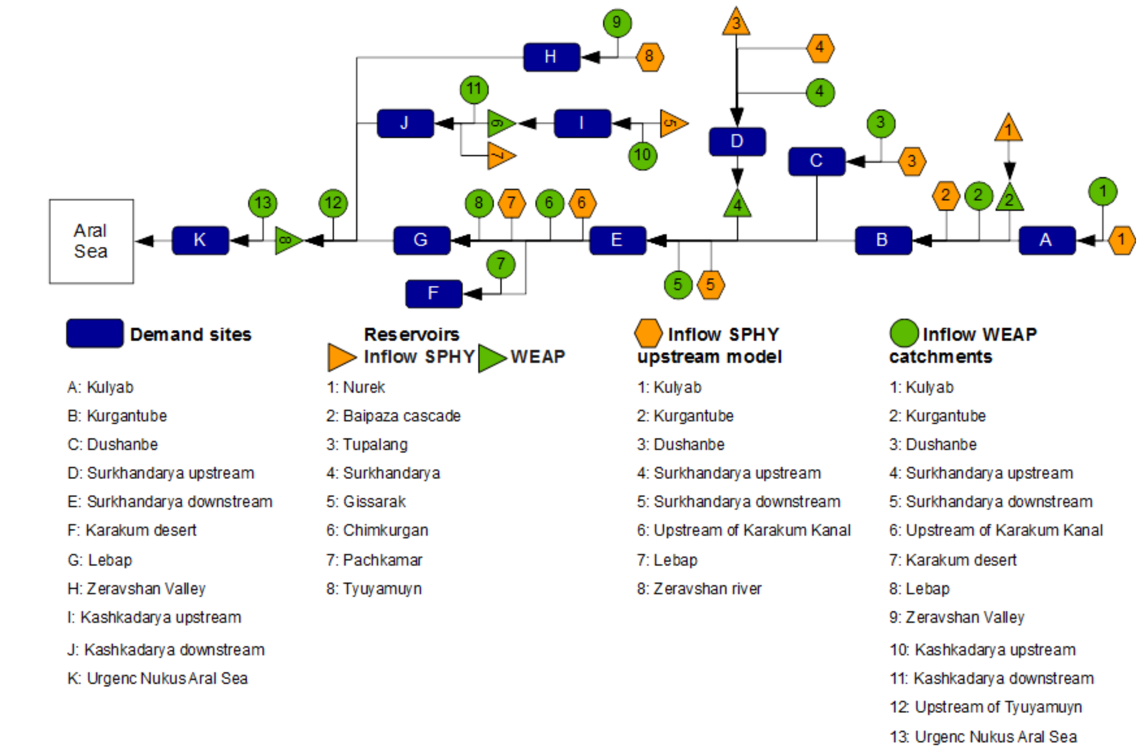

Figure 2-13: Schematic representation Amu Darya river basin in ARAL-WEAP model.

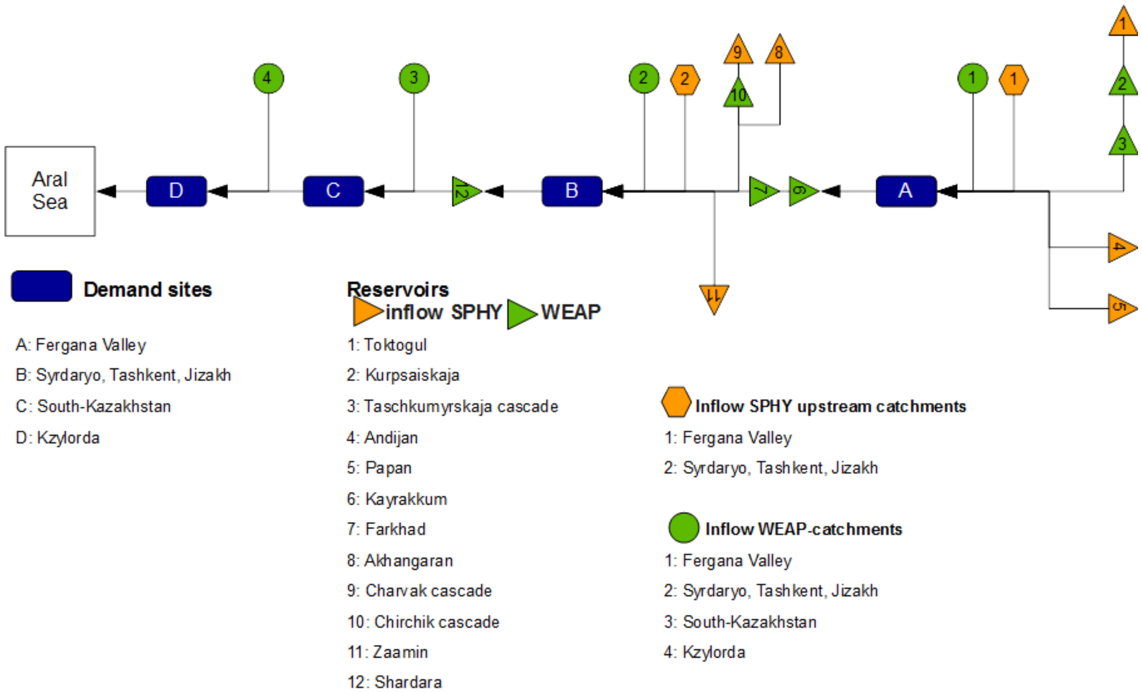

Figure 2-14: Schematic representation Syr Darya river basin in ARAL-WEAP model.

As explained previously (section 1.4 on Modelling approach), the division of the upstream and the downstream part approximates the division in areas without significant human interference and areas with significant human interference. Partly, this division is well defined where major reservoirs are located in the mountain ranges. Downstream of these locations, the stream flow is human-regulated. In some regions the division in upstream basin and downstream basin is less well defined. For those regions the division is made based on optical analysis of satellite imagery. This boundary approximates the division between the mountain environment and the lower land, extensively used by the human population. Figure 2-15 shows the upstream catchments for which the hydrological model SPHY was used. For the infrastructure scenarios the subcatchments draining to Nurek and Toktogul were further subdivided to obtain the flows at the upstream planned facilities.

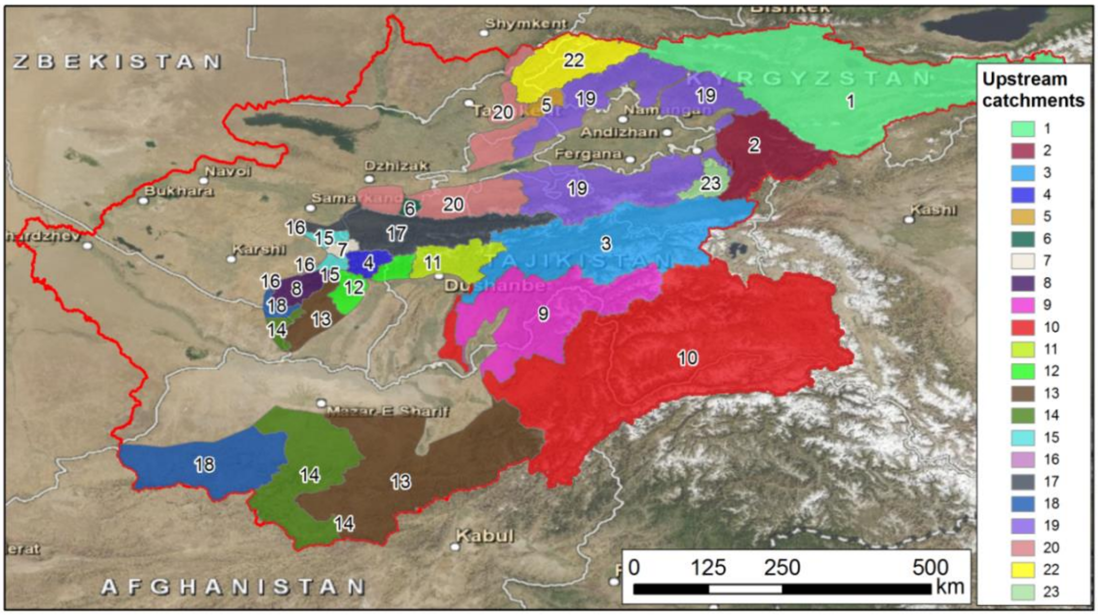

Figure 2-15: Subcatchments used in upstream model for input in downstream WEAP-model.

Figure 2-16 shows the geographical positioning of the rivers, demand sites, inflows, catchments, transmission links and return flows as represented schematically in Figure 2-13 and Figure 2-14.

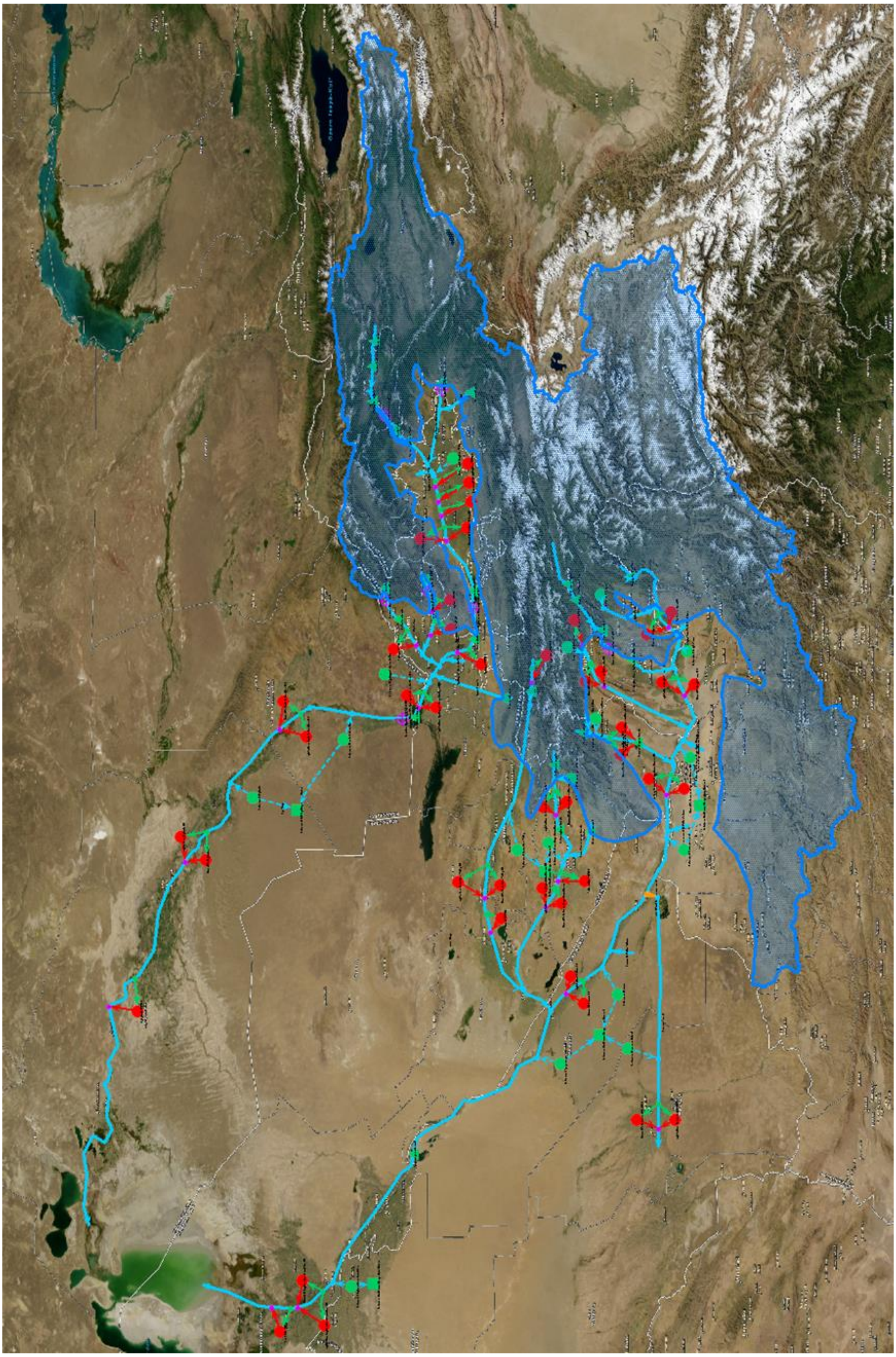

Figure 2-16: Geographical visualization of ARAL-WEAP2014 model. The spatial extent of the SPHY upstream model area is indicated with blue color. Demand sites are indicated with red dots, catchments are indicated with green dots.

The runoff that is generated in the downstream areas is simulated by WEAP, by assigning catchments that coincide with the demand sites. For these catchments monthly mean, maximum and minimum temperature and total monthly precipitation are extracted from the 2001-2010 climate data set prepared by the Finish Meteorological Institute (FMI). Based on this dataset, the monthly incoming water (from precipitation) and the water lost by evapotranspiration is calculated using the Modified Hargreaves method [*Droogers and Allen*, 2002]. The rainfall-runoff scheme used is the FAO rainfall-runoff model, which is incorporated in WEAP. A detailed discussion on data set used, model calibration and performance as well as impact and adaptation results can be found in [*Lutz et al.*, 2012].

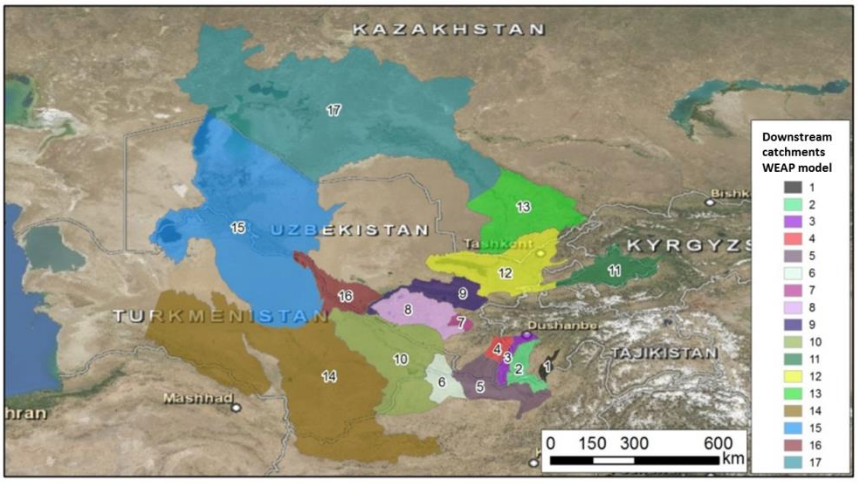

ID	Catchment name
1	Kulyab
2	KurganTube
3	Dushanbe
4	Surkhandarya upstream
5	Surkhandarya downstream
6	Karakum kanal
7	Kashkadarya upstream
8	Kashkadarya downstream
9	Zeravshan Valley
10	Lebap
11	Fergana Valley
12	Syrdaryo, Tashkent, Jizakh
13	South Kazakhstan
14	Karakum desert
15	Urgenc, Nukus, AralSea
16	Tyuyamuyn
17	Kzylorda

Figure 2-17: Downstream catchments used in WEAP model, see also

2.4.3 Hydropower facilities

To make the existing WEAP model suitable for the simulation of hydropower production, several additional data sources were added and incorporated in the tool. Table 2-3 summarizes the type of data and the data source that was used.

Table 2-3. Additional data and sources used to extend the WEAP-ARAL2014 model

Data	Source
Location and characteristics of Run-of-River (RoR) hydropower facilities	[*ADB*, 2012]; [*World Bank*, 2012]; [*EC IFAS*, 2012]; www.cawater-info.net
Planned reservoirs, rehabilitation and hydropower facilities	[*World Bank*, 2012]; [*World Bank*, 2014a]; [*EC IFAS*, 2012]; [*World Bank*, 2014b].
Installed capacity (GW)	[*ADB*, 2012]
Power generation (GWh) from 2000-2010	[*ADB*, 2012]
Volume elevation curves	[*USAID*, 2000]

2.4.3.1 Hydropower plants

Several reservoirs were added to the existing WEAP model (mainly RoR and planned ones). Table 2-4 provides a list of all the reservoirs in the WEAP model that have hydropower facilities and their main characteristics. The RoR facilities that are in cascade in a particular stream segment are included as one single node in the WEAP model.

The following future facilities were included:

- Rogun: 3200 MW, 311m head, 13 299 MCM storage capacity. The building of this facility is assumed to start in 2020 and finished after 12 years. Source: TEAS study for Rogun Project [*World Bank*, 2014b]
- RoR above Rogun, 1554 MW, 121m head. Source TEAS study for Rogun Project [*World Bank*, 2014b]
- Kambarata 1: 1900 MW, 210m head, 4650 MCM storage capacity. Source BEAM model [*EC IFAS*, 2012];
- Kambarata-II extension: 240 MW. Source BEAM model [*EC IFAS*, 2012];
- Upper Naryn RoR, 610 MW, 63m head. Source BEAM model [*EC IFAS*, 2012];

The TEAS study for Rogun Project [*World Bank*, 2014b] states that in 2020, "End of stage 1 dam" (FSL 1290 m), will be operational, while in 2025 the "End of Main Dam Construction" for the low option (FSL 1220 m) is foreseen to be operational. Therefore, the year 2025 was assumed to be the starting date of the Rogun options.

Based on the input data of the BEAM model [*EC IFAS*, 2012], it seems likely in the near future investments are expected for hydropower rehabilitation. This may increase capacity with around 5% (assumed from 2025 onwards).

Table 2-4. Reservoirs and other hydropower facilities and main characteristics per country

Country	Reservoir	From year	Full storage capacity (MCM)	Dead storage (MCM)	Dam height (m)	Available Capacity (MW)	Basin (S=Syr Darya, A=Amu Darya)
KYR	Kurpsaiskaja	<2000	372	74	94	796	S
	Papan	<2000	260	20	100	20	S
	Taschkumyrskaja_cascade[1]	<2000	222	44	108	864	S
	Toktogul reservoir	<2000	19500	5500	215	1192	S
	Kambarata-I	2025	4650	1220	210	1900	S
	Kambarata-II	2010			50	120	S
	Kambarata-II extension	2025			50	240	S
TAJ	Baipaza cascade[2]	<2000	2268	454	180	1510	A
	Kayrakkum reservoir	<2000	4160	1560	32	126	S
	Nurek reservoir	<2000	10500	6000	300	2997	A
	Rogun Low	2025	8228	2999	265	2000	A
	Rogun High	2025	13299	2999	311	3600	A
	RoR above Rogun	2025			121	1554	A
KAZ	Shardara reservoir	<2000	5700	1000	29	116	S
UZB	Akhangaran	<2000	198	13	100	21	S
	Andijan Reservoir	<2000	1900	300	121	189	S
	Charvak cascade[3]	<2000	2860	1122	200	899	S
	Chirchik cascade[4]	<2000			210	185	S
	Farkhad reservoir	<2000	350	70	28	126	S

Gissarak	<2000	170	8	139	45	A
Surkhandarya	<2000	800	100	30		A
Tupalangsku	<2000	500	30	40	30	A
Tyuyamuyun reservoir	<2000	7800	2530	80	149	A

[1]Taschkumyrskaja , Schamaldysaiskaja , Utschkurganskaja; [2]Baipaza, Sangtuda, Golovanaya; [3]Charvak, Chodjiket, Gasalkent; [4]Tawak, Chirchik, Akkawak

Additional reservoirs are included in the WEAP-ARAL2014 model that only serve irrigation and/or domestic use. These reservoirs can be found in Table 2-8.

2.4.3.2 Hydropower generation

Figure 2-18 shows the annual hydropower generation over the period 2001-2012, for all reservoirs for which data was available. The figure shows that there are significant differences in hydropower capacity, among countries and reservoirs and considerable annual variability related with the variable water availability.

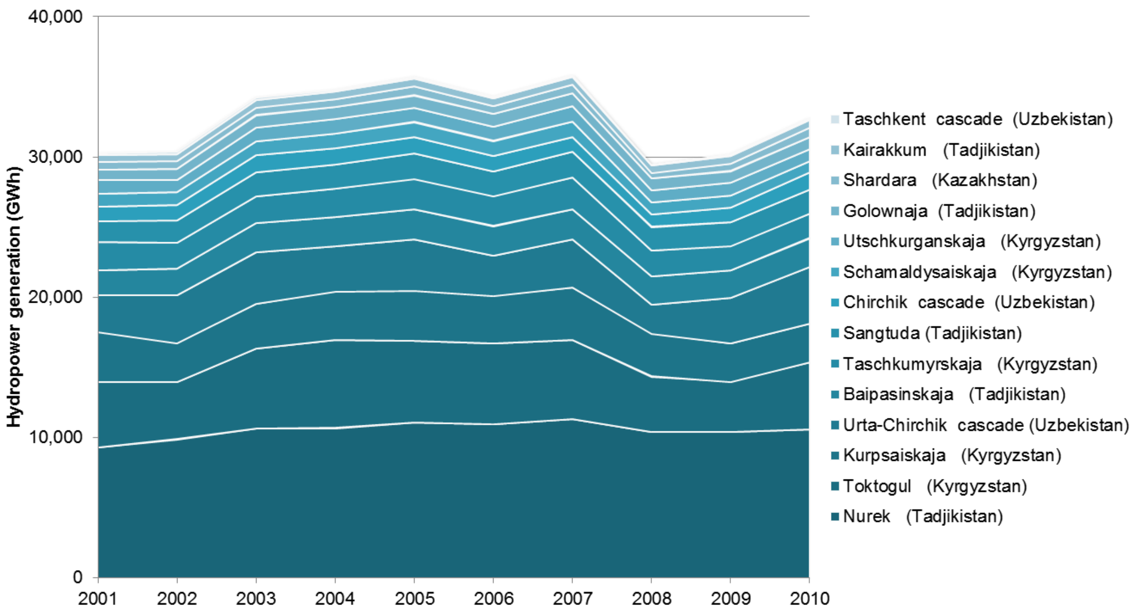

Figure 2-18: Annual hydropower generation 2001-2010 for the principal reservoirs in the region. Source: [*ADB*, 2012]

Hydropower generation in WEAP is computed from the flow passing through the turbine, based on the reservoir release or run-of-river streamflow, and constrained by the turbine's maximum flow capacity. If there is too much water, extra water is assumed to be released through spillways that do not generate electricity. So:

$$VolumeThroughTurbine = Min(\ Release_H\ ,\ MaxTurbineFlow_H\ )$$

The maximum turbine flow can be calculated by multiplying the installed generating capacity (MW) with the number of seconds in a month and dividing by what WEAP calls the *HydroGenerationFactor*:

$$MaxTurbineFlowGJ = InstalledCapacityMW * NoSecondsMonth\ /\ HydroGenerationFactor_H$$

The *HydroGenerationFactor* is calculated is a function of the mass of water (1000 kg / m^3) through the turbines multiplied by the drop in elevation, the plant factor (fraction of time on-line), the generating efficiency, and a conversion factor (9.806 kN/m3 is the specific weight of water, and from joules to gigajoules):

$HydroGenerationFactor_H = 1000\ (kg / m^3) * DropElevation_H \times PlantFactor_H \times PlantEfficiency_H * 9.806 / (1{,}000{,}000{,}000\ J / GJ)$

The *PlantEfficiency* factor was calibrated for all the hydropower plants for which power generation data were available. For the other reservoirs it was assumed to be 0.85. The *PlantFactor* was assumed to be 1. See section 2.6 Model Performance on page 40 for more details on the calibration.

2.4.3.3 Volume elevation curves

For hydropower assessments, volume elevation curves of the reservoirs are important to parameterize correctly. For the WEAP model, a similar approach and data from [*USAID*, 2000] were used. In this approach, the following power function is used to relate reservoir levels (h) with reservoir volume (W)

$$W = a * h^b$$

In this equation, b is a morphological constant, depending on the bathymetrical conditions of each reservoir. For the new planned reservoirs (Rogun and Kambarata) it was assumed that this constant is the same as the downstream reservoir (Nurek and Toktogul). The coefficient *a* can be derived directly knowing the total volume and total head. The following table shows the values for the two coefficients for the main reservoirs

Table 2-5. Coefficients used for the reservoir volume elevation curves

Reservoir	a	b
Toktogul	1.62E-01	2.18
Kayrakkum	1.98E-01	2.87
Charvak_cascade	7.05E-04	2.87
Chardara	3.78E-01	2.87
Nurek	3.89E-04	5.95
Baipaza cascade	3.89E-04	3.00
Chirchik cascade	1.08E-05	3.00
Kurpsaiskaja	8.02E-04	2.87
Taschkumyrskaja cascade	2.57E-04	3.00

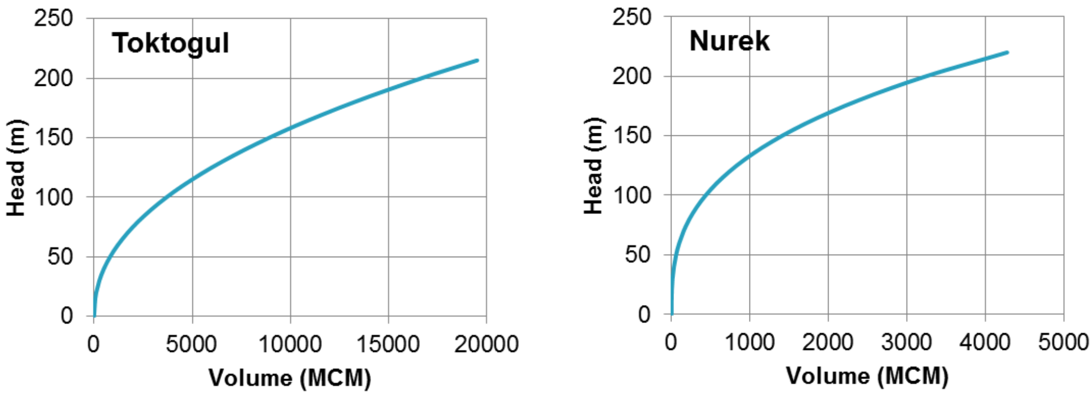

Figure 2-19. Volume elevation curves for Toktogul and Nurek reservoir

2.4.3.4 Reservoir evaporation

Losses through direct evaporation from the reservoirs were accounted for in the WEAP model by calculating monthly reference evapotranspiration (ET_{ref}) using the Modified Hargreaves method [*Droogers and Allen*, 2002]. According to the Modiefied Hargreaves method, the reference evapotranspiration is defined as:

$$\mathrm{ET}_{ref} = 0.0013 \cdot 0.408\mathrm{RA} \cdot (\mathrm{T}_{avg} + 17.0) \cdot (\mathrm{TD} - 0.0123\mathrm{P})^{0.76}$$

Where RA is the incoming extraterrestrial radiation in $MJm^{-2}d^{-1}$, Tavg is the average temperature, TD is the temperature range (Tmax – Tmin) and P is the incoming precipitation. All of these parameters are calculated on a monthly basis from the climate data set.

2.4.3.5 Reservoir outflow regimes

To obtain a correct simulation of the actual monthly outflow regime in the WEAP-ARAL2014 model, the current monthly release pattern was imposed on the WEAP-ARAL2014 model. This was done for the main reservoirs in the model for which monthly data was available. Thus, if enough water is available in the reservoir, the model meets this outflow regime based on the historical data.

The reservoirs for which this operational rule was imposed are listed in the performance section of the report (Section 2.6). For the other reservoirs, WEAP-ARAL2014 uses the optimization algorithm included in the WEAP model that by iteration tries to meet all downstream demands. Domestic demands are given a higher priority (1) then agricultural demands (2).

2.4.4 Cooling water needs for thermal power plants

Reductions in river flows due to climate change may result in shortages of cooling water for thermal power plants (TPPs), which will reduce their efficiency and potentially affect their reliability. Water shortages in the summer are already reported to affect the Syrdarya TPP [*World Bank*, 2013]. All existing TPPs and the planned ones of which data were available were included in WEAP to analyse their vulnerability to low flows.

The following data sources were used:

- [*World Bank*, 2012]: planned TPPs in Tajikistan
- [*ADB*, 2012]: capacity, future investments in TPPs and power production

2.4.4.1 Thermal plants

Table 2-6 shows the current and future TPPs included in the WEAP-ARAL2014 model and their main characteristics. Data on historical power production was obtained from [*ADB*, 2012]. This data allowed the calculation of an eficiency factor (plant factor) as shown in the last column. For those of which no data was available, a plant factor of 70% was assumed (estimated values indicated in italic).

Table 2-6. Thermal power plants and main characteristics included in the WEAP model

Name	**Country**	**Type**	**First year of operation**	**Capacity (MW)**	**Annual current production (GWh)**	**Plant factor (%)**
Sirdarya	UZB	Gas	<2000	3000	14053	53%
Taschkent	UZB	Gas	<2000	1860	8100	50%
Navoi	UZB	Gas	<2000	1250	6665	61%
Novo-Angren	UZB	Coal	<2000	2100	6188	34%
Talimardjan	UZB	Gas	<2000	800	5059	72%
Tachiatash	UZB	Gas	<2000	730	2753	43%
Fergana	UZB	Oil	<2000	420	590	16%
Angren	UZB	Coal	<2000	484	527	12%
Kyzylorda	KAZ	Gas	<2000	113	*693*	*70%*
Shurob_I	TAD	Coal	2018	300	*1214*	*70%*
Shurob_II	TAD	Coal	2020	300	*1840*	*70%*
Duschanbe_I	TAD	Gas/Oil	<2000	198	*1840*	*70%*
Duschanbe_II	TAD	Coal	2013	260	*1594*	*70%*
Fon Yaghnob I TPP	TAD	Coal	2020	500	*3066*	*70%*

2.4.4.2 Water withdrawal factor

Thermoelectric power plants boil water to create steam, which then spins turbines to generate electricity. Once steam has passed through a turbine, it must be cooled back into water before it can be reused to produce more electricity. Colder water cools the steam more effectively and allows more efficient electricity generation.

Thermoelectric plants take water from nearby sources (e.g., rivers, lakes, aquifers), circulate it through pipes to absorb heat from the steam in systems called condensers, and discharge the warmer water to the local source. These are called “once-through systems” which were initially the most popular because of their simplicity, low cost, and the possibility of siting power plants in places with abundant supplies of cooling water. As in other regions, these types of systems are common for the older power plants in Central Asia that have not been rehabilitated or modernized. New power plants tend to use a system in which cooling water is used in second cycle, so-called wet-recirculating or closed-loop systems. These systems have lower water withdrawals than once-through systems, but tend to have appreciably higher water consumption. Nevertheless, this water consumption tends to be very small compared to other consumptive use in a basin.

Data on cooling water needs is sparse in Central Asia. The Central Asia WaterInfo database has some data previous to 2000, but only on state level. This does not allow making reasonable assumptions on the extractions on plant-level. Fortunately, actual water extractions are almost a direct function of the actual generated power. This makes power generation a useful proxy to derive cooling water extractions from water system.

Another difficulty is to know the precise source of water. Given the strategic nature of power plants, a reliable source of water is needed so diversions are generally built from the main stem of the river, and not from smaller tributaries. Also aquifers may be a reliable source of water, but no data in Central Asia exists (as far as the consultant is aware of) on the source of the cooling water extractions for each plant.

For this study, the following assumptions were found reasonable, given the lack of data:

- Cooling water extractions are directly related with the actual power produced
- It was assumed that most of the TPPs are already or will be in the near future equipped with installations that reduce water withdrawals, including cooling towers or similar.
- Given the previous, a water withdrawal factor of 4500 m3/GWh was used [*Macknick et al.*, 2012]. It was assumed that 70% of the water withdrawal is consumed, and the rest returns to its source as returnflow [*Macknick et al.*, 2012].
- For most of the reservoirs included in the model it can be reasonably assumed that water is diverted from the nearby main stem of the Amu Darya or Syr Darya. For three of TPPs, this assumption does not hold: Talimardjan , Fergana and Shurob. These TPPs are located very much upstream of the main branches, and may either extract water from groundwater or from a smaller stream segment which is beyond the scale of the WEAP model.
- Based on the output of the hydrological model it was estimated that on average the ratio between the minimum monthly streamflow and the average monthly streamflow is 78%.

2.4.4.3 Power generation

Figure 2-20 shows annual power generation of several plants in the region. The average power production levels are also shown in Table 2-6. These annual values were obtained from the ADB Power Sector Regional Master Plan [*ADB*, 2012].

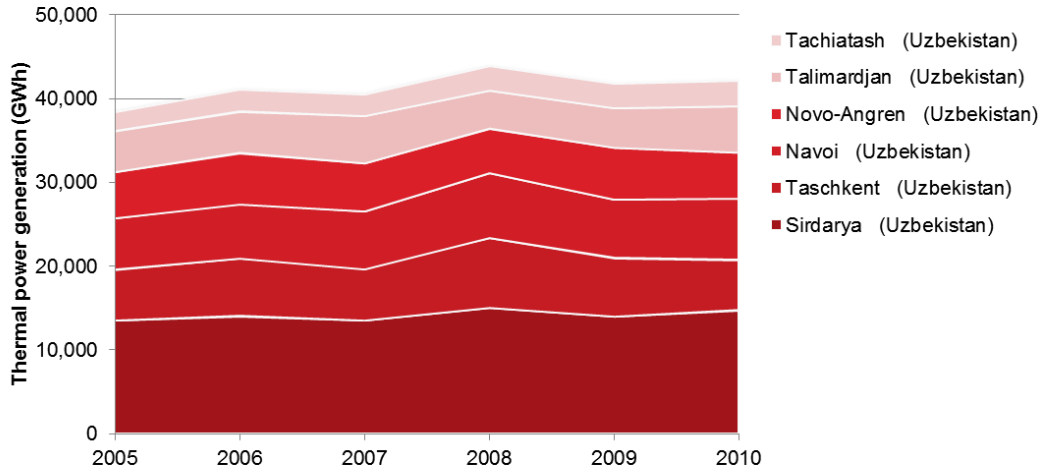

Figure 2-20: Annual thermal power generation 2005-2010 for several TPPs within the basins. Source: [*ADB*, 2012]**.**

Few data are available on *monthly* demand and electricity generation. For this study, data from [*World Bank*, 2012] were used on electricity demand and generation for Tajikistan, 2005-2010. The share of each month of the total annual demand was assumed to be representative for the region and for other years.

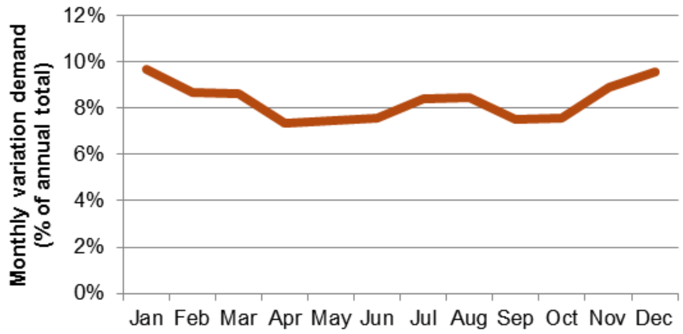

Figure 2-21. Relative monthly energy demand for Tajikistan (source [*World Bank*, 2012]**)**

2.4.5 Agriculture

Data on agricultural land use at the province level was taken from the online Central Asian Waterinfo portal.[1] for the five countries in the Amu Darya and Syr Darya river basins (Uzbekistan, Kazakhstan, Tadzhikistan, Kyrgyzstan and Turkmenistan). No data is available in the database for Afghanistan. These data, combined with FAOSTAT data on production and irrigated areas was used to define agricultural demand sites in WEAP. Table 2-7 shows the translation of provinces to demand sites as used in the model.

Table 2-7: Division of provinces over WEAP demand sites.

Demand site in WEAP	Provinces	
Dushanbe	Rayons of republican subordination (TJK)	
Fergana Valley	Andijan (UZB)	Jalalabad (KGZ)
	Namangan (UZB)	Osh (KGZ)
	Fergana (UZB)	

[1] www.cawater-info.net

Karakum desert	Mary (TKM)	
	Akhal (TKM)	
Kashkhadarya upstream	20% of Kashkhadarya (UZB)	
Kashkhadarya downstream	80% of Kashkhadarya (UZB)	
Kurgantube	80% of Khatlon (TJK)	
Kulyab	20% of Khatlon (TJK)	
Kzylorda	Kzylorda (KAZ)	
Lebap	Lebap (TKM)	
South Kazakhstan	South Kazakhstan (KAZ)	
Surkhandarya upstream	40% of Surkhandarya	
Surkhandaraya downstream	60% of Surkhandarya	
Syrdarya, Tashkent, Jizakh	Jizakh (UZB)	Tashkent (UZB)
	Syrdarya (UZB)	20% of Sughd (TJK)
Urgenc, Nukus, Aral Sea	Khorezm (UZB)	
	Karakalpakistan (UZB)	
	Dashoguz (TKM)	
Zeravshan Valley	Bukhara (UZB)	
	Navoiy (UZB)	
	Samarkand (UZB)	

In several agricultural demand nodes, reservoirs regulate and store water for irrigation. In some areas there are multiple smaller reservoirs, while also some bigger reservoirs exist in the region. The smaller reservoirs were aggregated to one single reservoir node in WEAP. Table 2-3 shows the characteristics of the irrigation reservoir nodes included in ARAL-WEAP2014.

Table 2-8: Irrigation reservoirs and their capacities included in WEAP-ARAL2014

Country	Reservoir	Full storage capacity (MCM)	Dead storage (MCM)	Basin
TUR	Turkmenistan reservoirs	4200	800	Amu Darya
UZB	Chimkurgan	500	50	Amu Darya
UZB	Pachkamar	260	10	Amu Darya
UZB	Surkhandarya	800	100	Amu Darya
UZB	Zaamin	51	21	Syr Darya
UZB	Fergana Valley reservoirs	1155	10	Syr Darya

The WEAP-ARAL2014 model assumes that domestic demand has always a higher priority than agricultural demand. Therefore, if not enough water is available in a certain river segment for domestic and agricultural demand, all unmet demand will go to the agricultural node in that particular river segment.

2.5 Modelling dimensions and scenarios

The upstream hydrological SPHY model and downstream WEAP model was set up for the future period 2001-2100, of which the first 10 years are the reference baseline years. The principal periods of interest for this study are:

- 2030s, from 2020-2039
- 2050s, from 2040-2059

Please note however that all model input is prepared till year 2100, so other periods could be studied if desired.

The climate scenarios analyzed are the four marker scenarios previously described. For consistency with a parallel study carried out by the World Bank [*Alford et al.*, 2014], an additional climate scenario was added that assumes a higher runoff at the headwaters of the Panj and Vakhsh rivers. This scenario re-scales the baseline flows for these two rivers with a multiplier, constant over time. The multipliers used are 1.11 for the Vaksh and 1.45 for the Panj river. For the other watersheds the Warm/wet flows were used as predicted by the SPHY model.

Also a “no climate change” scenario was analyzed, based on the same randomized trajectory of the climate change scenarios. The future trajectory was built randomizing the reference period uniformly on a yearly basis to a future series, where each year must be different than the previous four years.

So summarizing, the following climate change scenarios are analyzed:

1. No climate change
2. Hot/Dry: the most extreme climate scenario for water availability
3. Arid, with low precipitation but a more moderate temperature increase than the Hot/Dry.
4. Central, reflecting a small increase in precipitation and a temperature increase.
5. Warm/wet, which reflects a modest temperature increase but a large precipitation increase
6. Warm/wet+, based on warm/wet but including the increased runoff estimates for the Panj and Vaksh river of the parallel WB study

In terms of new infrastructure, the following scenarios were simulated in WEAP (for details on the properties of the simulated infrastructure see previous sections on hydropower and thermal facilities):

1. No new infrastructure (“CurrentInfrastructure”)
2. Partial Buildout, with
    - Planned thermal power plants:
        1. Shurob I – from 2018
        2. Shurob II – from 2020
        3. Fon Yaghnob – from 2020
    - New Run-of-river power facilities upstream
        1. RoR upstream Rogun – from 2025
        2. Upper Naryn RoR – from 2025
    - Refurbishment for all hydropower facilities, of 5% gradual increase from 2020-2025
3. Full Buildout, with same as Partial Buildout, and
    - Rogun gradually to be built from 2020 onwards
    - Kambarata-I - from 2025
    - Kambarata-II extension (RoR) – from 2025

2.6 Modelling performance

The total annual power simulated over the reference period 2001-2010 was compared with the data available on power production of several of the major hydropower facilities (source: [*ADB*, 2012]). Figure 2-22 compares the average annual power production that was simulated for these facilities compared with the actually produced ("observed") power for the reference period. As can be seen, the WEAP model simulates very similar production levels as actually produced.

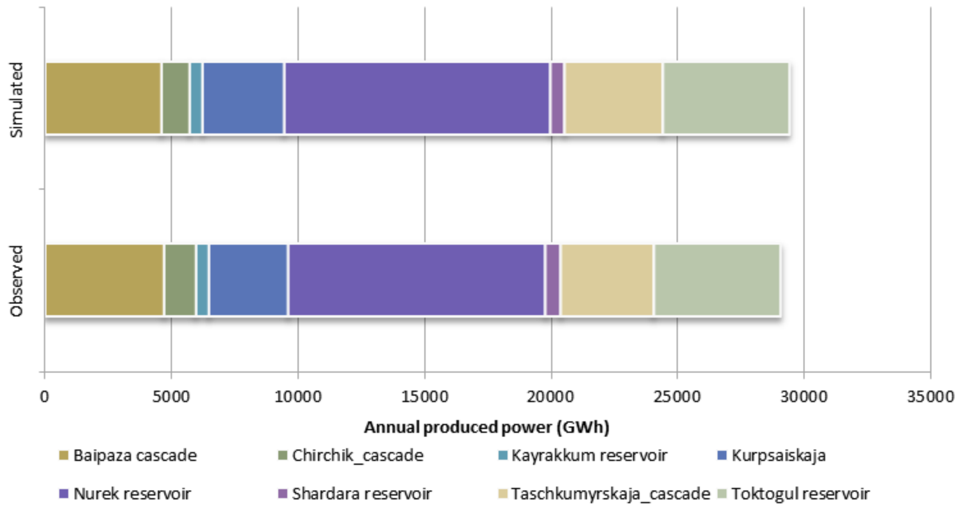

Figure 2-22. Produced versus simulated annual power production for the main reservoirs

Figure 2-23 is based on the same data but represented in the form of a scatterplot, indicating also the annual variability in power production (error bars based on the standard deviation of the annual series). Generally, the variability in simulated production levels are very much in the same range as actually produced power. This gives confidence in the model that it is able to mimic reasonably well the annual variability in production, mainly a function of water availability.

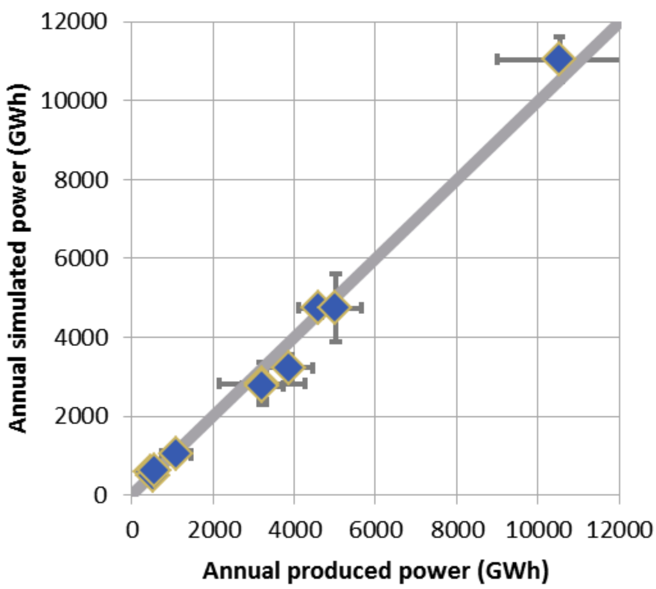

Figure 2-23. Scatterplot of produced versus simulated annual power production (GWh).

No data on monthly power production of the hydropower facilities is available. However, monthly data is available of the releases of most of the reservoirs (CAWATER database), being a good indicator of production levels. Figure 2-24 shows the average monthly release for several reservoirs. As can be seen in this figure, for these reservoirs the monthly pattern is quite similar between simulated and observed releases. The R^2 are ranging between 0.62 and 0.99 for these main reservoirs. This gives an indication that WEAP adequately mimics the outflow regime and operational rules in the current situation.

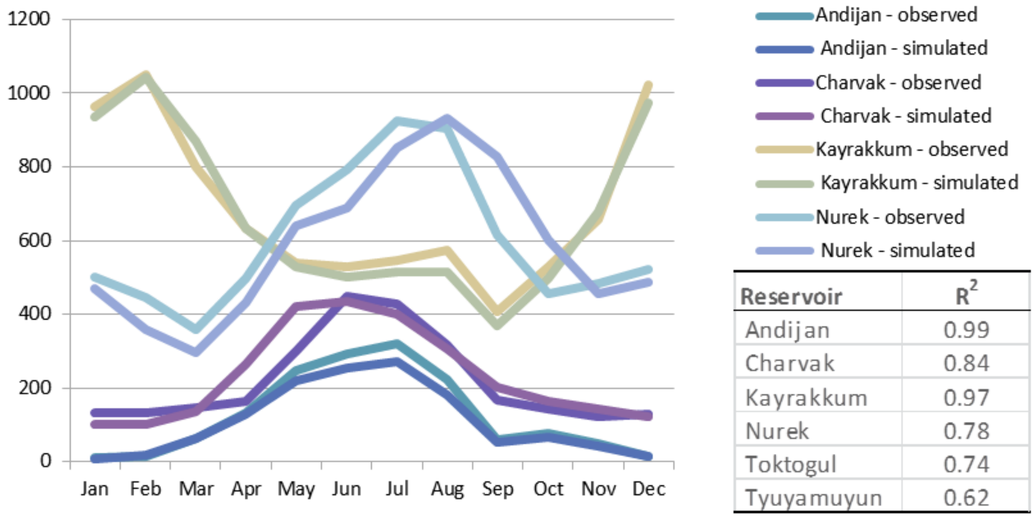

Reservoir	R^2
Andijan	0.99
Charvak	0.84
Kayrakkum	0.97
Nurek	0.78
Toktogul	0.74
Tyuyamuyun	0.62

Figure 2-24. Comparison of observed against simulated monthly reservoir releases

3 Results

Model outcomes are shown in the 1st section for the baseline (current climate) scenario, 2nd section under climate change with current infrastructure, and 3rd section with climate change and planned infrastructure. The following outcomes are shown in each of these sections:

1. Hydrology: inflow at several key reservoirs
2. Reservoir levels at the same reservoirs
3. Interannual variability of estimated hydropower production
4. Water supplied an unmet demand for key agricultural areas
5. River streamflow versus diverted flow for thermal electric plant cooling water

3.1 Baseline scenario

3.1.1 Hydrology

The upstream hydrological model SPHY, described in the methodological section, provides daily streamflow for all the upstream catchments that were discretized in the upstream modelling domain. Figure 3-1 and Figure 3-2 show the monthly variability in streamflow of some of the main catchments flowing into reservoirs, based on daily simulated flows over the 10-year period. As can be seen, maximum flows in the Syr Darya occur during May to July, while in the more glacierized Amu Darya basin, maximum flows are more delayed and occur in August and September. Also, note the extremely large differences between winter and summer streamflow.

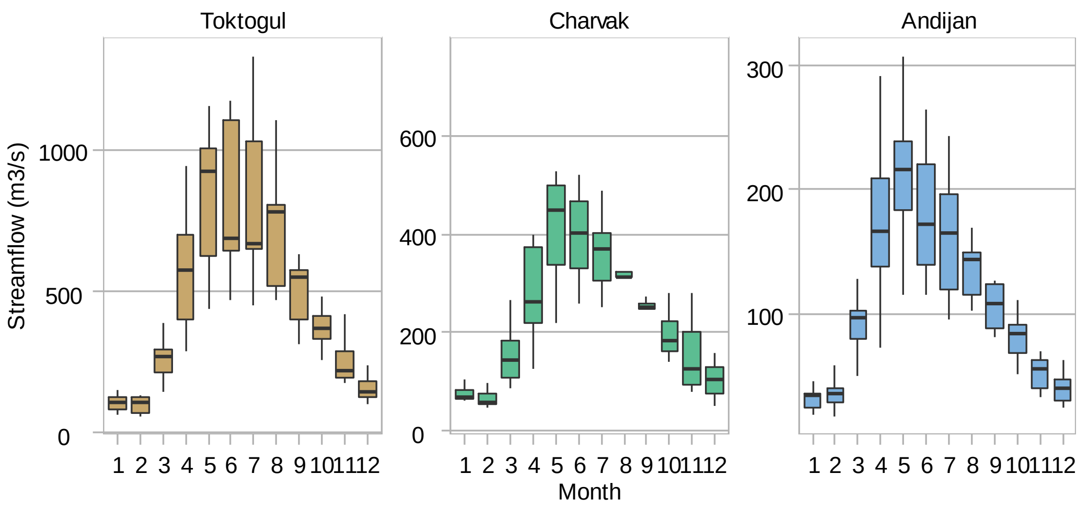

Figure 3-1. Monthly variability during the baseline period (2001-2010) of inflow of three main reservoirs in the Syr Darya basin

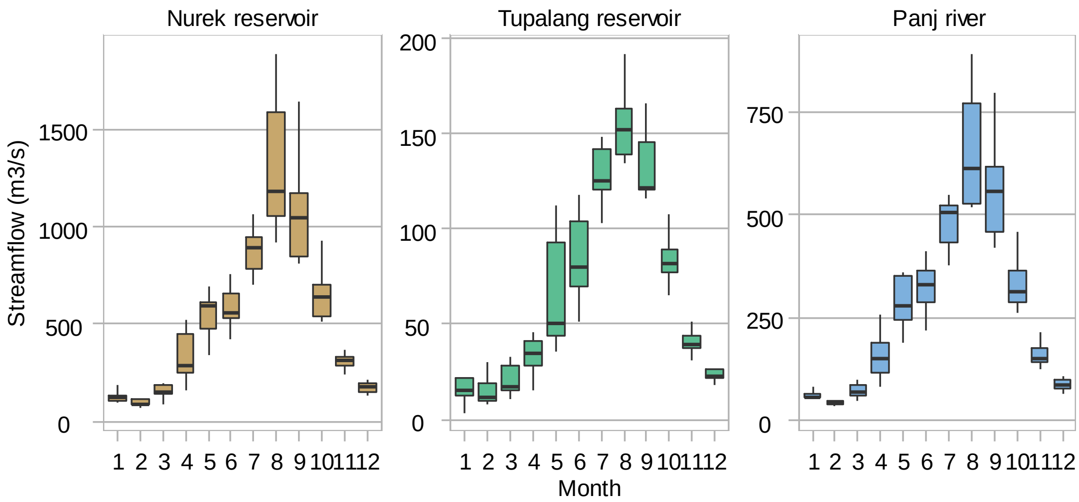

Figure 3-2. Monthly variability during the baseline period (2001-2010) of inflow of two reservoirs and the Panj river in the Amu Darya basin

3.1.2 Reservoir levels

Figure 3-3 shows the monthly variability in storage volume under the current climate, for the Nurek and Toktogul reservoirs. Nurek generally fills in September and October, while Toktogul fills earlier in summer.

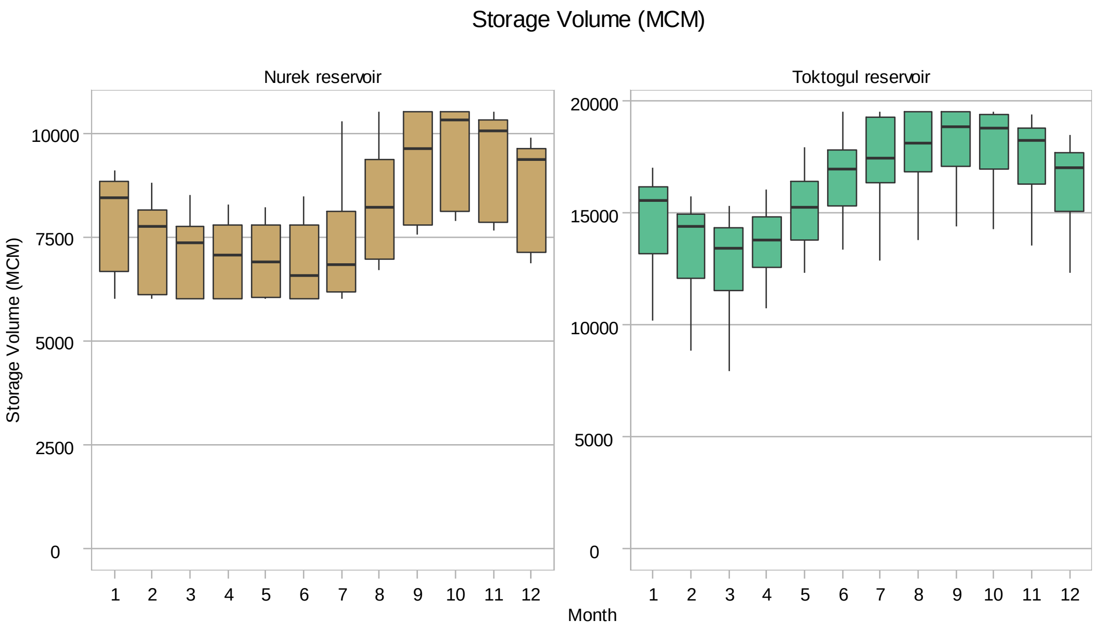

Figure 3-3. Monthly variability of storage volume in Nurek and Toktogul reservoirs under the current climate

The Andijan and Kayrakkum reservoirs demonstrated in Figure 3-3 are regulated principally for irrigation and have therefor maximum storage in winter and spring while lowest levels are seen in the summer period when irrigation demand is highest.

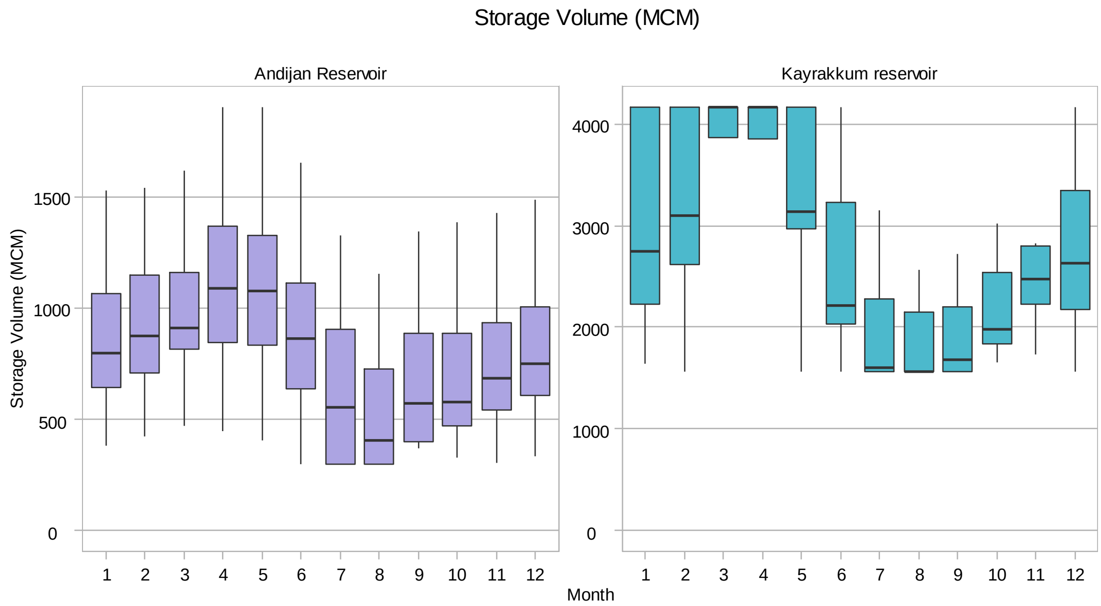

Figure 3-4. Monthly variability of storage volume in Andijan and Kayrakkum reservoirs under the current climate

For the other reservoirs in the region, the variability in storage for the baseline period can be observed from the figures included in Appendix III.1 (Reservoir storage variability with current infrastructure).

3.1.3 Hydropower production

Hydropower generation under the current climate is already quite variable, as water availability is highly variable over the years for some of the reservoirs. Table 3-1 shows the variability in annual hydropower production, as was simulated by the WEAP-ARAL2014 model under the current climate. The coefficient of variation (defined as the standard deviation divided by the mean) ranges between 4% and 35%, indicating considerable variability for some of the reservoirs under the current climate. Under climate change this variability is likely to increase as shown in the following sections.

Table 3-1. Hydropower generation for the main hydropower facilities in the region as simulated by WEAP-ARAL2014 under the current climate (GWh/year)

Reservoir	Mean	Standard deviation	Coefficient of variation
Andijan Reservoir	316	112	35%
Baipaza cascade	4684	525	11%
Charvak reservoir	3013	423	14%
Chirchik_cascade	1135	71	6%
Farkhad reservoir	574	67	12%
Kambarata_II	527	113	22%
Kayrakkum reservoir	485	46	10%
Kurpsaiskaja	2639	351	13%
Nurek reservoir	11002	1581	14%
Shardara reservoir	621	34	6%

Taschkumyrskaja_cascade	3082	398	13%
Toktogul reservoir	4595	552	12%
Tyuyamuyun reservoir	1009	36	4%
All Reservoirs	33847	2688	8%

3.1.4 Agriculture

The ARAL-WEAP model simulates the agricultural water demand and supplied water depending on the availability and allocation priorities. Figure 3-5 shows the variability in annual water demand of all the agricultural areas in the Syr Darya and Amu Darya basin, under the current climate. Figure 3-6 shows the same for the water supplied to these areas.

These figures show that under the current climate, the agricultural areas already deal with considerable variability in demand and supply. For some areas the ratio between minimum and maximum supply can be around 65%.

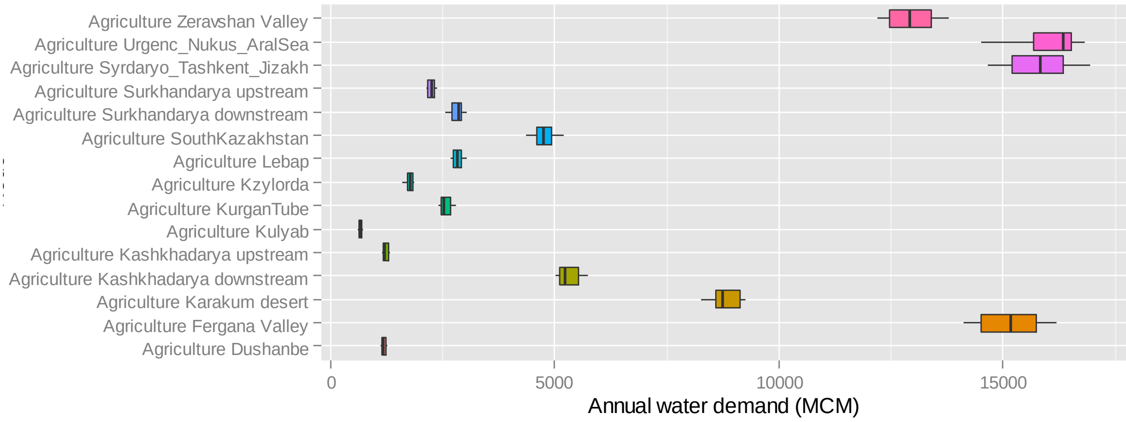

Figure 3-5. Annual variability in water demand of agricultural areas as simulated by WEAP-ARAL2014 under the current climate

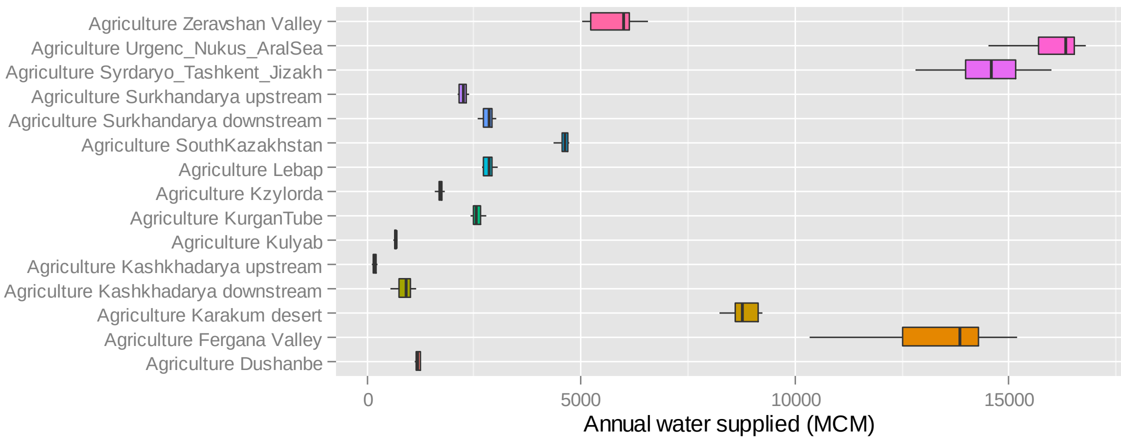

Figure 3-6. Annual variability in water supplied to agricultural areas as simulated by WEAP-ARAL2014 under the current climate

3.1.5 Thermal power plant cooling water

Based on data shown in the methodological section in Table 2-6, WEAP-ARAL2014 calculates the required abstractions for cooling of the thermal plants, shown in Figure 3-7. Also the consumed fraction (70% of abstracted, see methodological section) is visualized. These estimates are based on the actually produced power production based on data 2000-2010. For the future plants, this data was based on the projected capacity and the assumption that on average the plant runs on 70% of its full capacity. Table 3-2 shows the same data for abstraction but in m^3/s.

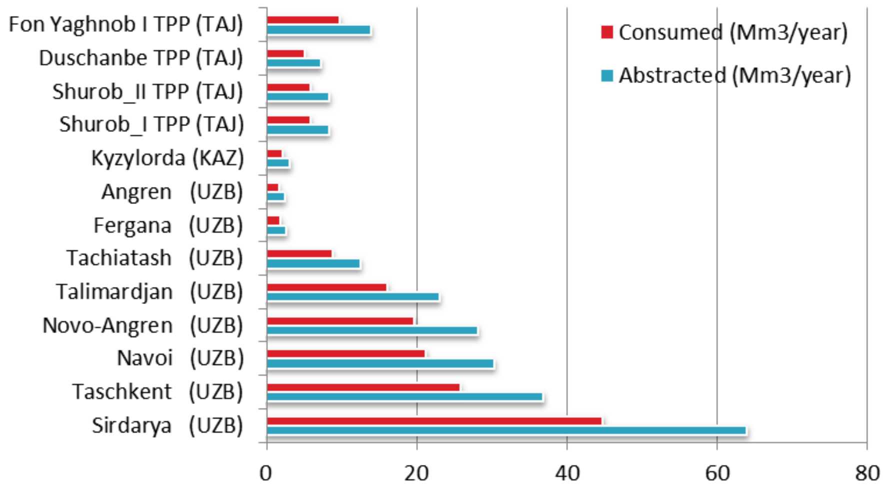

Figure 3-7. Annual water abstracted from the river and consumed for thermal power plants in the region

Table 3-2. Annual water abstracted for thermal power plant cooling in the region

TPP	Average water withdrawal (m3/s)	TPP	Average water withdrawal (m3/s)
Angren TPP	0.08	Shurob_I TPP	0.27
Dushanbe TPP	0.23	Shurob_II TPP	0.27
Fergana TPP	0.09	Sydarya TPP	2.03
Fon Yaghnob_I TPP	0.44	Tachiatash TPP	0.40
Kyzylorda TPP	0.10	Talimardjan TPP	0.73
Navoi TPP	0.96	Taschkent TPP	1.17
Novo_Angren TPP	0.89		

3.2 Climate change impacts with current infrastructure

This section summarizes the climate change impact analysis, without changes in infrastructure. It shows results on hydrology, reservoir levels, hydropower production, agriculture and thermal power cooling water.

3.2.1 Hydrology

The hydrological SPHY model was used to simulate the dynamics under the four climate change marker scenarios described earlier.

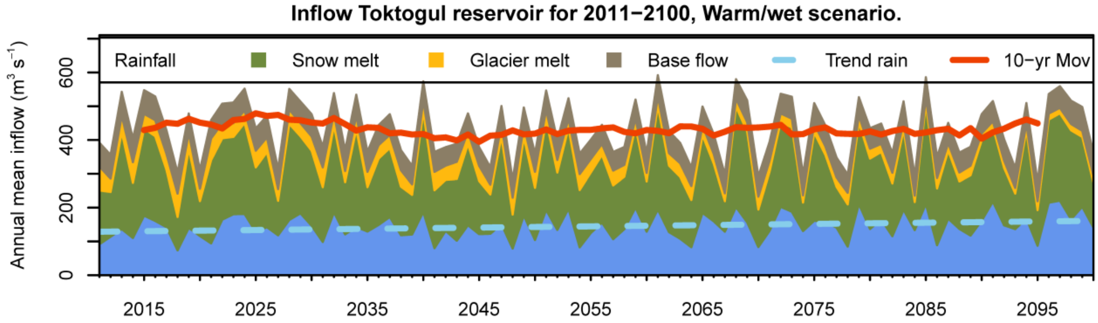

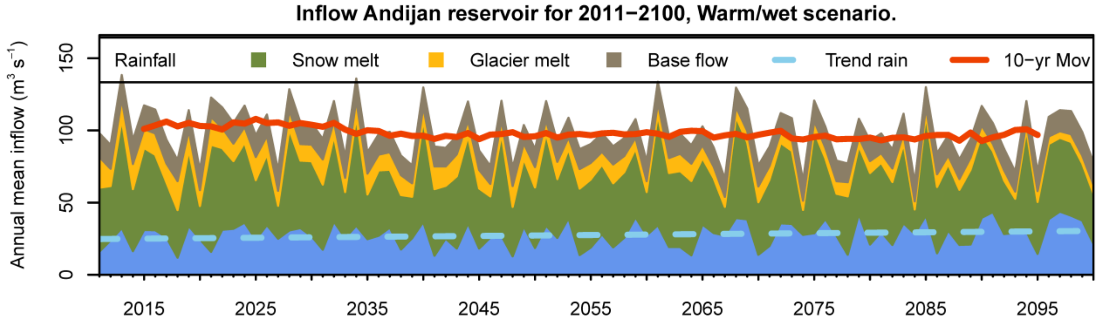

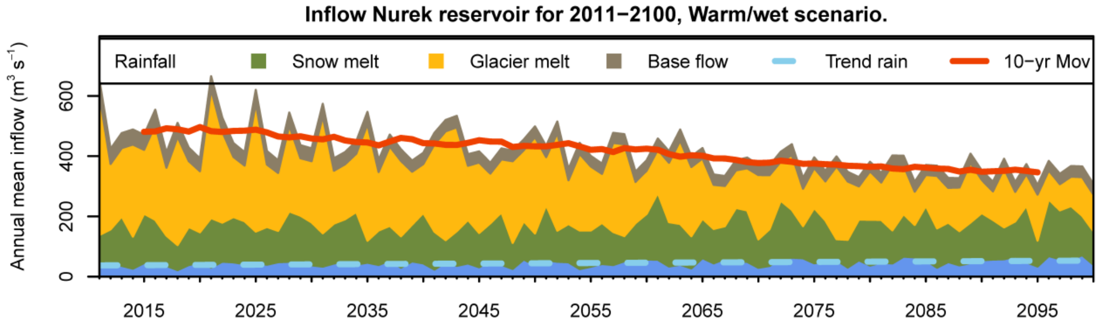

Figure 3-9 and Figure 3-8 show how for three of the in total 27 catchments included in the analysis the annual mean streamflow under the Warm/wet and the Arid marker scenario (for the other scenarios, see Appendix II).

The blue dashed line in the figures shows the trend in the streamflow component that is coming from direct rainfall. Under the warm/wet scenario this trend is positive because of two reasons: firstly because of the small projected increase in total precipitation, and secondly due to higher temperatures that cause more precipitation to fall as rainfall instead of snow. The complex interaction between precipitation and temperature changes in high mountain environments leads to sometimes contradictory outcomes: reductions in precipitation but increase in temperature may lead higher streamflow due to melting glaciers. Also the change from rainfall to snowfall can cause significant changes in the seasonality of the streamflow.

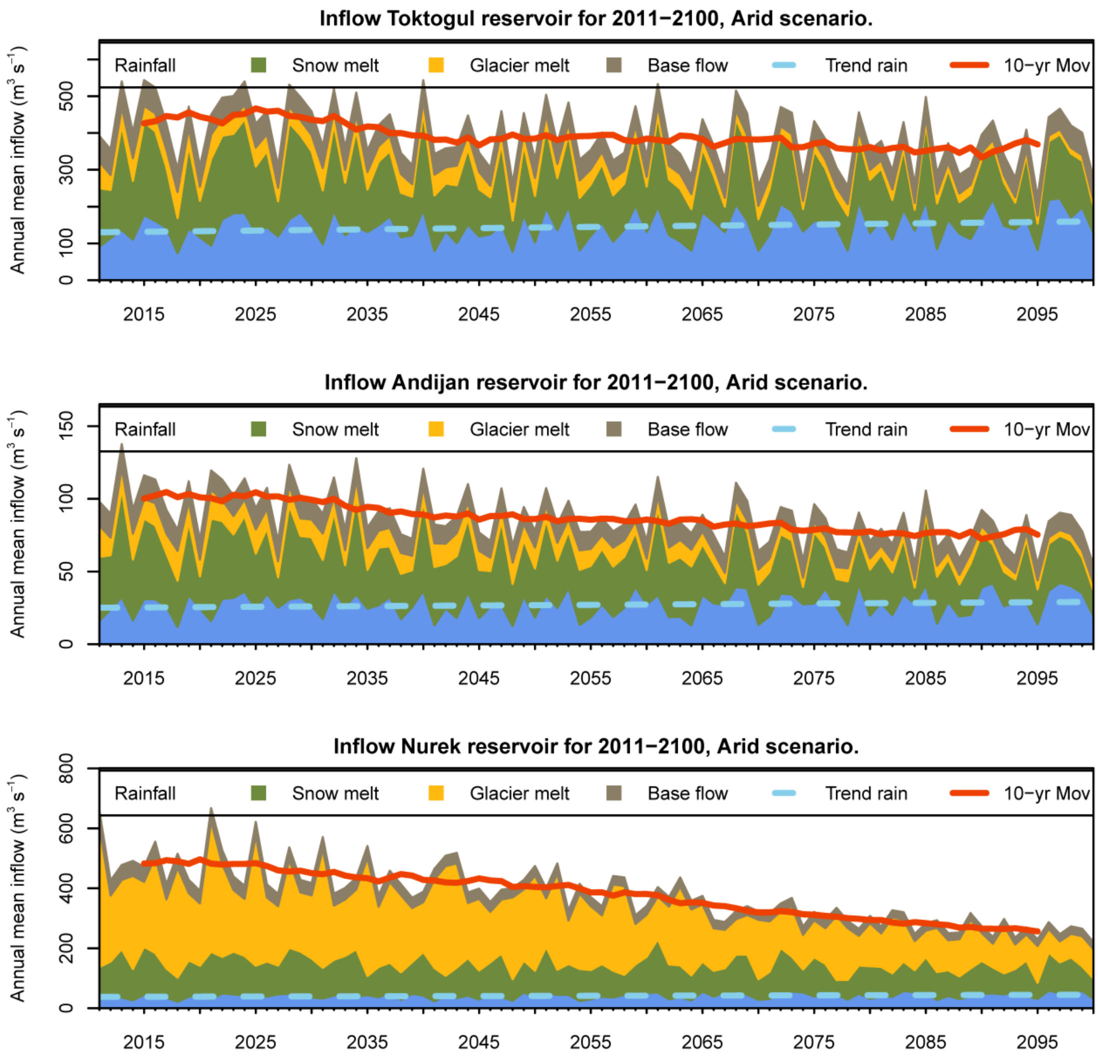

Figure 3-8. Future annual streamflow and its partitioning for the Nurek, Toktogul and Andijan reservoir under the Arid marker scenario

The figures show also the 10-year moving average of the total streamflow. For the warm/wet scenario, no clear trend can be observed for the Toktogul reservoir, while a clear downward trend happens under the Arid scenario. For the Nurek reservoir, a downward trend is observed for all the marker scenarios, especially after 2030, except for the Warm/wet+ scenario. This scenario was included for consistency with a parallel study of the World Bank and projects an increase for Nurek inflow and in the Panj river (see Section 2.5).

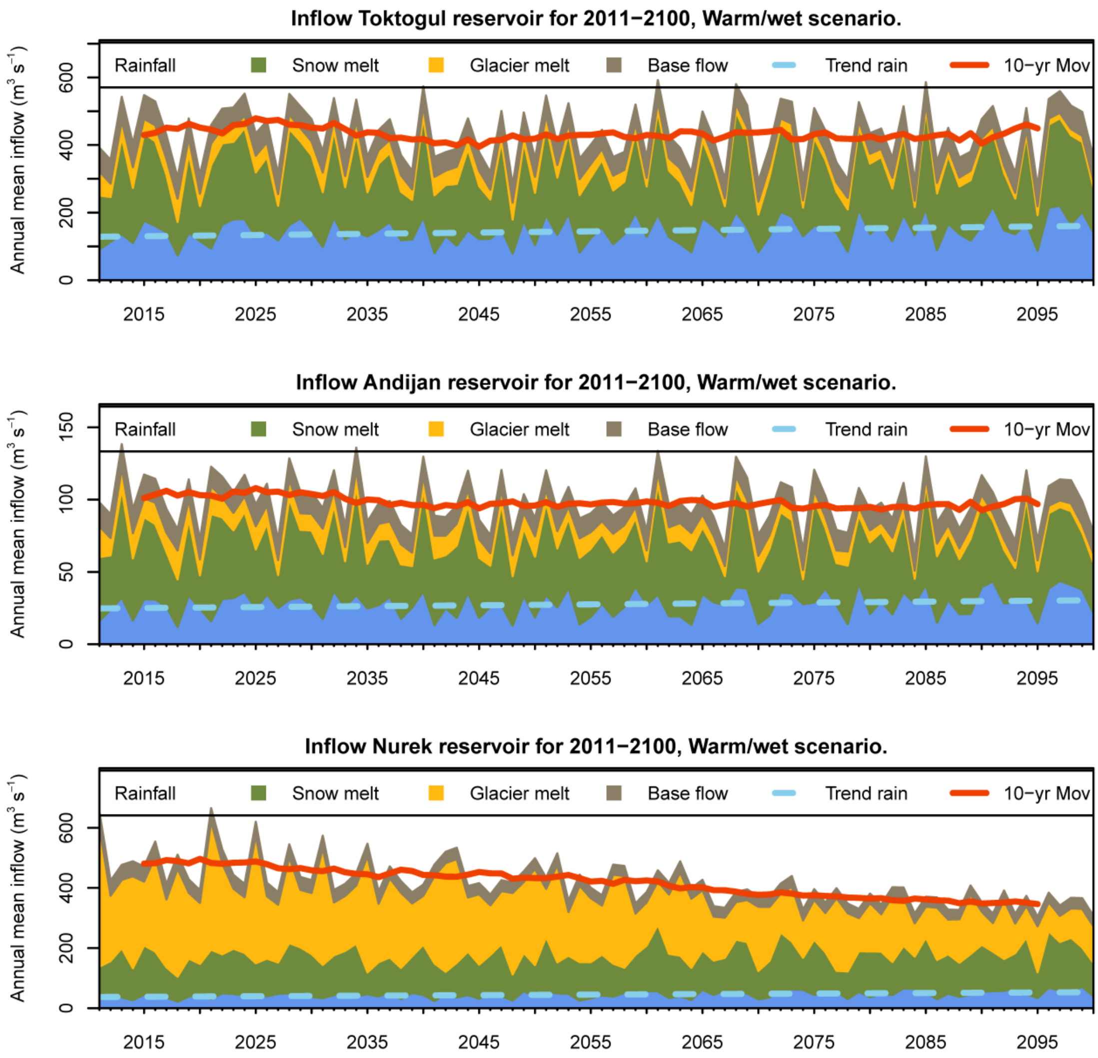

Figure 3-9. Future annual streamflow and its partitioning for the Nurek, Toktogul and Andijan reservoir under the Warm/wet marker scenario

Also the monthly flow regime is affected by climate change as is shown in Figure 3-10 and Figure 3-11 for the Nurek and Toktogul reservoirs. The range of future projections indicate that the high flow season is flattened out for the Nurek reservoir, so August and September will have comparable flows as in July. For the Toktogul reservoir, climate projections predict just a small decrease in flows in general for all seasons.

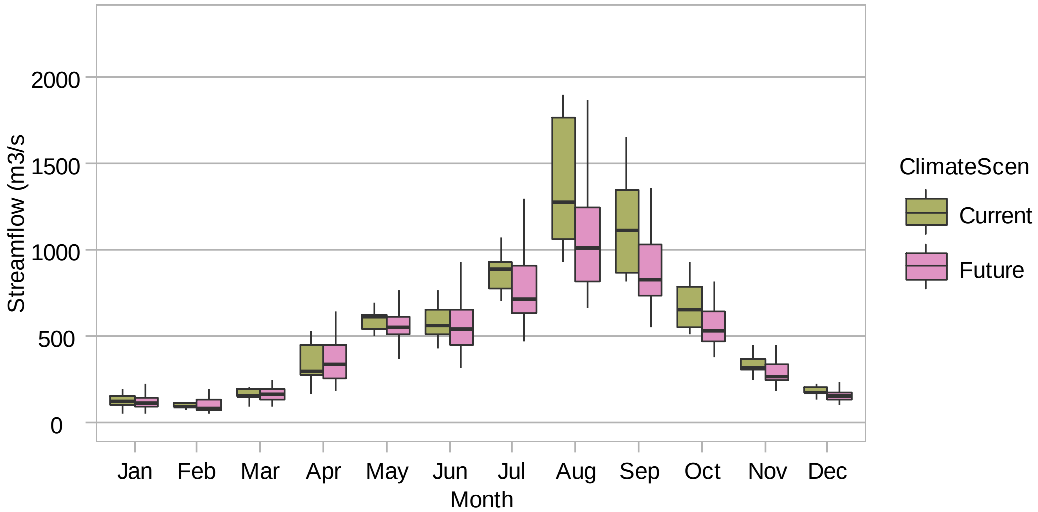

Figure 3-10. Monthly inflow for the Nurek reservoir under the current climate and the range of future climate change marker scenarios (including the fifth marker scenario)

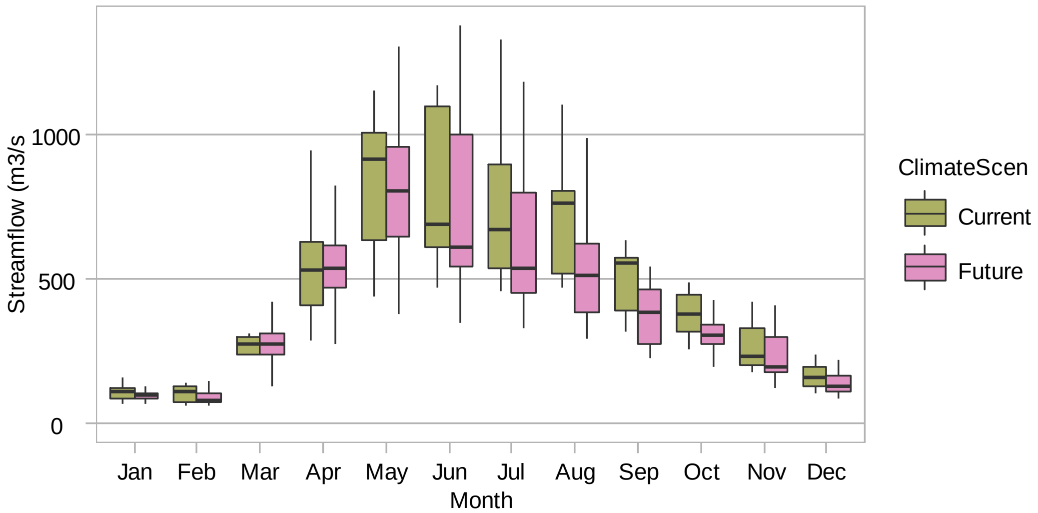

Figure 3-11. Monthly inflow for the Toktogul reservoir under the current climate and the entire range of future climate change marker scenarios

3.2.2 Reservoir levels

The reservoir storage dynamics were simulated using ARAL-WEAP2014 under the different climate change marker scenarios. Figure 3-12 to Figure 3-14 show the monthly variability of reservoir storage over two future periods (2030s and 2050s) of the Nurek, Toktogul and Andijan reservoir and for all climate change scenarios (including current climate “1Current”).

Results suggest that especially the Nurek reservoir will be highly affected. Only the additional 5th marker scenario deviates from the overall pattern and shows an increase in storage for this reservoir for both periods. Impacts for Toktogul are less severe. For Andijan the reservoir storage is clearly much more often close to minimum capacity putting at risk its combined use for hydropower and irrigation.

For the other reservoirs, impacts are shown in Appendix III.1.

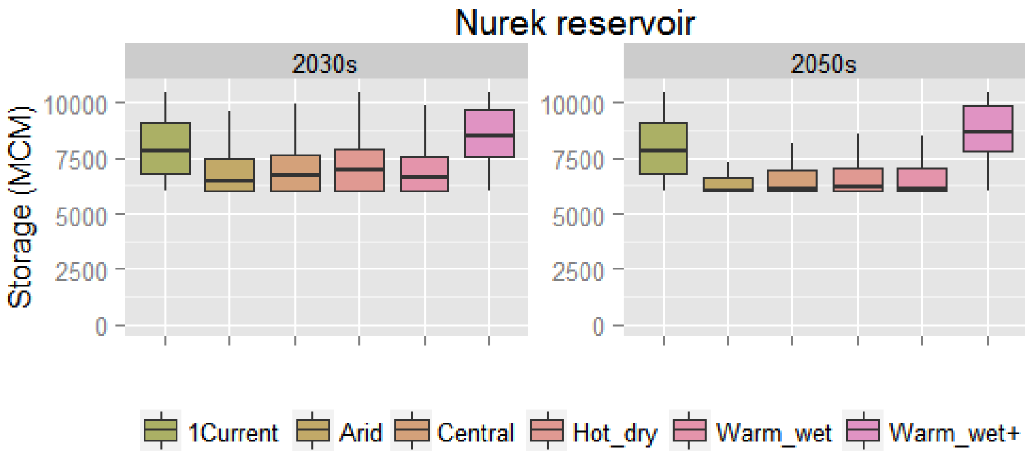

Figure 3-12. Reservoir storage variability of Nurek reservoir under climate change

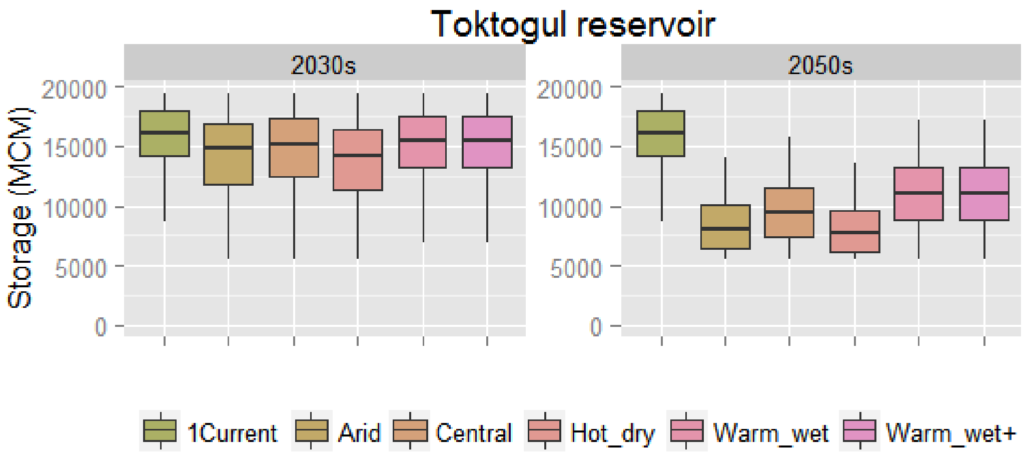

Figure 3-13. Reservoir storage variability of Toktogul reservoir under climate change

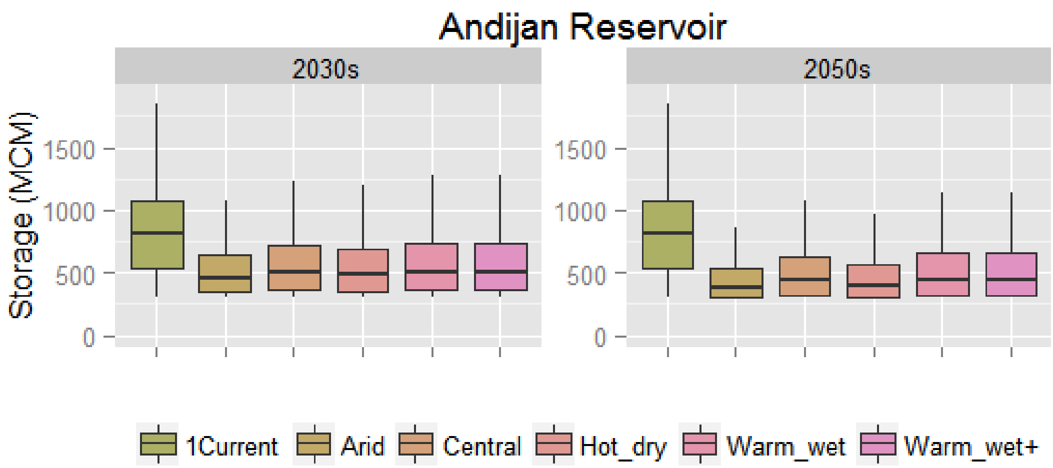

Figure 3-14. Reservoir storage variability of Andijan reservoir under climate change

3.2.3 Hydropower production

The ARAL-WEAP2014 model was used to simulate hydropower production, taking into account the installed power generating capacities, water inflows and simulated storage levels. Figure 3-15 shows the total power produced for all hydropower facilities that were simulated in the Amu Darya and Syr Darya basin, under different climate change scenarios, including the current climate (“1Current”).

Nurek (Figure 3-16) is one of the facilities highly affected by climate change as the principal four marker scenarios show similar decreases, except for the Warm/wet+ scenario. Impacts on Toktogul (Figure 3-17) are less severe in the 2030s, but will be likely seriously felt in the 2050s where in the most extreme scenario a reduction of more than 30% is projected.

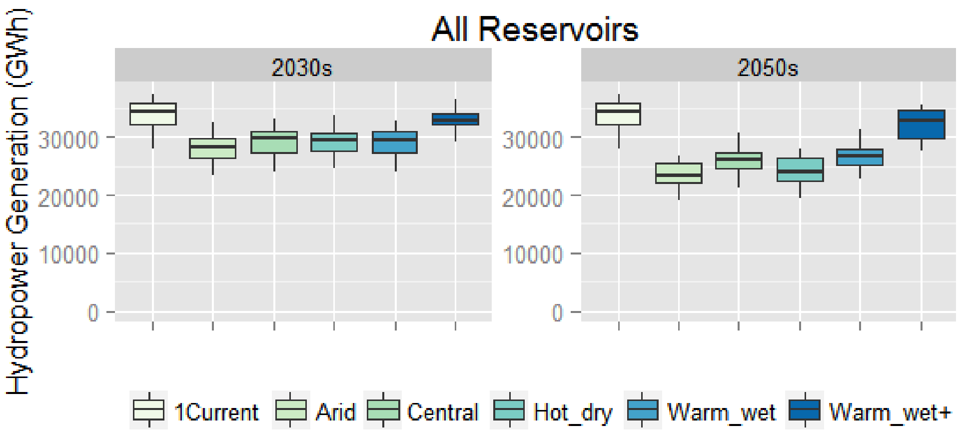

Figure 3-15. Annual hydropower production for all hydropower facilities installed in the Amu Darya and Syr Darya under different climate scenarios

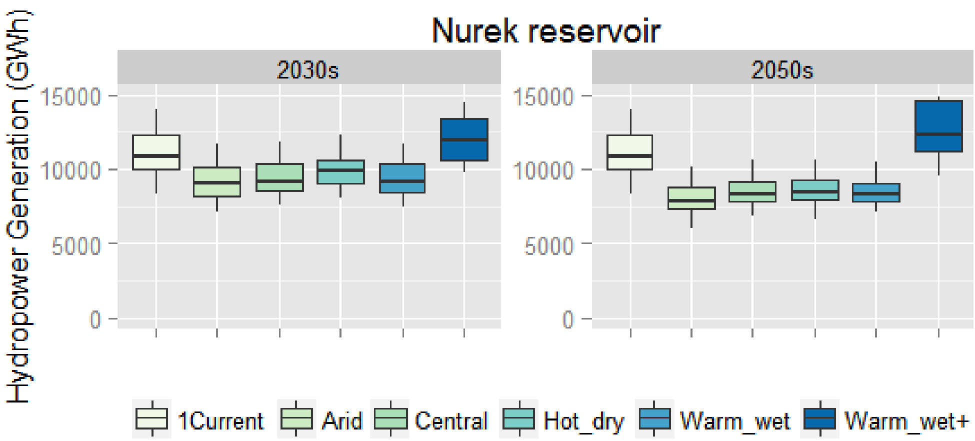

Figure 3-16. Annual variability of hydropower generation for the Nurek reservoir under the different climate change scenarios

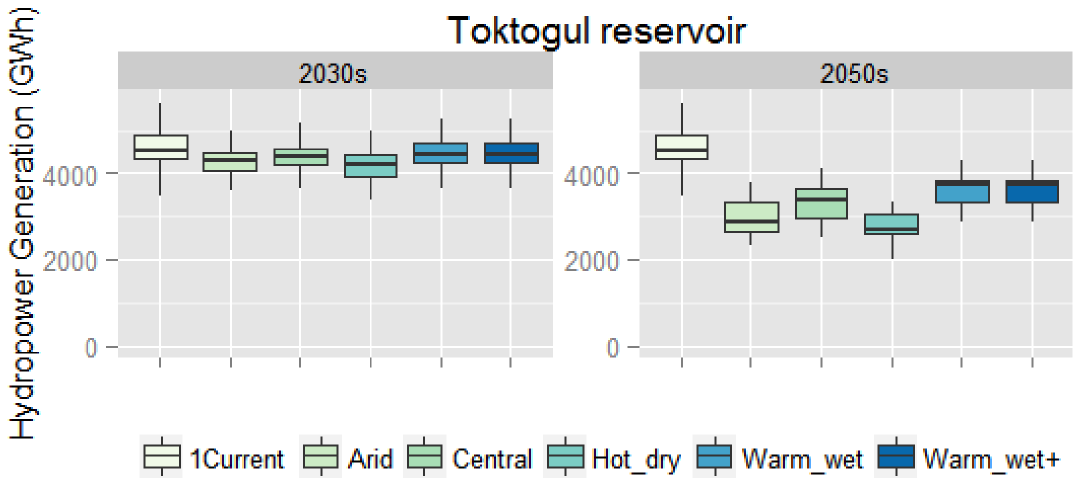

Figure 3-17. Annual variability of hydropower generation for the Toktogul reservoir under the different climate change scenarios

Table 3-3 shows for the 2050s how the production levels are predicted to be affected by climate change for all reservoirs. As can be seen for the total production the reductions are estimated to be between -5% and -31%. For all scenarios reductions are observed for all reservoirs except for the Warm/wet+ scenario which assumes an increase in flow in the Vaksh river benefiting Nurek and the Baipaza cascade. Clearly power production levels are seriously affected if no further investments are done.

Table 3-3. Current production (GWh) and percentual change under the different scenarios for all principal hydropower facilities in the 2050s

Reservoirs	1Current	Arid	Central	Hot_dry	Warm/ wet	Warm/ wet+
All Reservoirs	33847	-31%	-23%	-28%	-21%	-5%
Andijan Reservoir	316	-52%	-38%	-46%	-37%	-37%
Baipaza cascade	4684	-35%	-29%	-29%	-27%	4%
Charvak reservoir	3013	-29%	-13%	-27%	-16%	-16%
Chirchik_cascade	1135	-14%	-9%	-13%	-11%	-11%
Farkhad reservoir	574	-35%	-23%	-33%	-24%	-23%
Kambarata_II	527	-61%	-50%	-65%	-33%	-33%
Kayrakkum reservoir	485	-25%	-18%	-25%	-17%	-17%
Kurpsaiskaja	2639	-28%	-20%	-31%	-17%	-17%
Nurek reservoir	11002	-28%	-23%	-21%	-22%	13%
Shardara reservoir	621	-17%	-12%	-18%	-12%	-12%
Taschkumyrskaja_cascade	3082	-28%	-19%	-30%	-16%	-16%
Toktogul reservoir	4595	-35%	-28%	-39%	-21%	-21%
Tyuyamuyun reservoir	1009	-40%	-32%	-36%	-26%	-11%

3.2.4 Agriculture

Agricultural demand is affected under climate change (higher crop water requirements), while also the water availability and seasonality may change, affecting the water supply to agricultural areas. Figure 3-18 to Figure 3-20 show the water supply under future climate change (including the current climate) for three key agricultural areas in the Syr Darya and Amu Darya basin. For these areas, model simulations suggest that water supply will be reduced significantly under future climate change. Outcomes suggest that adaptation measures are necessary for downstream areas in order to copy with reduced water supply. For other areas similar patterns are predicted, as shown in Appendix V.1.

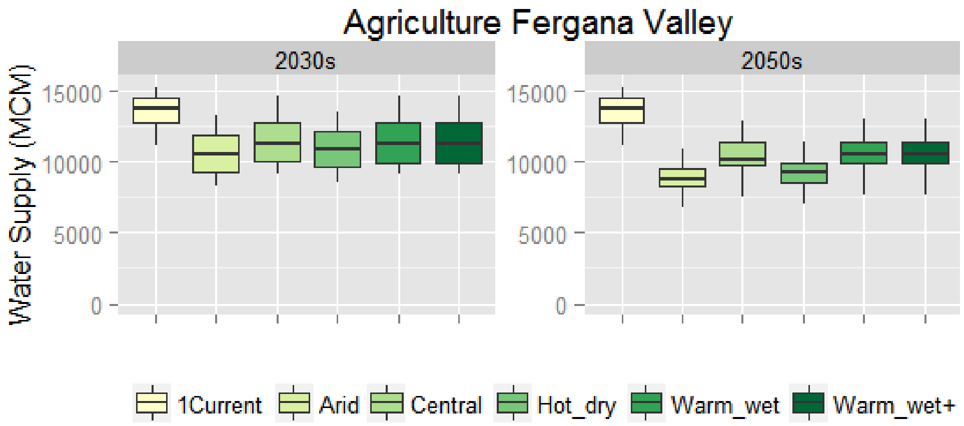

Figure 3-18. Annual variability of water supply to agriculture of Fergana Valley (UZB)

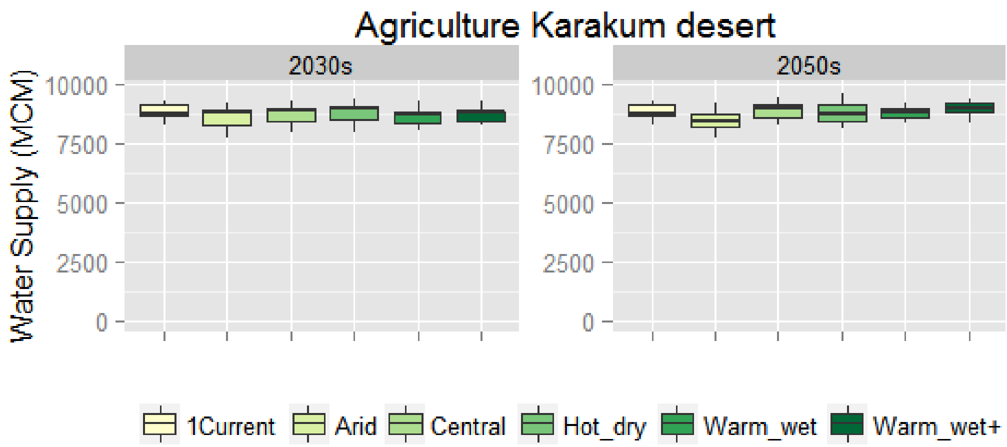

Figure 3-19. Annual variability of water supply to agriculture in Karakum desert (TUR).

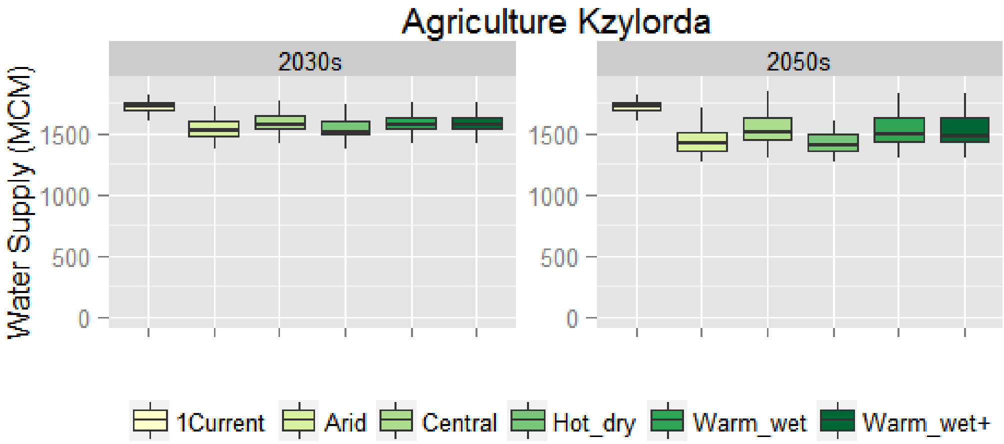

Figure 3-20. Annual variability of water supply to agriculture in Kzylorda (KAZ).

3.2.5 Thermal power plant cooling water

With limited data availability on thermal plant cooling water demands, cooling systems and plant types, WEAP was used to obtain a first-order assessment of cooling water supplies under future climate change. Abstractions from the river were simulated and compared with the streamflow over time. Even if sufficient streamflow is available, competing uses downstream (including environmental requirements) may seriously affect the availability of water for cooling. Therefore, for this assessment it was assumed that when more than 20% of the available water in the river needs to be abstracted, cooling water supply can be threatened.

Table 3-4 shows the outcomes for all TPPs, under the different climate scenarios. Results suggest that for most TPPs, no serious impacts can be expected, except for the Syr Darya TPP and to a lesser degree Tachiatash TPP. Please note that for this first-order assessment, it was assumed that all TPPs are equipped with cooling towers in the current or near-future situation. Cooling towers have a considerable lower water demand than the older once-through cooling system. Also, as commented in the methodological section, for the Talimardjan , Fergana and Shurob TPPs, these results need to be taken with caution, as the abstractions of these plants are most likely not directly related with the main river reaches but to tributaries that require a more detailed study.

Table 3-4. Percent of months in which more than 20% of streamflow is abstracted for cooling water of the thermal power plants

TPP	Current	Arid	Central	Hot_dry	Warm_wet
Angren TPP	0%	0%	0%	0%	0%
Dushanbe TPP	0%	0%	0%	0%	0%
*Fergana TPP**	0%	0%	0%	0%	0%
Fon Yaghnob_I TPP	0%	0%	0%	0%	0%
Kyzylorda TPP	0%	0%	0%	0%	0%
Navoi TPP	0%	0%	0%	0%	0%
Novo_Angren TPP	0%	0%	0%	0%	0%
*Shurob_I TPP**	0%	0%	0%	0%	0%
*Shurob_II TPP**	0%	0%	0%	0%	0%

Sydarya TPP	0%	11%	9%	10%	7%
Tachiatash TPP	0%	0%	0%	0%	0%
*Talimardjan TPP**	0%	0%	0%	0%	1%
Taschkent TPP	0%	0%	0%	0%	0%

** based on flow in main stem of river network*

Figure 3-21 shows the percent of months in which a certain flow level is exceeded. As can be seen, under several climate change scenarios, streamflow may be lower than 10 m3/s for around 10% of time. The SyrDarya TPP requires currently around 2 m3/s for cooling which means that under these conditions a considerable part of the river is abstracted and most of it (70%) consumed.

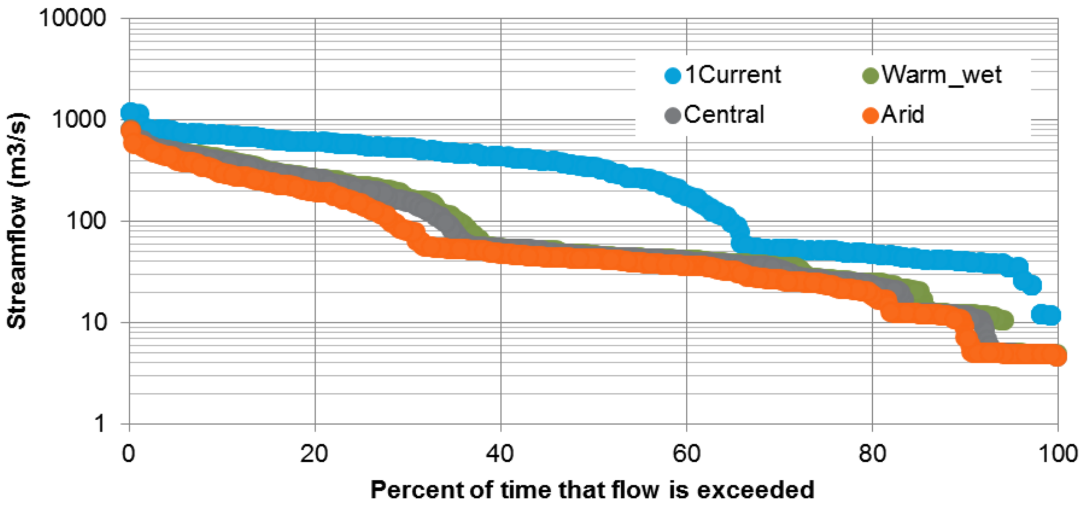

Figure 3-21. Exceedance curve for the Syrdarya TPP under different scenarios

For the Tachiatash TPP downstream in the Amu Darya basin, the average abstraction rate was assumed to be 0.40 m3/s. This is in the same order of magnitude as the low flows in this stream segment, as shown in Figure 3-21. Depending on the operational rules of the upstream reservoirs and allocations upstream this may become critical under climate change. For all the other TPPs, no critical water levels are predicted with climate change that may cause interruptions in cooling water provision for thermal plants. It has to be noted that this analysis assumes cooling towers to be installed at all the thermal plants as most of the plants are being or have been modernized.

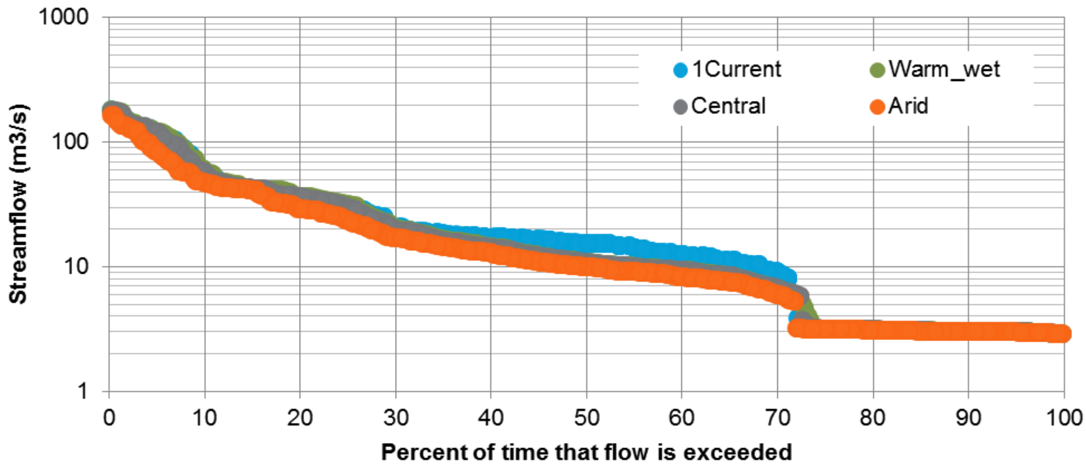

Figure 3-22. Exceedance curve for the Tachiatash TPP (downstream Amu Darya) under different scenarios

3.3 Climate change impacts with planned infrastructure

This section summarizes outcomes of the model simulations, including the planned infrastructure, according to the scenarios that were defined in the methodological section.

3.3.1 Hydrology

The SPHY model provided streamflow for the planned locations of Rogun and Kambarata-I, as shown in Figure 3-23 and Figure 3-24 respectively. Similar to their downstream neighbours, Rogun shows an overall decrease for all the marker scenarios. For Kambarata-I under the Warm/wet scenario streamflow remains constant while under the other scenarios also a slight decrease is seen.

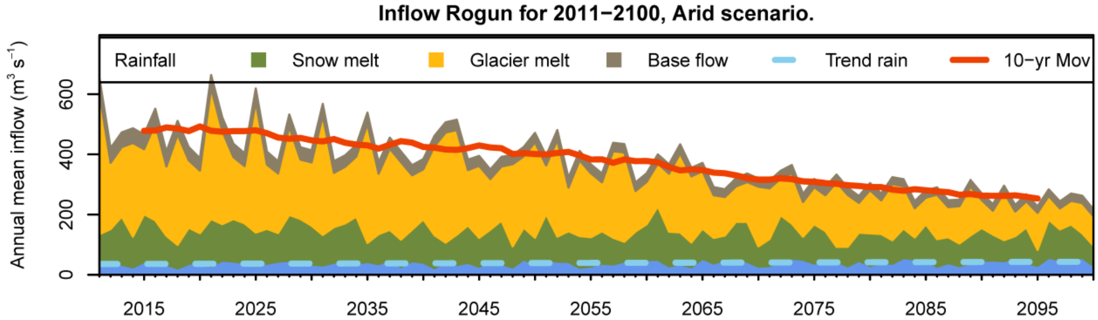

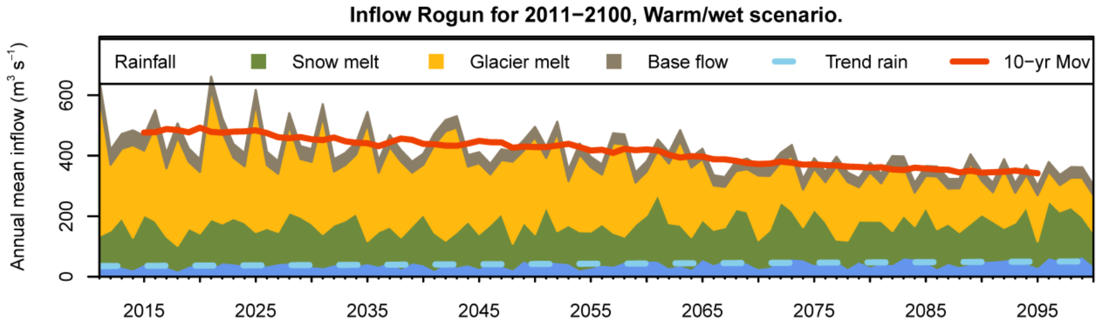

Figure 3-23. Flow upstream of Rogun site under the Arid and the Warm/wet marker scenario

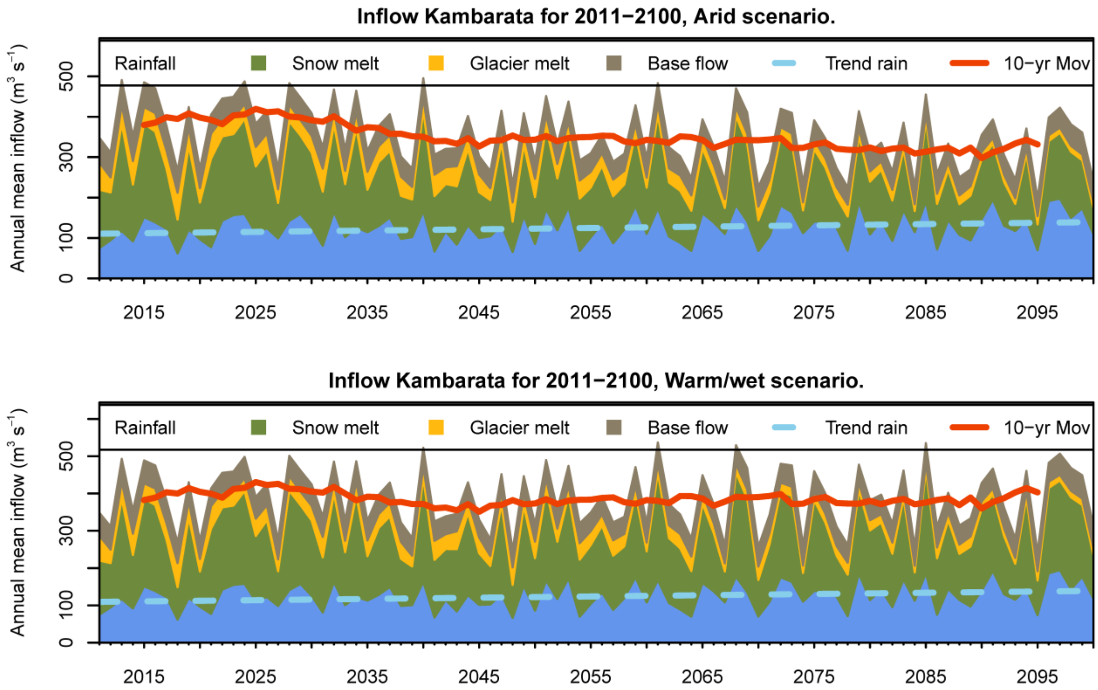

Figure 3-24. Flow upstream of Kamabarata-I site under the Arid and the Warm/wet marker scenario

Changing flow upstream due to climate change and planned infrastructure also impact inflows into downstream reservoirs. These impacts are reflected in the storage dynamics of these reservoirs as presented in the next section and more detailed in Appendix III.

3.3.2 Reservoir levels

Figure 3-25 to Figure 3-28 show how reservoir storage changes under the two different infrastructure scenarios that were defined. Results are shown for the current climate, the hot/dry and the warm/wet+ marker scenario. For other reservoirs outcomes can be found in Appendix III.2.

For Nurek reservoir, results indicate that the storage will likely increase under the Full Buildout scenario. However, for the Hot/dry scenario similar storage levels are predicted as with current infrastructure and current climate. For the 2050s storage levels are even much lower under the Full Buildout compared to the current infrastructure with current climate. In other words, the planned upstream storage facility Rogun will likely reduce the impact of climate change on Nurek storage variability. However, with the less favorable climate scenarios (less precipitation and higher temperatures) this positive impact will be offset by climate change.

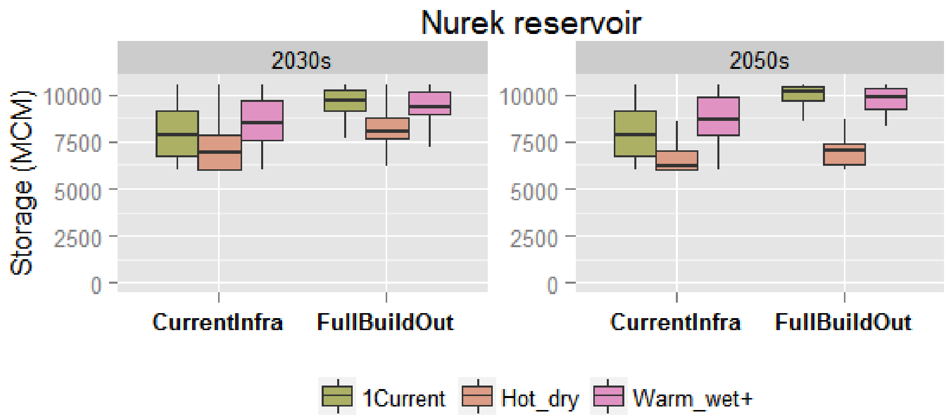

Figure 3-25. Reservoir storage variability of Nurek with Rogun upstream in Full Buildout scenario

For the downstream reservoir in the Amu Darya basins, no significant impact can be seen on storage dynamics under the Full Buildout scenario compared to current infrastructure as seen in the following figure. Climate change does clearly have an impact but new storage facilities upstream do not necessarily have a negative or positive impact, assuming no change in the current release regimes of the upstream reservoirs in the basins.

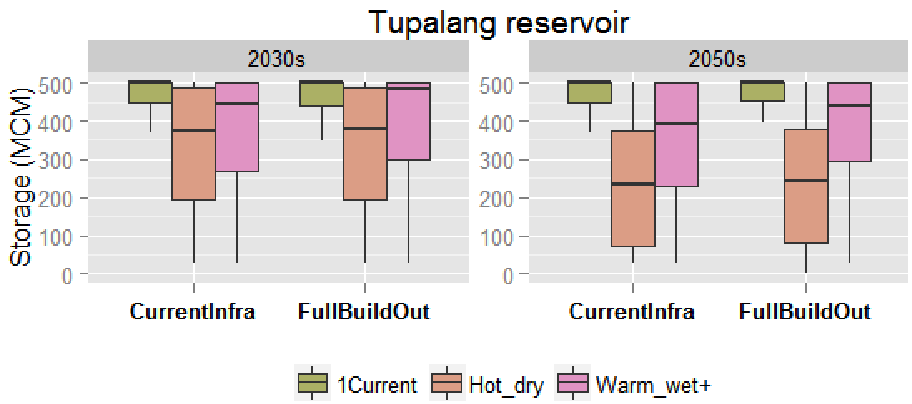

Figure 3-26. Reservoir storage variability of Tupalang with Rogun upstream in Full Buildout scenario

For the Toktogul reservoir, the inclusion of the upstream reservoir Kambarata-I will likely not alter significantly the reservoir storage of Toktogul and the downstream Shardara reservoir. However, it has to be noted that this simulation assumes no altering outflow regime of the Toktogul reservoir.

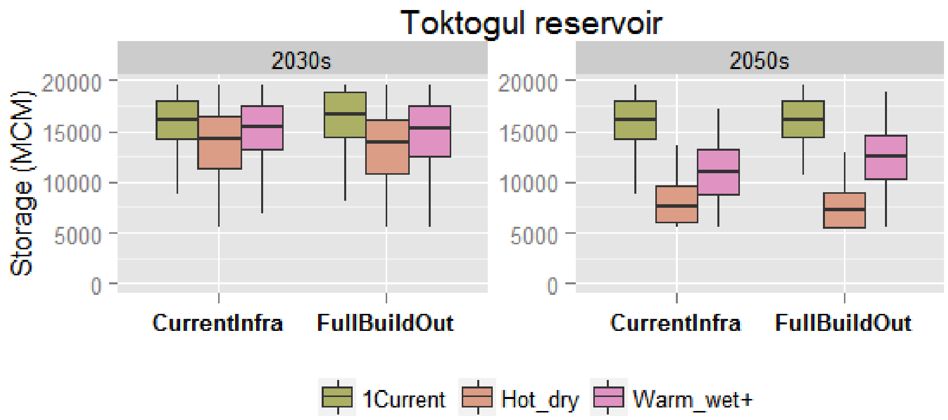

Figure 3-27. Reservoir storage variability of Toktogul with Kambarata-I upstream in Full Buildout scenario

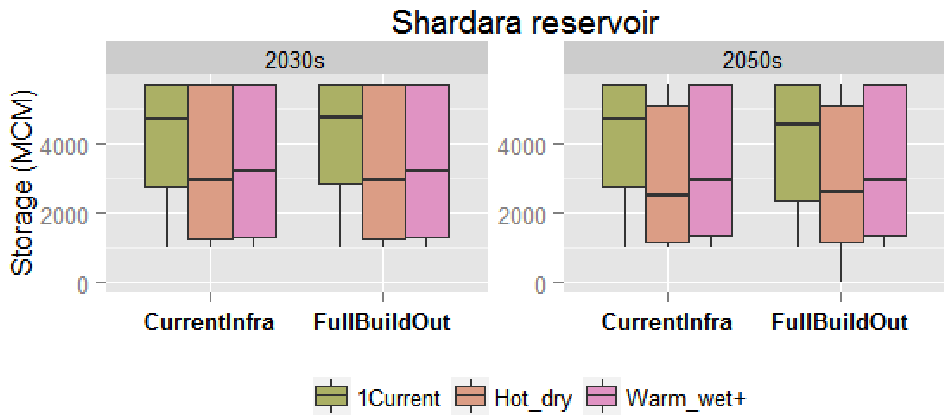

Figure 3-28. Reservoir storage variability of Shardara with Kambarata-I upstream in Full Buildout scenario

3.3.3 Hydropower production

This section shows hydropower production with the two planned infrastructure scenarios. The Partial Buildout includes several new RoR facilities and refurbishment of facilities (5% increase between 2020-2025). The Full Buildout includes the new upstream storage facilities Rogun and Kambarata-I (more details in Modelling dimensions and scenarios, section 2.5).

Figure 3-29 shows the total annual power production of all reservoirs. For the Full Buildout an increase is predicted in production for the current and the warm/wet+ scenario. However, for the Hot/dry scenario, production levels would remain similar as under the Partial Buildout, or even slightly lower in the 2050s.

This same pattern is seen for Rogun and Nurek (Figure 3-30). For Toktogul and Kambarata-I (Figure 3-31) also for Hot/dry scenario an increase is predicted in production for the Full Buildout compared to Partial although considerably less than under the current climate scenario.

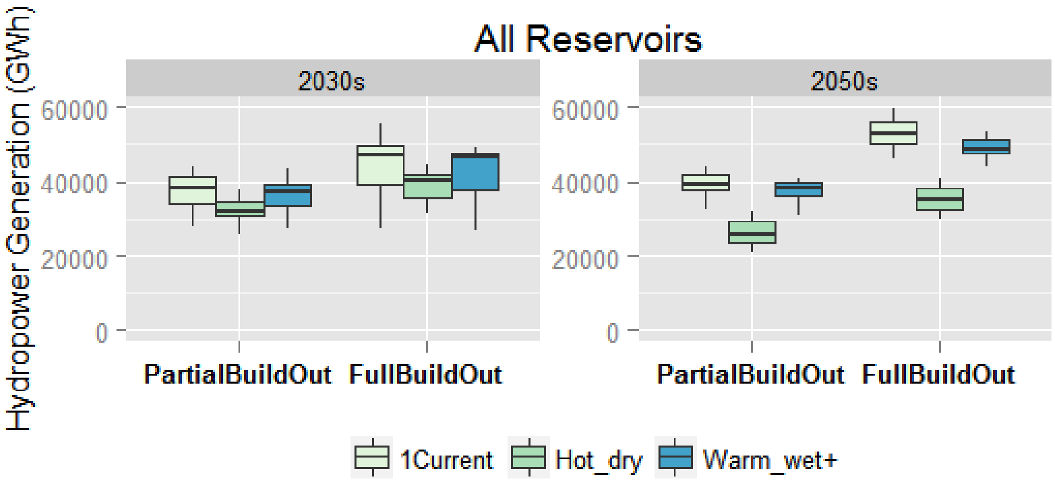

Figure 3-29. Annual hydropower generation of all the simulated hydropower facilities in the region for the two buildout scenarios

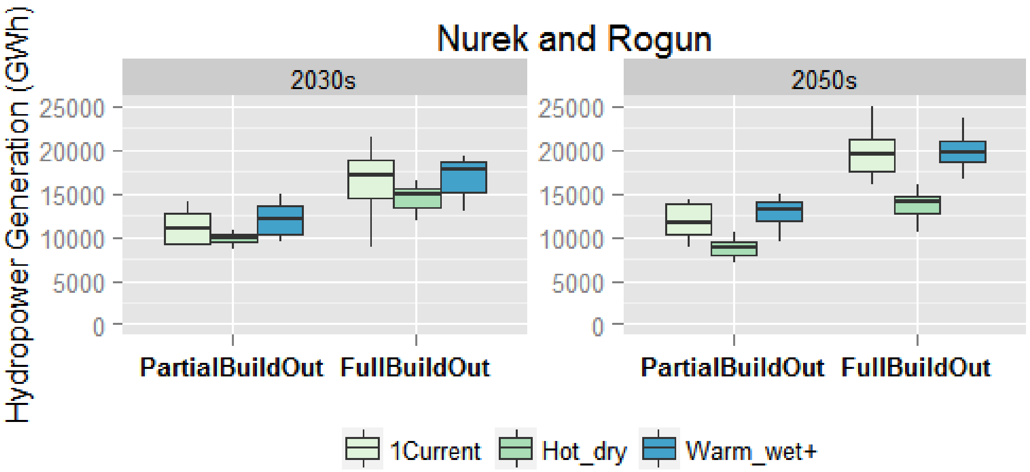

Figure 3-30. Hydropower generation for Nurek and Rogun for the two buildout scenarios

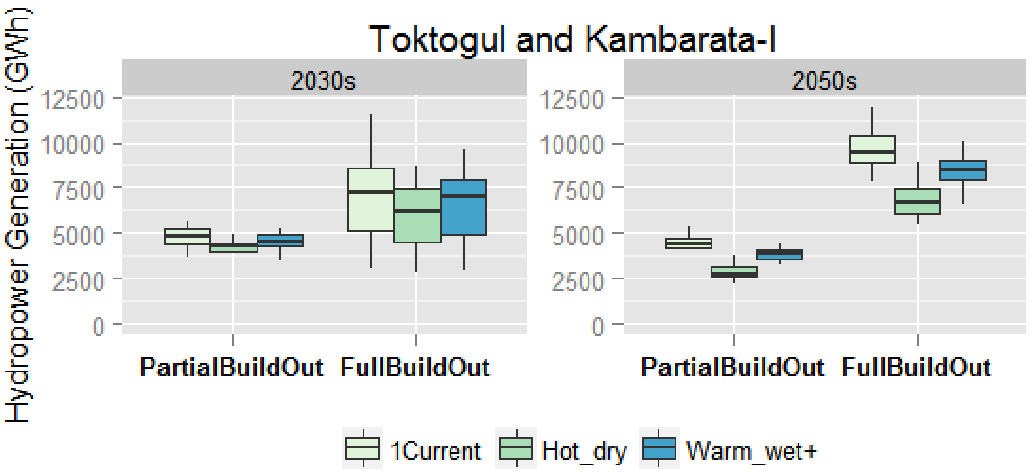

Figure 3-31. Hydropower generation for Toktogul and Kambarata-I for the two buildout scenarios

3.3.4 Agriculture

Water supply to domestic use is not affected by climate change or planned infrastructure as predicted by the WEAP-ARAL2014, as priority was given to this use above agriculture. Hosever, impacts on water supply to agriculture of climate change are considerable as shown previously, and could potentially also be affected by planned infrastructure (positively and negatively).

Outcomes of the simulations indicate that under the current release regimes of the upstream reservoirs agricultural water supply is not affected by the planned infrastructure as shown in the following figures. Clearly climate change impacts are of much greater concern for agricultural water supply (for more details check Appendix V.2).

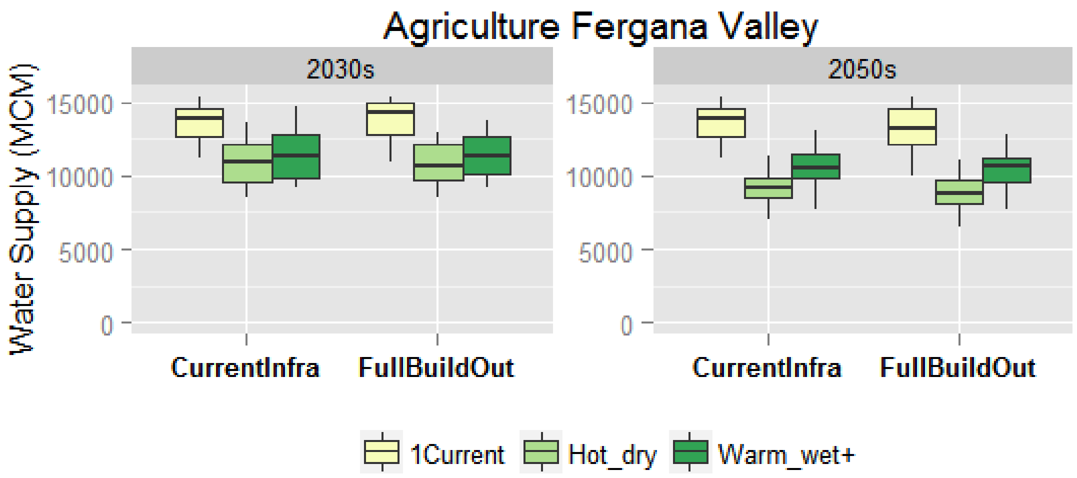

Figure 3-32. Water supplied to three agricultural areas in the 2050s for the infrastructure scenarios under the current climate

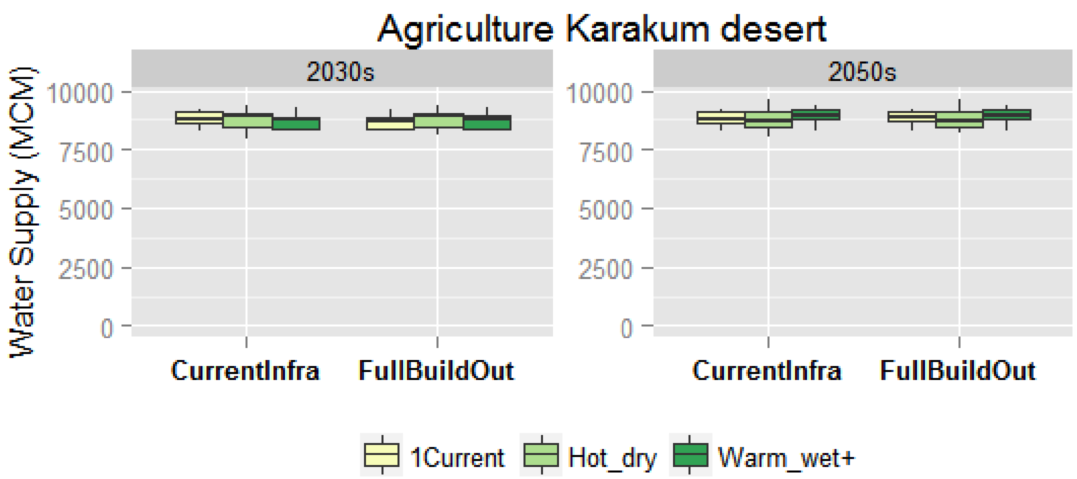

Figure 3-33. Unmet demand of the same agricultural areas in the 2050s for the infrastructure scenarios under the current climate

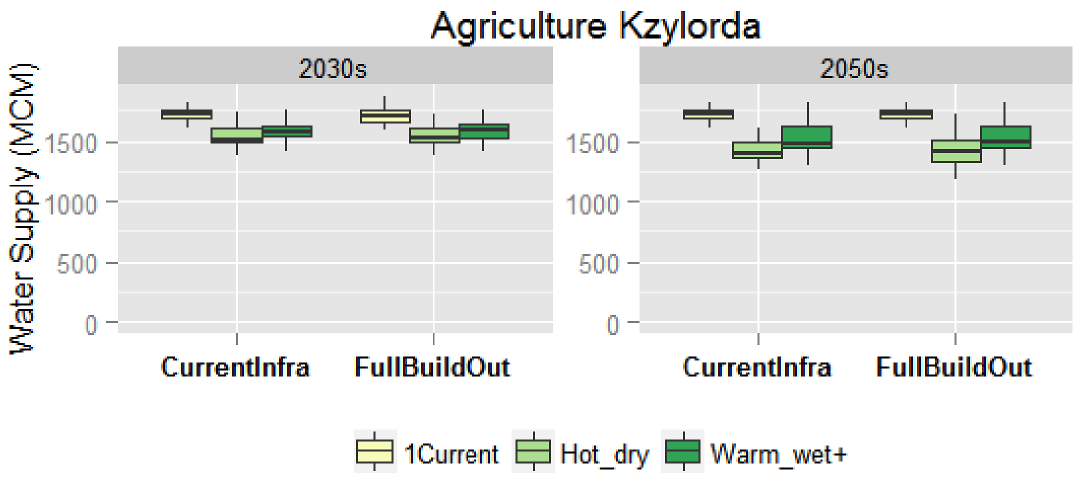

Figure 3-34. Unmet demand of the same agricultural areas in the 2050s for the infrastructure scenarios under the current climate

4 Conclusions

This study carries out a risk assessment under climate change for water availability and water related energy sector impacts in the Central Asian region (Syr Darya and Amu Darya basins), building on several previous studies and tools that have been developed over the last years. Several advancements were included compared to previous studies, in terms of input data and modeling tools.

For the upstream parts of the basins, the hydrological model SPHY was used while for the downstream areas a water allocation model was built including all the main infrastructure, supplies and demands, using the Water Evaluation and Planning (WEAP) tool. This modelling framework was used to study impacts of climate change on water availability, allocations and water for the energy facilities (hydropower and thermal).

The study uses climate modeling results of the latest fifth assessment report (AR5) published by the IPCC in 2014. This updated model ensemble projects greater warming and a wider range in projections for temperature as well as precipitation compared to the projections used for the studies so far in the region. Besides this observed larger uncertainty, the different ensembles showed significant seasonal differences in the projections, which have major implications for the impacts on the cryosphere (glaciers and snow) in the region, where the hydrology is dominated by runoff generated in the cryosphere.

Currently still a large debate is taking place in the scientific arena on the implications of climate change on glaciers in Central Asia and South Asia. The hydrological modelling approach used in this study includes some of the latest insights in glacier response to climate change. Modelling outcomes suggest an overall reduction in flows even in the near term for most of the watersheds and climate scenarios. Clearly this will have considerable impacts on the services that rely on the reservoirs in the region, both due to changes in seasonality as in total flows.

Overall, most climate change scenarios included in the study predict more variable and lower reservoir levels, for both the upstream as the downstream reservoirs. Impacts are noticeable, both in the Syr Darya as in the Amu Darya. The impacts in terms of hydropower are very variable for each basin and reservoir. Overall, the reduction in total hydropower production is predicted to be between 5% and 30% in the 2050s. For several reservoirs this impact is likely to be even much higher. Only for the reservoirs in the Vaksh river, one of the climate scenarios predicts an increase in production.

Cooling water provision to thermal power plants in the region is hardly affected by climate change, assuming that all power plants are equipped with cooling towers in the very near future. Results suggest it is unlikely that the power plans will suffer water shortages due to the relatively low abstraction rates plants using this technology. It has to be noted though that this part of the assessment was done with relatively scarce data and that more detailed studies are recommendable for particular sites where water scarcity and competing uses are an issue.

Planned investments in infrastructure, both in generating capacity as in storage, will increase overall power production levels but for some of the reservoirs and under some of the climate change scenarios the increase can be offset by lower water availabilities due to climate change. From this study it becomes evident that the impacts of climate change on the future infrastructural investments in the region should be taken into account as they can highly affect their return.

5 References

ADB (2012), *Central Asia Regional Economic Cooperation: Power Sector Regional Master Plan*, ADB.

Alford, D., U. Kamp, and C. Pan (2014), *The Role of Glaciers in the Hydrologic Regime of the Amu Darya and Syr Darya Headwaters. Draft.*

Arnell, N. W. (1999), Climate change and global water resources, *Glob. Environ. Chang.*, *9*, S31–S49.

Bliss, A., R. Hock, and V. Radić (2014), Global response of glacier runoff to twenty-first century climate change, *J. Geophys. Res. Earth Surf.*, *119*, 1–14, doi:10.1002/2013JF002931.

Bolch, T. et al. (2012), The State and Fate of Himalayan Glaciers, *Science (80-.).*, *336*, 310–314, doi:10.1126/science.1215828.

Bookhagen, B., and D. W. Burbank (2010), Toward a complete Himalayan hydrological budget: Spatiotemporal distribution of snowmelt and rainfall and their impact on river discharge, *J. Geophys. Res.*, *115*(F3), 1–25, doi:10.1029/2009JF001426.

Deque, M. (2007), Frequency of precipitation and temperature extremes over France in an anthropogenic scenario: Model results and statistical correction according to observed values, *Glob. Planet. Change*, *57*(1-2), 16–26, doi:10.1016/j.gloplacha.2006.11.030.

Droogers, P., and R. G. Allen (2002), Estimating reference evapotranspiration under inaccurate data conditions, *Irrig. Drain. Syst.*, *16*, 33–45.

EC IFAS (2012), *Aral Sea BEAM (Basin Economic Allocation Model). User's Manual*, edited by Global Water Partnership, DHI, and COWI.

Gardelle, J., E. Berthier, and Y. Arnaud (2012), Slight mass gain of Karakoram glaciers in the early twenty-first century, *Nat. Geosci.*, *5*(5), 322–325, doi:10.1038/ngeo1450.

Gardelle, J., E. Berthier, Y. Arnaud, and a. Kääb (2013), Region-wide glacier mass balances over the Pamir-Karakoram-Himalaya during 1999–2011, *Cryosph.*, *7*(4), 1263–1286, doi:10.5194/tc-7-1263-2013.

Hewitt, K. (2005), The Karakoram Anomaly? Glacier Expansion and the “Elevation Effect,” Karakoram Himalaya, *Mt. Res. Dev.*, *25*(4), 332 – 340.

Hock, R. (2005), Glacier melt: a review of processes and their modelling, *Prog. Phys. Geogr.*, *29*(3), 362–391, doi:10.1191/0309133305pp453ra.

Immerzeel, W. W., and A. F. Lutz (2012), *Regional knowledge sharing on climate change scenario downscaling. FutureWater technical report 116.*, Wageningen, The Netherlands.

Immerzeel, W. W., L. P. H. van Beek, and M. F. P. Bierkens (2010), Climate change will affect the Asian water towers., *Science*, *328*(5984), 1382–5, doi:10.1126/science.1183188.

Immerzeel, W. W., A. F. Lutz, and P. Droogers (2012), *Climate Change Impacts on the Upstream Water Resources of the Amu and Syr Darya River Basins*, Wageningen, The Netherlands.

Immerzeel, W. W., F. Pellicciotti, and M. F. P. Bierkens (2013), Rising river flows throughout the twenty-first century in two Himalayan glacierized watersheds, *Nat. Geosci.*, *6*(9), 742–745, doi:10.1038/ngeo1896.

IPCC (2013), *Climate Change 2013: The Physical Science Basis. Contribution of Working Group I to the Fifth Assessment Report of the Intergovernmental Panel on Climate Change*, Cambridge, UK.

Kääb, A., E. Berthier, C. Nuth, J. Gardelle, and Y. Arnaud (2012), Contrasting patterns of early twenty-first-century glacier mass change in the Himalayas., *Nature*, *488*(7412), 495–8, doi:10.1038/nature11324.

Kapnick, S. B., T. L. Delworth, M. Ashfaq, S. Malyshev, and P. C. D. Milly (2014), Snowfall less sensitive to warming in Karakoram than in Himalayas due to a unique seasonal cycle, *Nat. Geosci.*, (October), 1–7, doi:10.1038/ngeo2269.

Kargel, J. S., J. G. Cogley, G. J. Leonard, U. Haritashya, and A. Byers (2011), Himalayan glaciers: The big picture is a montage, *Proc. Natl. Acad. Sci. U. S. A.*, *108*(34), 14709–14710, doi:10.1073/pnas.1111663108.

Karssenberg, D., P. Burrough, R. Sluiter, and K. de Jong (2001), The PCRASTER software and course materials for teaching numerical modelling in the environmental sciences, *Trans. GIS*, *5*, 99–110, doi:10.1111/1467-9671.00070.

Kay, A. L., H. N. Davies, V. A. Bell, and R. G. Jones (2008), Comparison of uncertainty sources for climate change impacts: flood frequency in England, *Clim. Change*, *92*, 41–63, doi:10.1007/s10584-008-9471-4.

Lutz, A. F., and W. W. Immerzeel (2013), *Water Availability Analysis for the Upper Indus , Ganges , Brahmaputra , Salween and Mekong River Basins*, FutureWater Report 127, Wageningen, Netherlands.

Lutz, A. F., P. Droogers, and W. W. Immerzeel (2012), *Climate Change Impact and Adaptation on the Water Resources in the Amu Darya and Syr Darya River Basins*, FutureWater Report 110, Wageningen, Netherlands.

Lutz, A. F., W. W. Immerzeel, A. Gobiet, F. Pellicciotti, and M. F. P. Bierkens (2013), Comparison of climate change signals in CMIP3 and CMIP5 multi-model ensembles and implications for Central Asian glaciers, *Hydrol. Earth Syst. Sci.*, *17*(9), 3661–3677, doi:10.5194/hess-17-3661-2013.

Lutz, A. F., W. W. Immerzeel, A. B. Shrestha, and M. F. P. Bierkens (2014a), Consistent increase in High Asia ' s runo due to increasing glacier melt and precipitation, *Nat. Clim. Chang.*, (June), 1–6, doi:10.1038/NCLIMATE2237.

Lutz, A. F., W. W. Immerzeel, A. B. Shrestha, and M. F. P. Bierkens (2014b), Consistent increase in High Asia's runoff due to increasing glacier melt and precipitation, *Nat. Clim. Chang.*, *4*(7), doi:10.1038/NCLIMATE2237.

Macknick, J., R. Newmark, G. Heath, and K. C. Hallett (2012), Operational water consumption and withdrawal factors for electricity generating technologies: a review of existing literature, *Environ. Res. Lett.*, *7*(4), 045802, doi:10.1088/1748-9326/7/4/045802.

Radić, V., A. Bliss, a. C. Beedlow, R. Hock, E. Miles, and J. G. Cogley (2013), Regional and global projections of twenty-first century glacier mass changes in response to climate scenarios from global climate models, *Clim. Dyn.*, 37–58, doi:10.1007/s00382-013-1719-7.

Raskin, P., E. Hansen, Z. Zhu, and M. Iwra (1992), Simulation of Water Supply and Demand in the Aral Sea Region, *Water Int.*, *17*, 55–67.

Taylor, K. E., R. J. Stouffer, and G. A. Meehl (2012), An Overview of CMIP5 and the Experiment Design, *Bull. Am. Meteorol. Soc.*, *93*(4), 485–498, doi:10.1175/BAMS-D-11-00094.1.

USAID (2000), *Optimization of the use of water and energy resources in the Syrdarya basin under current conditions. Volume II: National Groups*, edited by D. C. McKinney and A. K. Kenshimov.

World Bank (2012), *Tajikistan ' s Winter Energy Crisis : Electricity Supply and Demand Alternatives*, edited by D. Fields, A. Kochnakyan, G. Stuggins, and J. Besant-Jones.

World Bank (2013), *Uzbekistan Energy / Power Sector Issues Note*, edited by A. Kochnakyan, S. Hofer Kumar, I. Buranov, K. Buranov, D. Hankinson, and J. Finn.

World Bank (2014a), *From Volume to Value : Managing Water in Central Asia. Draft Report*, edited by B. Blarel and G. Peszko.

World Bank (2014b), *Techno-Economic Assessment Study For Rogun Hydroelectric Construction Project. Phase II Report (Final): Project Definition Options. Volume 3 : Engineering And Design. Chapter 5: Reservoir Operation Study*.

Appendix I - Delta change downscaling approach

I.1 Approach

An efficient way to do downscale GCM projections is applying the 'delta change' approach. When applying this approach the final generated grids are monthly delta change data for a future period (e.g. 2071-2100) relative to a reference period (e.g. 1971-2000). The delta change values reflect the change in temperature and precipitation over a period years (in this case that would be 100 years. These change data are in Kelvin for temperature and in % for precipitation. This well established delta change approach is an efficient way to assess climatic changes [*Arnell*, 1999; *Deque*, 2007; *Kay et al.*, 2008]. This approach becomes necessary due to the large scale discrepancy between the climate models and the hydrological models operating at a much higher resolution. We cut out the grid cells of the climate models over the study region to calculate monthly climate change signals, which are subsequently superimposed on a local reference time series, which is available from the ADB project. The "delta change" approach removes large parts of model biases, which cancel out in the climate change signals. Based on these change data the annual change can be calculated (assuming linear change) and be used to generate transient time series to force the models.

The following paragraphs discuss the procedure in detail, and show examples how this was done for the Himalayan region (based on [*Immerzeel and Lutz*, 2012]).
Downloading of GCMs

The selected GCMs are downloaded from the CMIP5 portal. (http://cmip-pcmdi.llnl.gov/cmip5/data_portal.html). For the selected GCMs the files containing the monthly summed precipitation (pr, [$kgm^{-2}s^{-1}$]) and monthly averaged near-surface air temperature (tas, [K]) for the historical period (January 1971 – December 2000) and future period (January 2071 – December 2100) are downloaded. The data is available in netCDF format. Each file contains a time series of worldwide rasters for each month in the resolution specific for the GCM.

I.2 Downscaling of GCMs

The downscaling of the GCMs consists of the following processing steps:

- Extracting temperature and precipitation grid per month for study domain from NetCDF files
- Calculate average temperature and precipitation per month for Jan-Dec for 1971-2000
- Calculate average temperature and precipitation per month for Jan-Dec for 2071-2100
- Calculate delta change values for Jan-Dec for 2071-2100 compared to 1971-2000
- Interpolate delta change values from GCM resolution to 0.25° resolution

The processing steps are done using the 'raster' package in the open access R statistical computing software (http://www.r-project.org/), and ArcGIS scripting with Python. In the following paragraphs these processing steps are discussed in detail.

I.2.1 Extracting one grid per month for study domain from NetCDF files

For each month within the periods 1971-2000 and 2071-2100 a grid with temperature and a grid with precipitation is extracted for the rough extent of the study domain. This results for each GCM in:

- 360 temperature grids reference period (each month from January 1971 to December 2000)
- 360 temperature grids future period (each month from January 2071 to December 2100)
- 360 precipitation grids reference period (each month from January 1971 to December 2000
- 360 precipitation grids future period (each month from January 2071 to December 2100)

In total 4 * 360 * 8 = 11520 grids are extracted. Figure 5-1 shows examples of extracted temperature and precipitation grids for July 1971 for the CanESM2-r4ip1 RCP 4.5 projection.

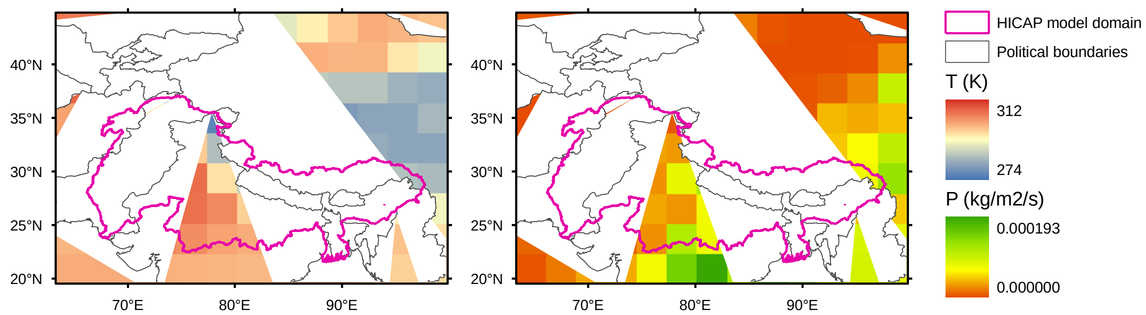

Figure 5-1: Average T (K) and summed P (kg/m^2/s) for July 1971 (CanESM2-r4i1p1_rcp45).

I.2.2 Calculate average monthly temperature and precipitation for Jan-Dec 1971-2000

For each month in the reference period (1971-2000) a grid with the average temperature is calculated using the grids extracted in the previous step (section I.2.1). This is done by summing all temperature grids for the specific month and dividing by the number of summed months. For example for January this is:

1971-2000 January average = (January 1971 + January 1972 + … + January 2000) / 30

The same is done for the months February to December.

The same procedure is applied to calculate average precipitation per month. For each month in the reference period (1971-2000) a grid with the average monthly summed precipitation is calculated using the grids extracted in the previous step (section I.2.1). This is done by summing all precipitation grids for the specific month and dividing by the number of summed months. For example for January this is:

1971-2000 January average = (January 1971 + January 1972 + … + January 2000) / 30

The same is done for the months February to December.

This yields:

- 12 grids for average temperature (Jan-Dec)
- 12 grids for average summed precipitation (Jan-Dec)

The procedure is repeated for each of the selected GCMs resulting in a total of 24 x 8 = 192 grids. Figure 5-2 shows examples of average July temperature and precipitation grids for the reference period (1971-2000) and the future period (2071-2100) for the the CanESM2-r4ip1 RCP 4.5 projection.

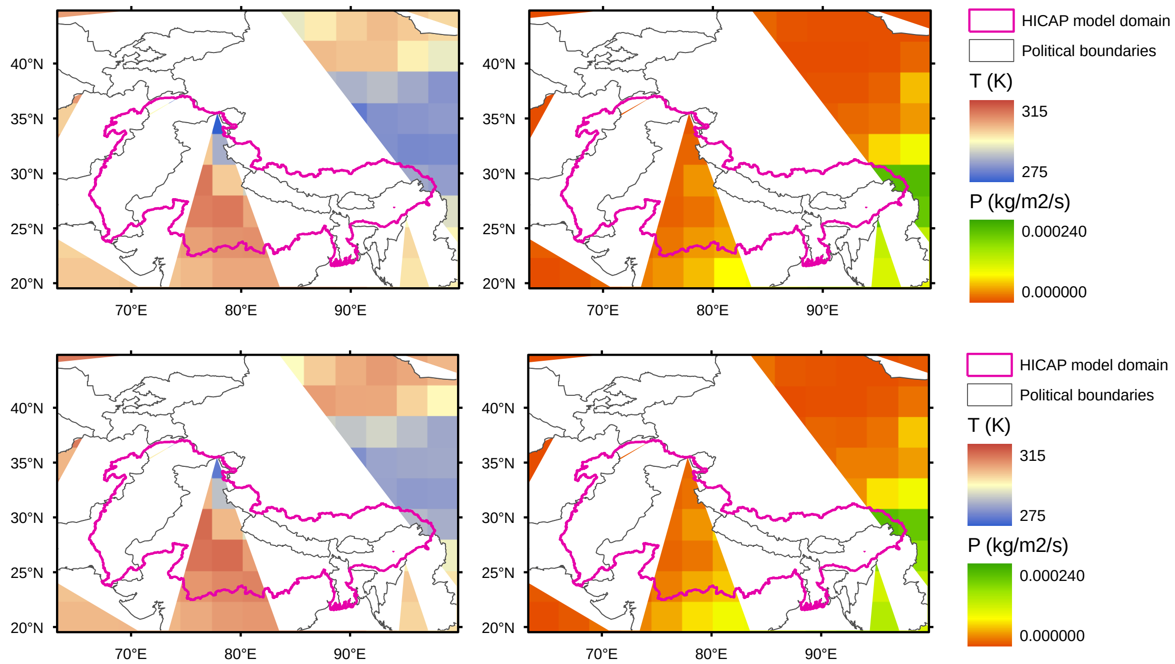

Figure 5-2: Average July temperature and average July precipitation 1971-2000 (upper panels) and 2071-2100 (lower panels) (CanESM2-r4i1p1_rcp45).

I.2.3 Calculate average monthly temperature and precipitation for Jan-Dec for 2071-2100

Following the same procedure as in section I.2.2 average monthly temperature and precipitation grids are calculated for the future period (2071 – 2100).

For each month in the future period (2071-2100) a grid with the average temperature is calculated using the grids extracted in the previous step (section I.2.1). This is done by summing all temperature grids for the specific month and dividing by the number of summed months. For example for January this is:

2071-2100 January average = (January 2071 + January 2072 + … + January 2100) / 30

The same is done for the months February to December.

The same procedure is applied to calculate average precipitation per month. For each month in the future period (2071-2100) a grid with the average monthly summed precipitation is calculated using the grids extracted in the previous step (section I.2.1). This is done by summing all precipitation grids for the specific month and dividing by the number of summed months. For example for January this is:

2071-2100 January average = (January 2071 + January 2072 + … + January 2100) / 30

The same is done for the months February to December.

This yields:

- 12 grids for average temperature (Jan-Dec)
- 12 grids for average summed precipitation (Jan-Dec)

The procedure is repeated for each of the selected GCMs resulting in a total of 24 x 8 = 192 grids. Figure 5-2 shows examples of average July temperature and precipitation grids for the reference period (1971-2000) and the future period (2071-2100) for the the CanESM2-r4ip1 RCP 4.5 projection.

I.2.4 Calculate delta change values for Jan-Dec for 2071-2100 compared to 1971-2000

For each month (Jan-Dec) a delta change value [*Arnell*, 1999; *Deque*, 2007; *Kay et al.*, 2008] is calculated using the grids calculated in sections I.2.2 and I.2.3. For temperature the delta change value is calculated in Kelvin and for precipitation the delta change value is calculated as a percentage.

For example, the ΔT value for January is calculated as follows:

ΔT Jan = T Jan 2071-2100 – T Jan 1971-2000

The same is done for February – December.

This leads to 12 (Jan-Dec) ΔT grids per selected GCM. For eight GCMs this means 12 x 8 = 96 ΔT grids. As an example, Figure 5-3 shows the ΔT grids for January and July for the CanESM2-r4ip1 RCP 4.5 projection.

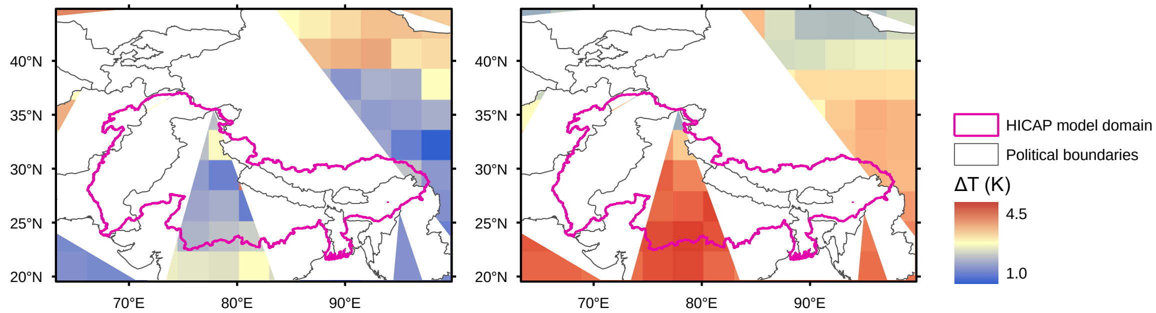

Figure 5-3: Delta change for temperature January (left panel) and July (right panel) (CanESM2-r4i1p1_rcp45).

For precipitation, the calculation of the delta change value requires extra steps. Because some parts of the study area are characterized by very low amounts of precipitation during parts of the year this can lead to very extreme values when calculating the ΔP value. To avoid this, the ΔP value for months with low precipitation (< 15 mm per month), is calculated using the annual precipitation instead of precipitation per month.

In addition, a maximum boundary is set at 200% of the precipitation value in the reference period.

For each selected GCM an annual ΔP value is calculated using the monthly precipitation grids calculated in sections I.2.2 and I.2.3. With these grids annual precipitation grids can be calculated for the reference period and the future period:

Annual P 1971-2000 = P Jan 1971-2000 + P Feb 1971-2000 + … + P Dec 1971-2000

Annual P 2071-2100 = P Jan 2071-2100 + P Feb 2071-2100 + … + P Dec 2071-2100

If monthly precipitation in 1971-2000 > 15 mm:

Jan ΔP = ((Jan P 2071-2100 – Jan P 1971-2000) / Jan P 1971-2000)) * 100

If monthly precipitation in 1971-2000 < 15 mm:

Jan ΔP = ((Annual P 2071-2100 – Annual P 1971-2000) / Annual P 1971-2000) * 100

If Jan ΔP < 200%:
Jan ΔP = Jan delta change P

If Jan ΔP > 200%:
Jan ΔP = 200%

The same is done for February – December.
This leads to 12 ΔP grids (Jan-Dec) for precipitation per selected GCM. For eight GCMs this means 12 x 8 = 96 ΔP grids.

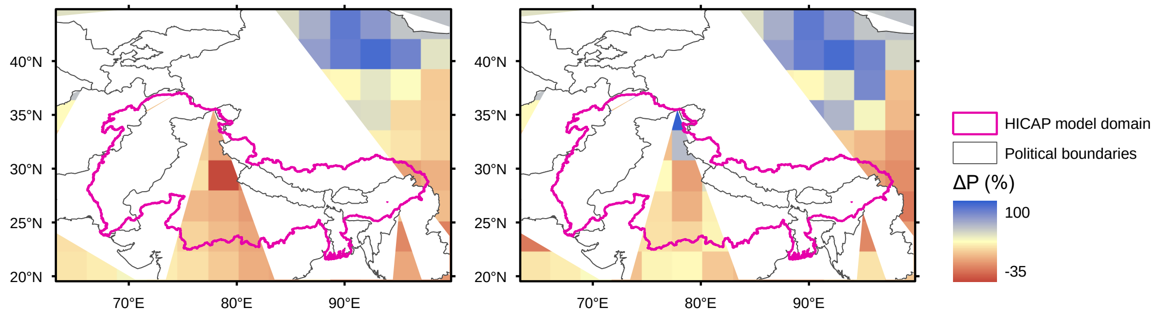

Figure 5-4: Delta change value for precipitation in January (left panel) and July (right panel) (CanESM2-r4i1p1_rcp45).

I.2.5 Interpolate delta change values from GCM resolution to 0.25° resolution

The 192 delta change grids calculated in section I.2.4 are spatially interpolated to 0.25° resolution using a spline interpolation. This interpolation is done from the central points of the grid cells. A tension spline with spline tension 10 and 4 neighbours is applied.

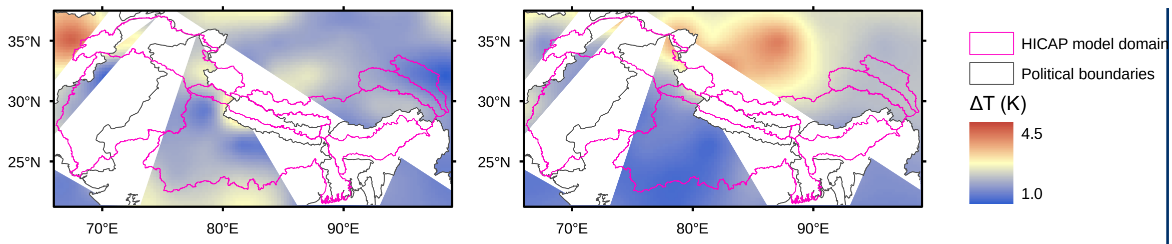

Figure 5-5: Delta change for temperature January (left panel) and July (right panel) at 0.25° resolution (CanESM2-r4i1p1_rcp45).

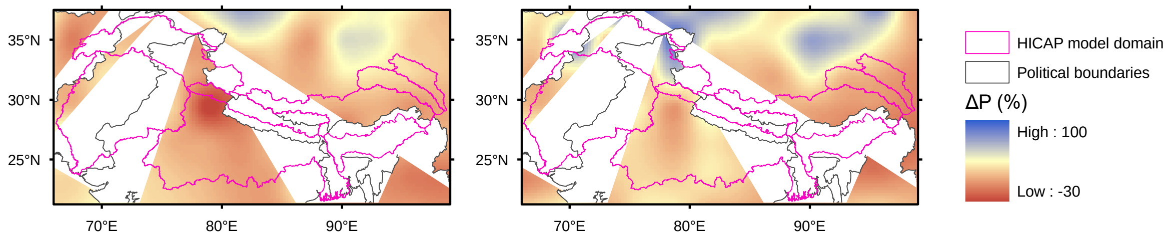

Figure 5-6: Delta change value for precipitation in January (left panel) and July (right panel) at 0.25° resolution (CanESM2-r4i1p1_rcp45).

Appendix II – Annual hydrographs under climate change

II.1 Marker scenario: Arid

Inflow Toktogul reservoir for 2011–2100, Arid scenario.

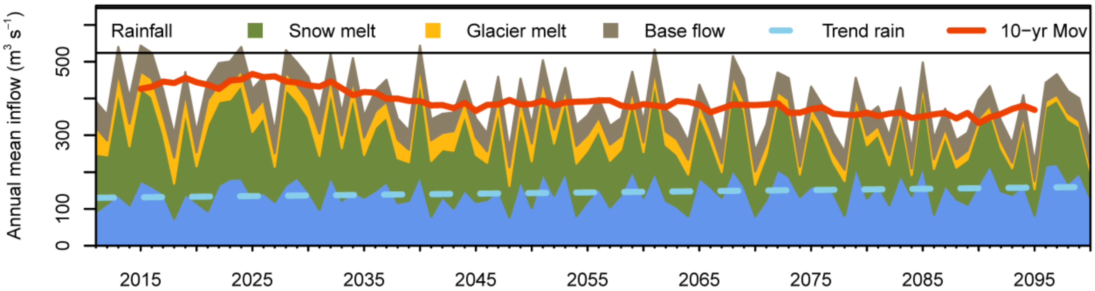

Inflow Andijan reservoir for 2011–2100, Arid scenario.

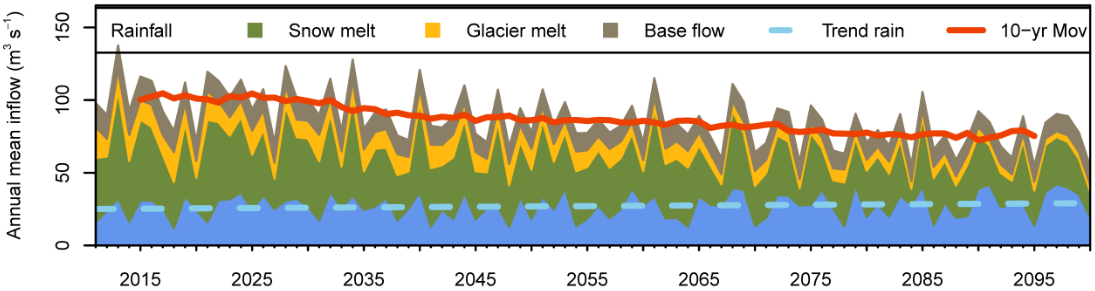

Inflow Nurek reservoir for 2011–2100, Arid scenario.

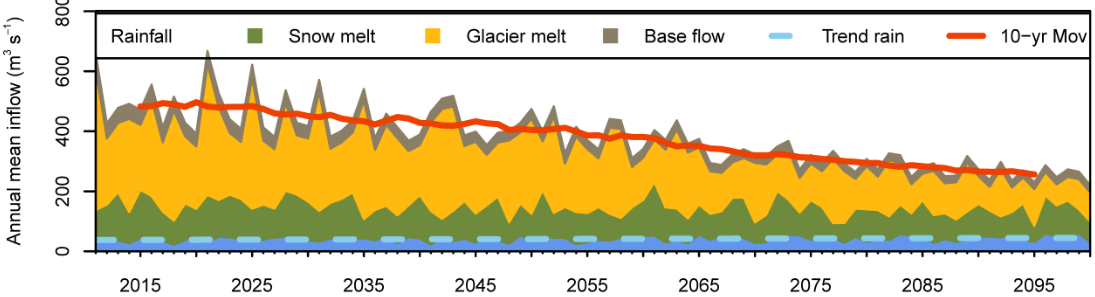

Inflow Tupalangskoe reservoir for 2011–2100, Arid scenario.

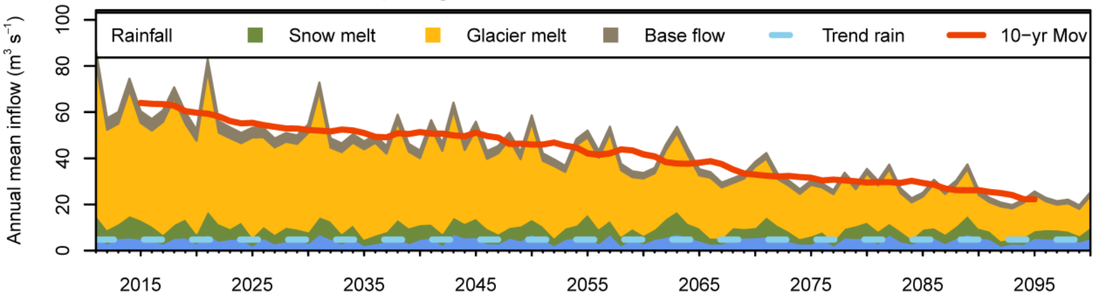

Inflow Akhangaran reservoir for 2011–2100, Arid scenario.

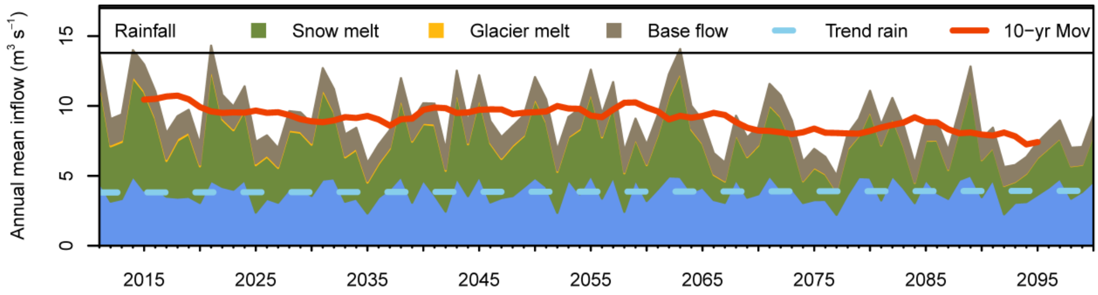

Inflow Zaamin reservoir for 2011–2100, Arid scenario.

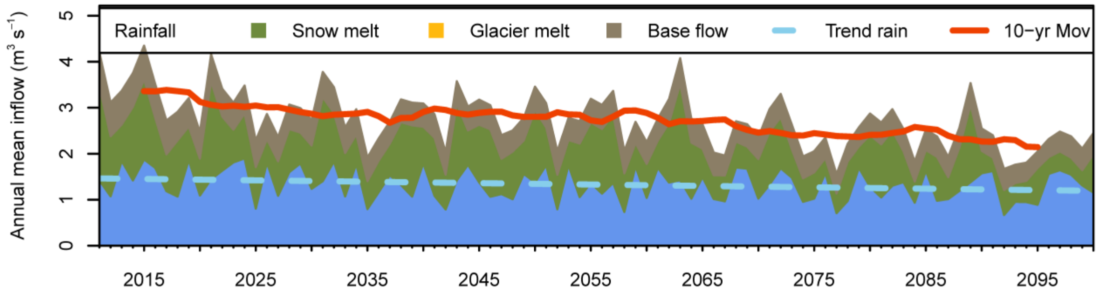

Inflow Gissarak reservoir for 2011–2100, Arid scenario.

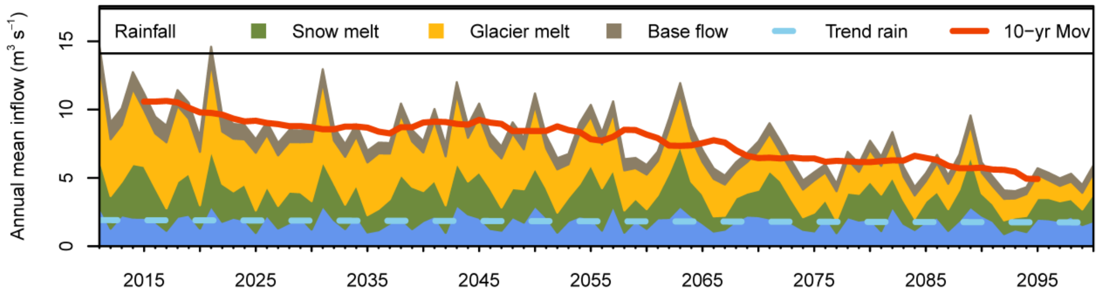

Inflow Pachkamar reservoir for 2011–2100, Arid scenario.

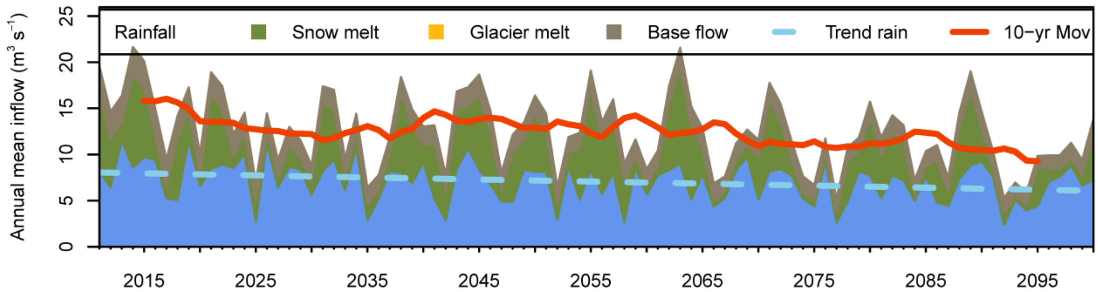

Inflow Kulyab catchment for 2011–2100, Arid scenario.

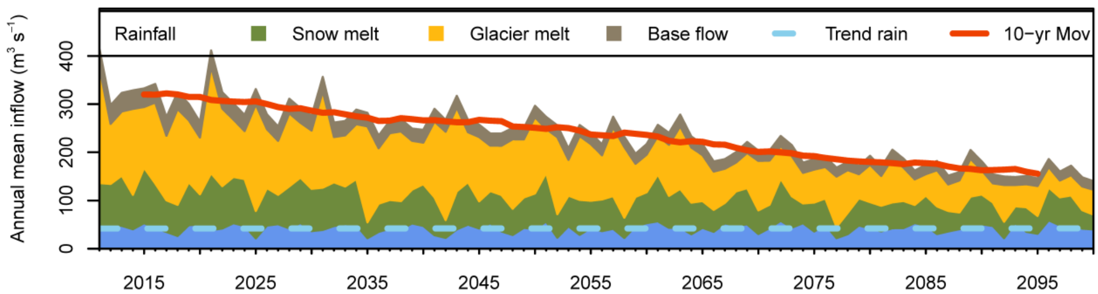

Inflow Kurgantube catchment for 2011−2100, Arid scenario.

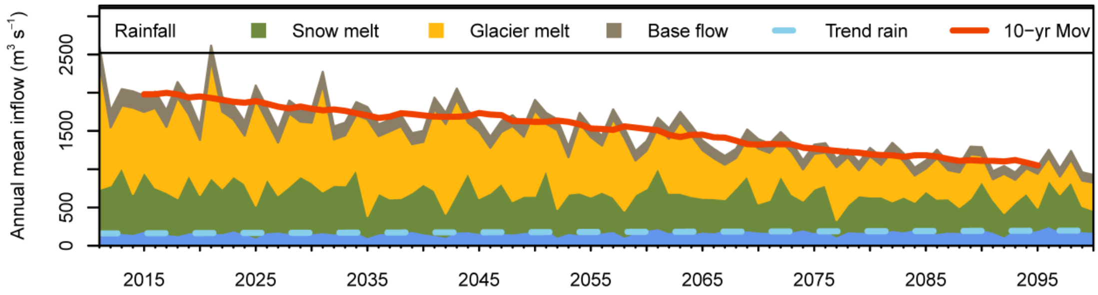

Inflow Dushanbe catchment for 2011−2100, Arid scenario.

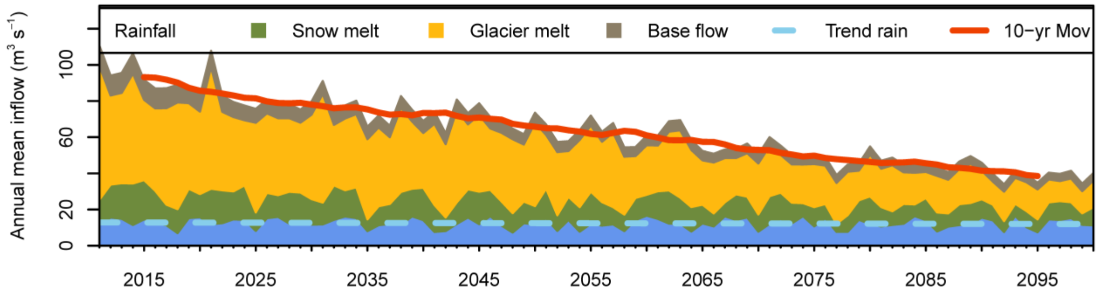

Inflow Surkhandarya upstream catchment for 2011−2100, Arid scenario.

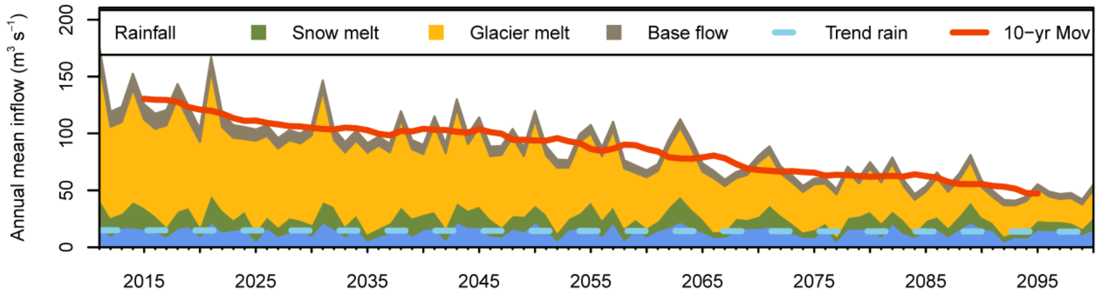

Inflow Surkhandarya downstream catchment for 2011−2100, Arid scenario.

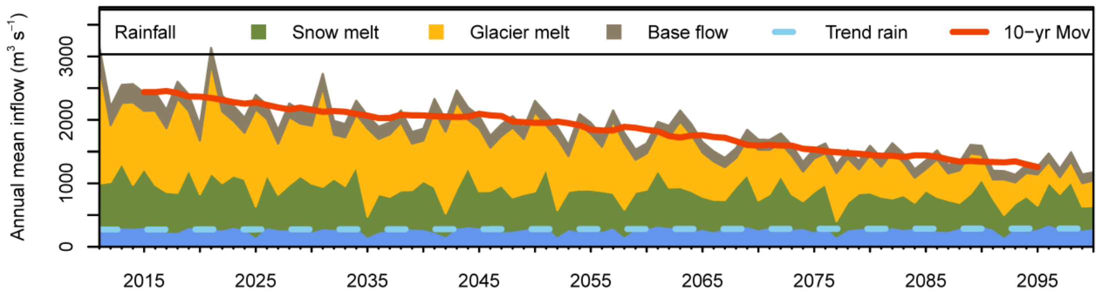

Inflow Karukum kanal catchment for 2011−2100, Arid scenario.

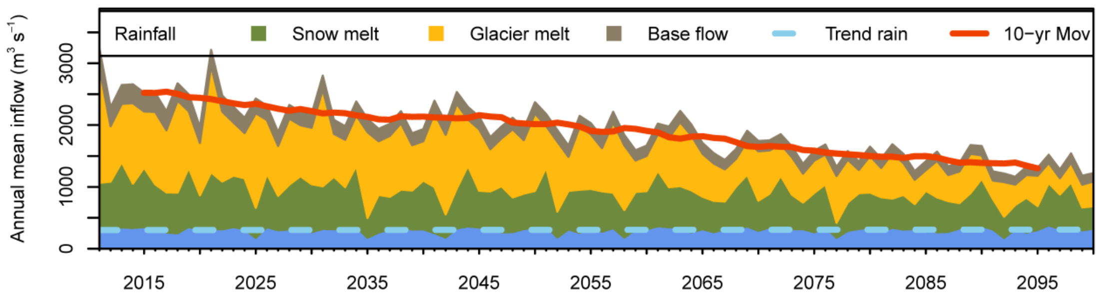

Inflow Kashkadarya upstream catchment for 2011−2100, Arid scenario.

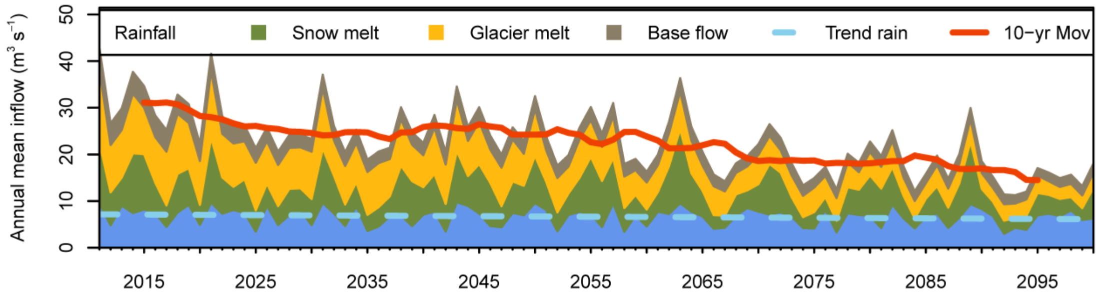

Inflow Kashkadarya downstream catchment for 2011−2100, Arid scenario.

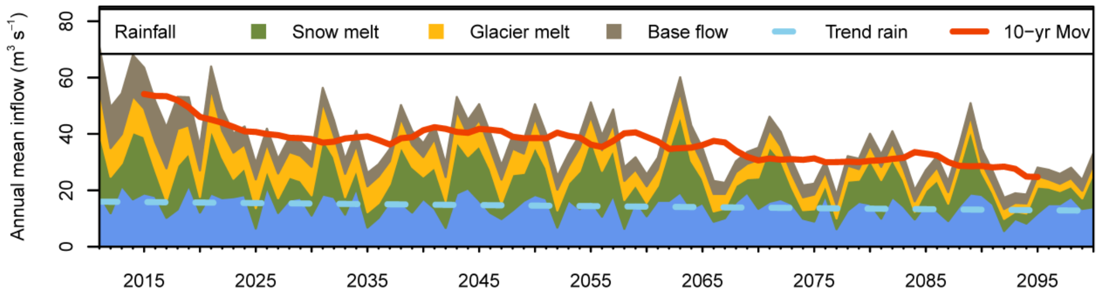

Inflow Zeravshan Valley catchment for 2011−2100, Arid scenario.

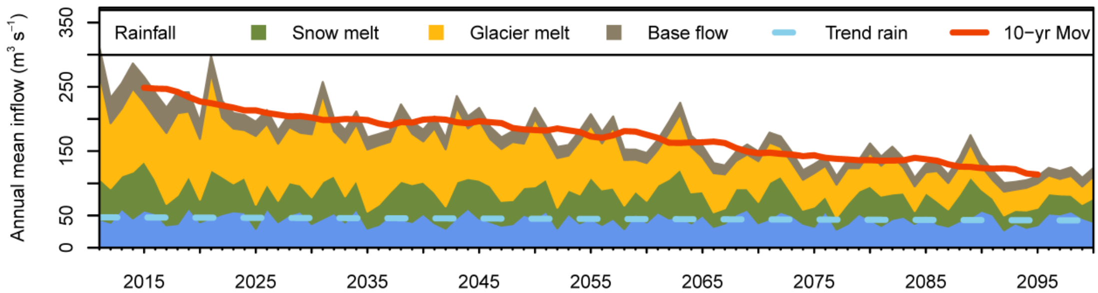

Inflow Lebap upstream catchment 1 for 2011−2100, Arid scenario.

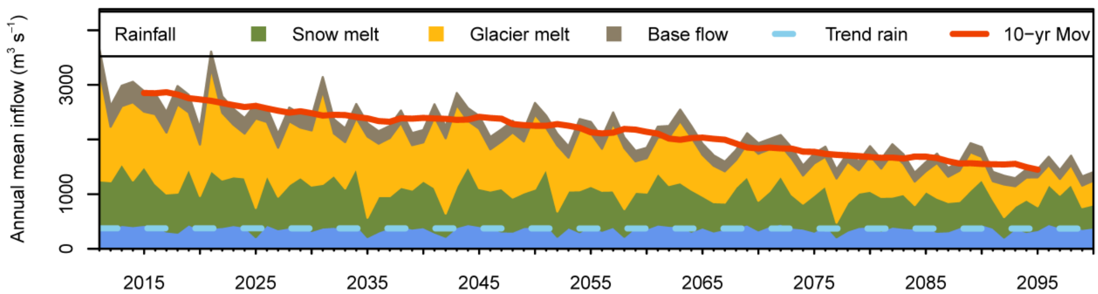

Inflow Fergana Valley catchment for 2011−2100, Arid scenario.

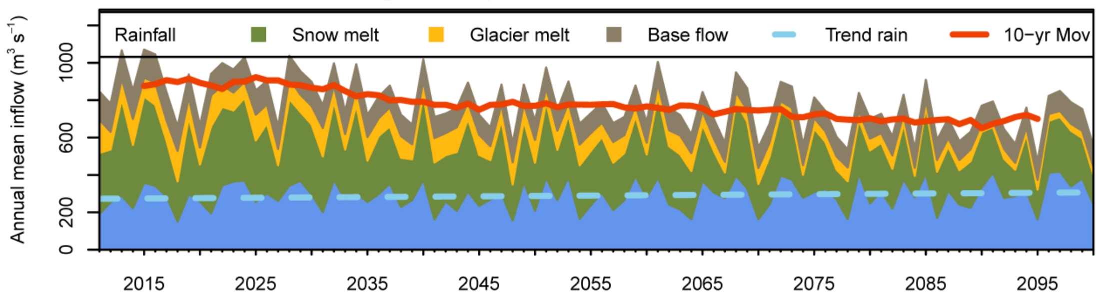

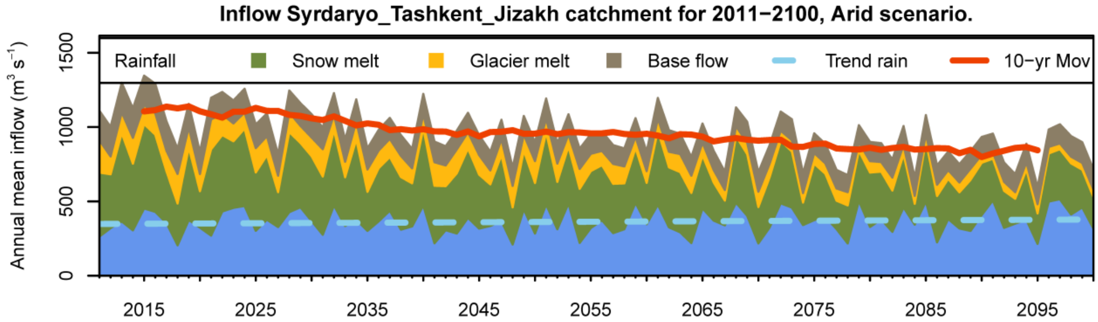
Inflow Syrdaryo_Tashkent_Jizakh catchment for 2011−2100, Arid scenario.
Rainfall
Snow melt
Glacier melt
Base flow
Trend rain
10−yr Mov
Annual mean inflow ($m^3 s^{-1}$)
0
500
1000
1500
2015
2025
2035
2045
2055
2065
2075
2085
2095

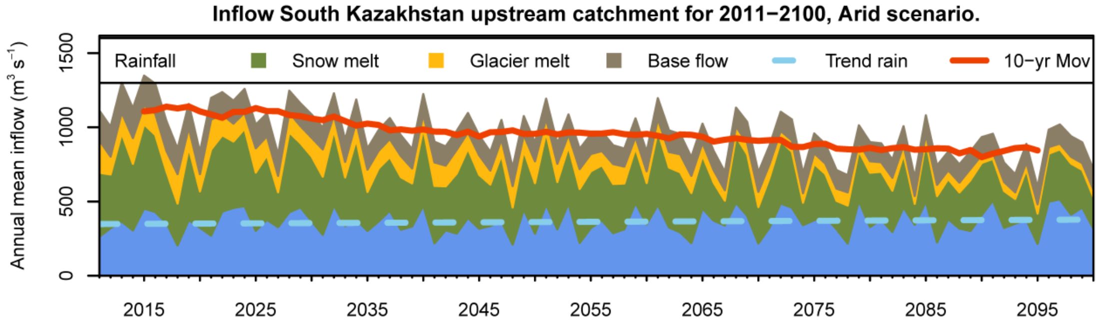
Inflow South Kazakhstan upstream catchment for 2011−2100, Arid scenario.
Rainfall
Snow melt
Glacier melt
Base flow
Trend rain
10−yr Mov
Annual mean inflow ($m^3 s^{-1}$)
0
500
1000
1500
2015
2025
2035
2045
2055
2065
2075
2085
2095

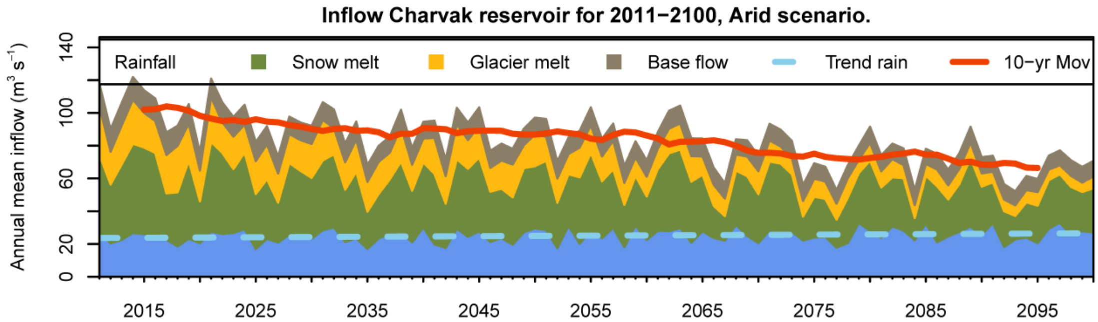
Inflow Charvak reservoir for 2011−2100, Arid scenario.
Rainfall
Snow melt
Glacier melt
Base flow
Trend rain
10−yr Mov
Annual mean inflow ($m^3 s^{-1}$)
0
20
60
100
140
2015
2025
2035
2045
2055
2065
2075
2085
2095

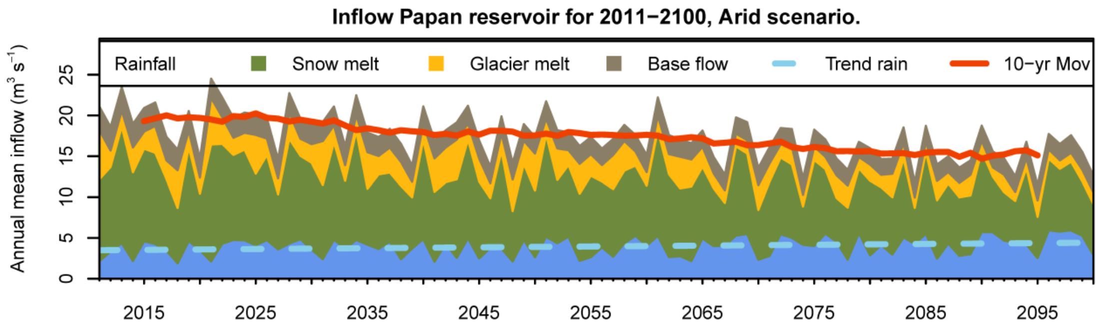
Inflow Papan reservoir for 2011−2100, Arid scenario.
Rainfall
Snow melt
Glacier melt
Base flow
Trend rain
10−yr Mov
Annual mean inflow ($m^3 s^{-1}$)
0
5
10
15
20
25
2015
2025
2035
2045
2055
2065
2075
2085
2095

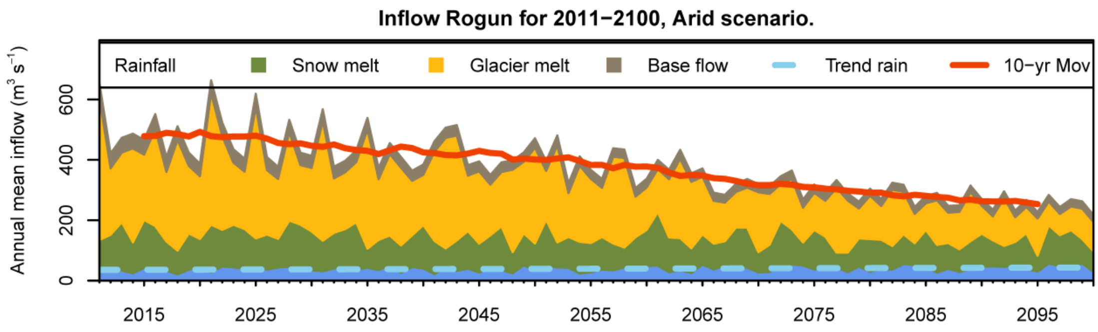

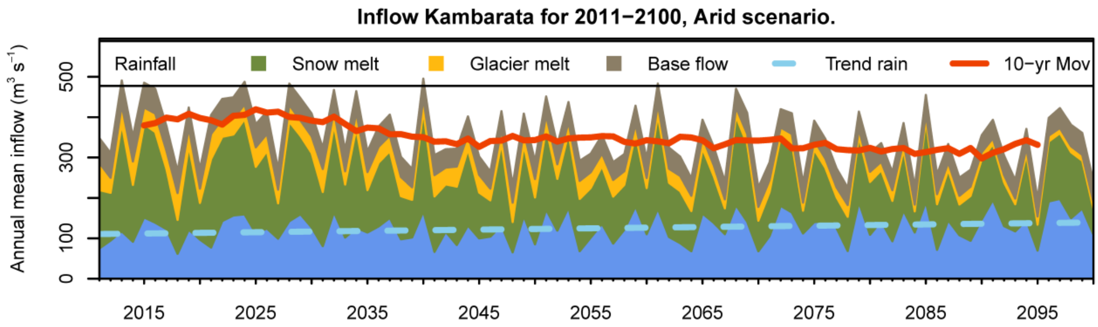

II.2 Marker scenario: Hot/dry

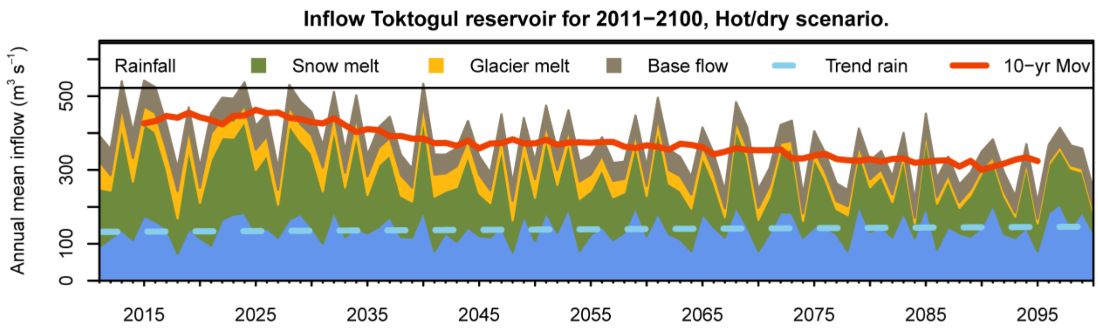

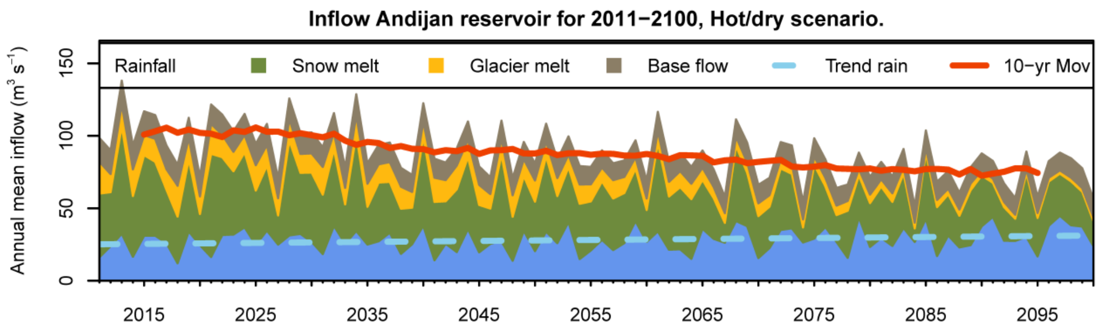

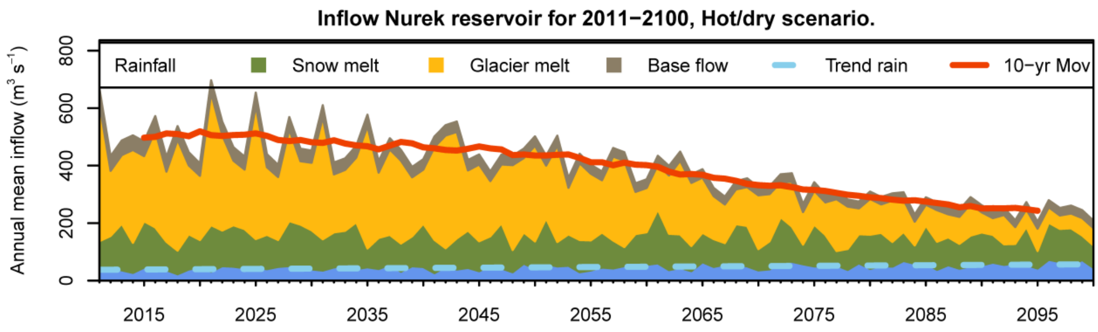
Inflow Nurek reservoir for 2011–2100, Hot/dry scenario.
Rainfall
Snow melt
Glacier melt
Base flow
Trend rain
10–yr Mov
Annual mean inflow (m3 s−1)
0
200
400
600
800
2015
2025
2035
2045
2055
2065
2075
2085
2095

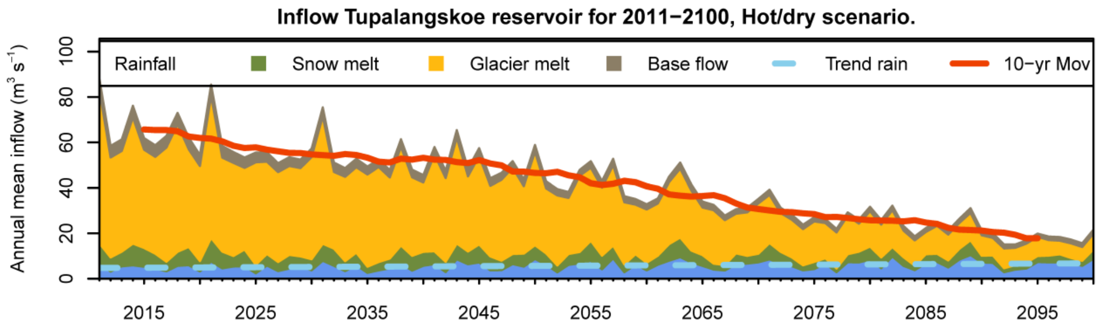
Inflow Tupalangskoe reservoir for 2011–2100, Hot/dry scenario.
Rainfall
Snow melt
Glacier melt
Base flow
Trend rain
10–yr Mov
Annual mean inflow (m3 s−1)
0
20
40
60
80
100
2015
2025
2035
2045
2055
2065
2075
2085
2095

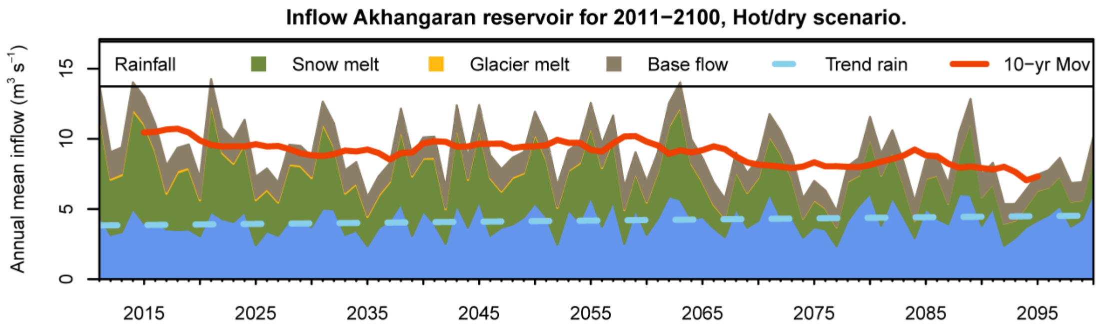
Inflow Akhangaran reservoir for 2011–2100, Hot/dry scenario.
Rainfall
Snow melt
Glacier melt
Base flow
Trend rain
10–yr Mov
Annual mean inflow (m3 s−1)
0
5
10
15
2015
2025
2035
2045
2055
2065
2075
2085
2095

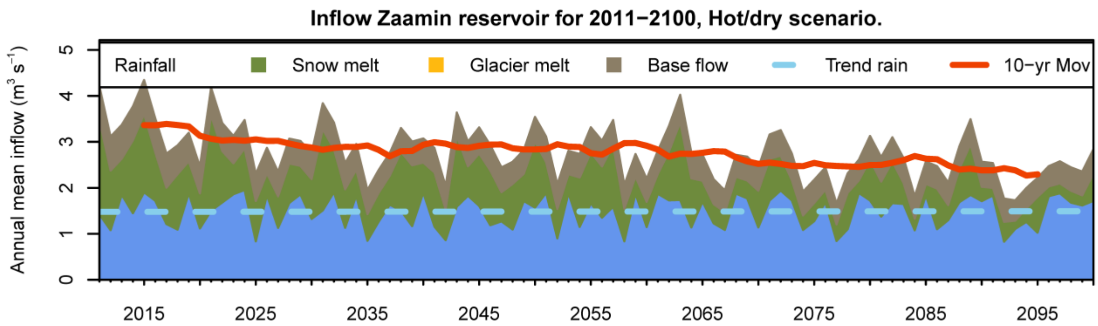
Inflow Zaamin reservoir for 2011–2100, Hot/dry scenario.
Rainfall
Snow melt
Glacier melt
Base flow
Trend rain
10–yr Mov
Annual mean inflow (m3 s−1)
0
1
2
3
4
5
2015
2025
2035
2045
2055
2065
2075
2085
2095

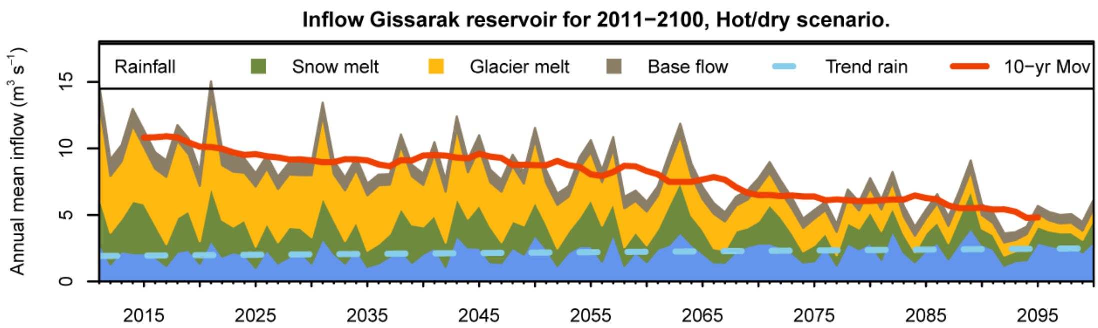
Inflow Gissarak reservoir for 2011–2100, Hot/dry scenario.
Rainfall
Snow melt
Glacier melt
Base flow
Trend rain
10–yr Mov
Annual mean inflow (m3 s−1)
0
5
10
15
2015
2025
2035
2045
2055
2065
2075
2085
2095

Inflow Pachkamar reservoir for 2011–2100, Hot/dry scenario.

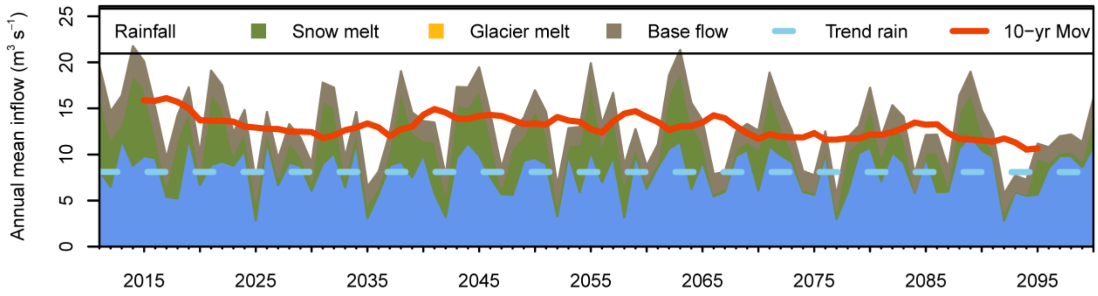

Inflow Kulyab catchment for 2011–2100, Hot/dry scenario.

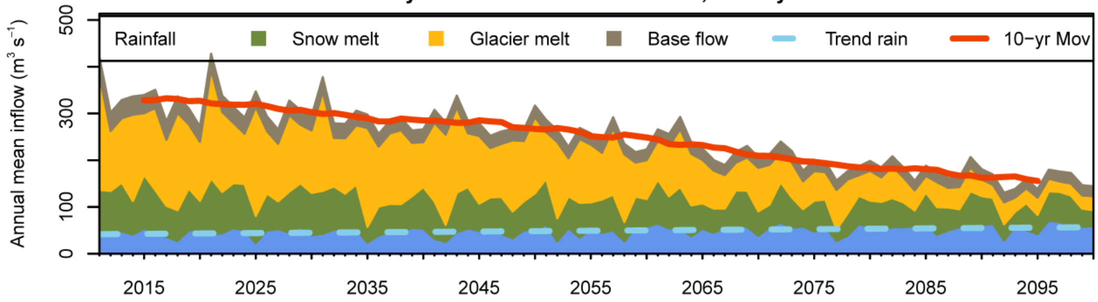

Inflow Kurgantube catchment for 2011–2100, Hot/dry scenario.

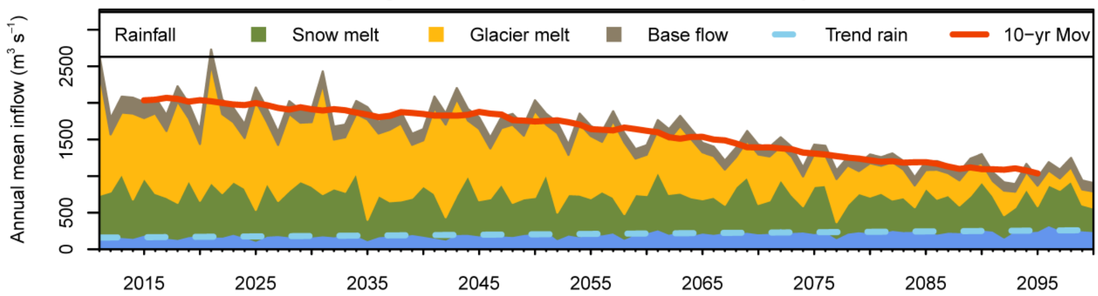

Inflow Dushanbe catchment for 2011–2100, Hot/dry scenario.

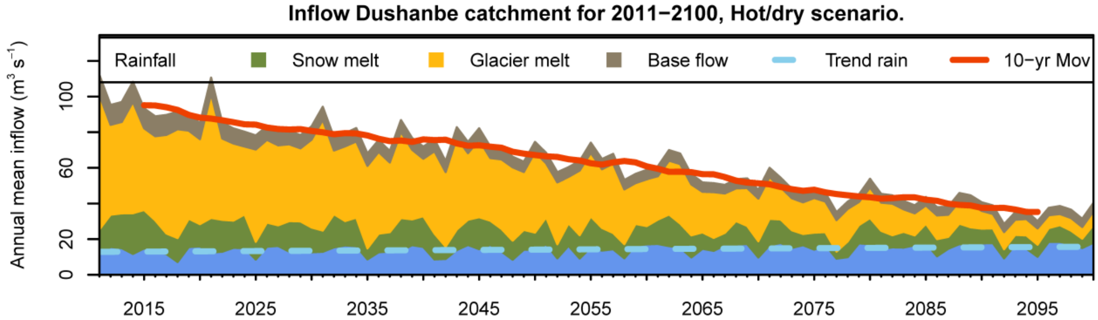

Inflow Surkhandarya upstream catchment for 2011–2100, Hot/dry scenario.

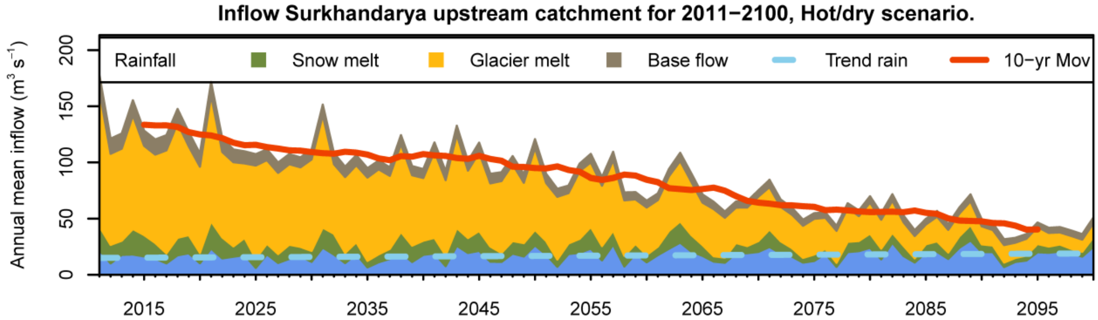

Inflow Surkhandarya downstream catchment for 2011−2100, Hot/dry scenario.

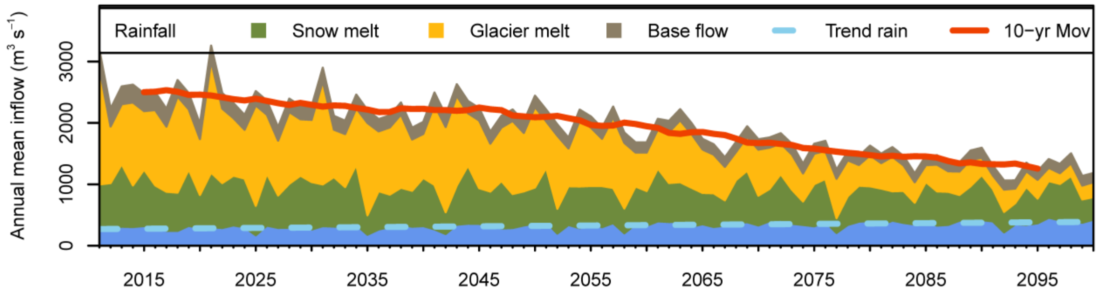

Inflow Karukum kanal catchment for 2011−2100, Hot/dry scenario.

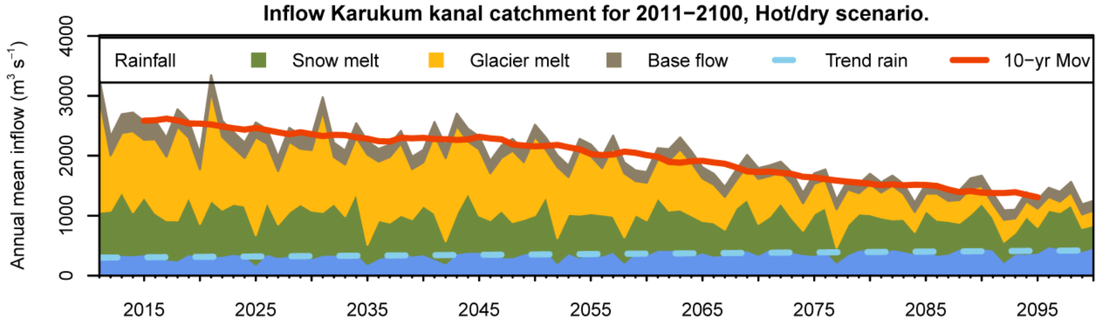

Inflow Kashkadarya upstream catchment for 2011−2100, Hot/dry scenario.

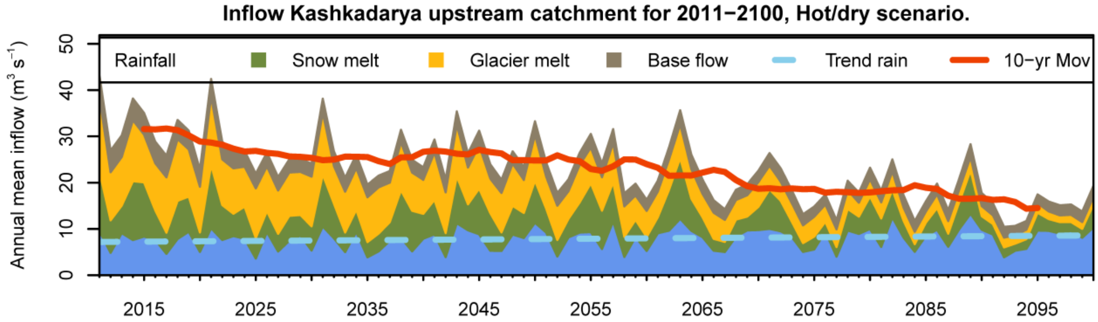

Inflow Kashkadarya downstream catchment for 2011−2100, Hot/dry scenario.

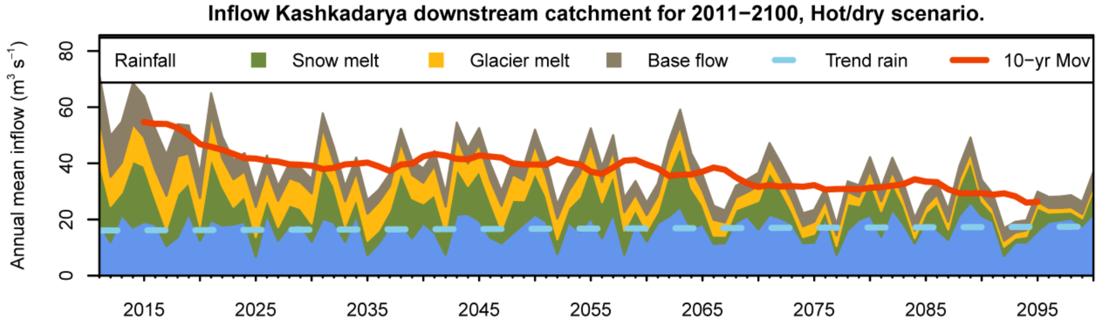

Inflow Zeravshan Valley catchment for 2011−2100, Hot/dry scenario.

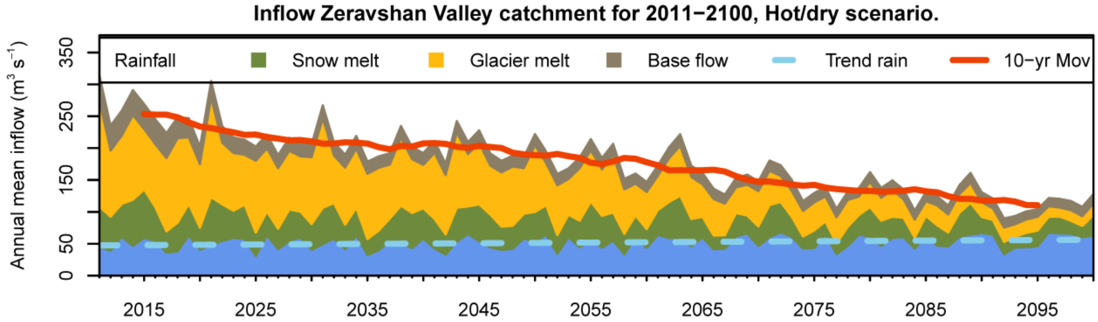

Inflow Lebap upstream catchment 1 for 2011−2100, Hot/dry scenario.

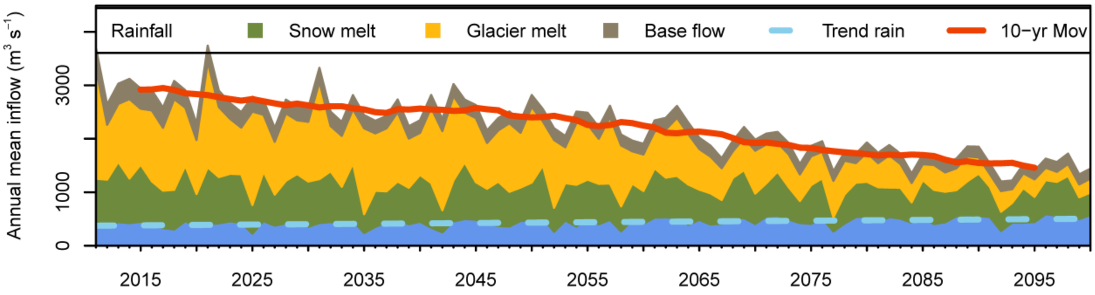

Inflow Fergana Valley catchment for 2011−2100, Hot/dry scenario.

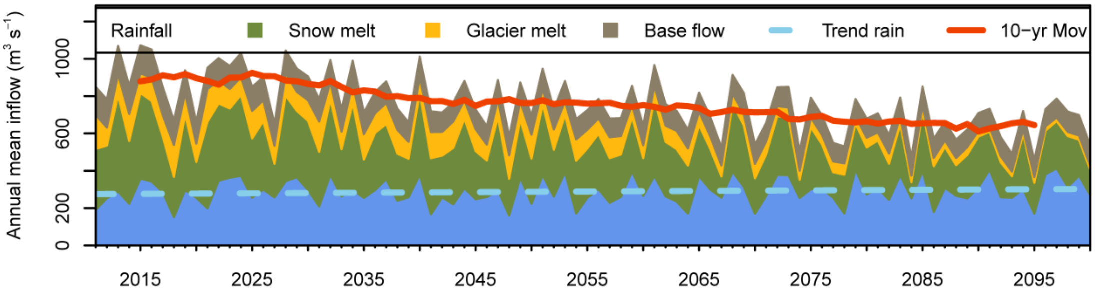

Inflow Syrdaryo_Tashkent_Jizakh catchment for 2011−2100, Hot/dry scenario.

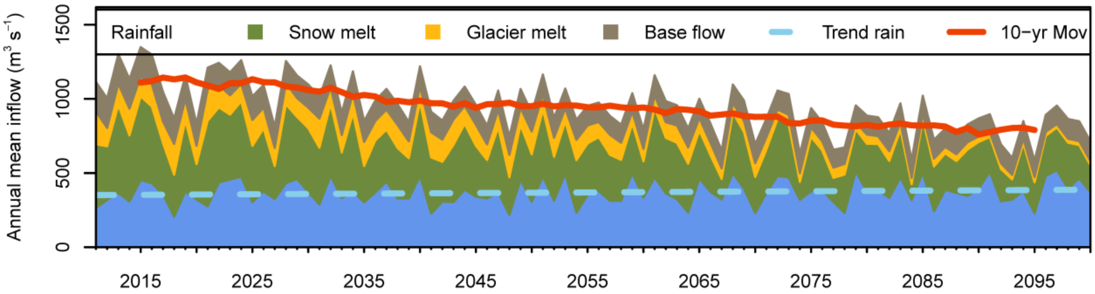

Inflow South Kazakhstan upstream catchment for 2011−2100, Hot/dry scenario.

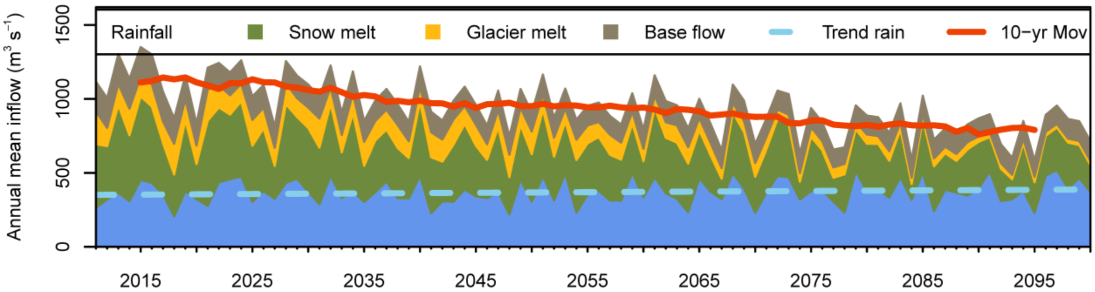

Inflow Charvak reservoir for 2011−2100, Hot/dry scenario.

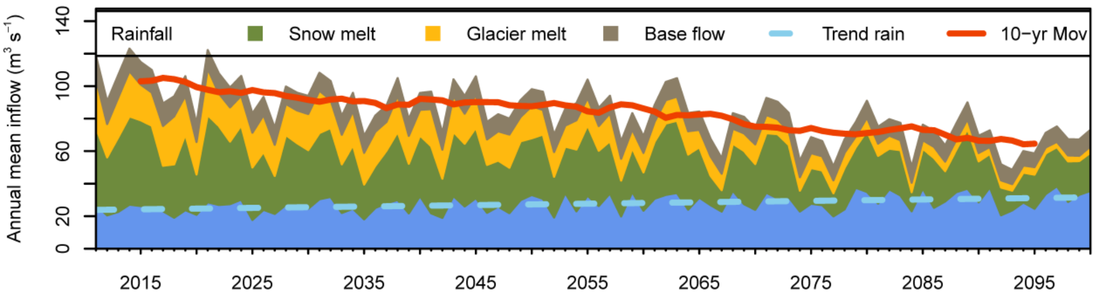

Inflow Papan reservoir for 2011−2100, Hot/dry scenario.

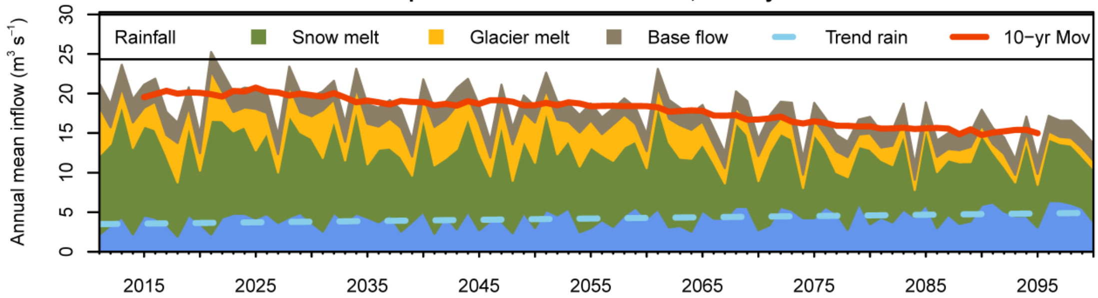

Inflow Rogun for 2011−2100, Hot/dry scenario.

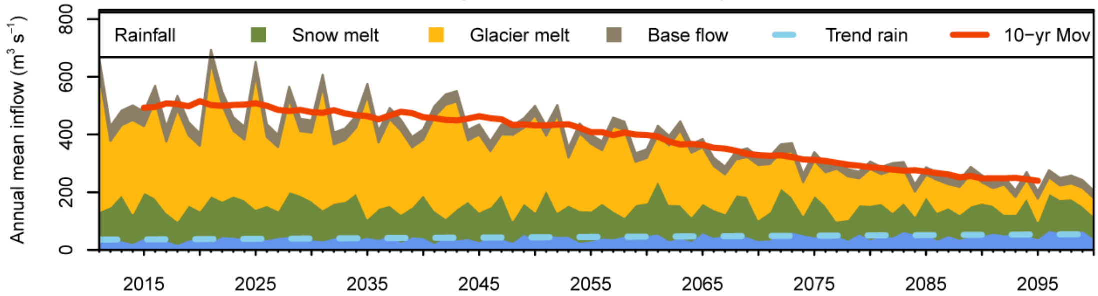

Inflow Kambarata for 2011−2100, Hot/dry scenario.

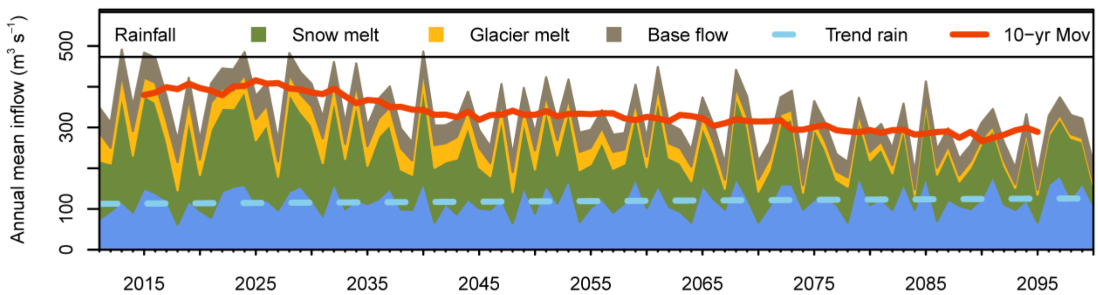

II.3 Marker scenario: Central

Inflow Toktogul reservoir for 2011–2100, Central scenario.

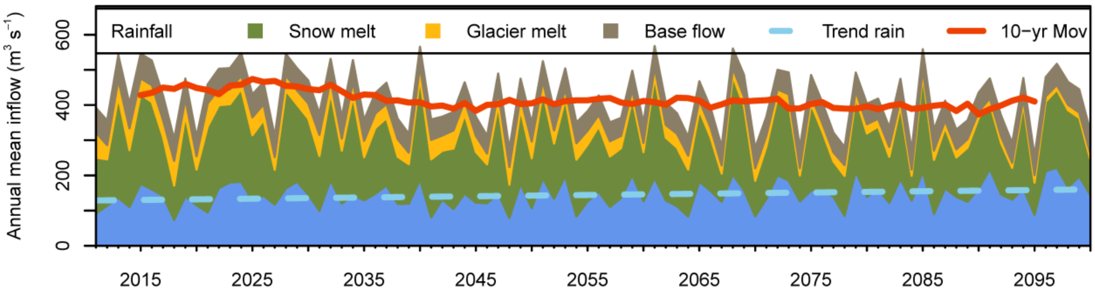

Inflow Andijan reservoir for 2011–2100, Central scenario.

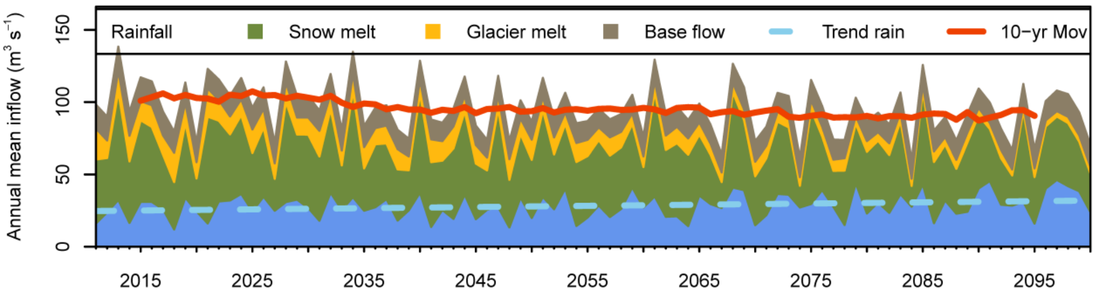

Inflow Nurek reservoir for 2011–2100, Central scenario.

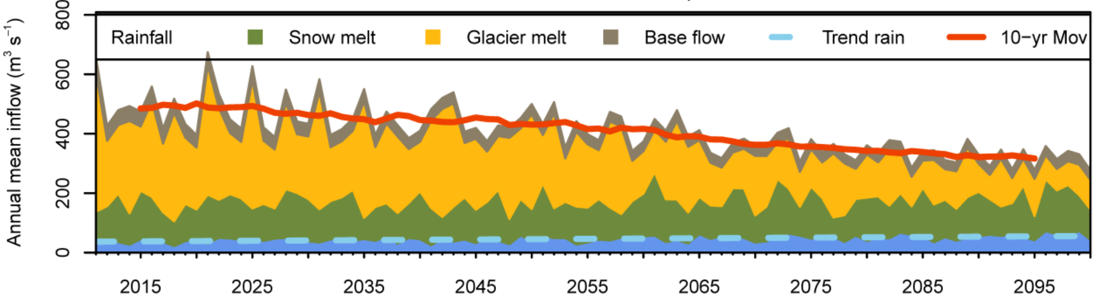

Inflow Tupalangskoe reservoir for 2011–2100, Central scenario.

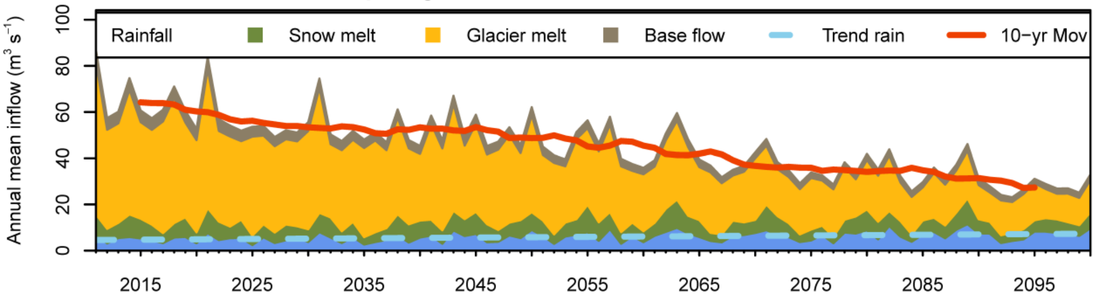

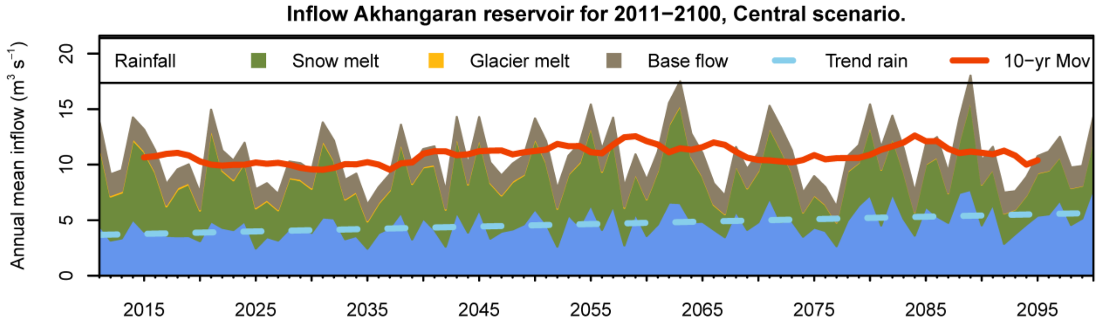
Inflow Akhangaran reservoir for 2011−2100, Central scenario.
Rainfall
Snow melt
Glacier melt
Base flow
Trend rain
10−yr Mov
Annual mean inflow ($m^3 s^{-1}$)
0
5
10
15
20
2015
2025
2035
2045
2055
2065
2075
2085
2095

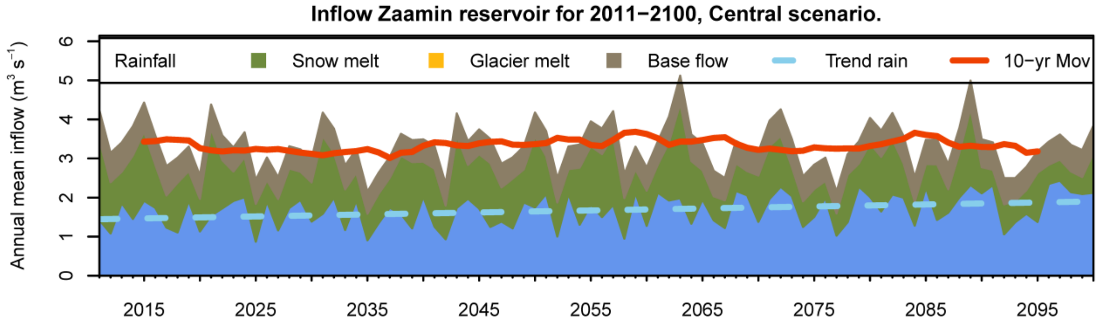
Inflow Zaamin reservoir for 2011−2100, Central scenario.
Rainfall
Snow melt
Glacier melt
Base flow
Trend rain
10−yr Mov
Annual mean inflow ($m^3 s^{-1}$)
0
1
2
3
4
5
6
2015
2025
2035
2045
2055
2065
2075
2085
2095

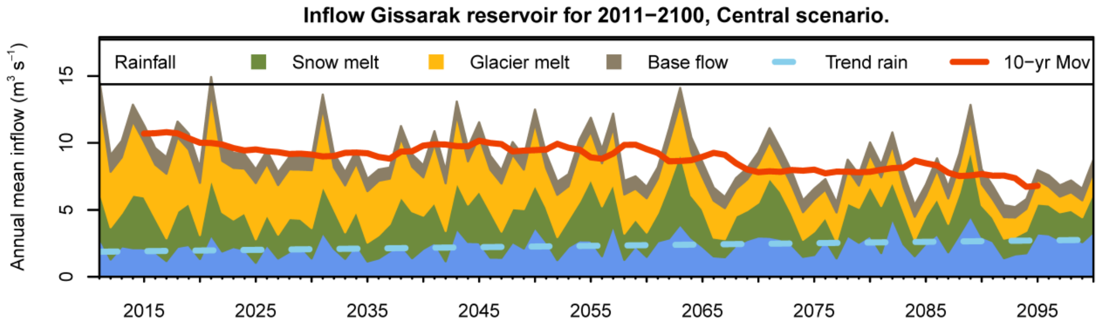
Inflow Gissarak reservoir for 2011−2100, Central scenario.
Rainfall
Snow melt
Glacier melt
Base flow
Trend rain
10−yr Mov
Annual mean inflow ($m^3 s^{-1}$)
0
5
10
15
2015
2025
2035
2045
2055
2065
2075
2085
2095

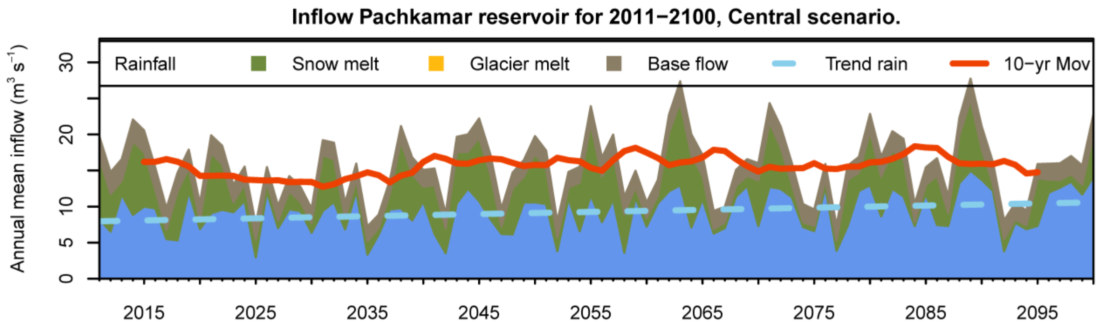
Inflow Pachkamar reservoir for 2011−2100, Central scenario.
Rainfall
Snow melt
Glacier melt
Base flow
Trend rain
10−yr Mov
Annual mean inflow ($m^3 s^{-1}$)
0
5
10
20
30
2015
2025
2035
2045
2055
2065
2075
2085
2095

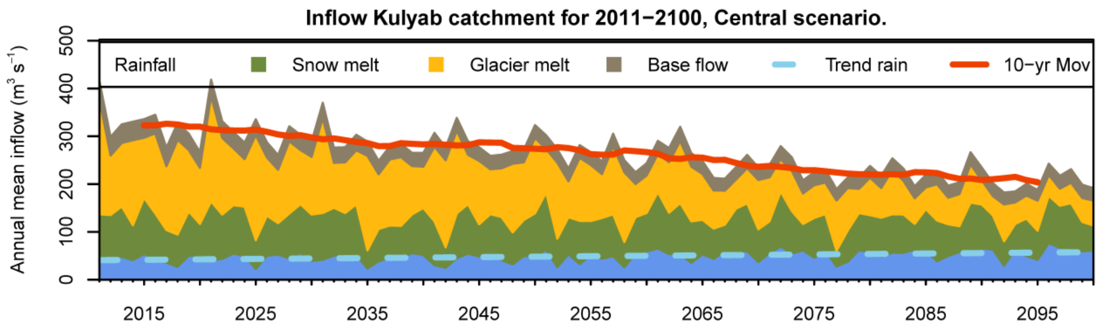
Inflow Kulyab catchment for 2011−2100, Central scenario.
Rainfall
Snow melt
Glacier melt
Base flow
Trend rain
10−yr Mov
Annual mean inflow ($m^3 s^{-1}$)
0
100
200
300
400
500
2015
2025
2035
2045
2055
2065
2075
2085
2095

Inflow Kurgantube catchment for 2011−2100, Central scenario.

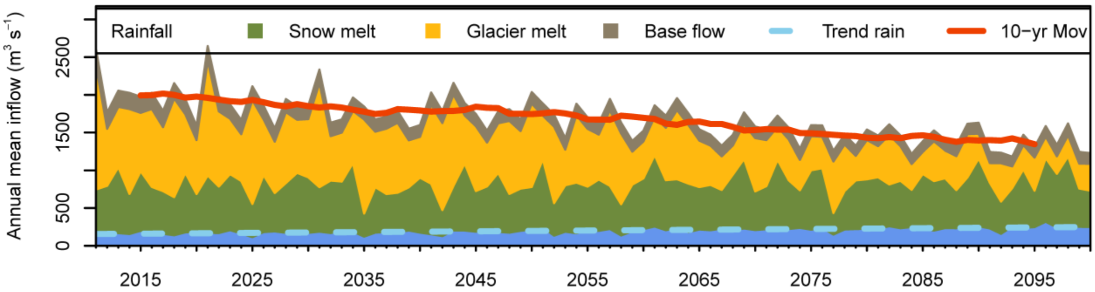

Inflow Dushanbe catchment for 2011−2100, Central scenario.

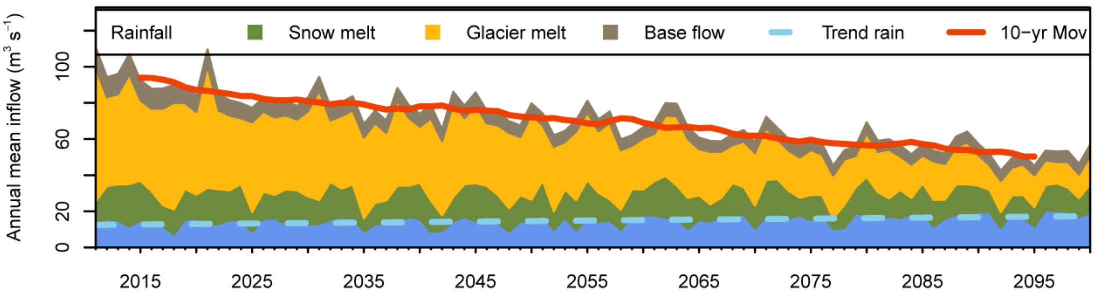

Inflow Surkhandarya upstream catchment for 2011−2100, Central scenario.

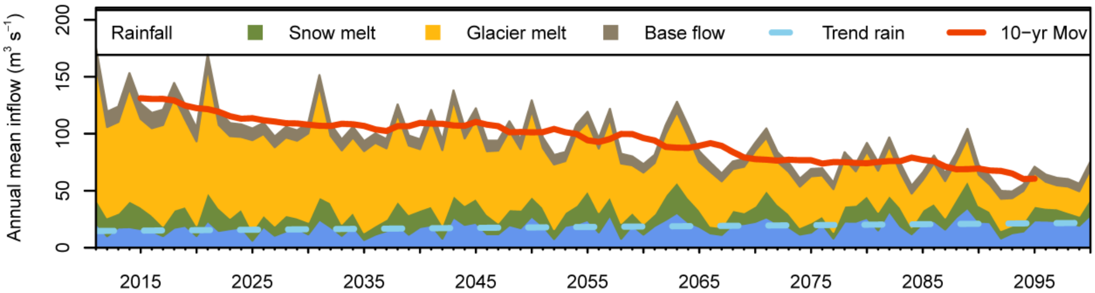

Inflow Surkhandarya downstream catchment for 2011−2100, Central scenario.

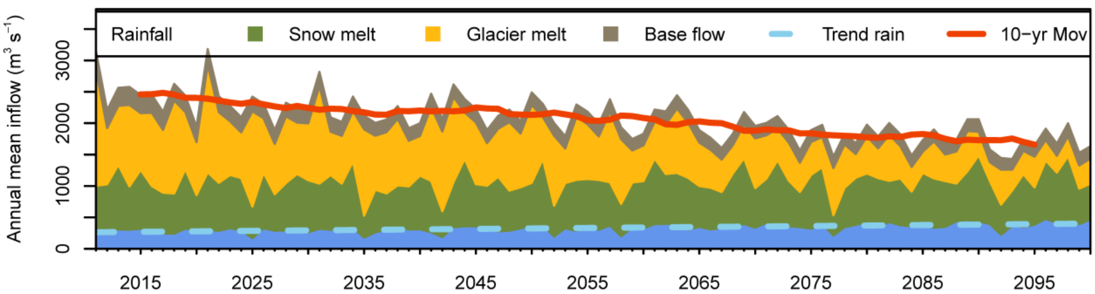

Inflow Karukum kanal catchment for 2011−2100, Central scenario.

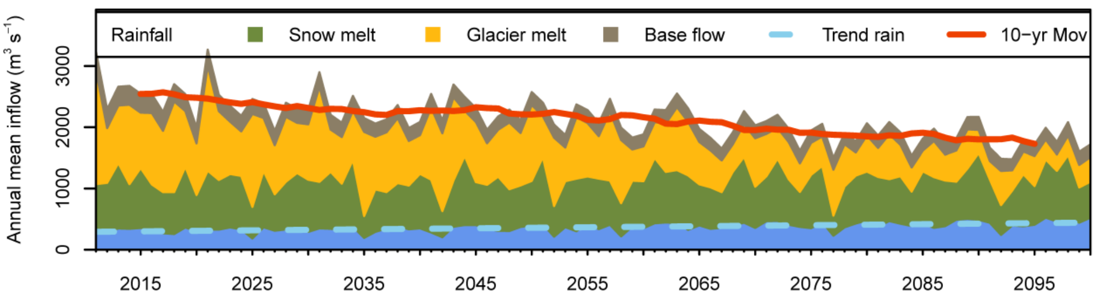

Inflow Kashkadarya upstream catchment for 2011−2100, Central scenario.

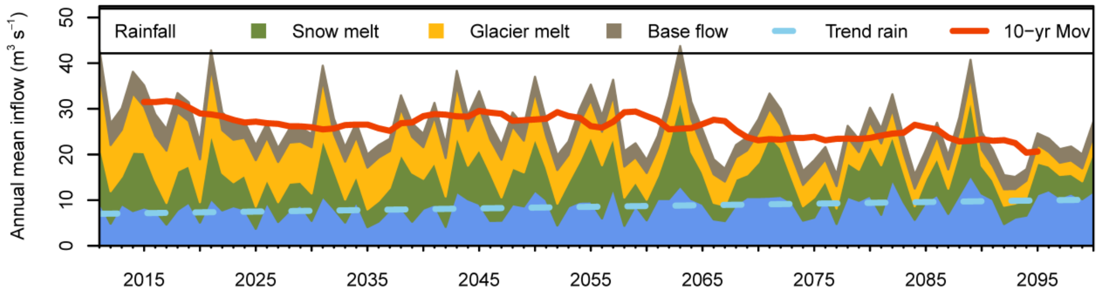

Inflow Kashkadarya downstream catchment for 2011−2100, Central scenario.

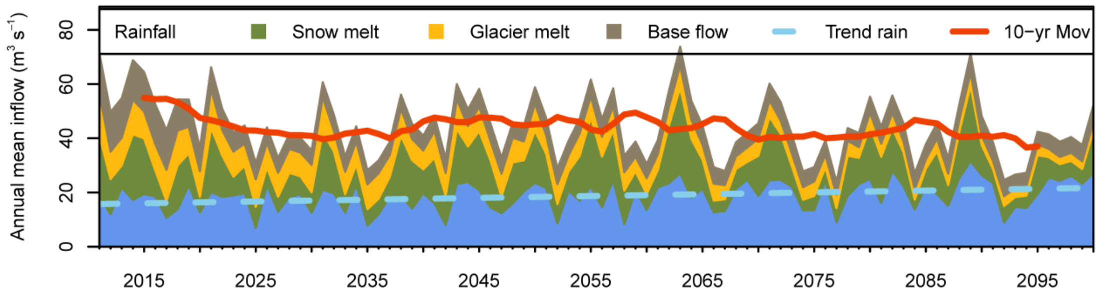

Inflow Zeravshan Valley catchment for 2011−2100, Central scenario.

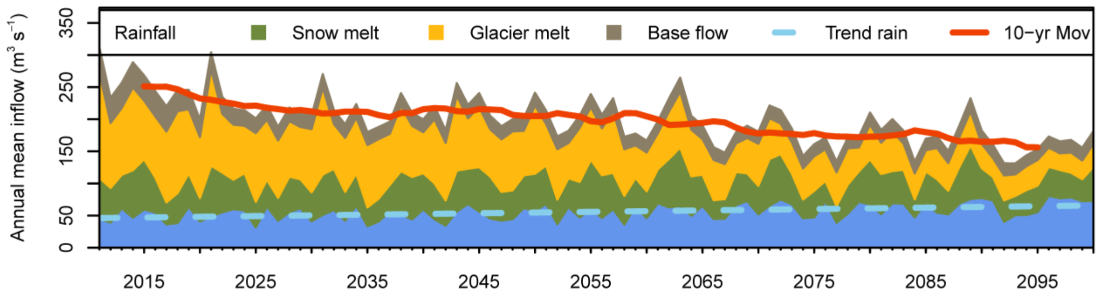

Inflow Lebap upstream catchment 1 for 2011−2100, Central scenario.

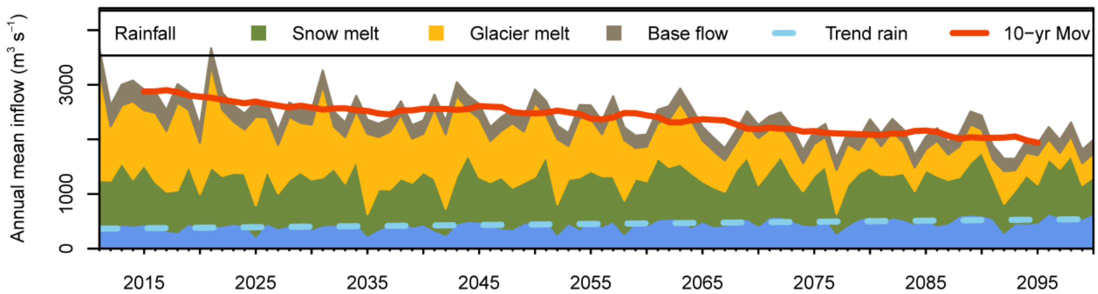

Inflow Fergana Valley catchment for 2011−2100, Central scenario.

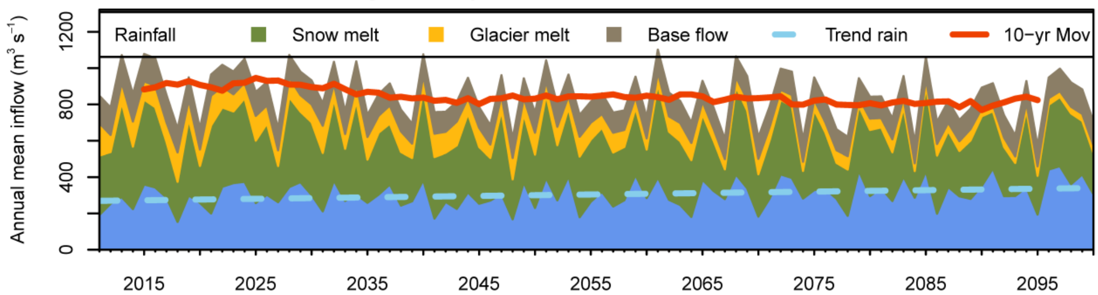

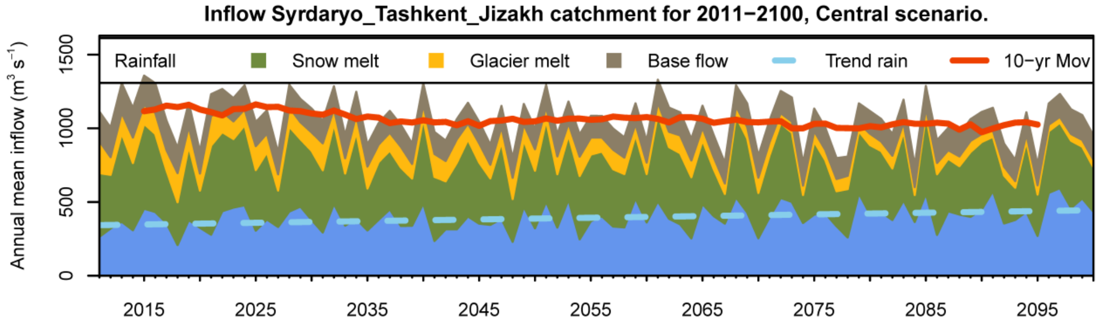
Inflow Syrdaryo_Tashkent_Jizakh catchment for 2011−2100, Central scenario.
Rainfall
Snow melt
Glacier melt
Base flow
Trend rain
10−yr Mov
Annual mean inflow (m³ s⁻¹)
0
500
1000
1500
2015
2025
2035
2045
2055
2065
2075
2085
2095

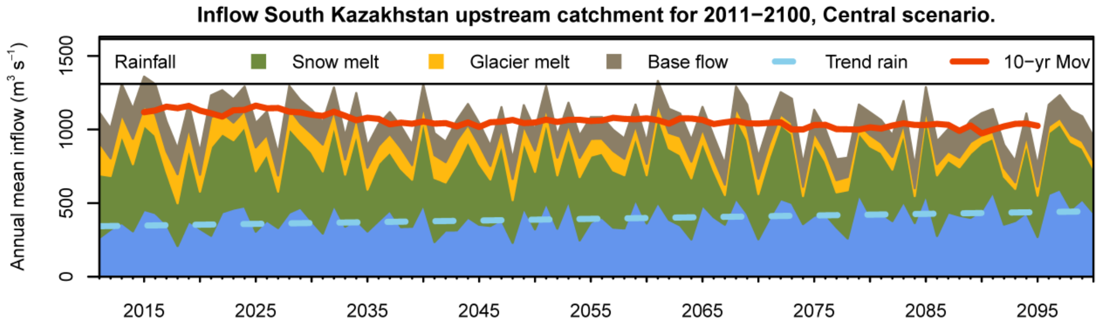
Inflow South Kazakhstan upstream catchment for 2011−2100, Central scenario.
Rainfall
Snow melt
Glacier melt
Base flow
Trend rain
10−yr Mov
Annual mean inflow (m³ s⁻¹)
0
500
1000
1500
2015
2025
2035
2045
2055
2065
2075
2085
2095

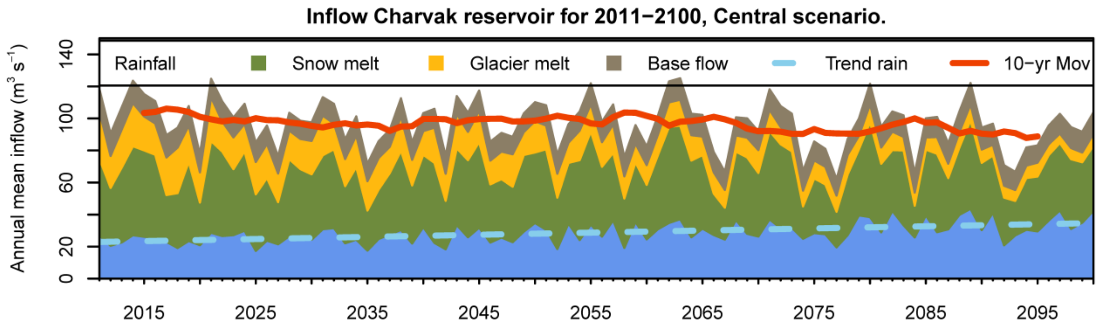
Inflow Charvak reservoir for 2011−2100, Central scenario.
Rainfall
Snow melt
Glacier melt
Base flow
Trend rain
10−yr Mov
Annual mean inflow (m³ s⁻¹)
0
20
60
100
140
2015
2025
2035
2045
2055
2065
2075
2085
2095

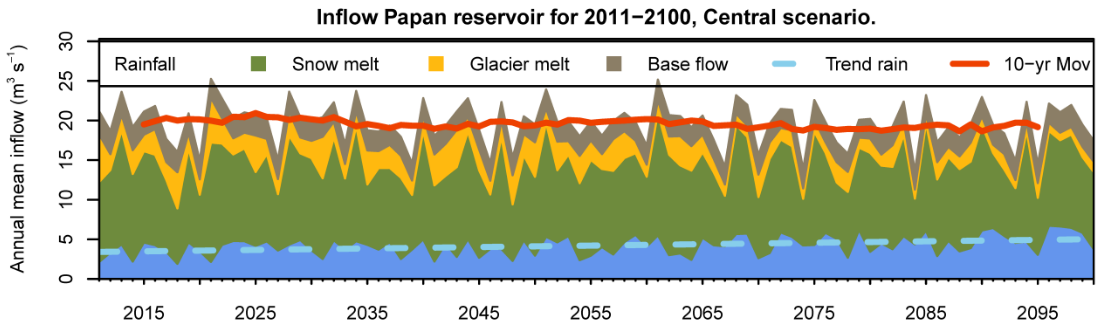
Inflow Papan reservoir for 2011−2100, Central scenario.
Rainfall
Snow melt
Glacier melt
Base flow
Trend rain
10−yr Mov
Annual mean inflow (m³ s⁻¹)
0
5
10
15
20
25
30
2015
2025
2035
2045
2055
2065
2075
2085
2095

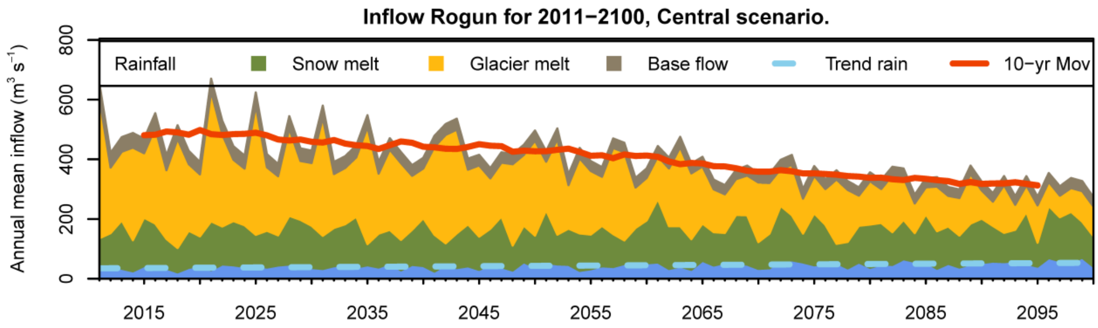

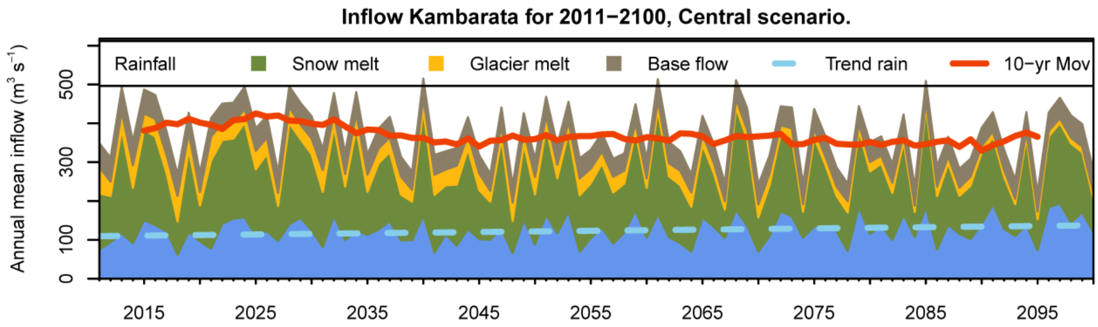

II.4 Marker scenario: Warm/wet

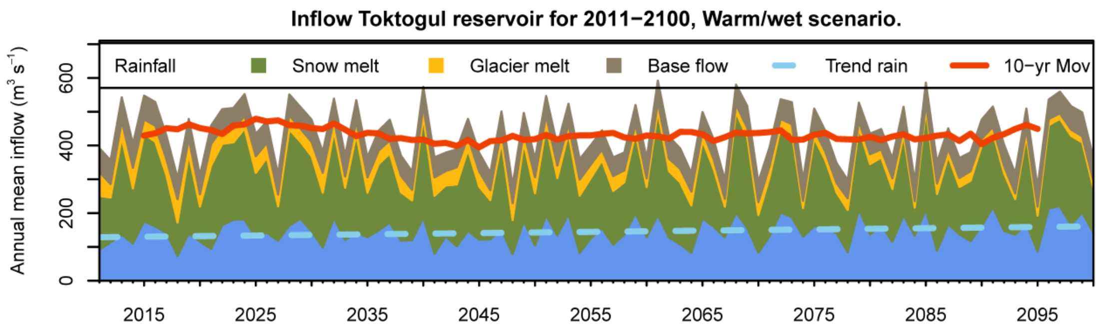

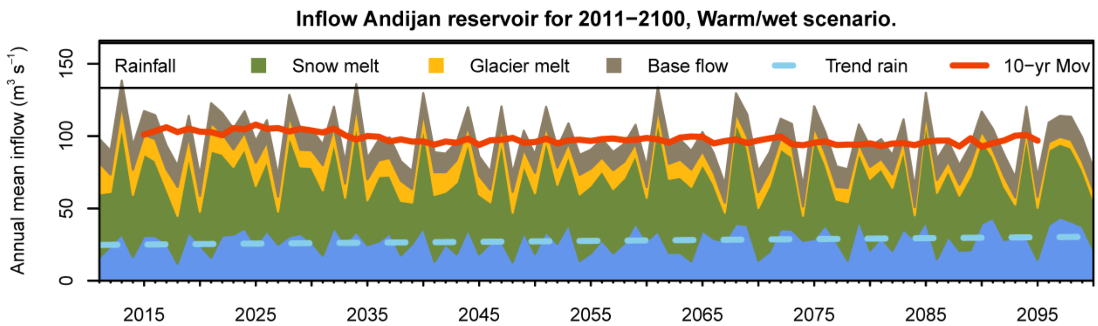

Inflow Nurek reservoir for 2011−2100, Warm/wet scenario.

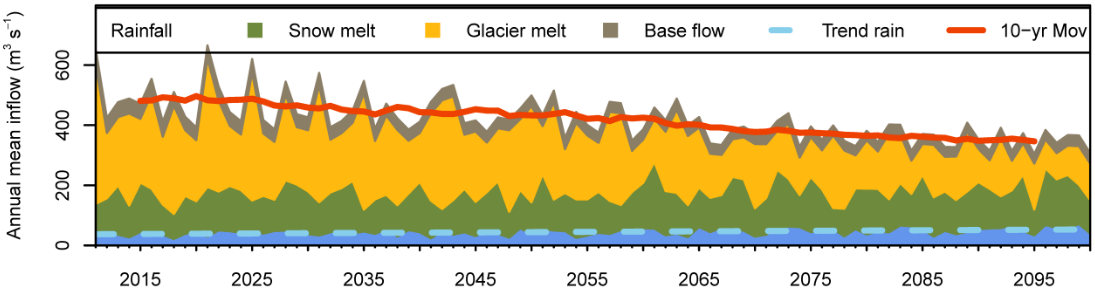

Inflow Tupalangskoe reservoir for 2011−2100, Warm/wet scenario.

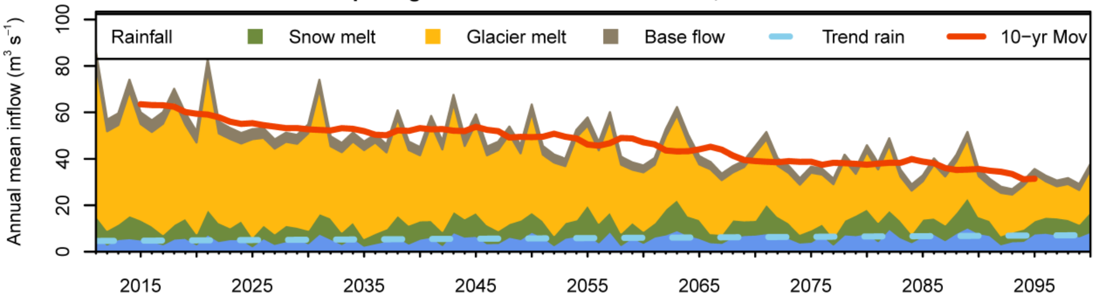

Inflow Akhangaran reservoir for 2011−2100, Warm/wet scenario.

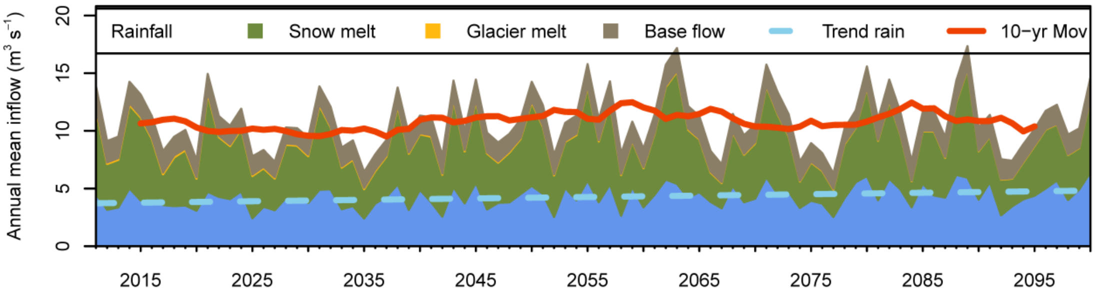

Inflow Zaamin reservoir for 2011−2100, Warm/wet scenario.

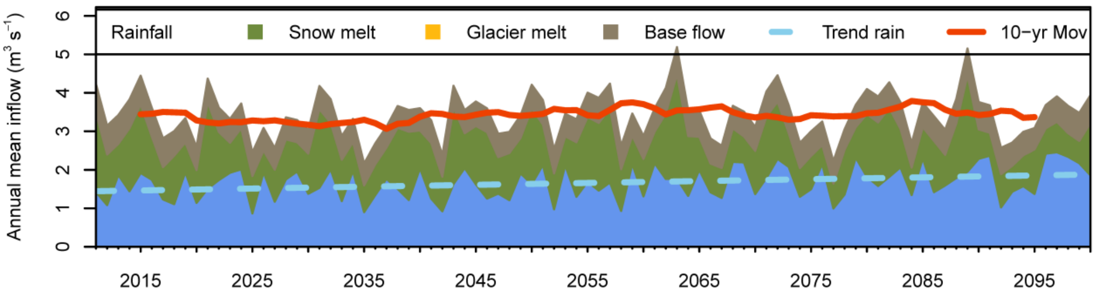

Inflow Gissarak reservoir for 2011−2100, Warm/wet scenario.

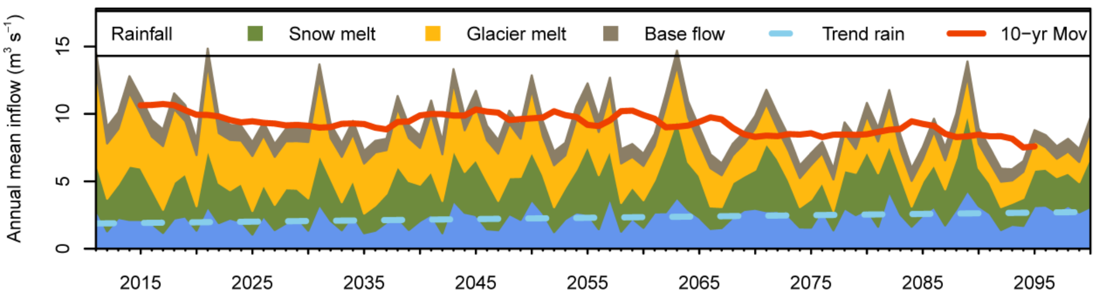

Inflow Pachkamar reservoir for 2011−2100, Warm/wet scenario.

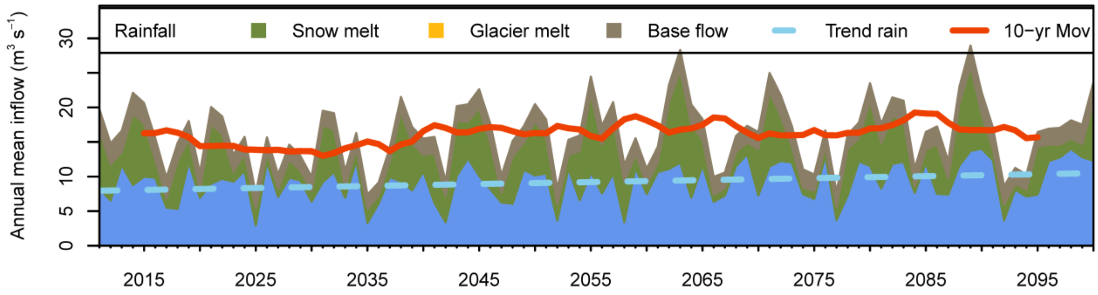

Inflow Kulyab catchment for 2011−2100, Warm/wet scenario.

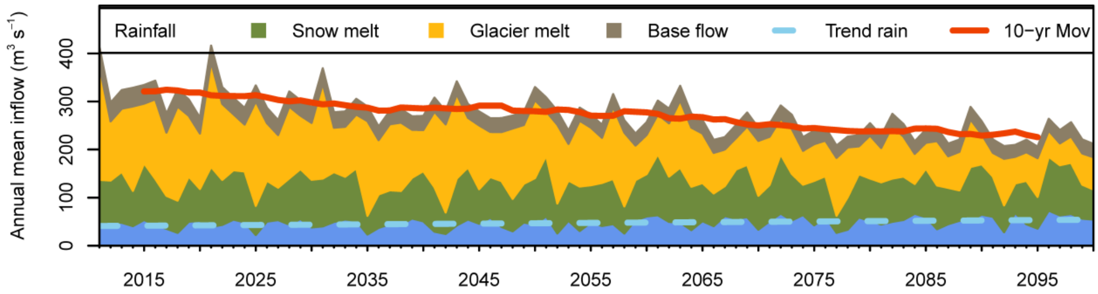

Inflow Kurgantube catchment for 2011−2100, Warm/wet scenario.

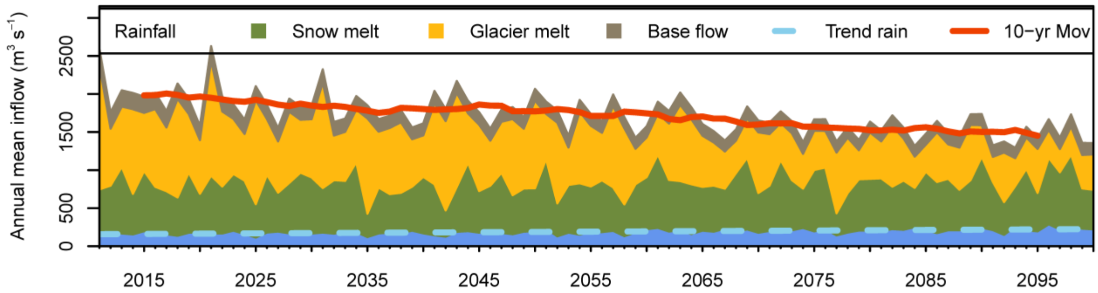

Inflow Dushanbe catchment for 2011−2100, Warm/wet scenario.

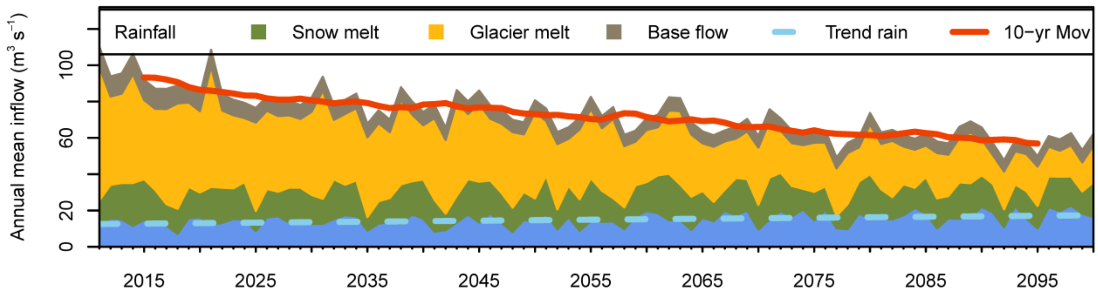

Inflow Surkhandarya upstream catchment for 2011−2100, Warm/wet scenario.

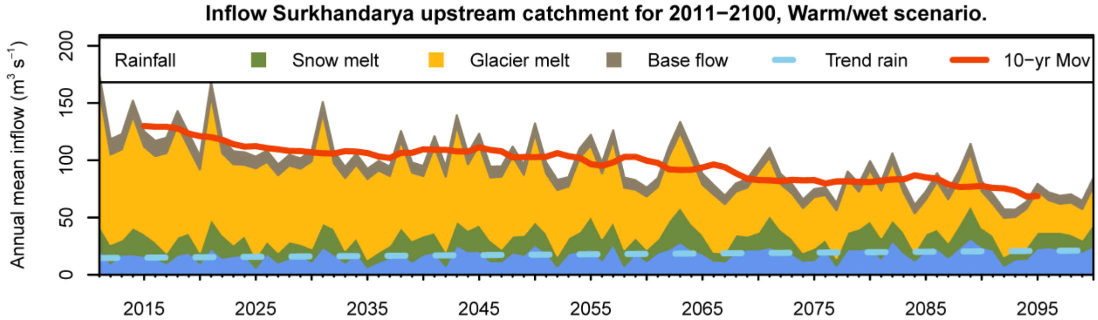

Inflow Surkhandarya downstream catchment for 2011−2100, Warm/wet scenario.

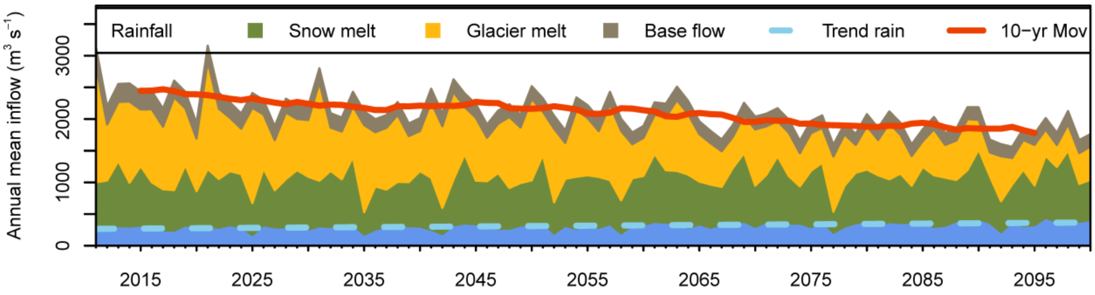

Inflow Karukum kanal catchment for 2011−2100, Warm/wet scenario.

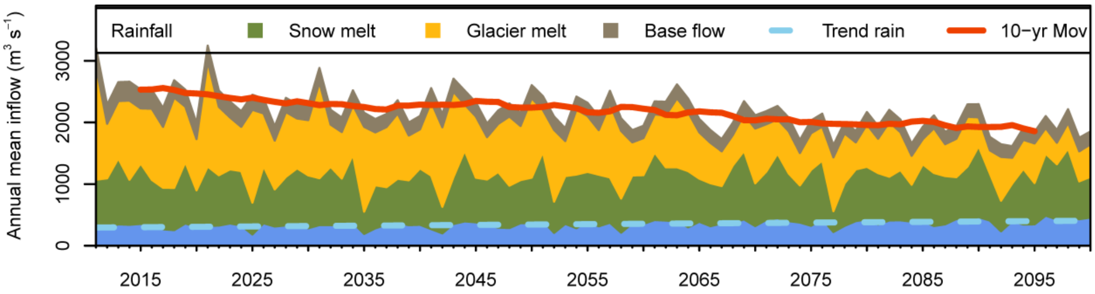

Inflow Kashkadarya upstream catchment for 2011−2100, Warm/wet scenario.

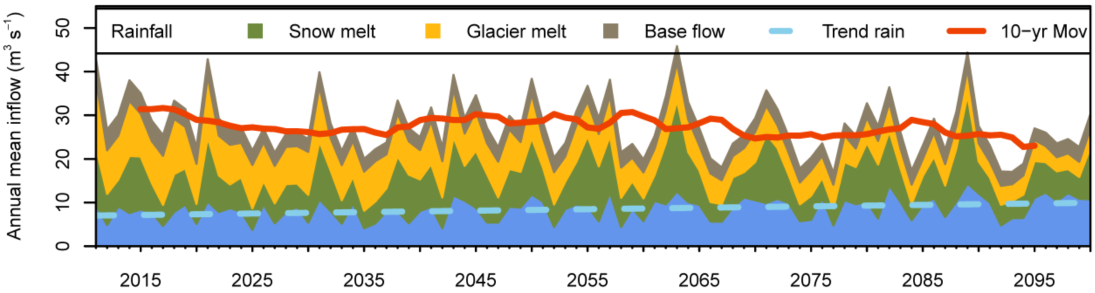

Inflow Kashkadarya downstream catchment for 2011−2100, Warm/wet scenario.

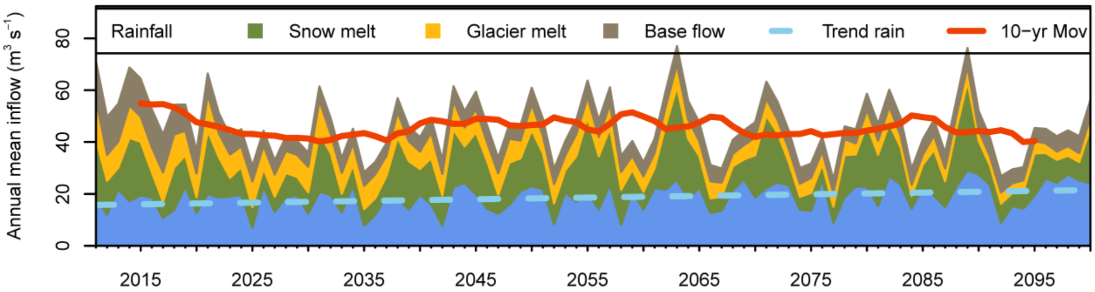

Inflow Zeravshan Valley catchment for 2011−2100, Warm/wet scenario.

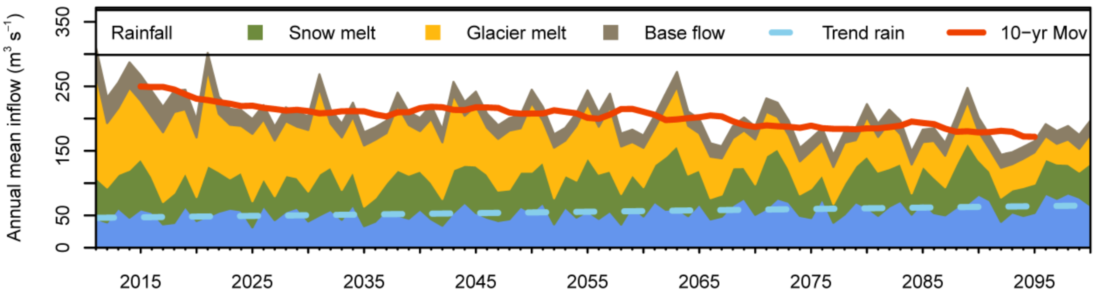

Inflow Lebap upstream catchment 1 for 2011–2100, Warm/wet scenario.

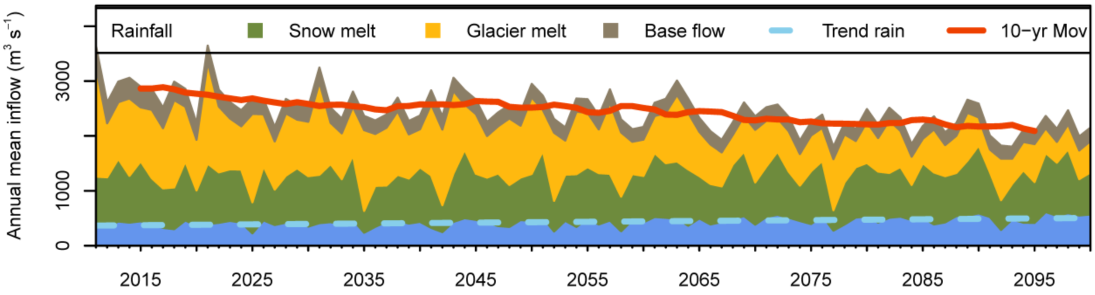

Inflow Fergana Valley catchment for 2011–2100, Warm/wet scenario.

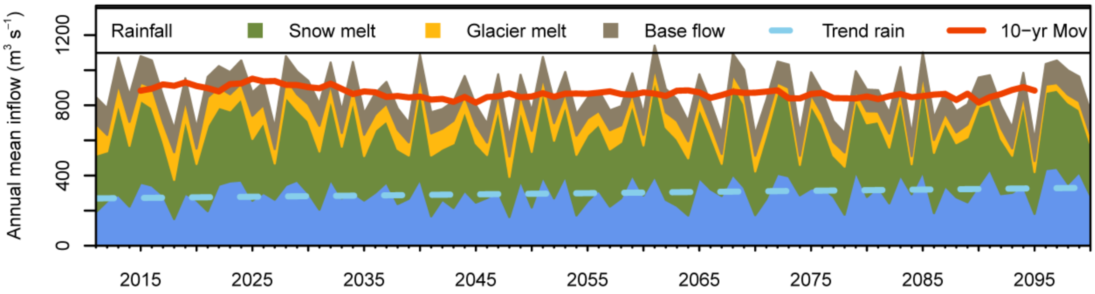

Inflow Syrdaryo_Tashkent_Jizakh catchment for 2011–2100, Warm/wet scenario.

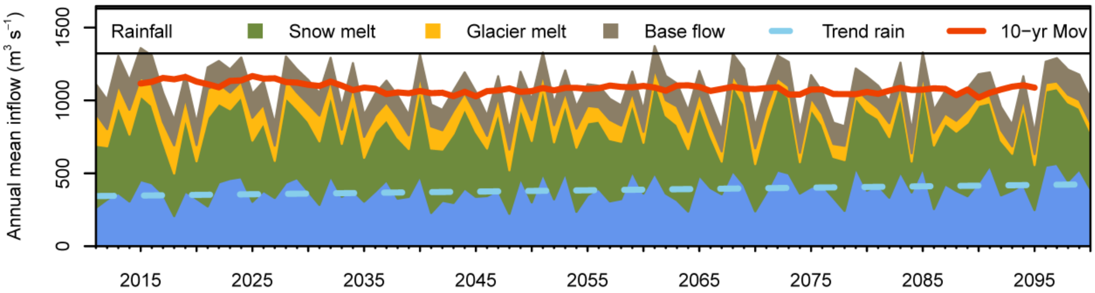

Inflow South Kazakhstan upstream catchment for 2011–2100, Warm/wet scenario.

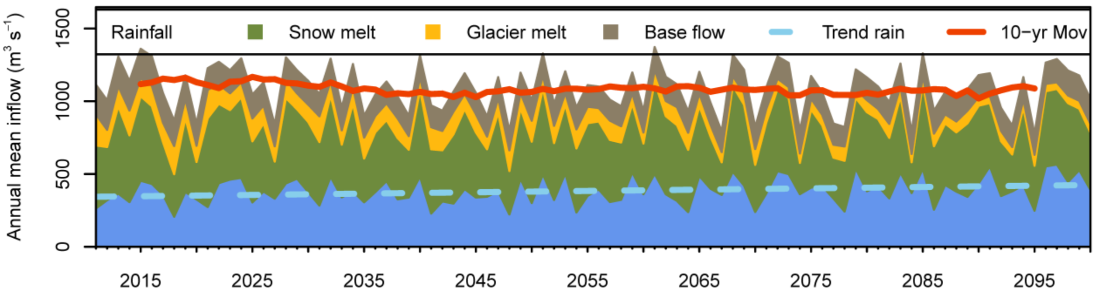

Inflow Charvak reservoir for 2011–2100, Warm/wet scenario.

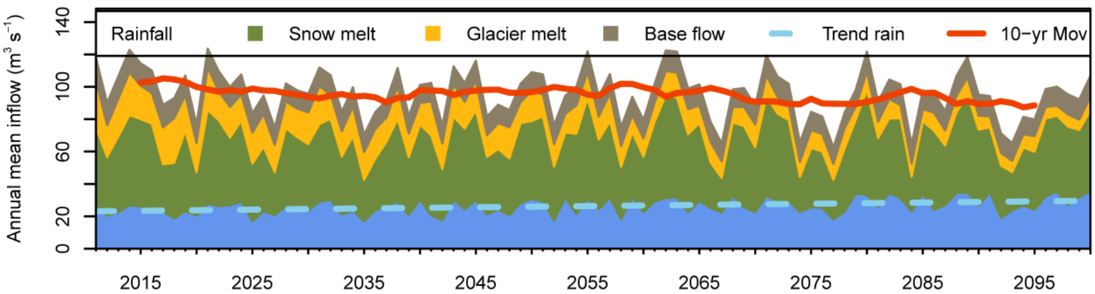

Inflow Papan reservoir for 2011−2100, Warm/wet scenario.

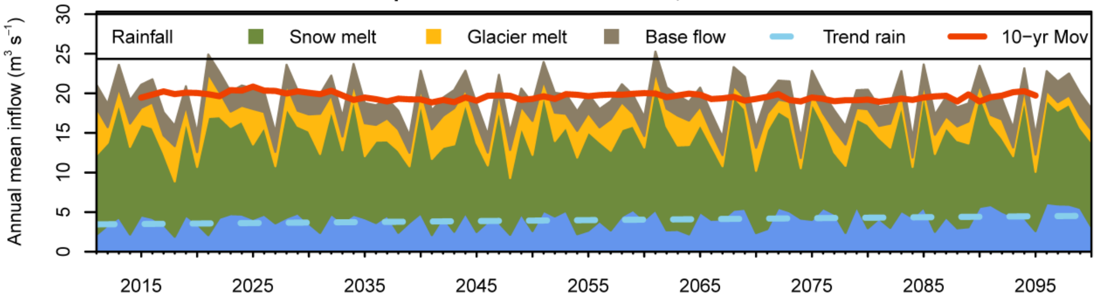

Inflow Rogun for 2011−2100, Warm/wet scenario.

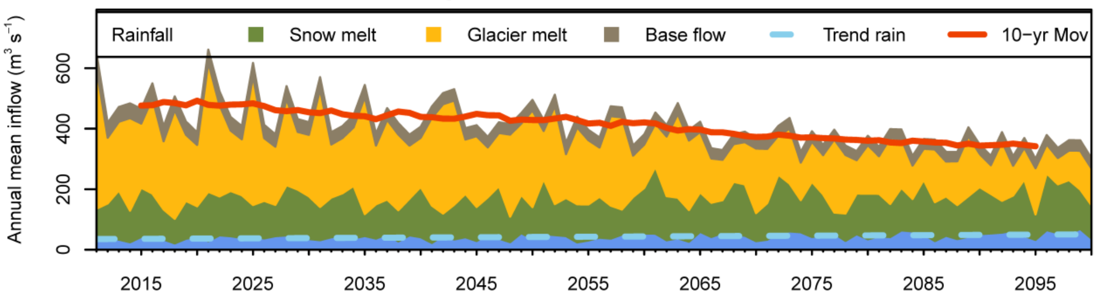

Inflow Kambarata for 2011−2100, Warm/wet scenario.

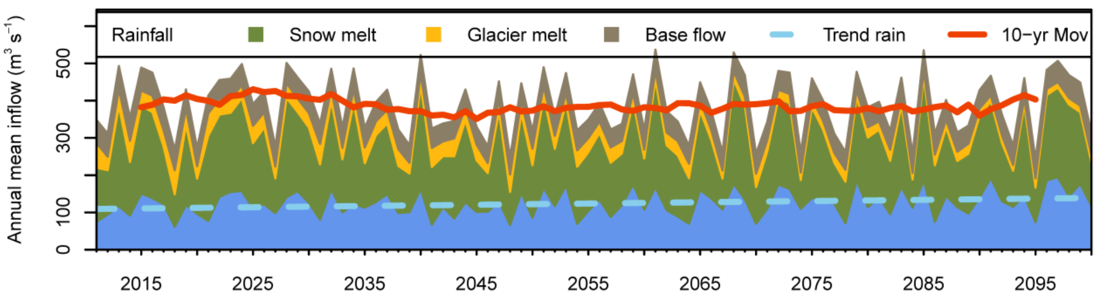

Appendix III Reservoir storage variability

III.1 With current infrastructure

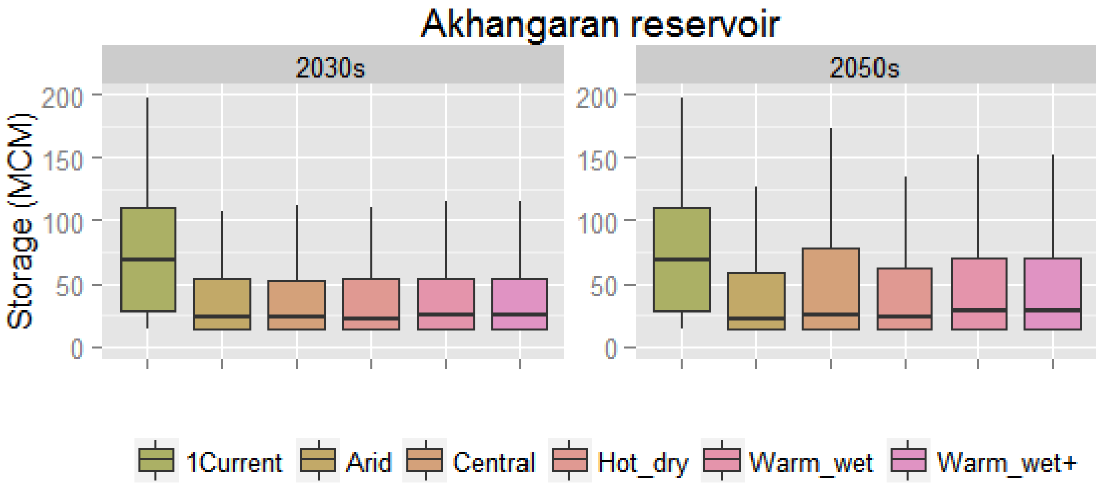

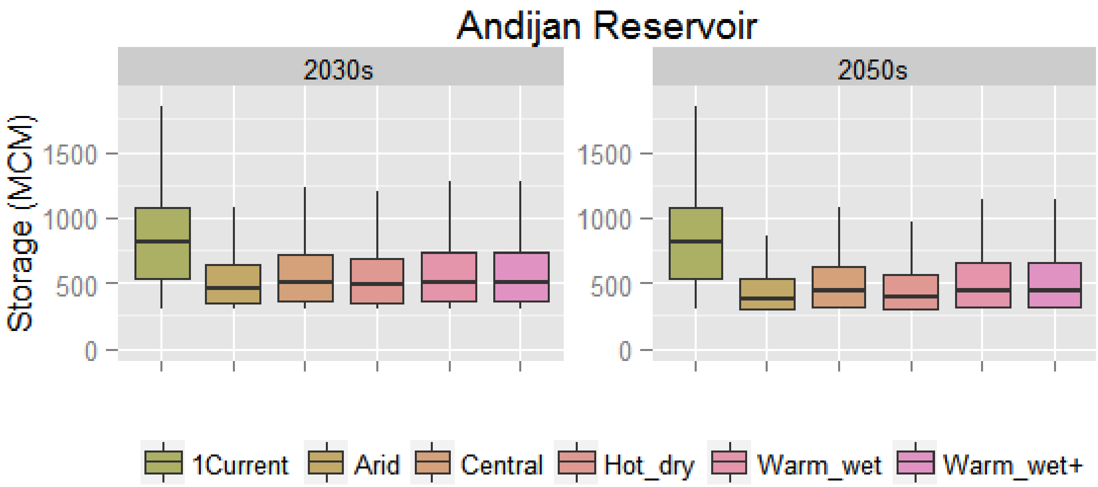

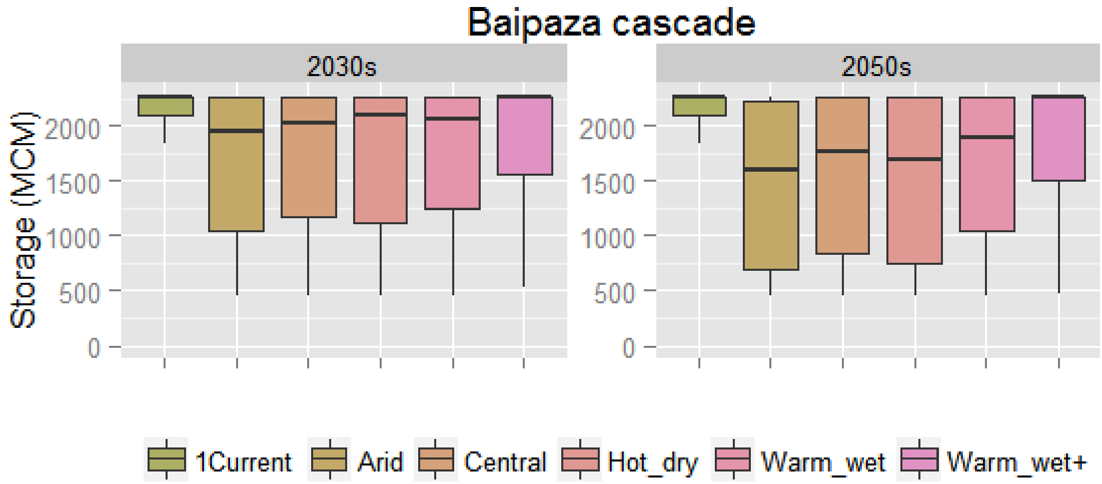
Baipaza cascade
2030s
2050s
Storage (MCM)
0
500
1000
1500
2000
1Current
Arid
Central
Hot_dry
Warm_wet
Warm_wet+

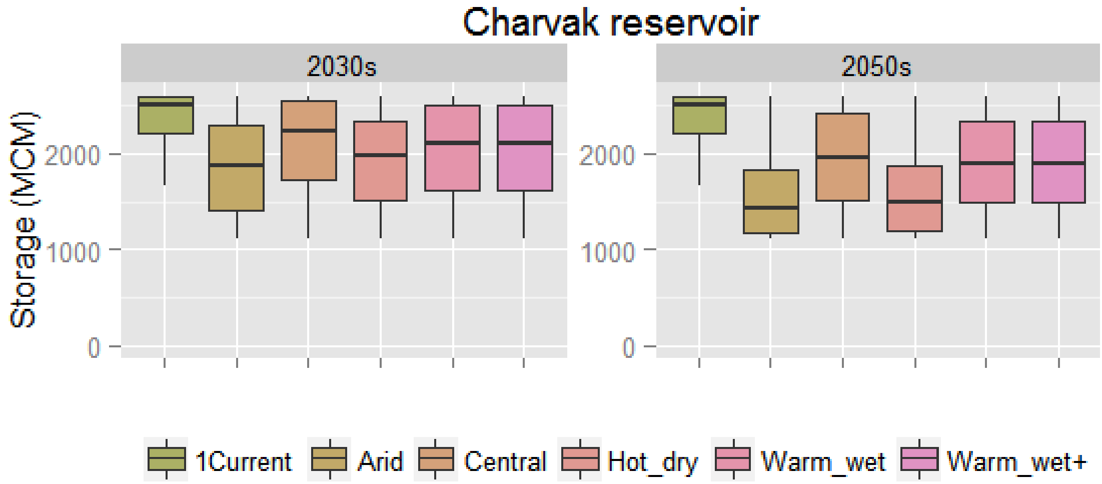
Charvak reservoir
2030s
2050s
Storage (MCM)
0
1000
2000
1Current
Arid
Central
Hot_dry
Warm_wet
Warm_wet+

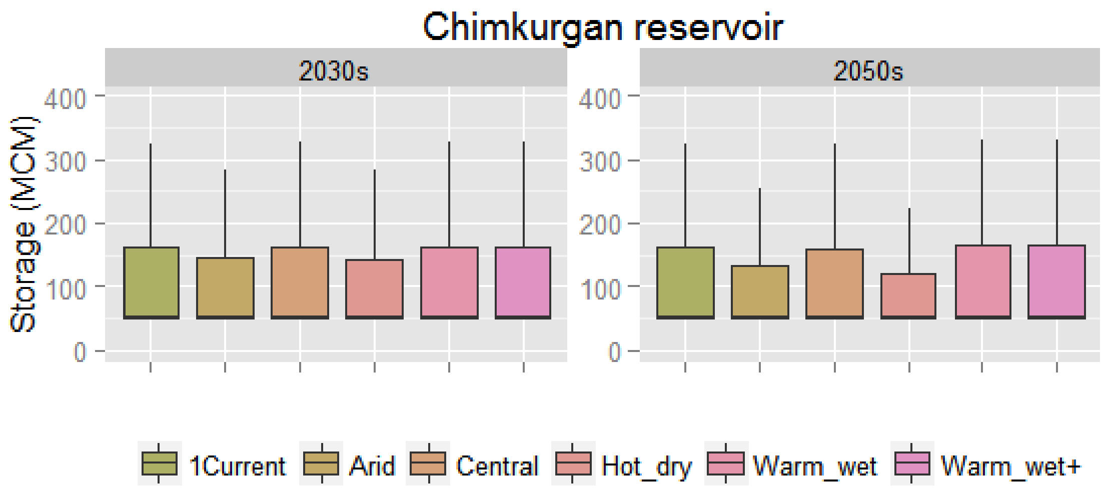
Chimkurgan reservoir
2030s
2050s
Storage (MCM)
0
100
200
300
400
1Current
Arid
Central
Hot_dry
Warm_wet
Warm_wet+

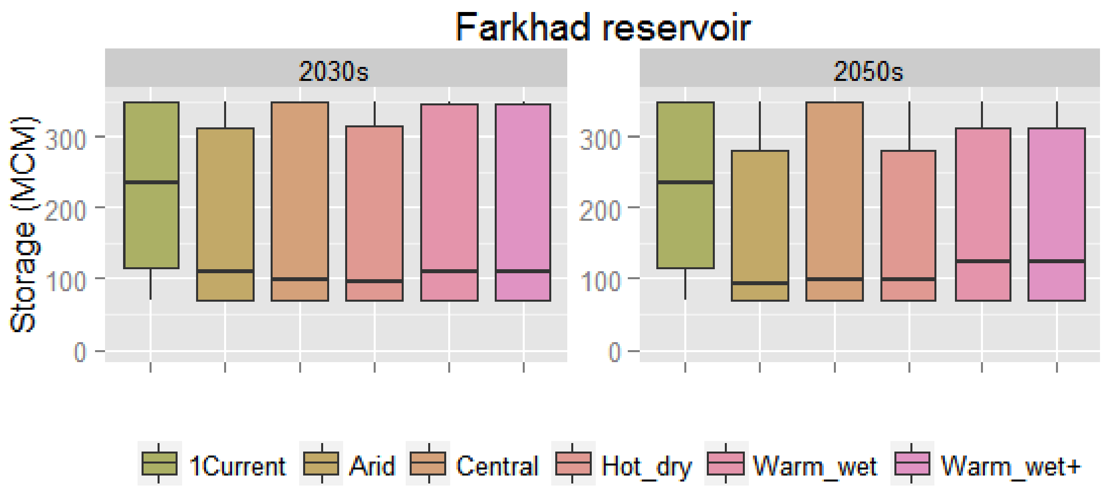
Farkhad reservoir
2030s
2050s
Storage (MCM)
0
100
200
300
1Current
Arid
Central
Hot_dry
Warm_wet
Warm_wet+

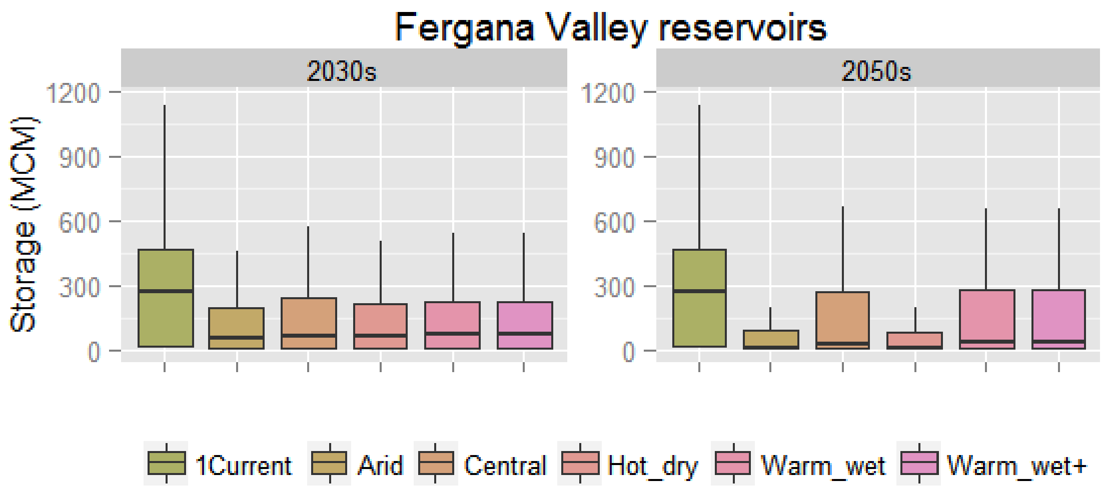
Fergana Valley reservoirs
2030s
2050s
Storage (MCM)
0
300
600
900
1200
1Current
Arid
Central
Hot_dry
Warm_wet
Warm_wet+

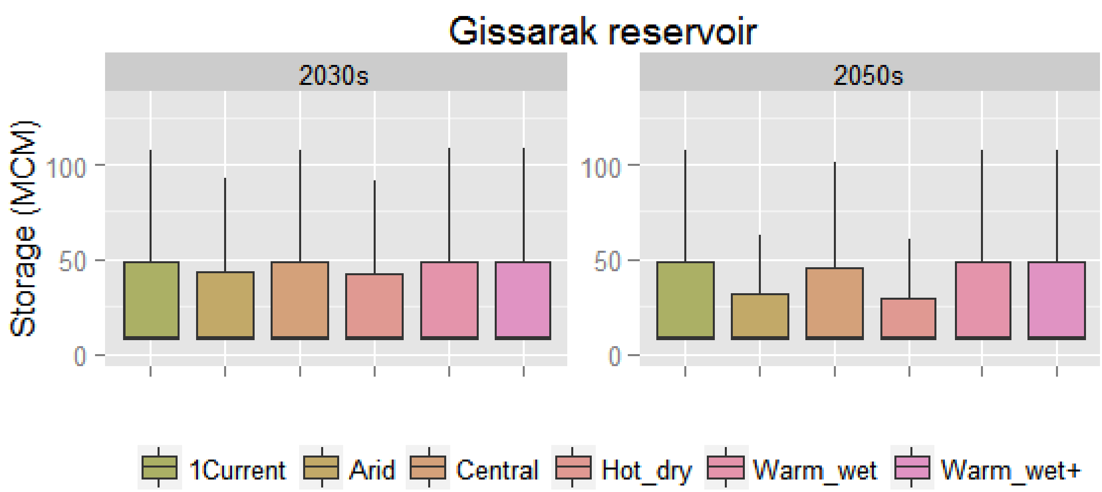
Gissarak reservoir
2030s
2050s
Storage (MCM)
0
50
100
1Current
Arid
Central
Hot_dry
Warm_wet
Warm_wet+

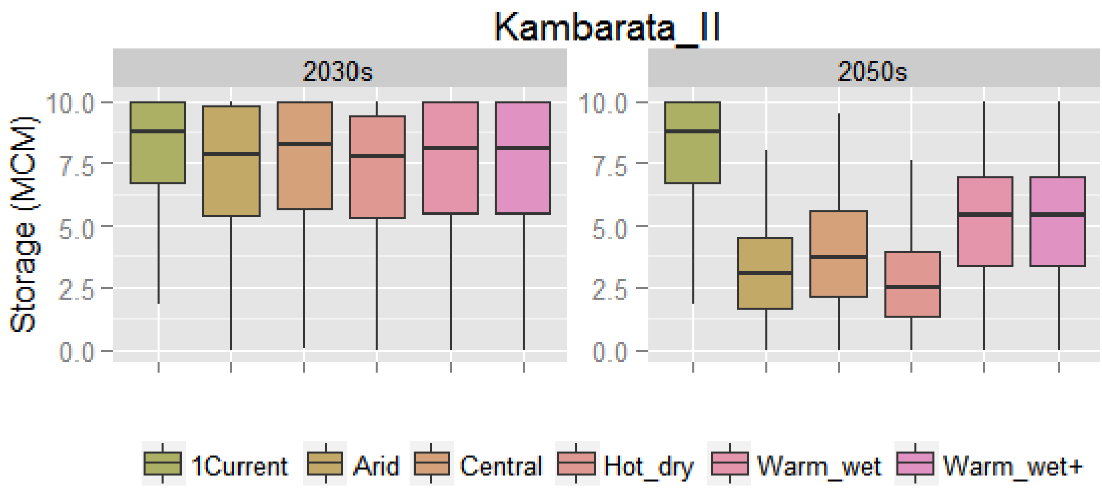
Kambarata_II
2030s
2050s
Storage (MCM)
10.0
7.5
5.0
2.5
0.0
1Current
Arid
Central
Hot_dry
Warm_wet
Warm_wet+

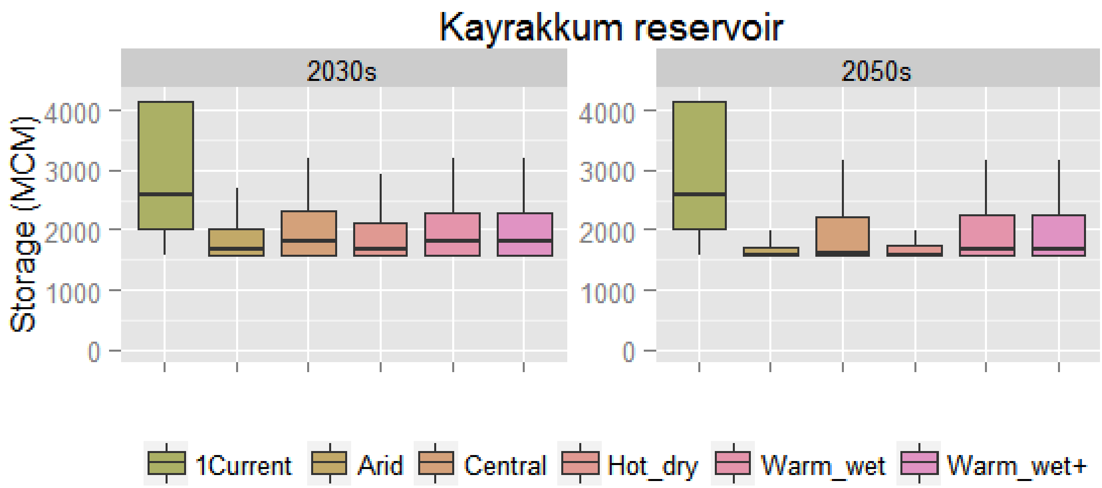
Kayrakkum reservoir
2030s
2050s
Storage (MCM)
4000
3000
2000
1000
0
1Current
Arid
Central
Hot_dry
Warm_wet
Warm_wet+

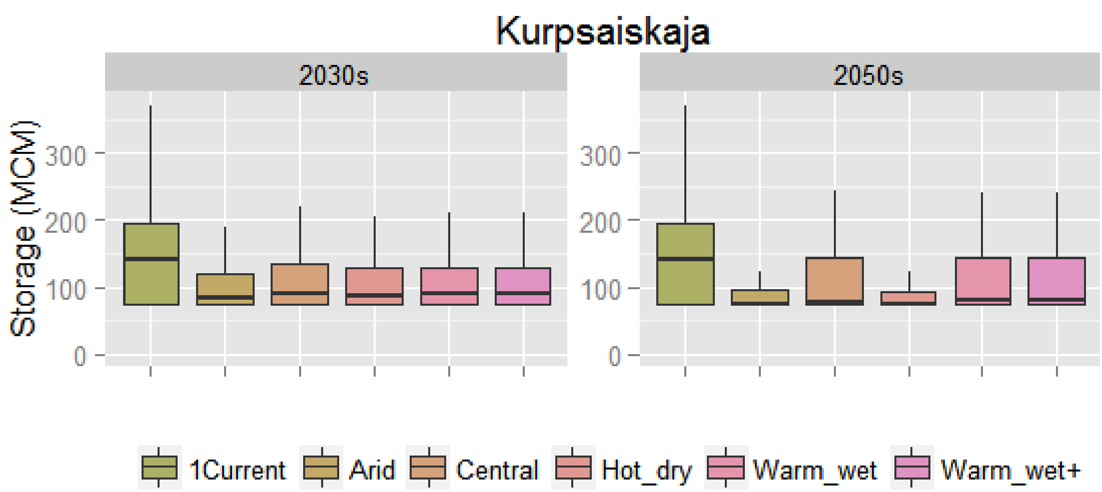
Kurpsaiskaja
2030s
2050s
Storage (MCM)
300
200
100
0
1Current
Arid
Central
Hot_dry
Warm_wet
Warm_wet+

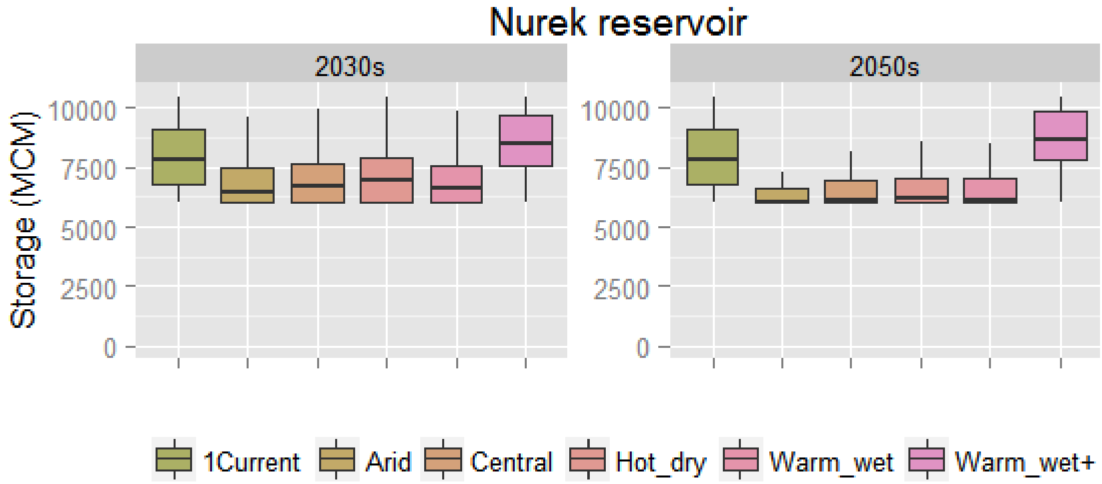
Nurek reservoir
2030s
2050s
Storage (MCM)
10000
7500
5000
2500
0
1Current
Arid
Central
Hot_dry
Warm_wet
Warm_wet+

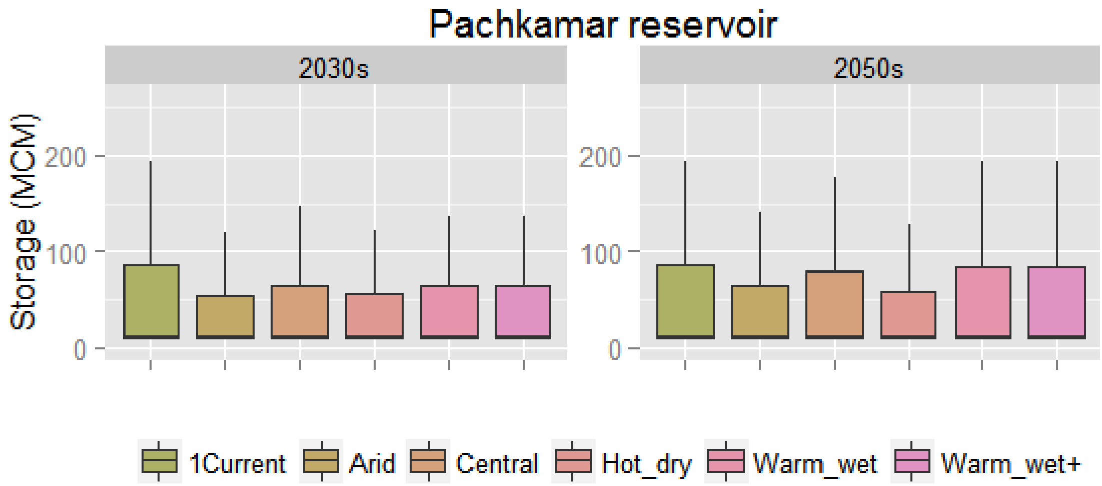
Pachkamar reservoir
2030s
2050s
Storage (MCM)
200
100
0
1Current
Arid
Central
Hot_dry
Warm_wet
Warm_wet+

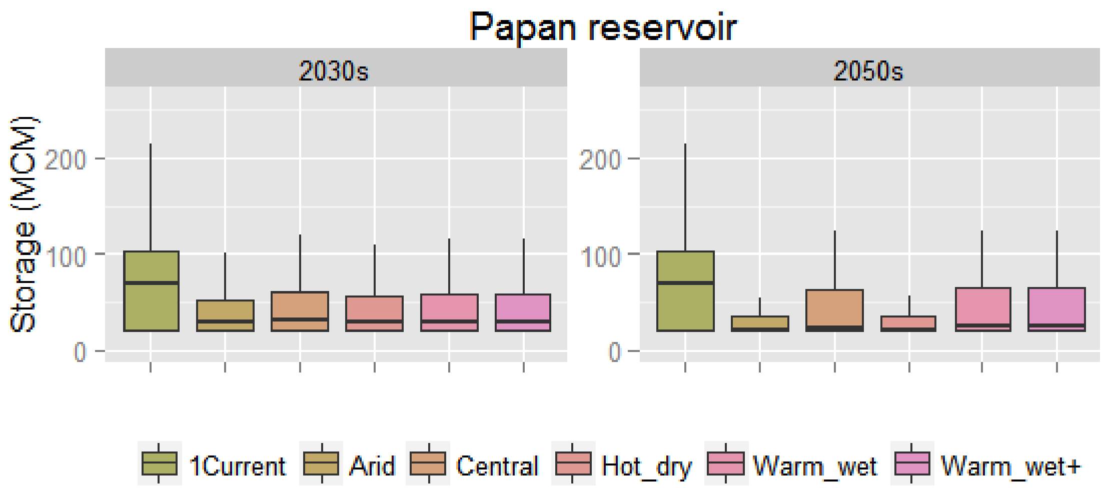
Papan reservoir
2030s
2050s
Storage (MCM)
200
100
0
1Current
Arid
Central
Hot_dry
Warm_wet
Warm_wet+

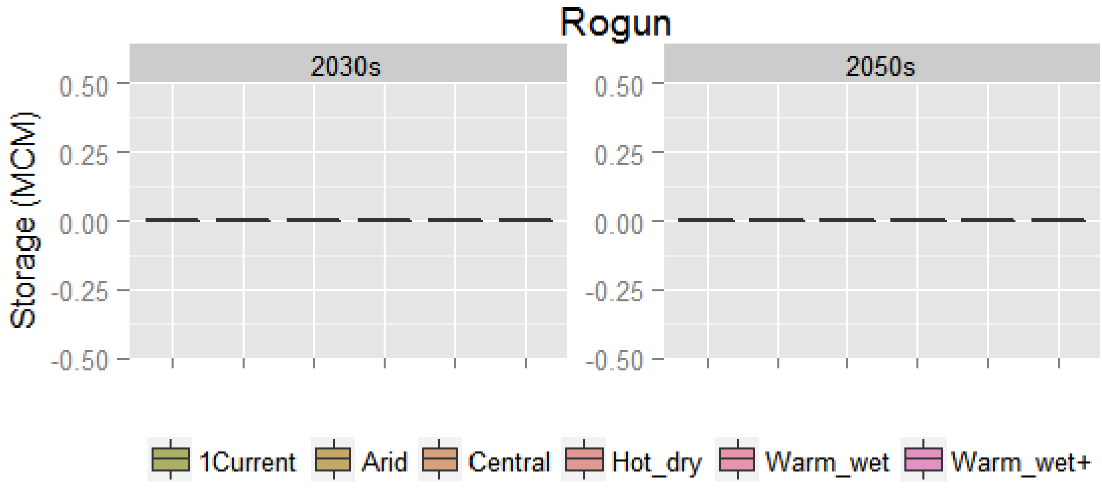
Rogun
2030s
2050s
Storage (MCM)
0.50
0.25
0.00
-0.25
-0.50
1Current
Arid
Central
Hot_dry
Warm_wet
Warm_wet+

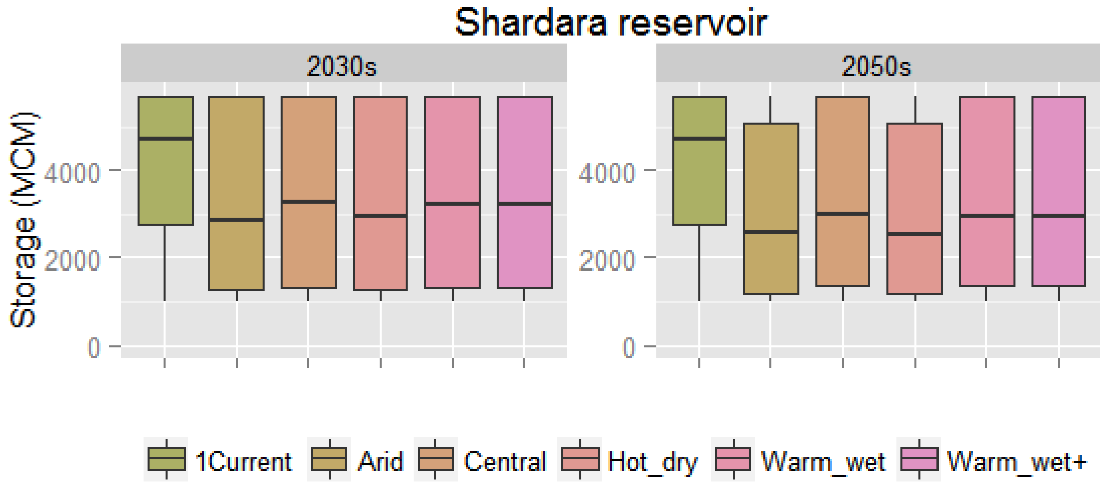
Shardara reservoir
2030s
2050s
Storage (MCM)
4000
2000
0
1Current
Arid
Central
Hot_dry
Warm_wet
Warm_wet+

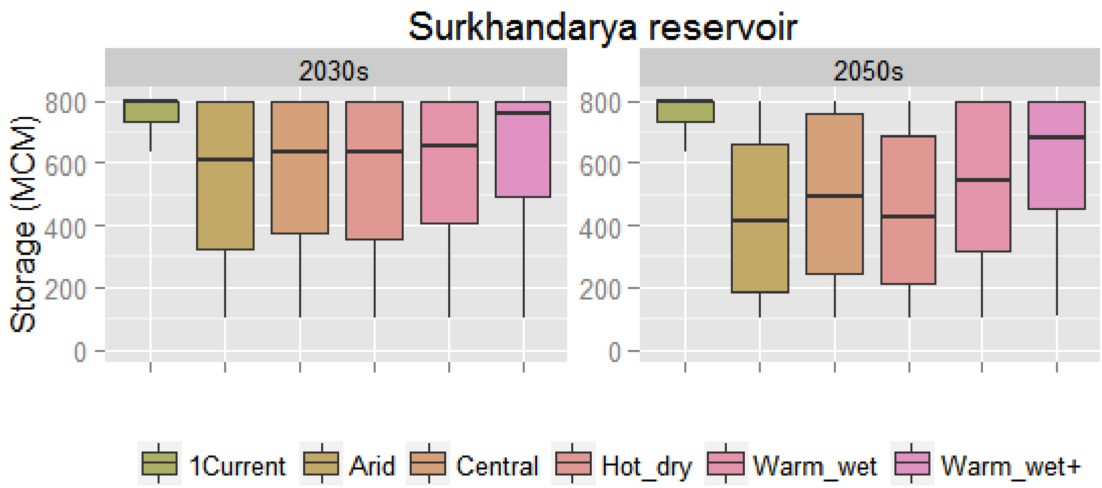
Surkhandarya reservoir
2030s
2050s
Storage (MCM)
800
600
400
200
0
1Current
Arid
Central
Hot_dry
Warm_wet
Warm_wet+

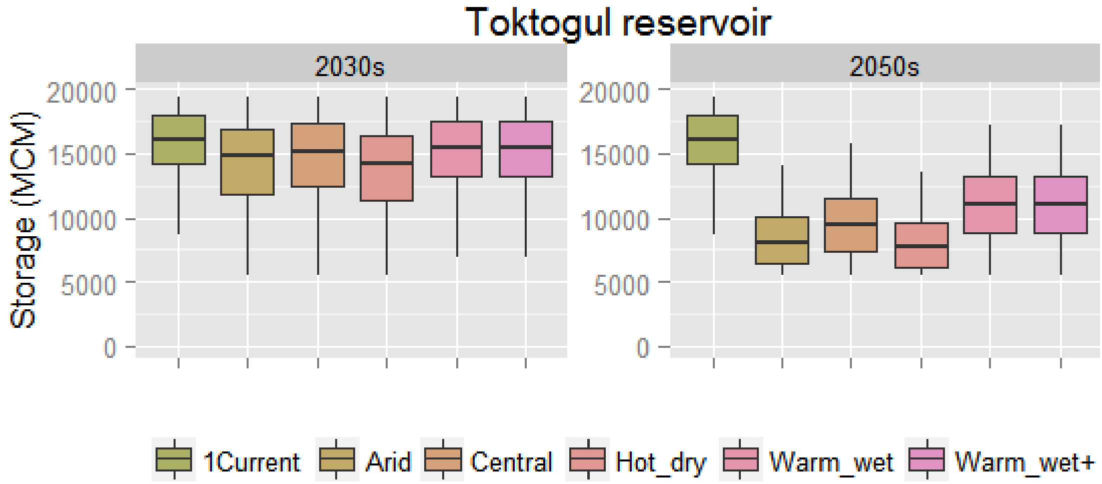
Toktogul reservoir
2030s
2050s
Storage (MCM)
20000
15000
10000
5000
0
1Current
Arid
Central
Hot_dry
Warm_wet
Warm_wet+

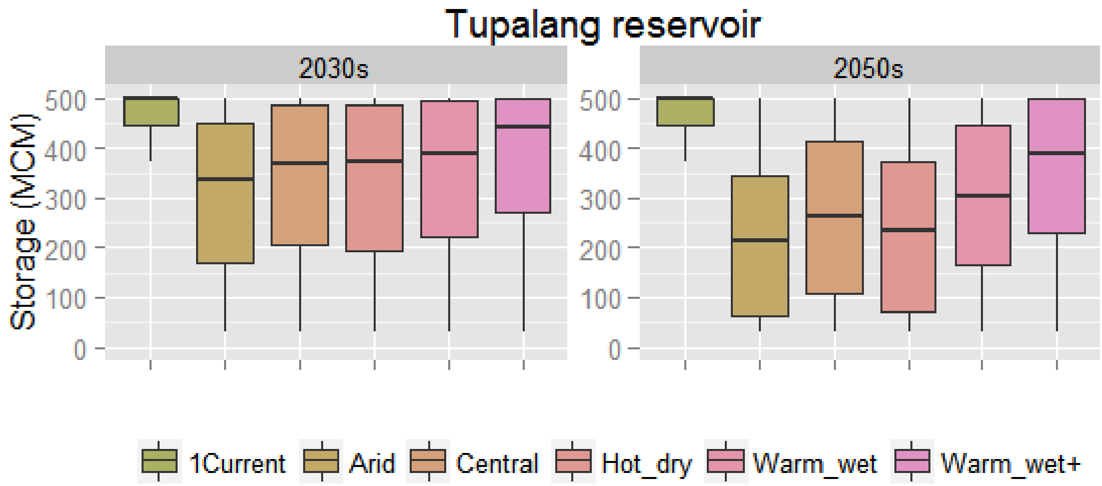
Tupalang reservoir
2030s
2050s
Storage (MCM)
500
400
300
200
100
0
1Current
Arid
Central
Hot_dry
Warm_wet
Warm_wet+

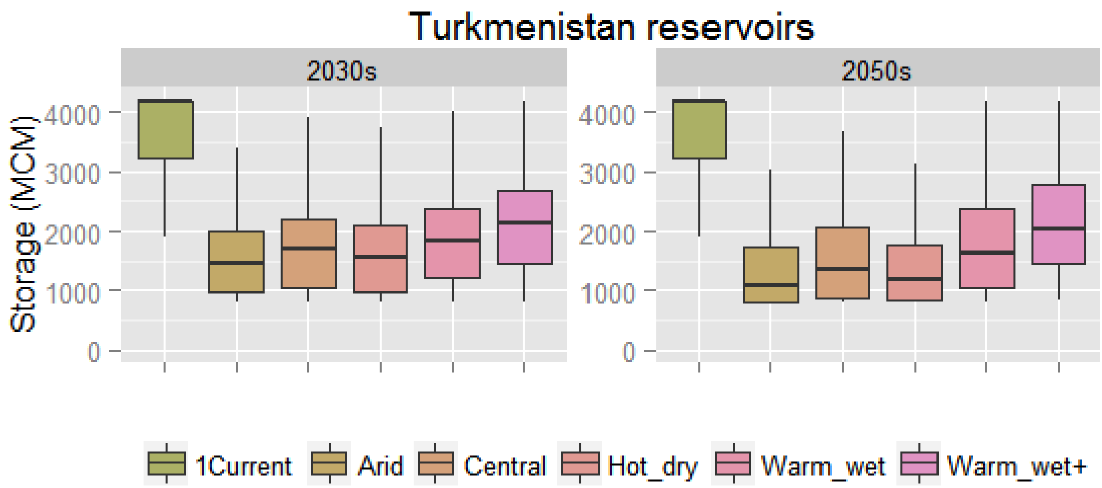
Turkmenistan reservoirs
2030s
2050s
Storage (MCM)
4000
3000
2000
1000
0
1Current
Arid
Central
Hot_dry
Warm_wet
Warm_wet+

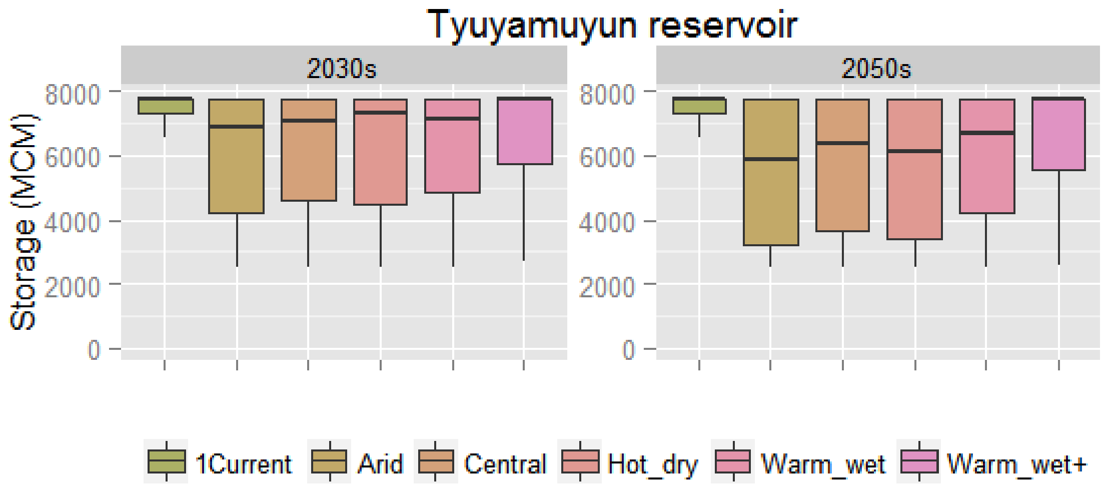
Tyuyamuyun reservoir
2030s
2050s
Storage (MCM)
0
2000
4000
6000
8000
1Current
Arid
Central
Hot_dry
Warm_wet
Warm_wet+

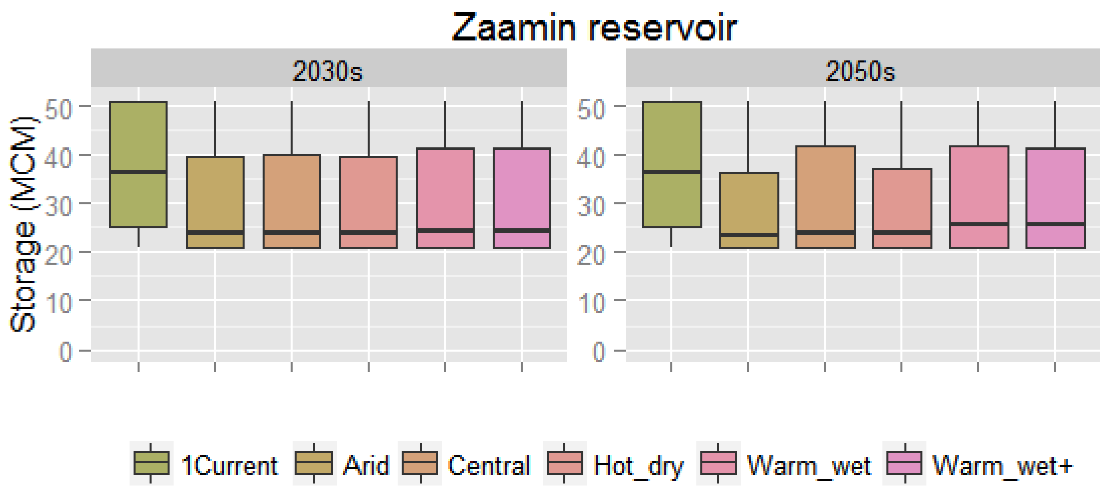
Zaamin reservoir
2030s
2050s
Storage (MCM)
0
10
20
30
40
50
1Current
Arid
Central
Hot_dry
Warm_wet
Warm_wet+

III.2 With planned infrastructure

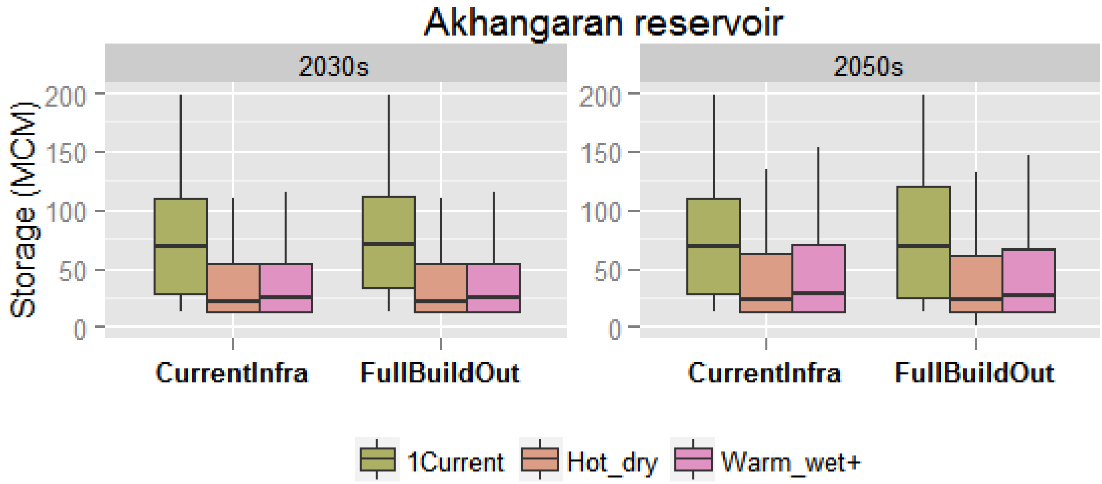

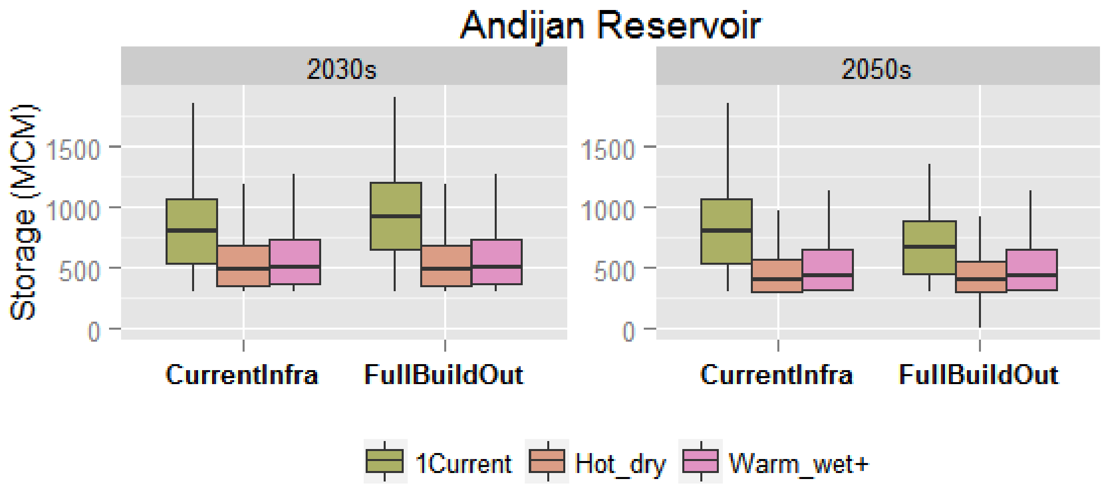

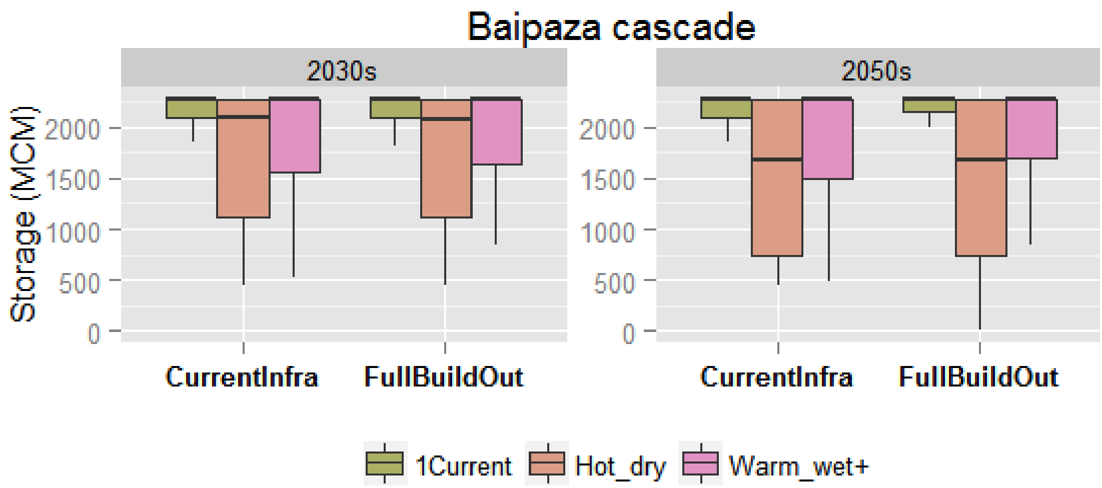

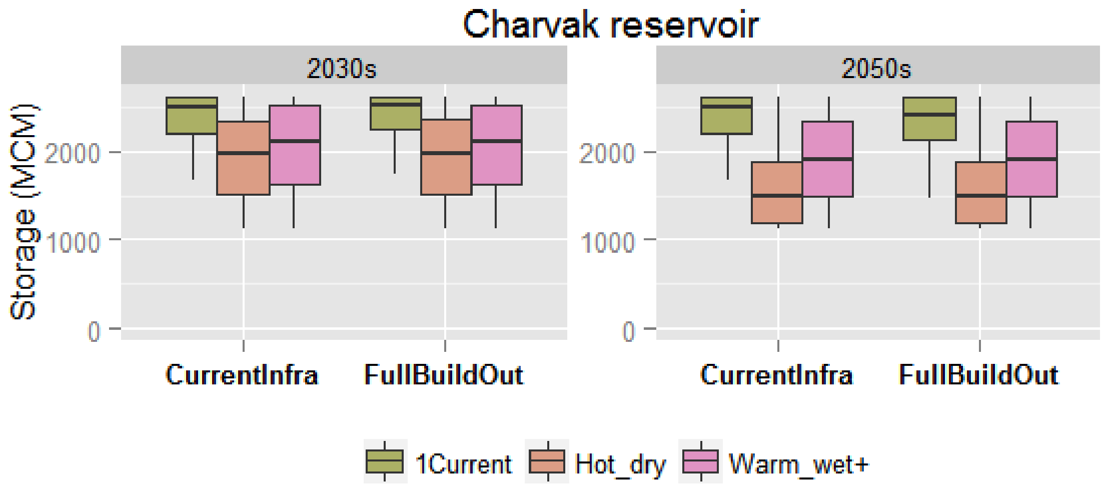
Charvak reservoir
2030s
2050s
Storage (MCM)
0
1000
2000
CurrentInfra
FullBuildOut
1Current
Hot_dry
Warm_wet+

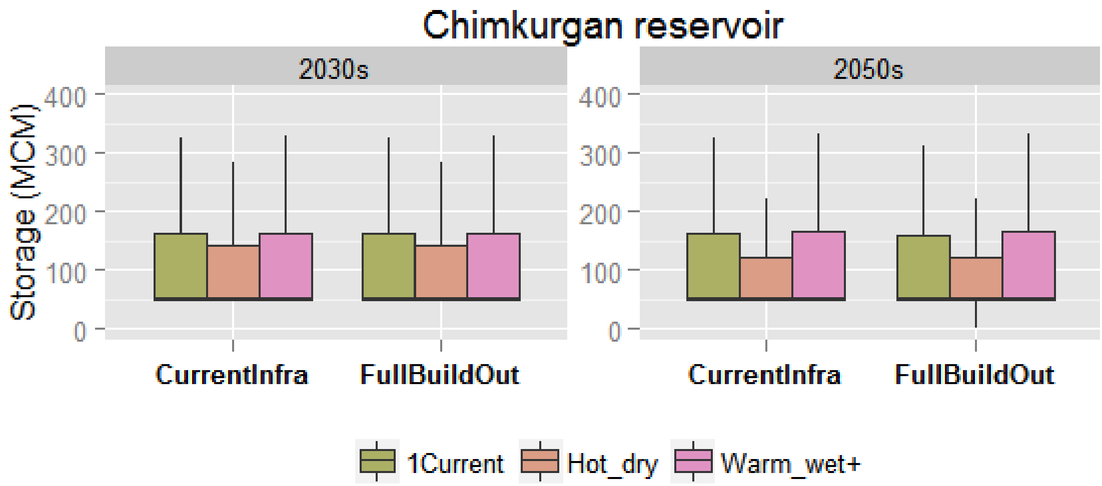
Chimkurgan reservoir
2030s
2050s
Storage (MCM)
0
100
200
300
400
CurrentInfra
FullBuildOut
1Current
Hot_dry
Warm_wet+

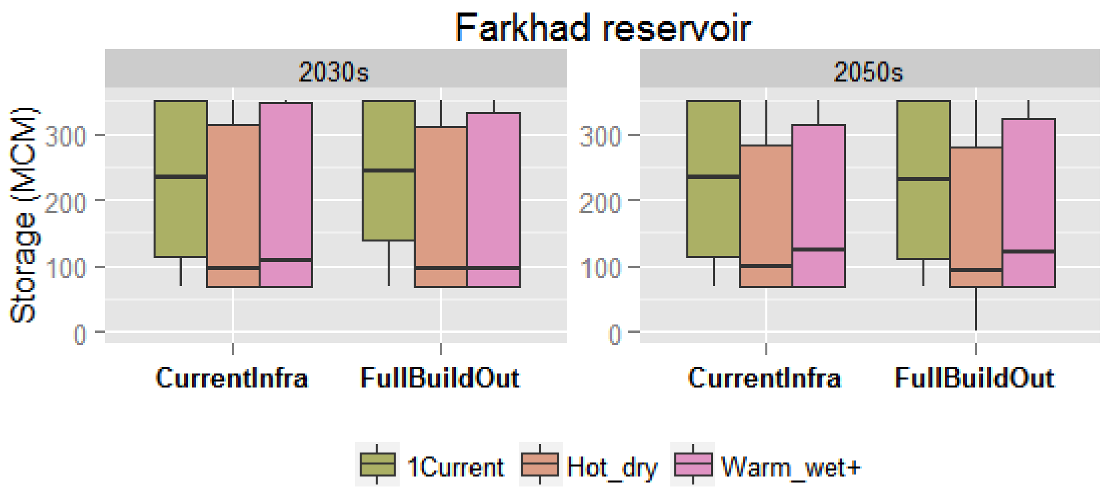
Farkhad reservoir
2030s
2050s
Storage (MCM)
0
100
200
300
CurrentInfra
FullBuildOut
1Current
Hot_dry
Warm_wet+

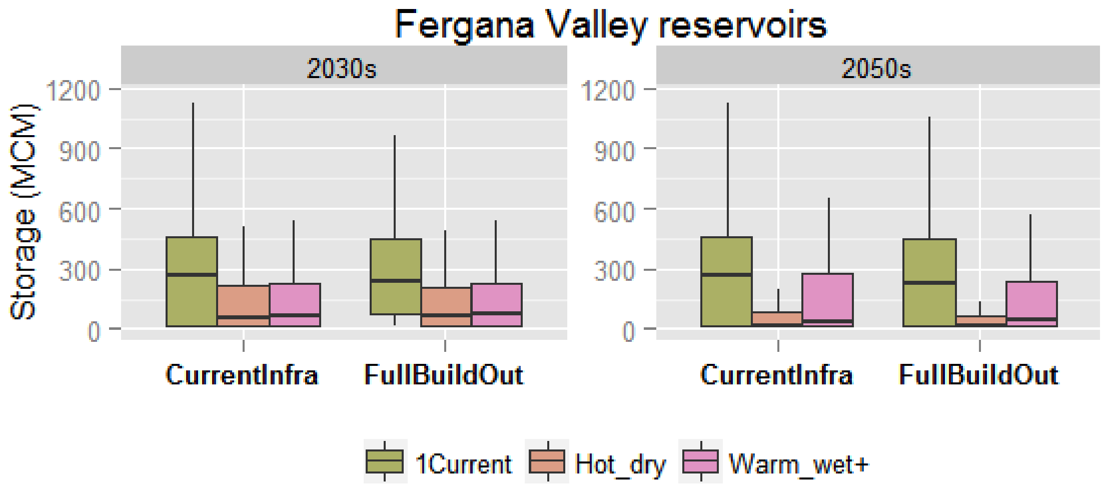
Fergana Valley reservoirs
2030s
2050s
Storage (MCM)
0
300
600
900
1200
CurrentInfra
FullBuildOut
1Current
Hot_dry
Warm_wet+

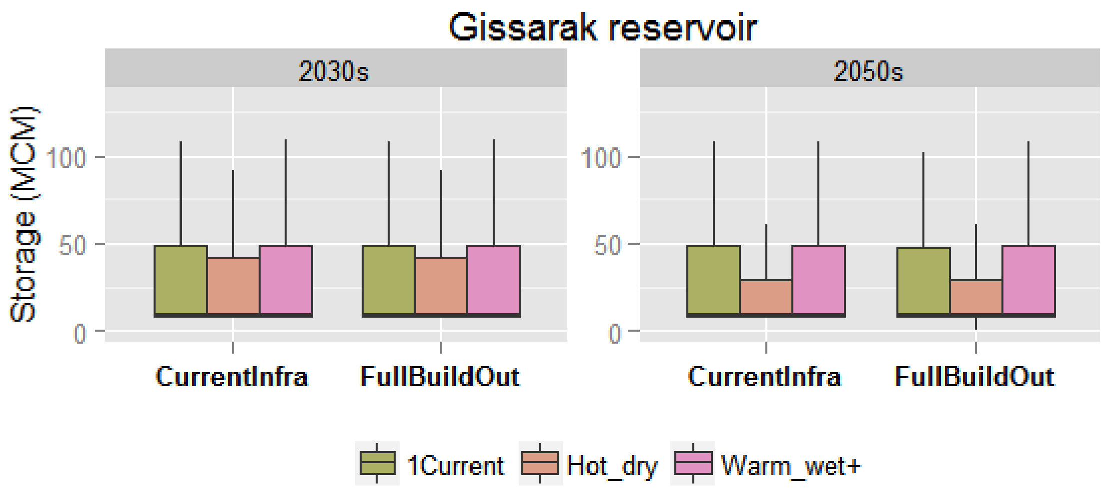
Gissarak reservoir
2030s
2050s
Storage (MCM)
0
50
100
CurrentInfra
FullBuildOut
1Current
Hot_dry
Warm_wet+

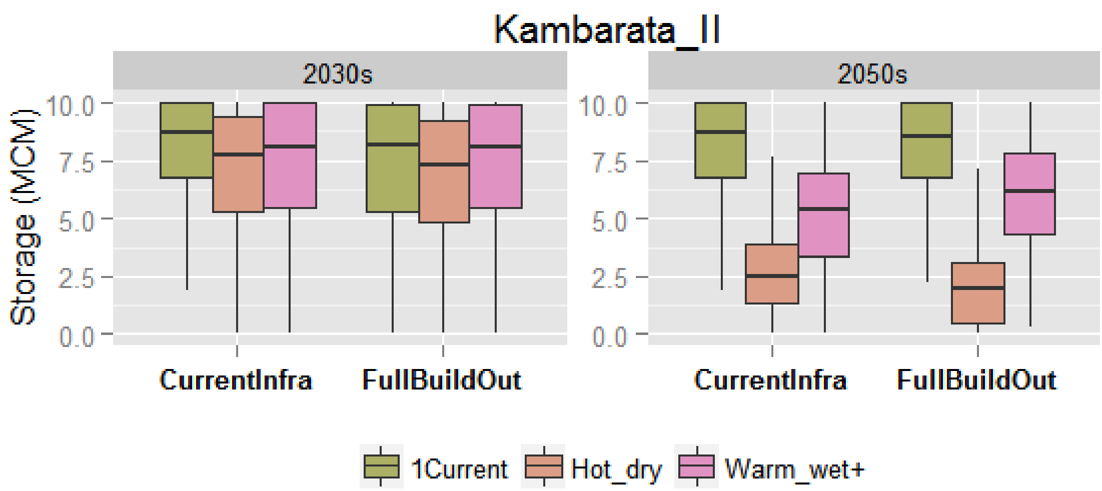
Kambarata_II
2030s
2050s
Storage (MCM)
0.0
2.5
5.0
7.5
10.0
CurrentInfra
FullBuildOut
1Current
Hot_dry
Warm_wet+

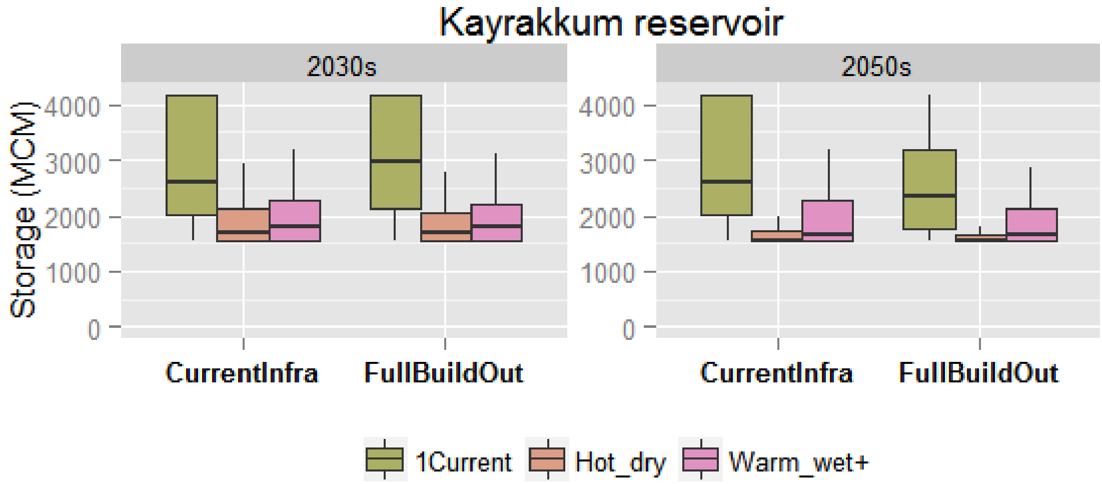
Kayrakkum reservoir
2030s
2050s
Storage (MCM)
4000
3000
2000
1000
0
CurrentInfra
FullBuildOut
1Current
Hot_dry
Warm_wet+

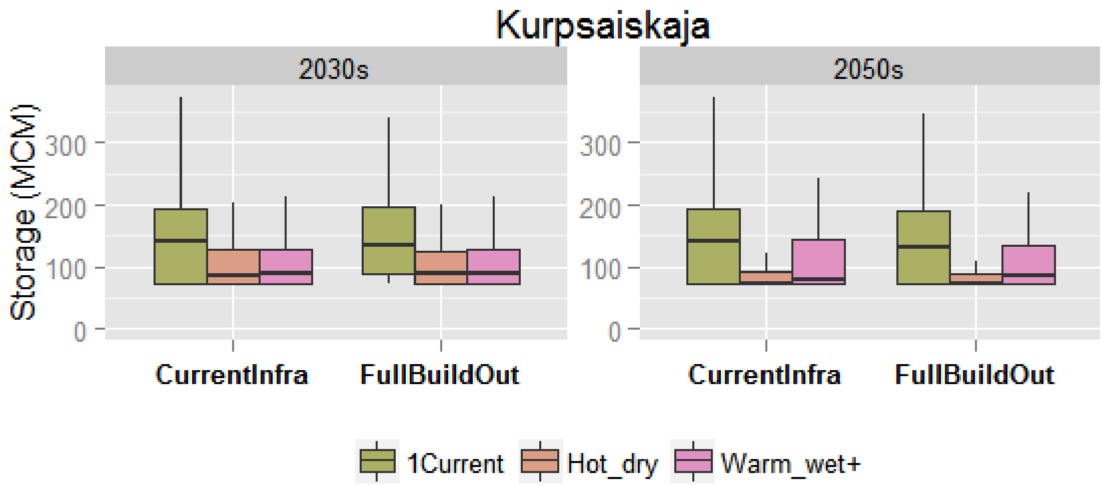
Kurpsaiskaja
2030s
2050s
Storage (MCM)
300
200
100
0
CurrentInfra
FullBuildOut
1Current
Hot_dry
Warm_wet+

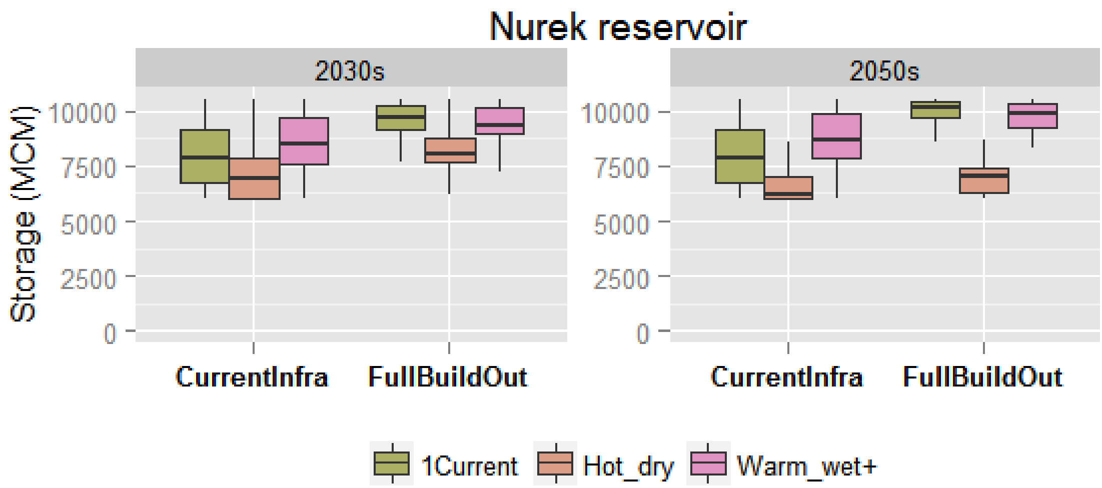
Nurek reservoir
2030s
2050s
Storage (MCM)
10000
7500
5000
2500
0
CurrentInfra
FullBuildOut
1Current
Hot_dry
Warm_wet+

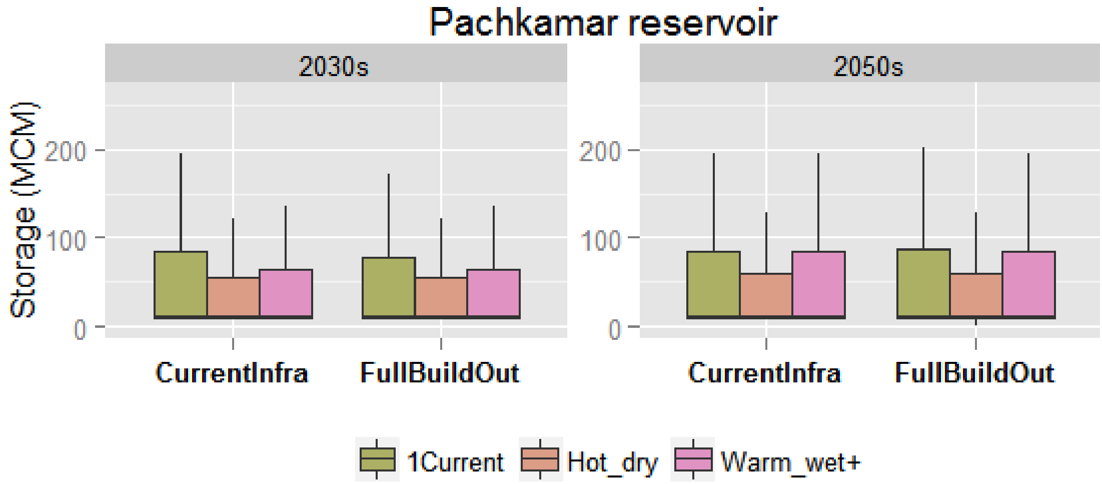
Pachkamar reservoir
2030s
2050s
Storage (MCM)
200
100
0
CurrentInfra
FullBuildOut
1Current
Hot_dry
Warm_wet+

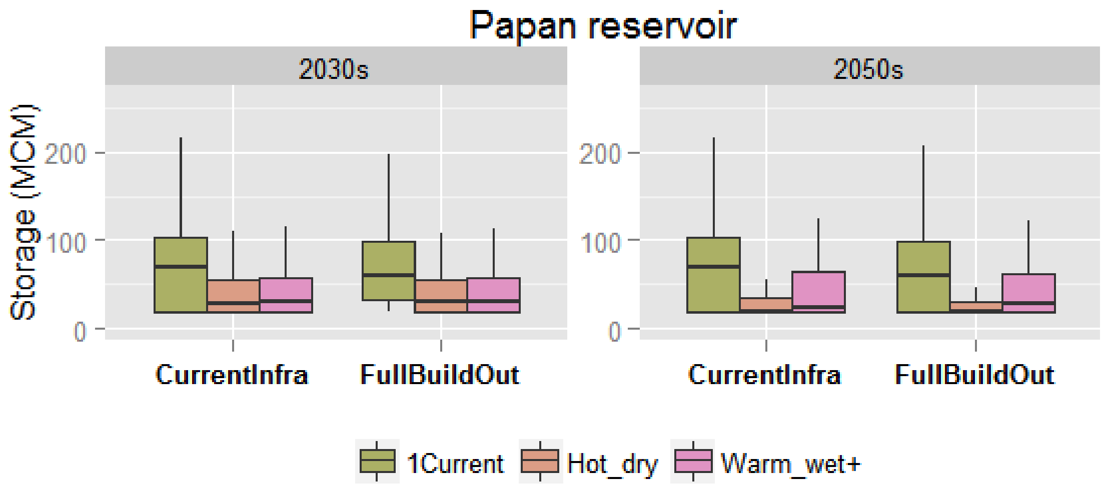
Papan reservoir
2030s
2050s
Storage (MCM)
200
100
0
CurrentInfra
FullBuildOut
1Current
Hot_dry
Warm_wet+

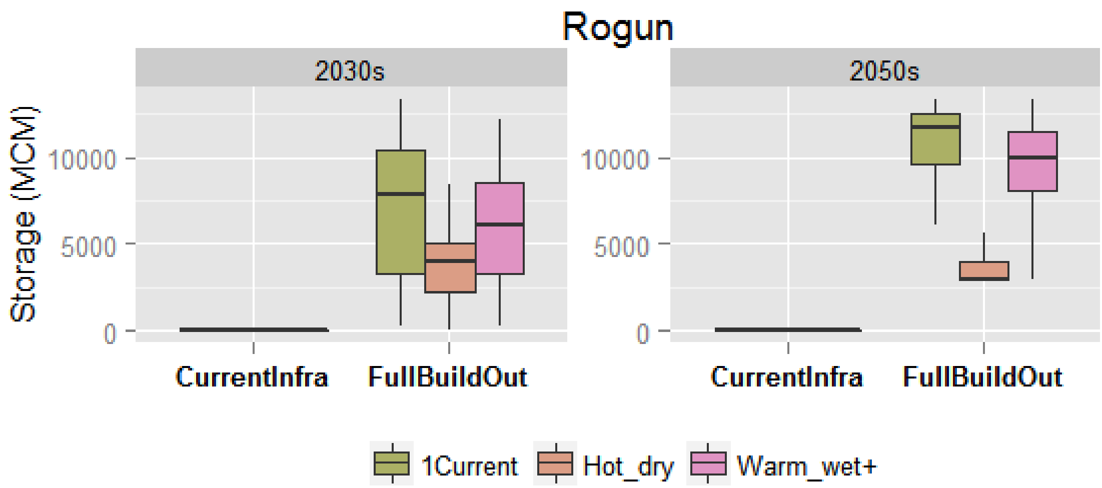
Rogun
2030s
2050s
Storage (MCM)
10000
5000
0
CurrentInfra
FullBuildOut
1Current
Hot_dry
Warm_wet+

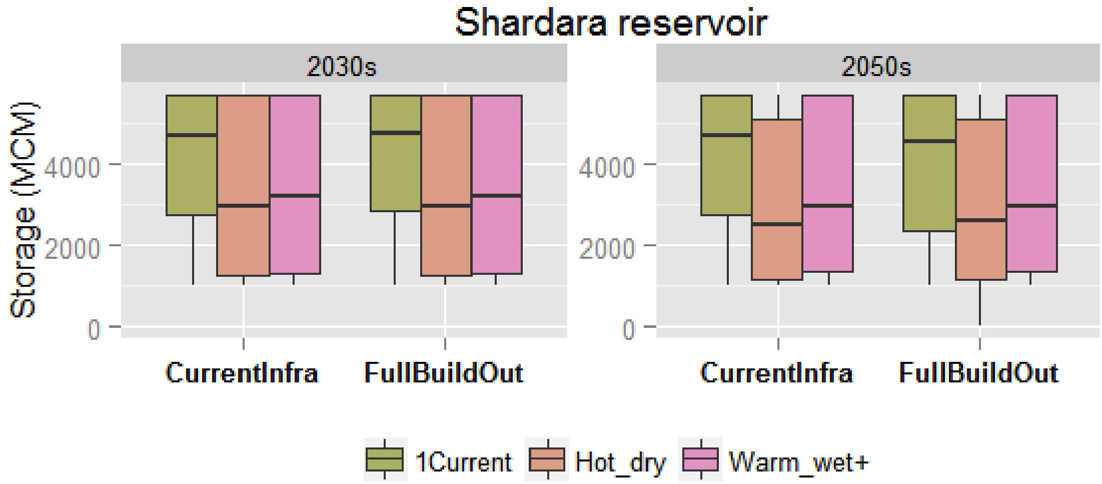

Shardara reservoir
2030s
2050s
Storage (MCM)
4000
2000
0
CurrentInfra
FullBuildOut
1Current
Hot_dry
Warm_wet+

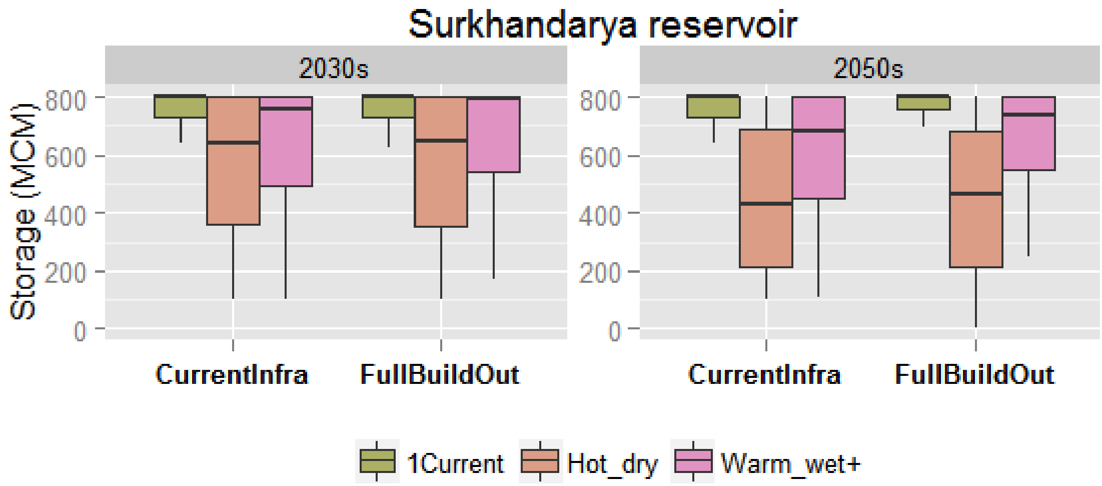

Surkhandarya reservoir
2030s
2050s
Storage (MCM)
800
600
400
200
0
CurrentInfra
FullBuildOut
1Current
Hot_dry
Warm_wet+

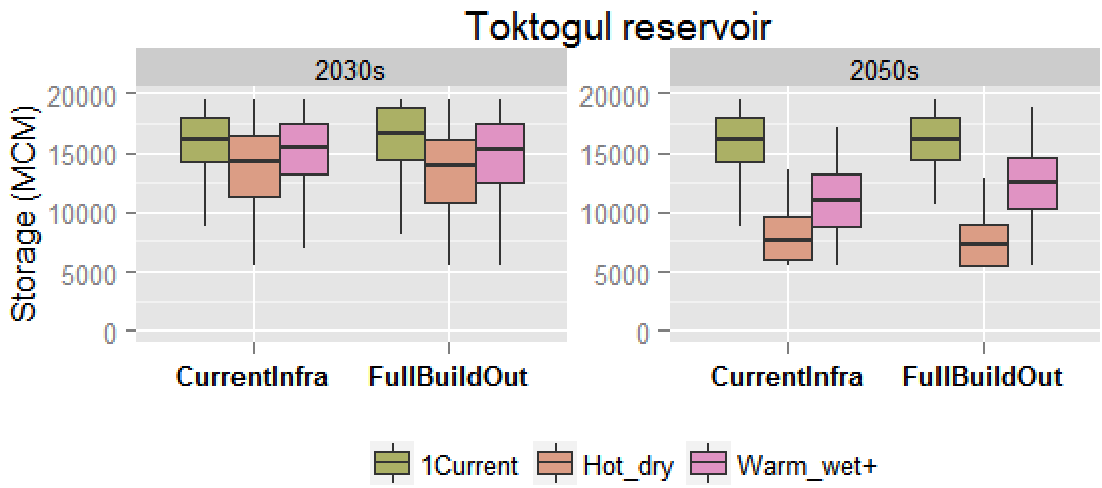

Toktogul reservoir
2030s
2050s
Storage (MCM)
20000
15000
10000
5000
0
CurrentInfra
FullBuildOut
1Current
Hot_dry
Warm_wet+

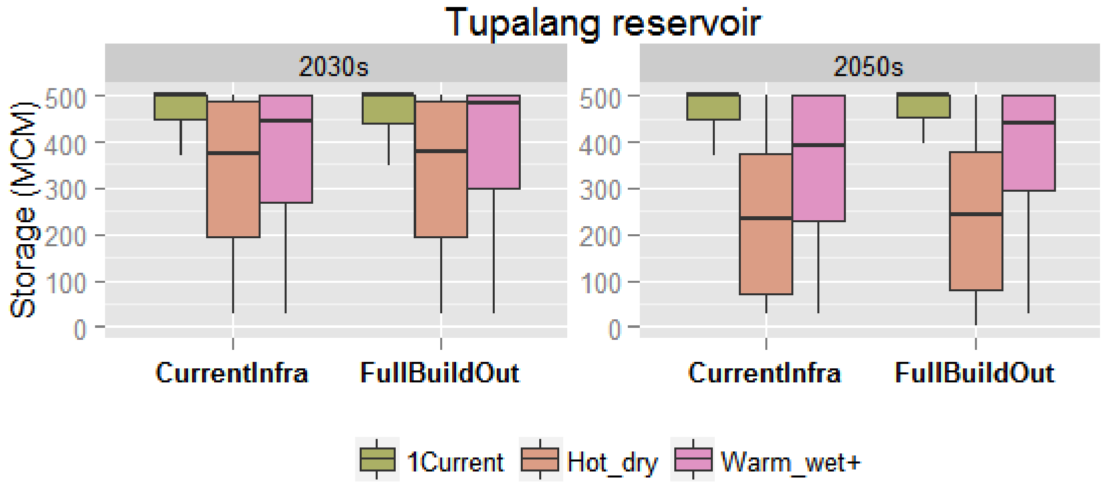

Tupalang reservoir
2030s
2050s
Storage (MCM)
0
100
200
300
400
500
CurrentInfra
FullBuildOut
1Current
Hot_dry
Warm_wet+

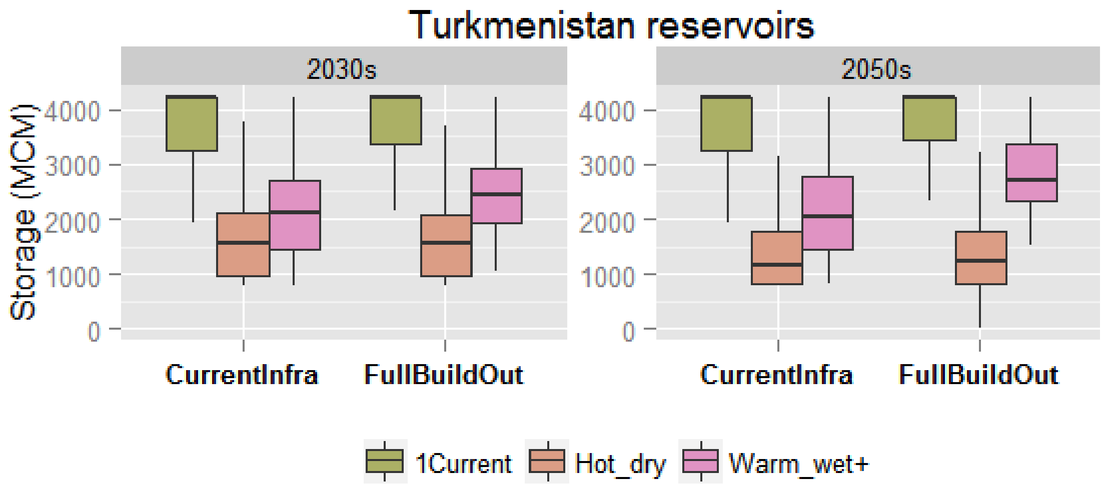

Turkmenistan reservoirs
2030s
2050s
Storage (MCM)
0
1000
2000
3000
4000
CurrentInfra
FullBuildOut
1Current
Hot_dry
Warm_wet+

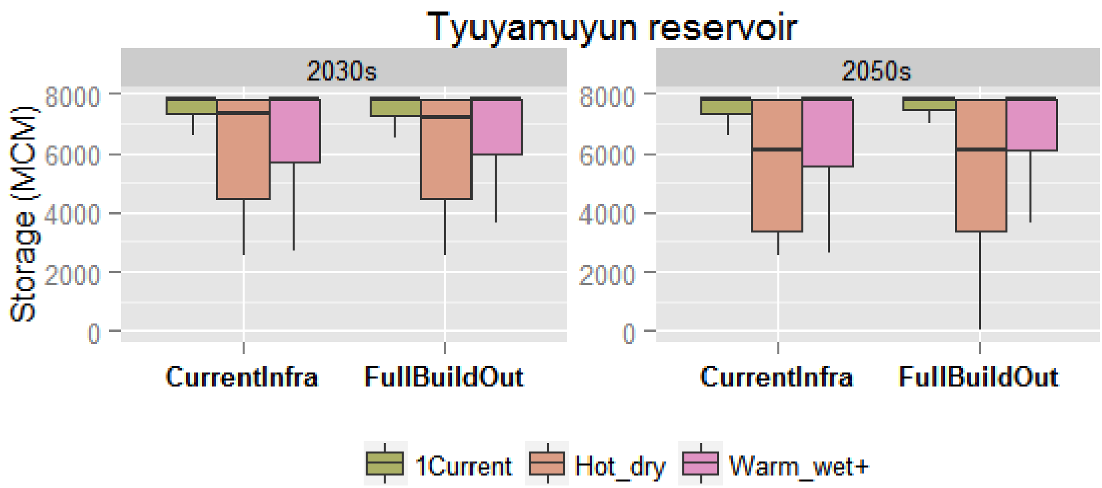

Tyuyamuyun reservoir
2030s
2050s
Storage (MCM)
0
2000
4000
6000
8000
CurrentInfra
FullBuildOut
1Current
Hot_dry
Warm_wet+

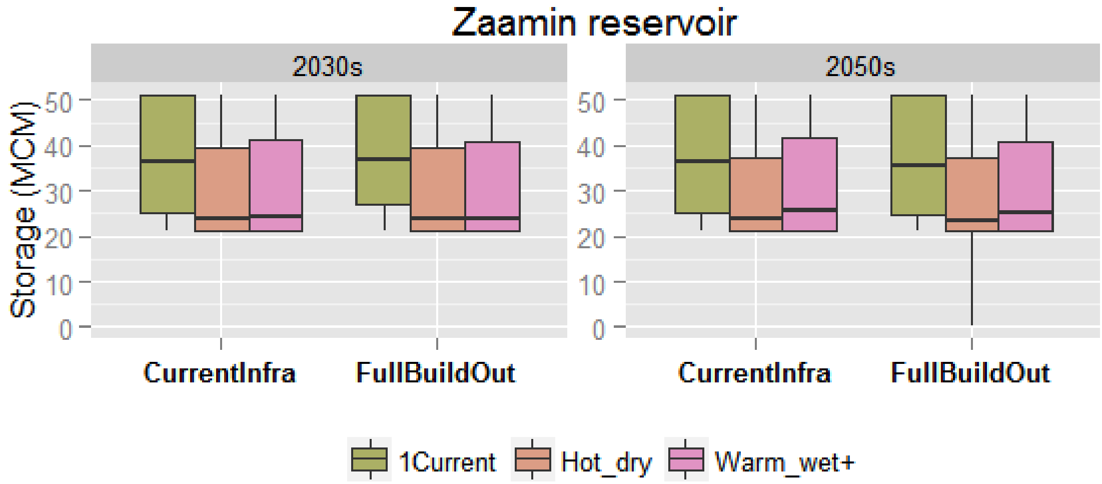

Zaamin reservoir
2030s
2050s
Storage (MCM)
0
10
20
30
40
50
CurrentInfra
FullBuildOut
1Current
Hot_dry
Warm_wet+

Appendix IV Reservoir hydropower production

IV.1 With current infrastructure

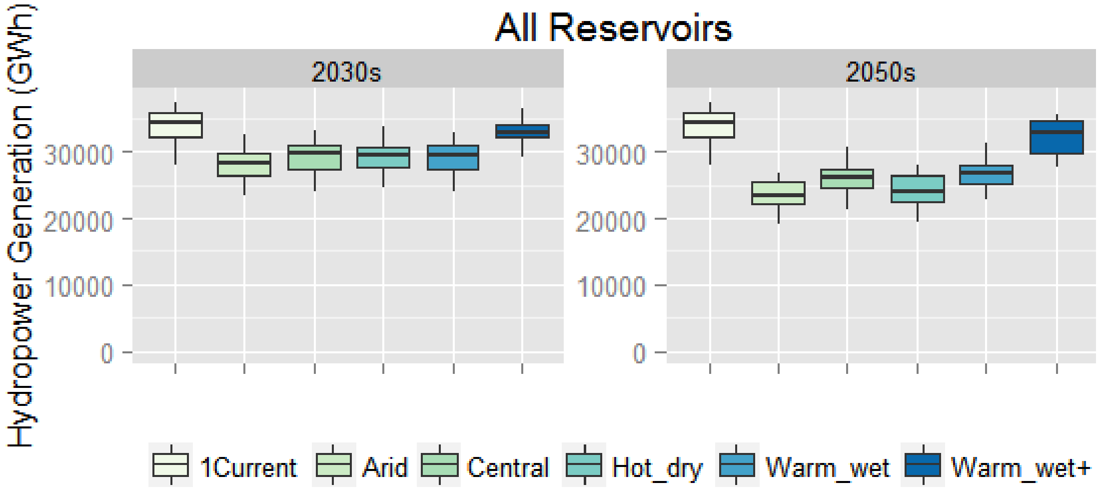

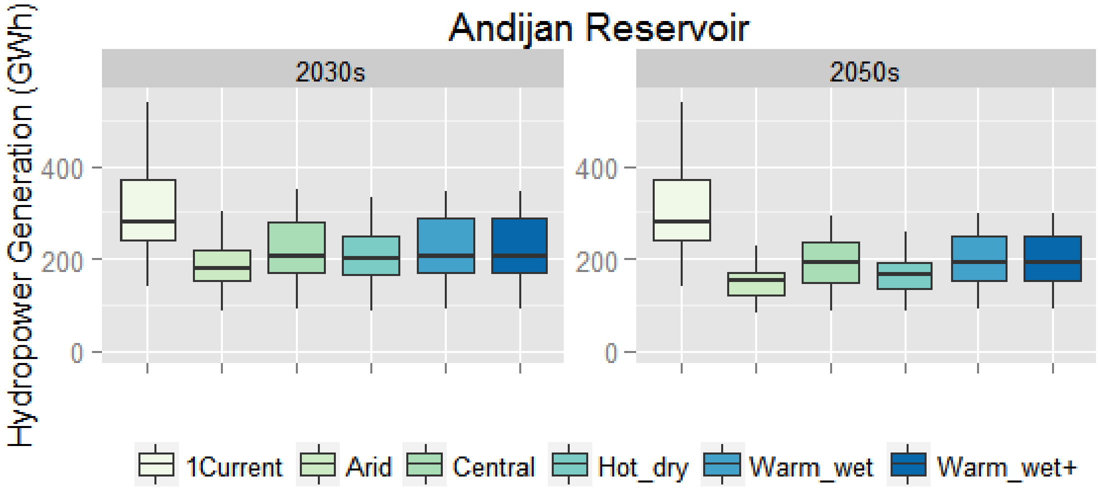

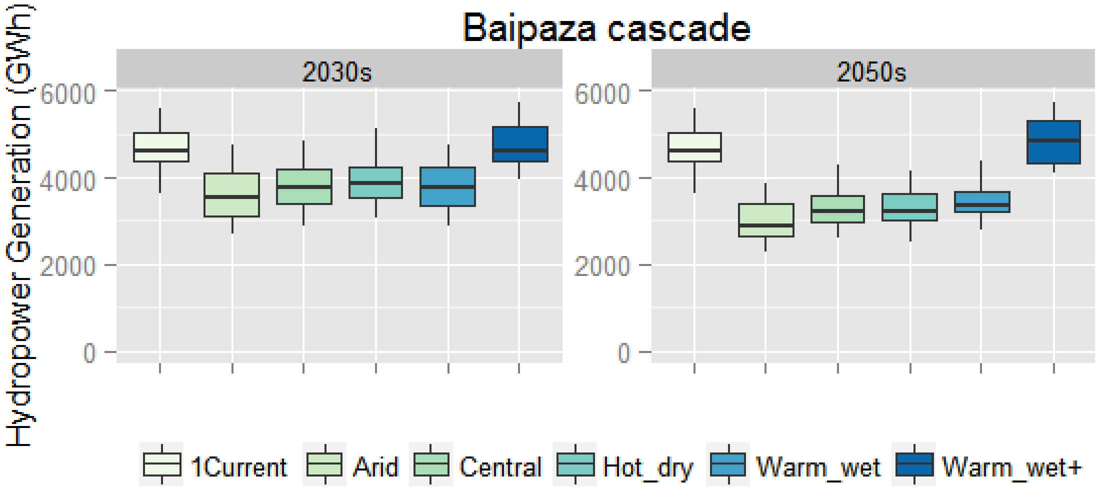
Baipaza cascade
2030s
2050s
Hydropower Generation (GWh)
6000
4000
2000
0
1Current
Arid
Central
Hot_dry
Warm_wet
Warm_wet+

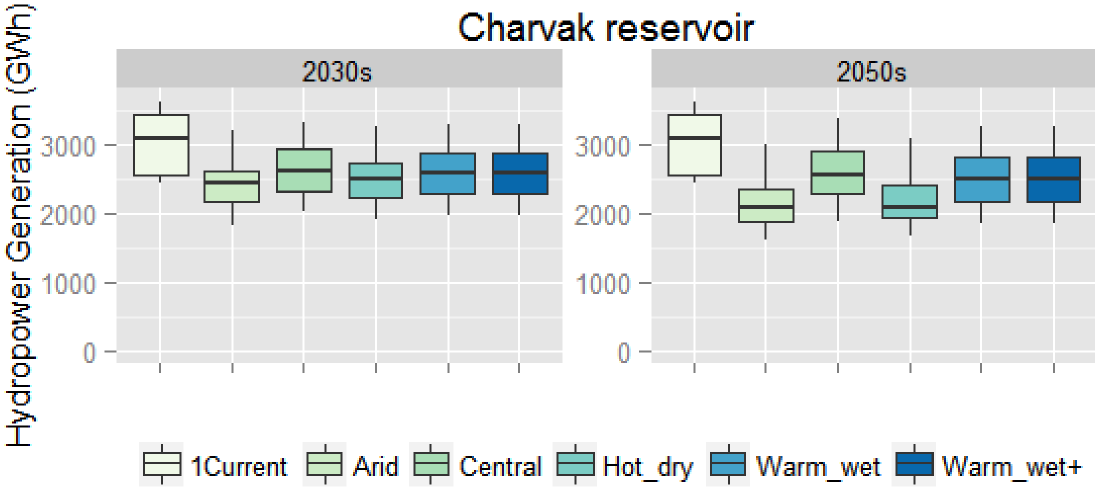
Charvak reservoir
2030s
2050s
Hydropower Generation (GWh)
3000
2000
1000
0
1Current
Arid
Central
Hot_dry
Warm_wet
Warm_wet+

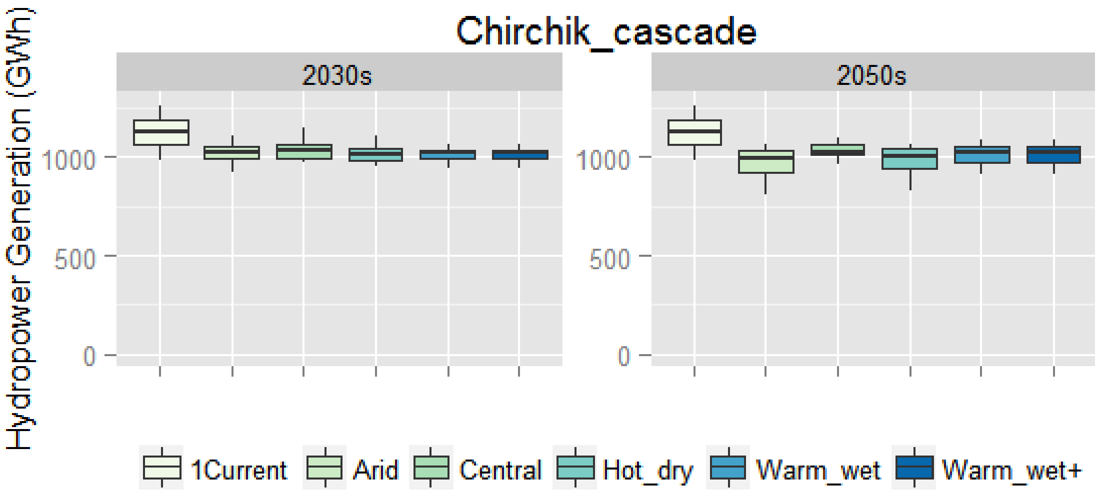
Chirchik_cascade
2030s
2050s
Hydropower Generation (GWh)
1000
500
0
1Current
Arid
Central
Hot_dry
Warm_wet
Warm_wet+

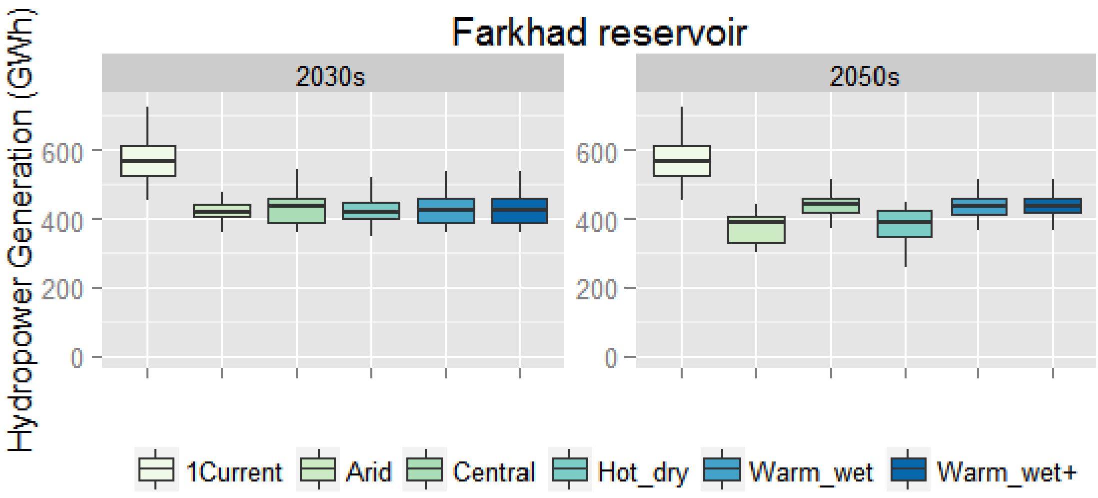
Farkhad reservoir
2030s
2050s
Hydropower Generation (GWh)
0
200
400
600
1Current
Arid
Central
Hot_dry
Warm_wet
Warm_wet+

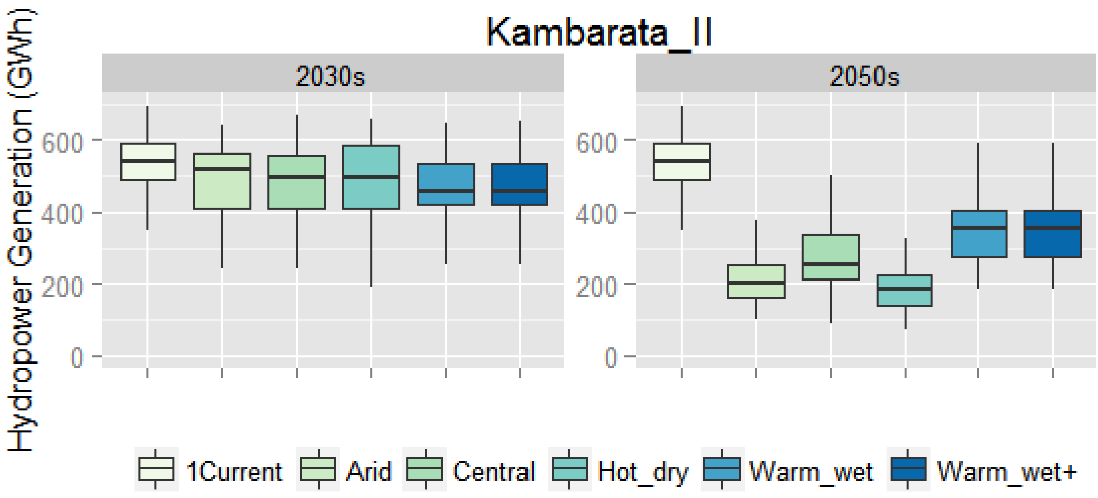
Kambarata_II
2030s
2050s
Hydropower Generation (GWh)
0
200
400
600
1Current
Arid
Central
Hot_dry
Warm_wet
Warm_wet+

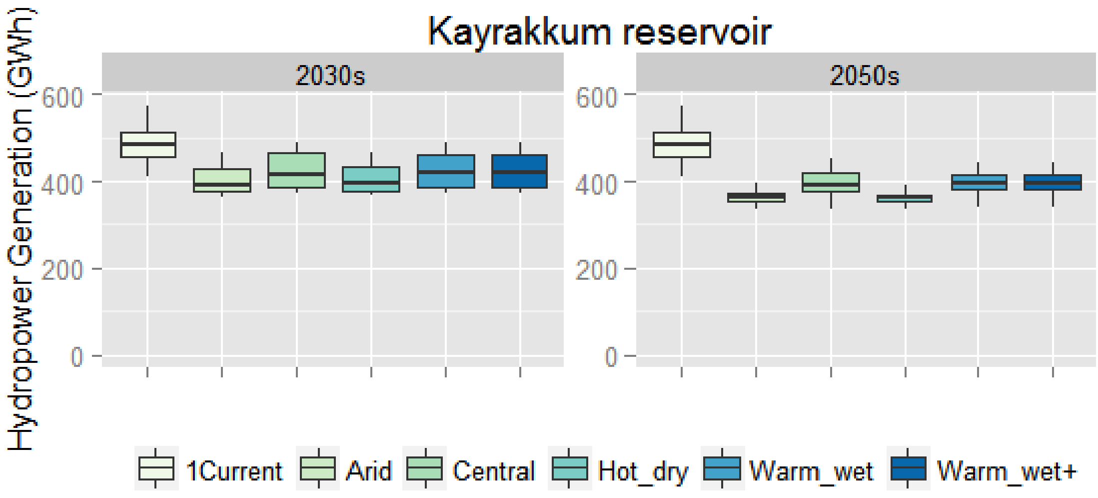
Kayrakkum reservoir
2030s
2050s
Hydropower Generation (GWh)
0
200
400
600
1Current
Arid
Central
Hot_dry
Warm_wet
Warm_wet+

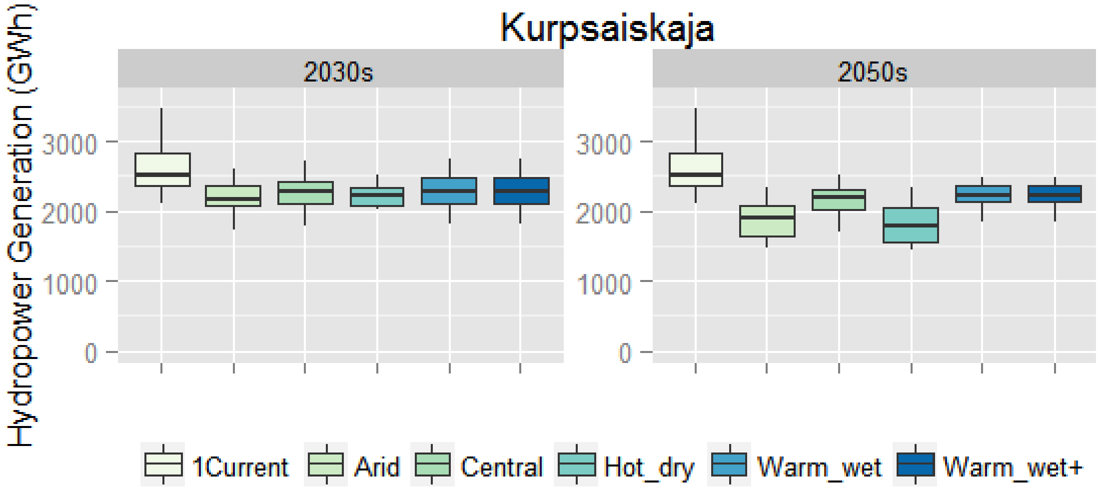
Kurpsaiskaja
2030s
2050s
Hydropower Generation (GWh)
3000
2000
1000
0
1Current
Arid
Central
Hot_dry
Warm_wet
Warm_wet+

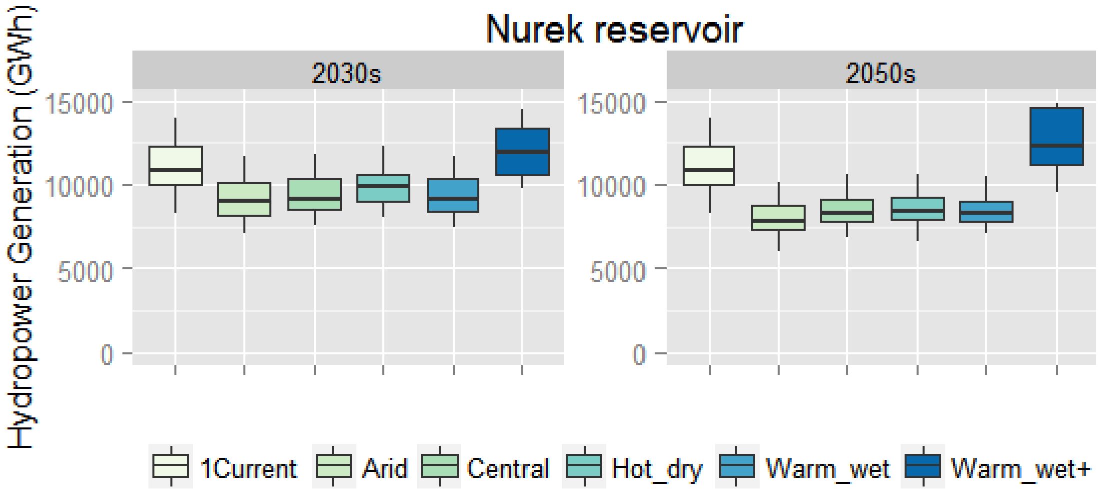
Nurek reservoir
2030s
2050s
Hydropower Generation (GWh)
15000
10000
5000
0
1Current
Arid
Central
Hot_dry
Warm_wet
Warm_wet+

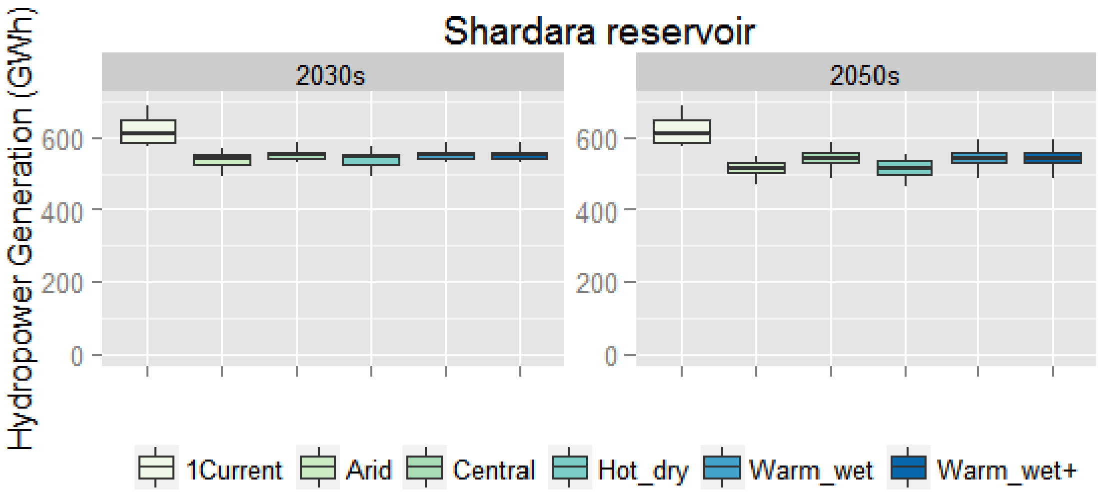
Shardara reservoir
2030s
2050s
Hydropower Generation (GWh)
600
400
200
0
1Current
Arid
Central
Hot_dry
Warm_wet
Warm_wet+

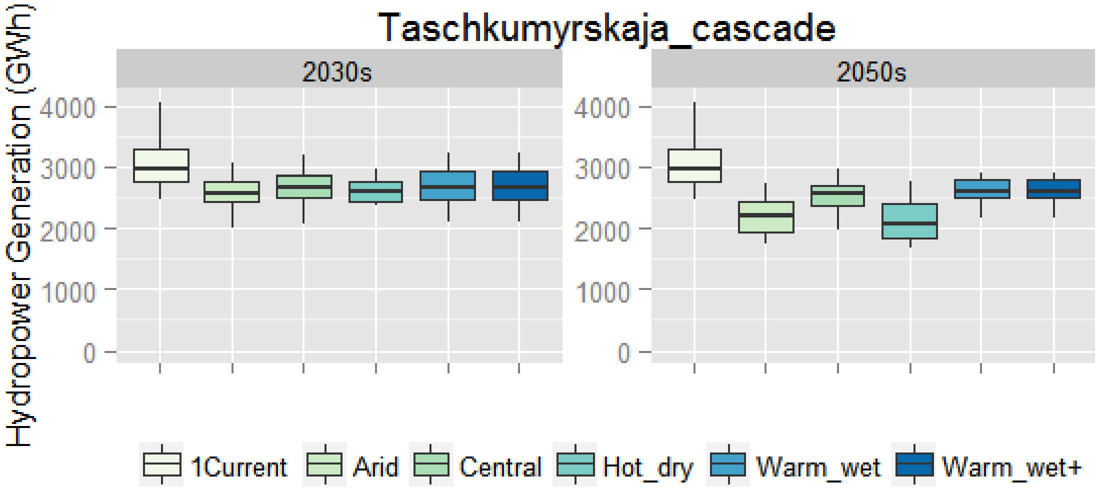
Taschkumyrskaja_cascade
2030s
2050s
Hydropower Generation (GWh)
4000
3000
2000
1000
0
1Current
Arid
Central
Hot_dry
Warm_wet
Warm_wet+

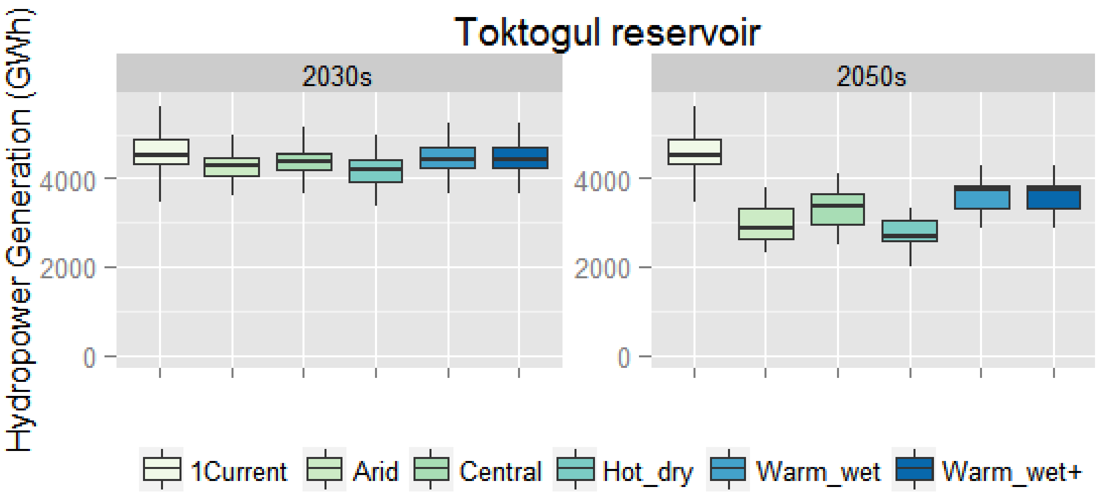
Toktogul reservoir
2030s
2050s
Hydropower Generation (GWh)
4000
2000
0
1Current
Arid
Central
Hot_dry
Warm_wet
Warm_wet+

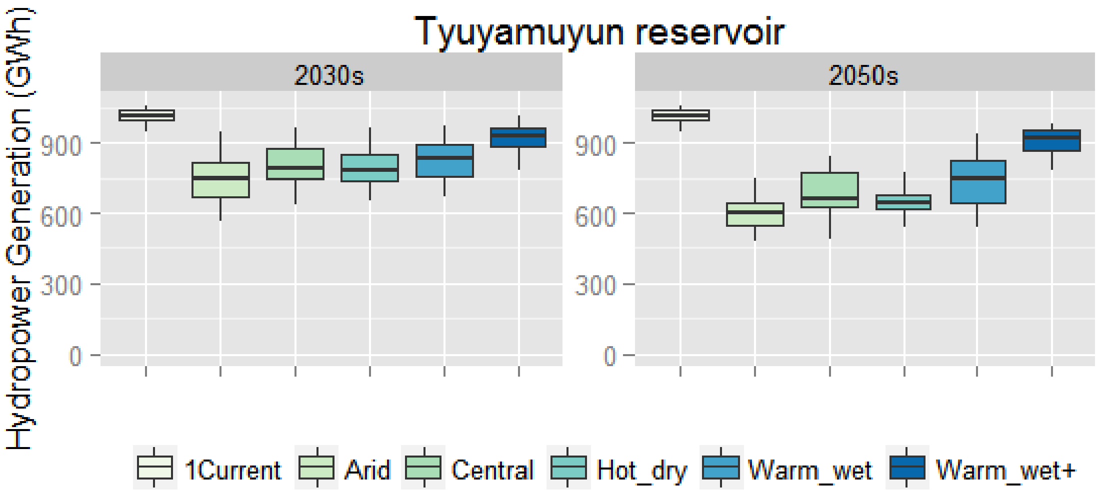
Tyuyamuyun reservoir
2030s
2050s
Hydropower Generation (GWh)
900
600
300
0
1Current
Arid
Central
Hot_dry
Warm_wet
Warm_wet+

IV.2 With planned infrastructure

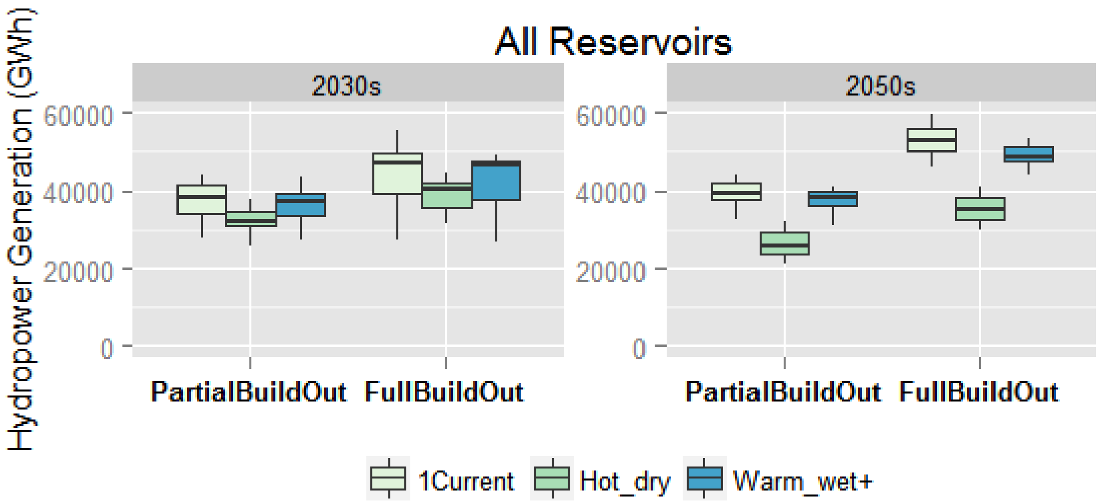

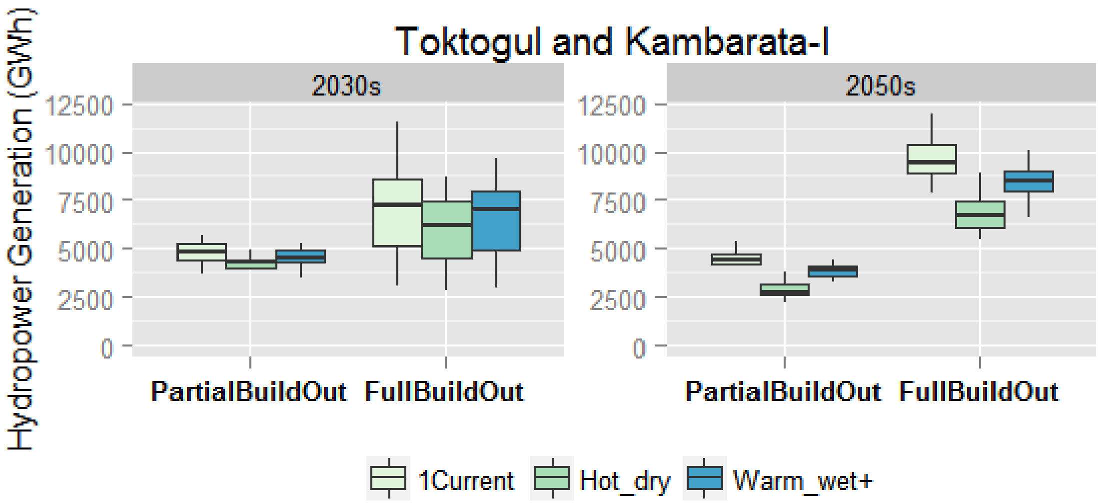

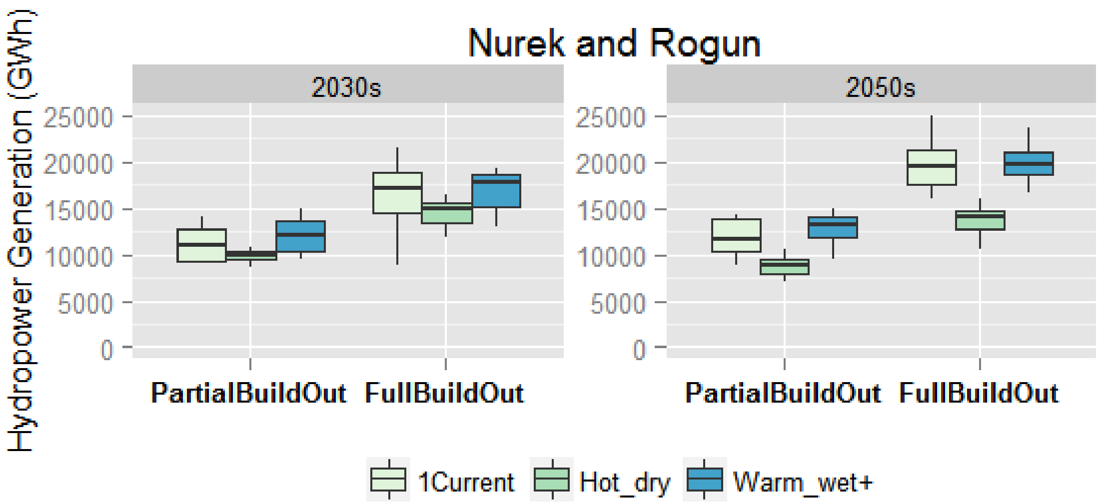

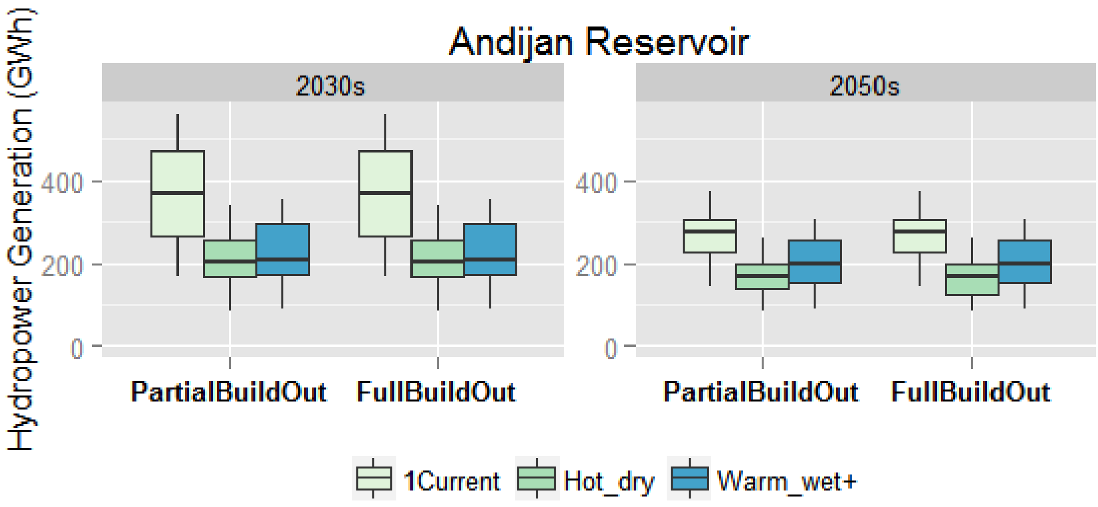
Andijan Reservoir
2030s
2050s
Hydropower Generation (GWh)
0
200
400
PartialBuildOut
FullBuildOut
1Current
Hot_dry
Warm_wet+

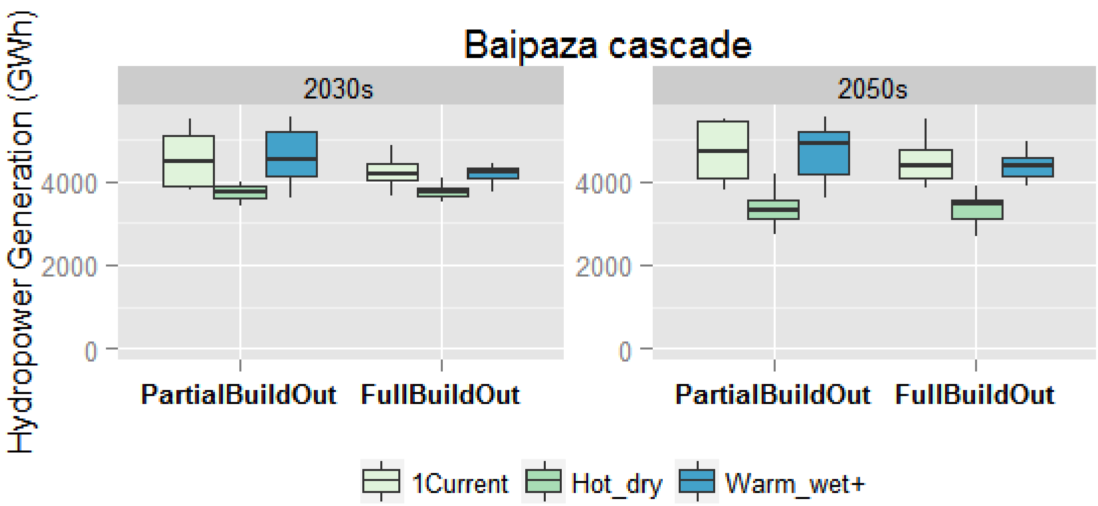
Baipaza cascade
2030s
2050s
Hydropower Generation (GWh)
0
2000
4000
PartialBuildOut
FullBuildOut
1Current
Hot_dry
Warm_wet+

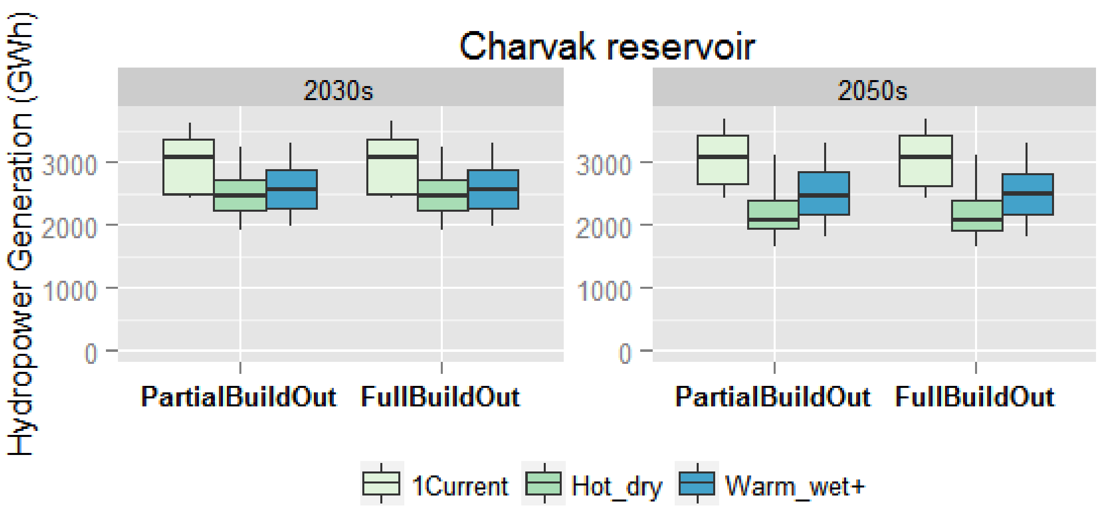
Charvak reservoir
2030s
2050s
Hydropower Generation (GWh)
0
1000
2000
3000
PartialBuildOut
FullBuildOut
1Current
Hot_dry
Warm_wet+

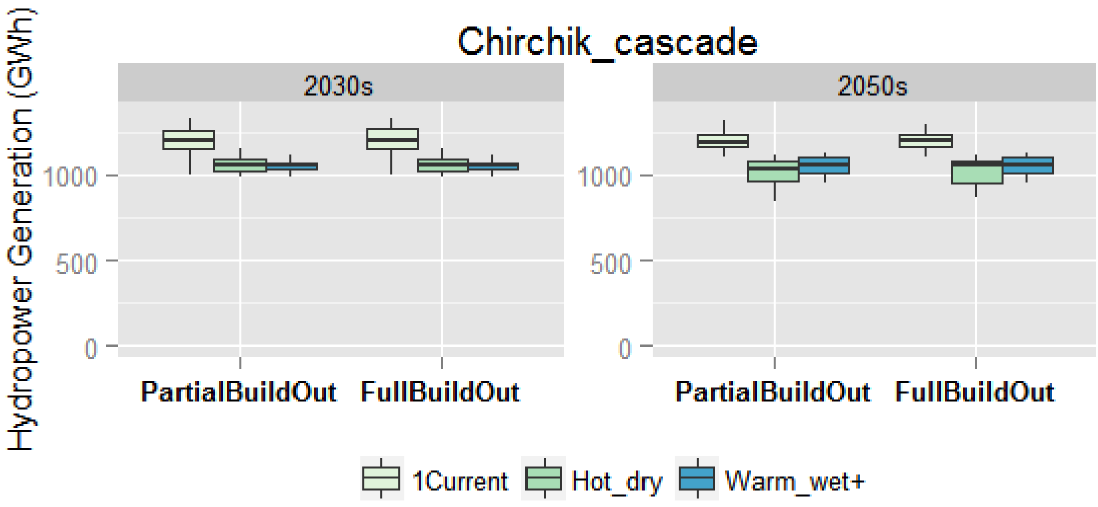
Chirchik_cascade
Hydropower Generation (GWh)
2030s
2050s
1000
500
0
PartialBuildOut
FullBuildOut
1Current
Hot_dry
Warm_wet+

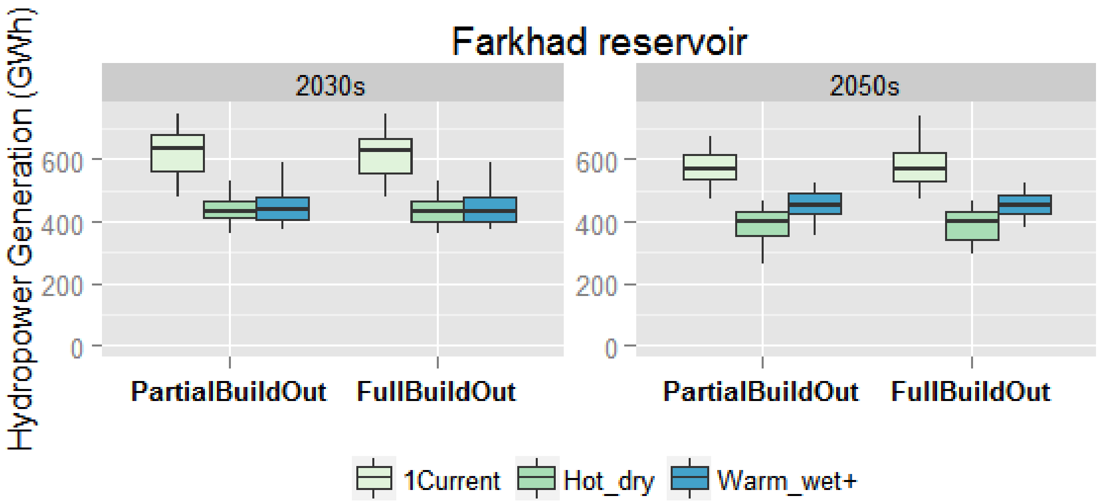
Farkhad reservoir
Hydropower Generation (GWh)
2030s
2050s
600
400
200
0
PartialBuildOut
FullBuildOut
1Current
Hot_dry
Warm_wet+

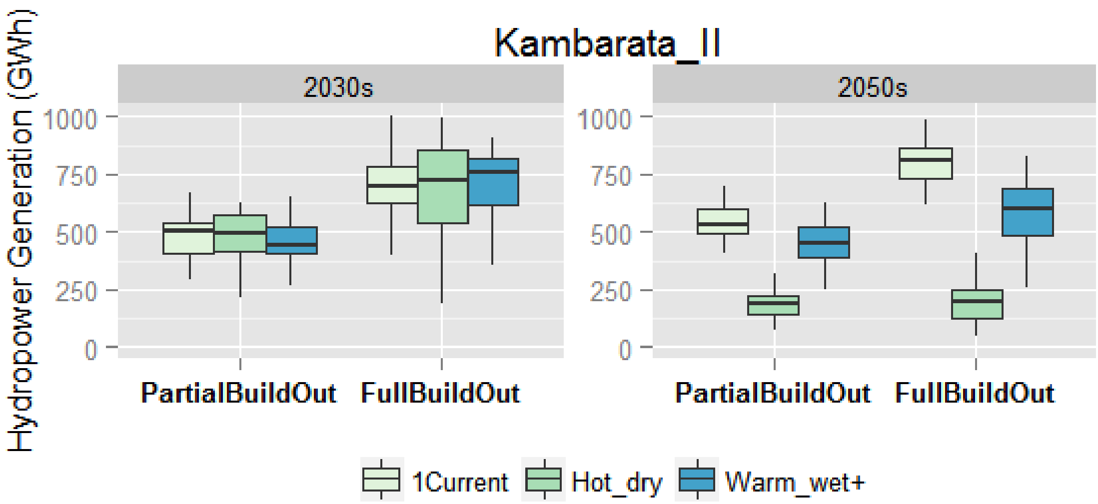
Kambarata_II
Hydropower Generation (GWh)
2030s
2050s
1000
750
500
250
0
PartialBuildOut
FullBuildOut
1Current
Hot_dry
Warm_wet+

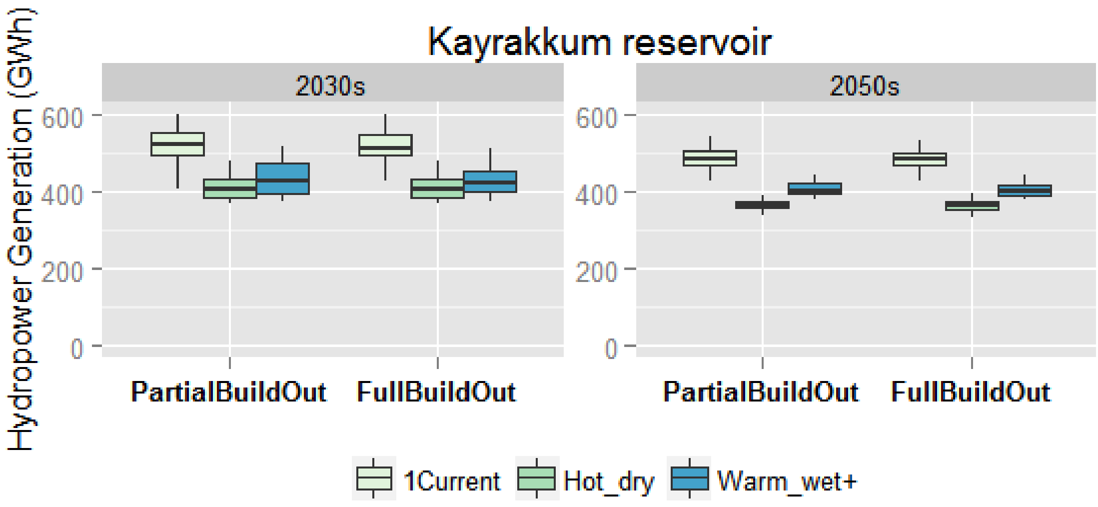
Kayrakkum reservoir
Hydropower Generation (GWh)
2030s
2050s
0
200
400
600
PartialBuildOut
FullBuildOut
1Current
Hot_dry
Warm_wet+

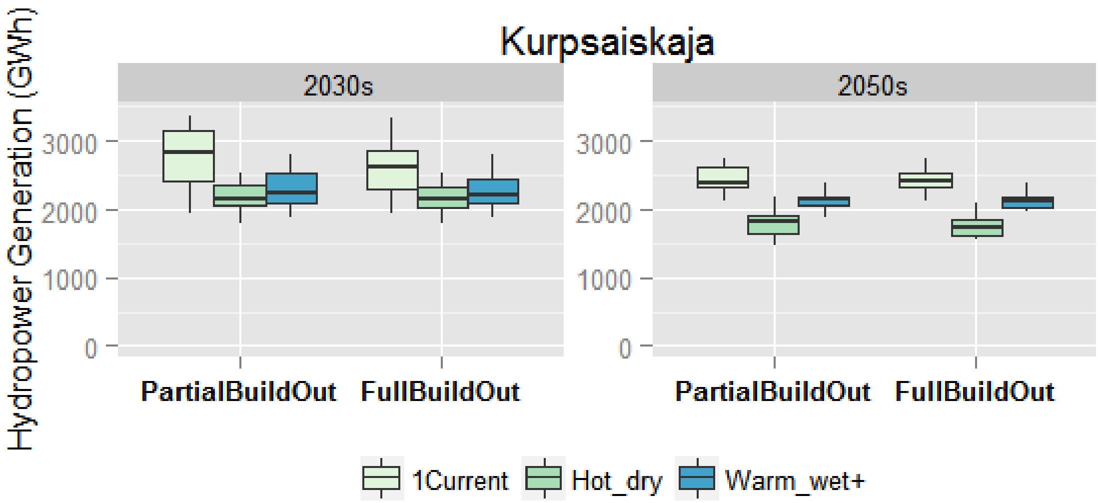
Kurpsaiskaja
Hydropower Generation (GWh)
2030s
2050s
0
1000
2000
3000
PartialBuildOut
FullBuildOut
1Current
Hot_dry
Warm_wet+

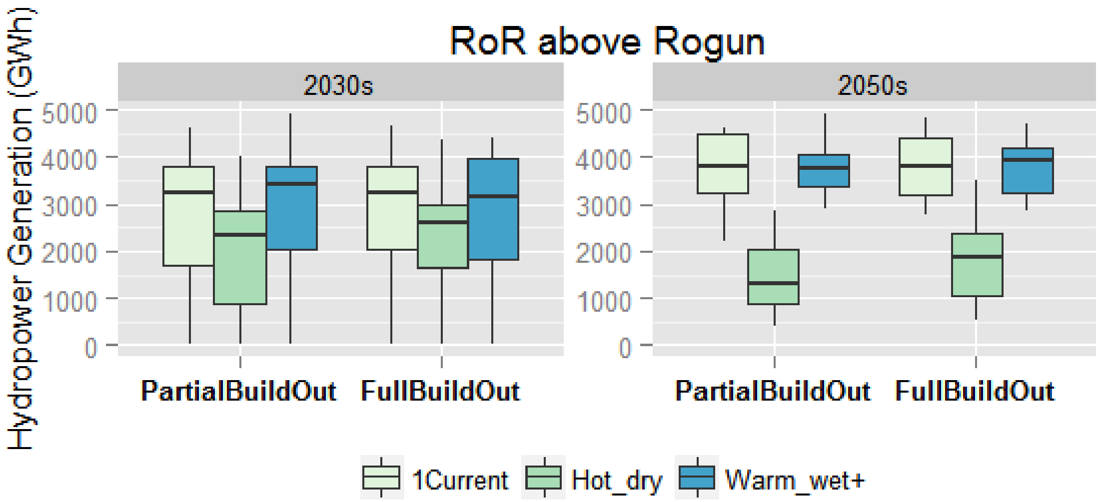
RoR above Rogun
Hydropower Generation (GWh)
2030s
2050s
0
1000
2000
3000
4000
5000
PartialBuildOut
FullBuildOut
1Current
Hot_dry
Warm_wet+

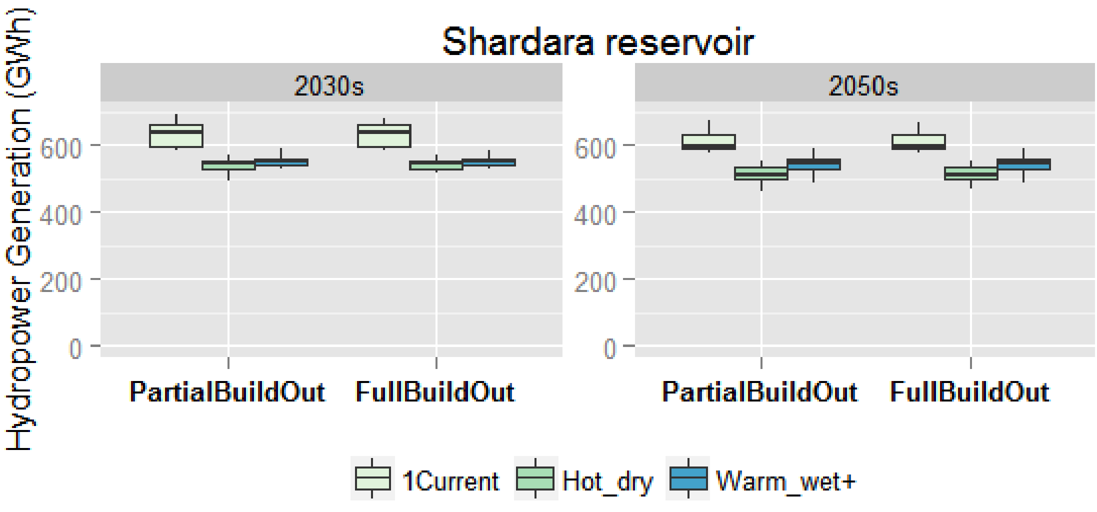
Shardara reservoir
Hydropower Generation (GWh)
2030s
2050s
600
400
200
0
PartialBuildOut
FullBuildOut
1Current
Hot_dry
Warm_wet+

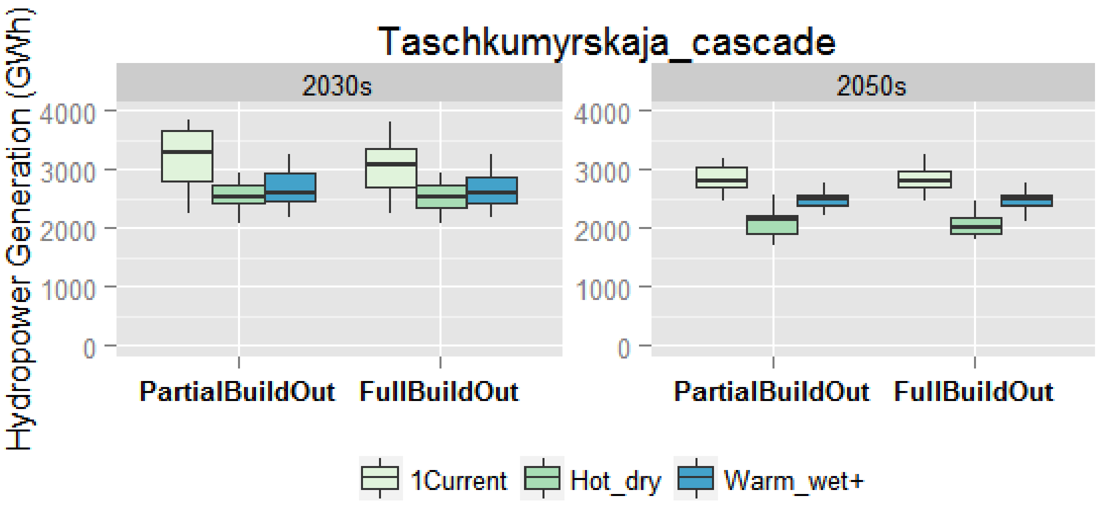
Taschkumyrskaja_cascade
Hydropower Generation (GWh)
2030s
2050s
4000
3000
2000
1000
0
PartialBuildOut
FullBuildOut
1Current
Hot_dry
Warm_wet+

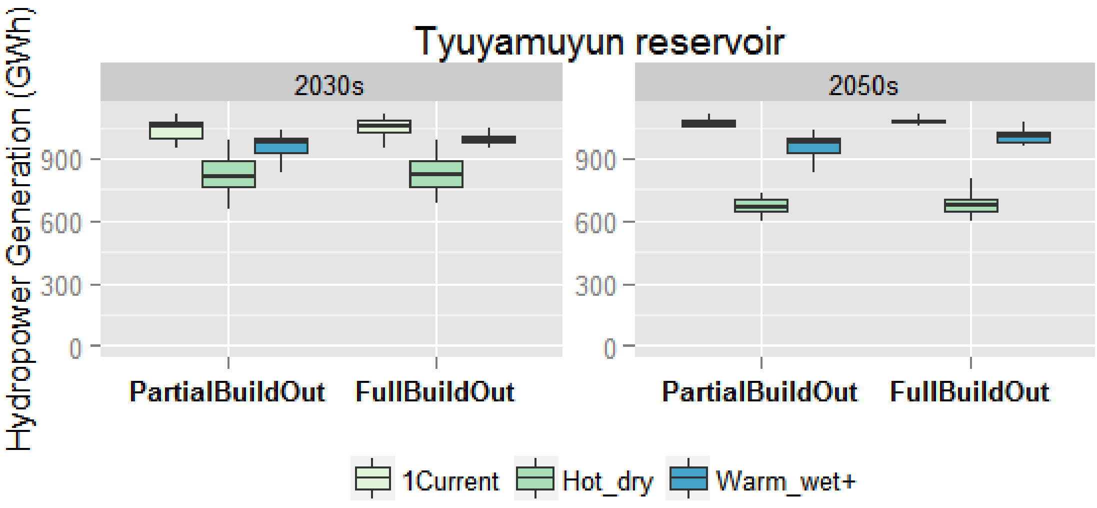
Tyuyamuyun reservoir
Hydropower Generation (GWh)
2030s
2050s
900
600
300
0
PartialBuildOut
FullBuildOut
1Current
Hot_dry
Warm_wet+

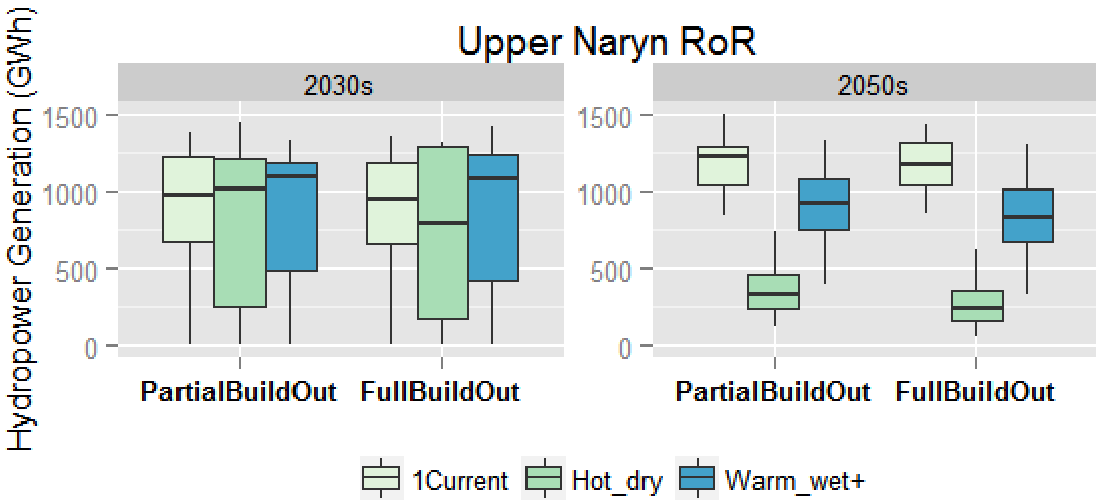

Upper Naryn RoR
2030s
2050s
Hydropower Generation (GWh)
1500
1000
500
0
PartialBuildOut
FullBuildOut
1Current
Hot_dry
Warm_wet+

Appendix V Agriculture Water Supply

V.1 With current infrastructure

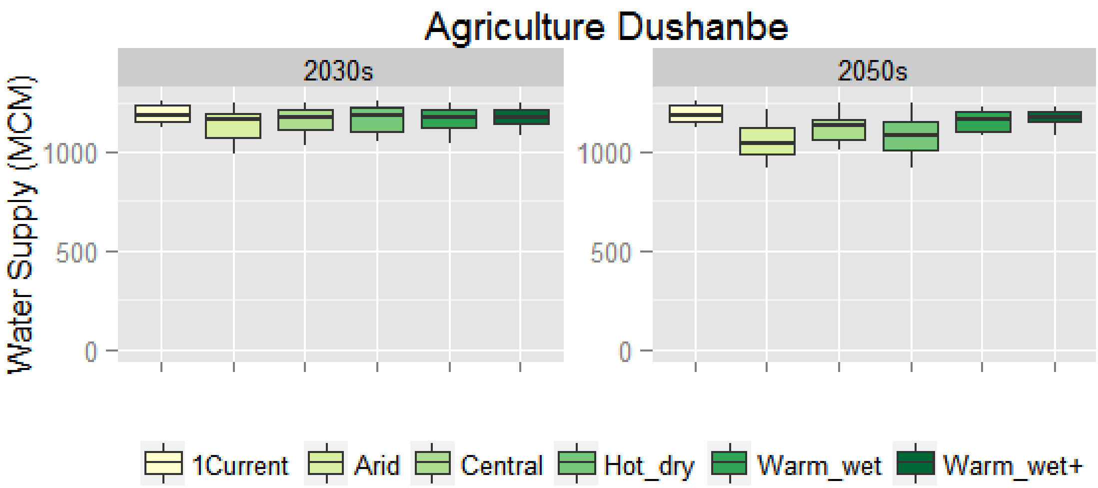

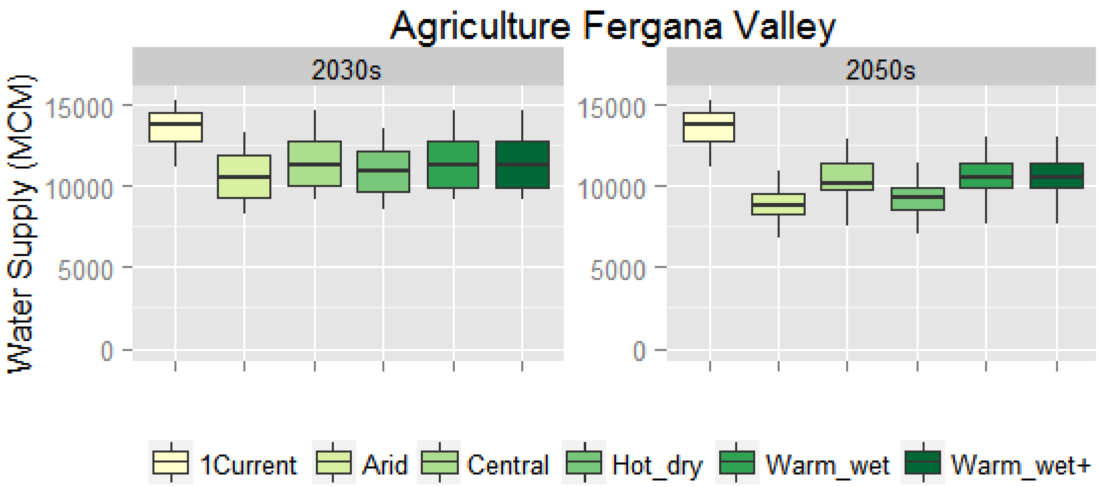

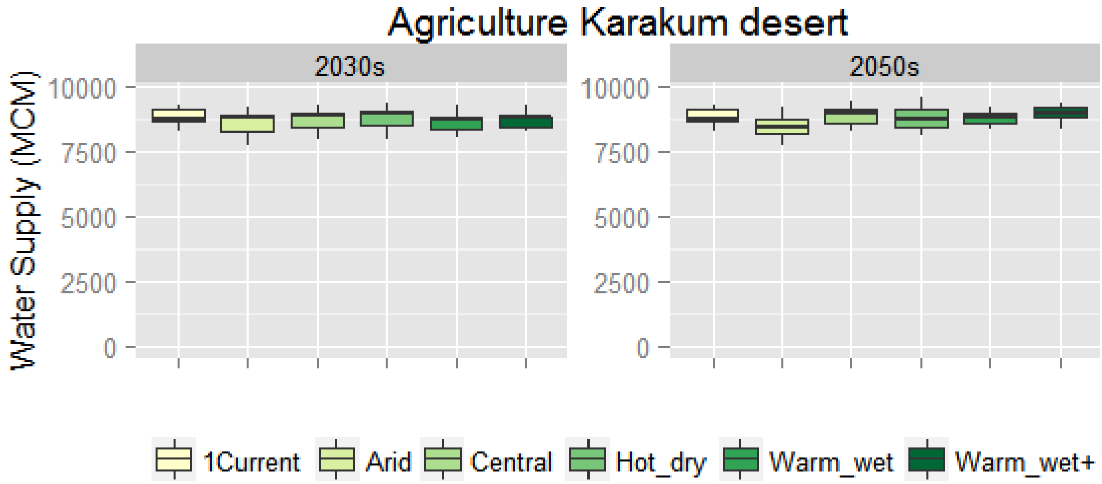
Agriculture Karakum desert
2030s
2050s
Water Supply (MCM)
10000
7500
5000
2500
0
1Current
Arid
Central
Hot_dry
Warm_wet
Warm_wet+

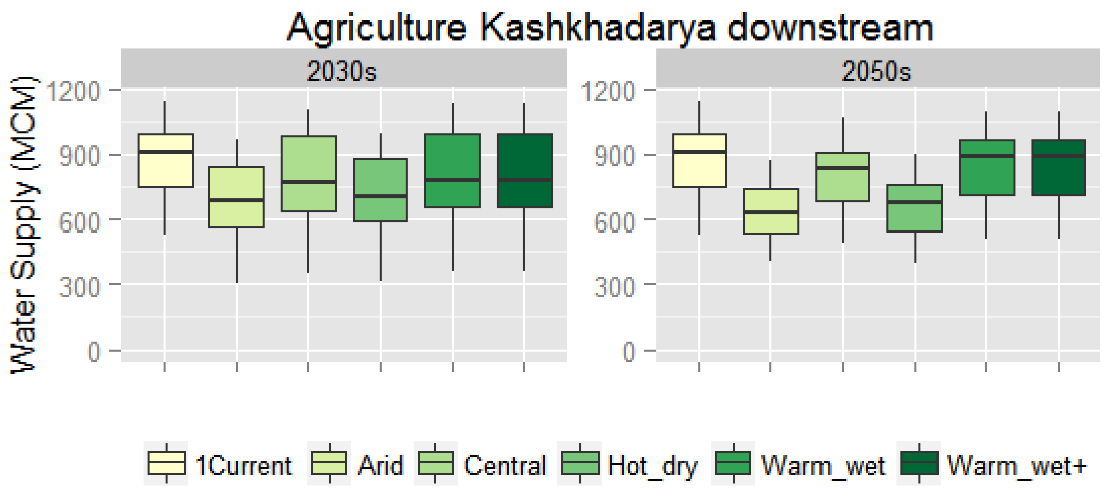
Agriculture Kashkhadarya downstream
2030s
2050s
Water Supply (MCM)
1200
900
600
300
0
1Current
Arid
Central
Hot_dry
Warm_wet
Warm_wet+

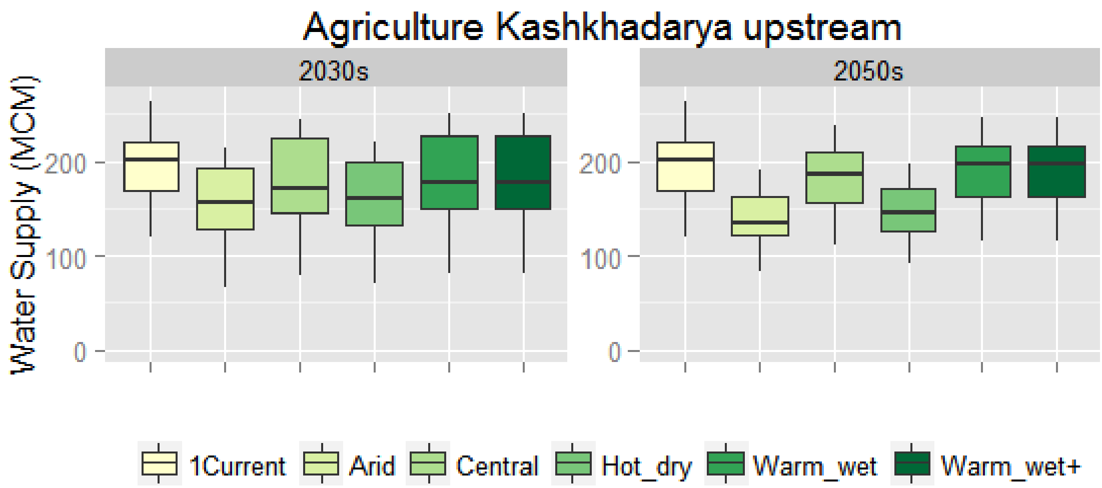
Agriculture Kashkhadarya upstream
2030s
2050s
Water Supply (MCM)
200
100
0
1Current
Arid
Central
Hot_dry
Warm_wet
Warm_wet+

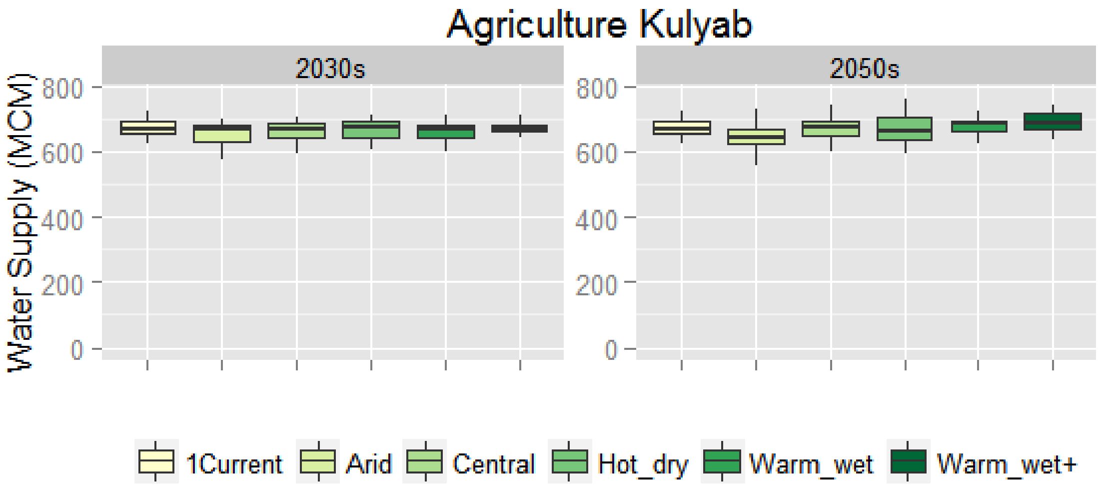

Agriculture Kulyab
2030s
2050s
Water Supply (MCM)
800
600
400
200
0
1Current
Arid
Central
Hot_dry
Warm_wet
Warm_wet+

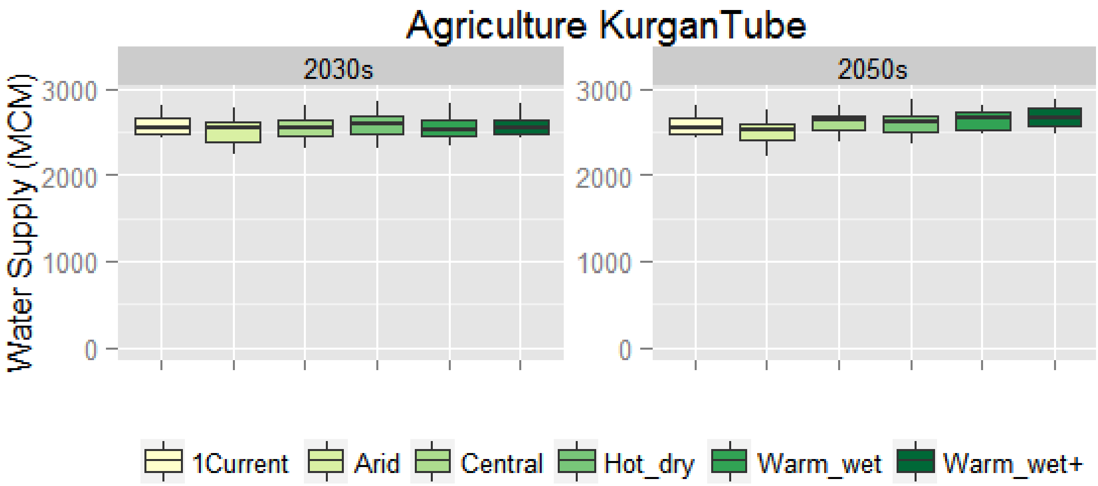

Agriculture KurganTube
2030s
2050s
Water Supply (MCM)
3000
2000
1000
0
1Current
Arid
Central
Hot_dry
Warm_wet
Warm_wet+

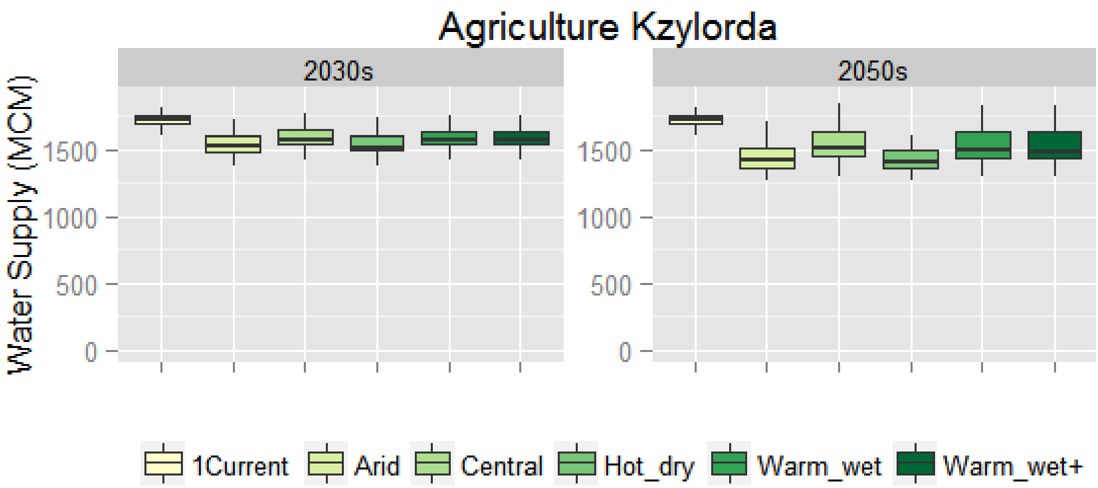

Agriculture Kzylorda
2030s
2050s
Water Supply (MCM)
1500
1000
500
0
1Current
Arid
Central
Hot_dry
Warm_wet
Warm_wet+

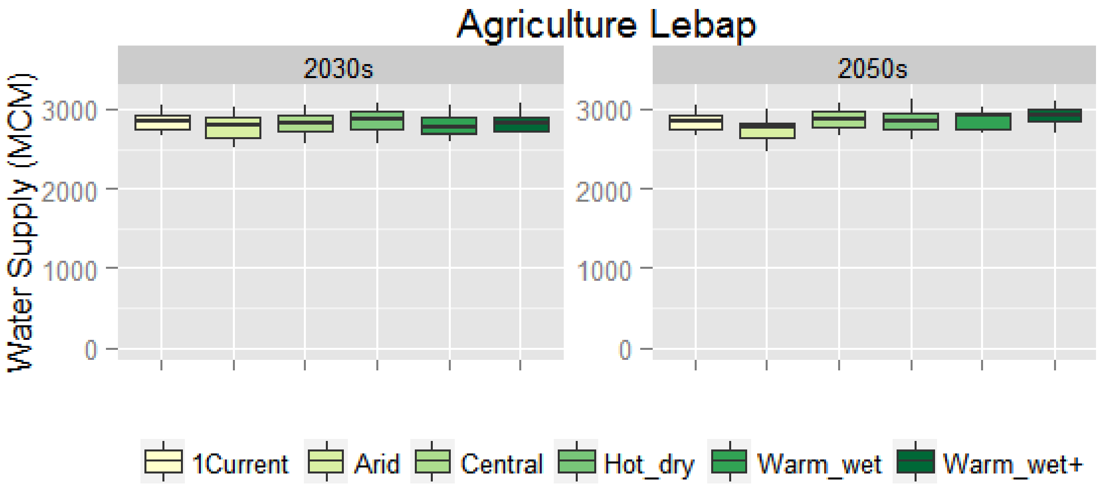
Agriculture Lebap
2030s
2050s
Water Supply (MCM)
0
1000
2000
3000
1Current
Arid
Central
Hot_dry
Warm_wet
Warm_wet+

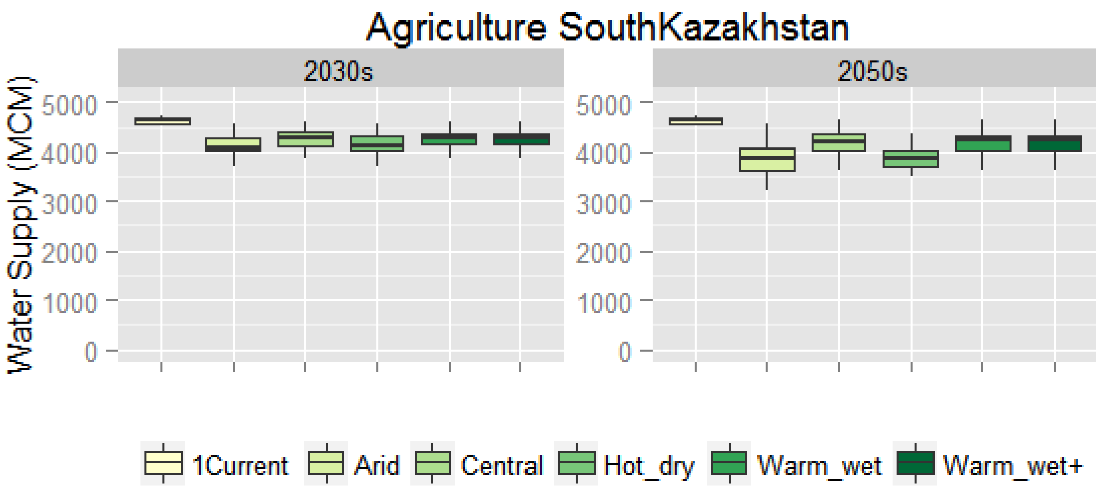
Agriculture SouthKazakhstan
2030s
2050s
Water Supply (MCM)
0
1000
2000
3000
4000
5000
1Current
Arid
Central
Hot_dry
Warm_wet
Warm_wet+

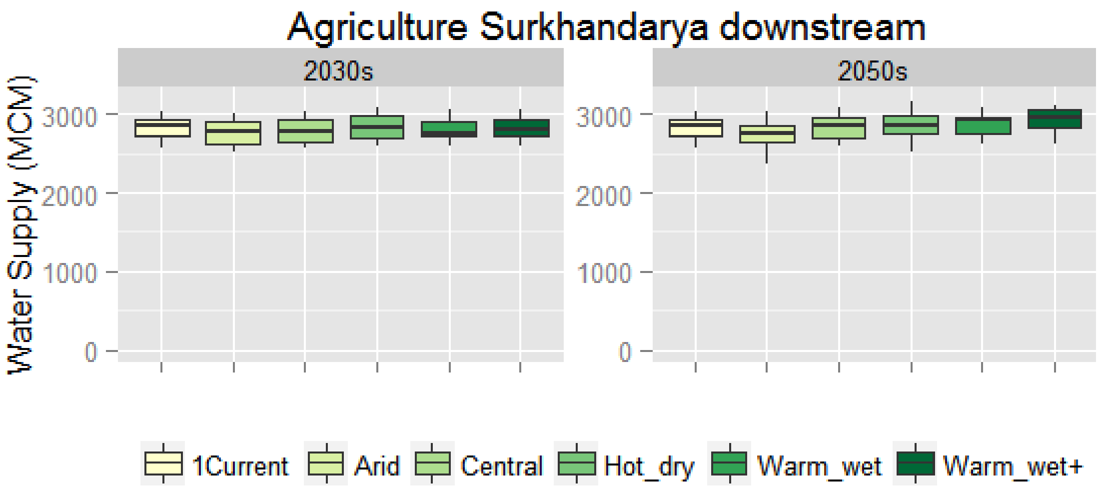
Agriculture Surkhandarya downstream
2030s
2050s
Water Supply (MCM)
0
1000
2000
3000
1Current
Arid
Central
Hot_dry
Warm_wet
Warm_wet+

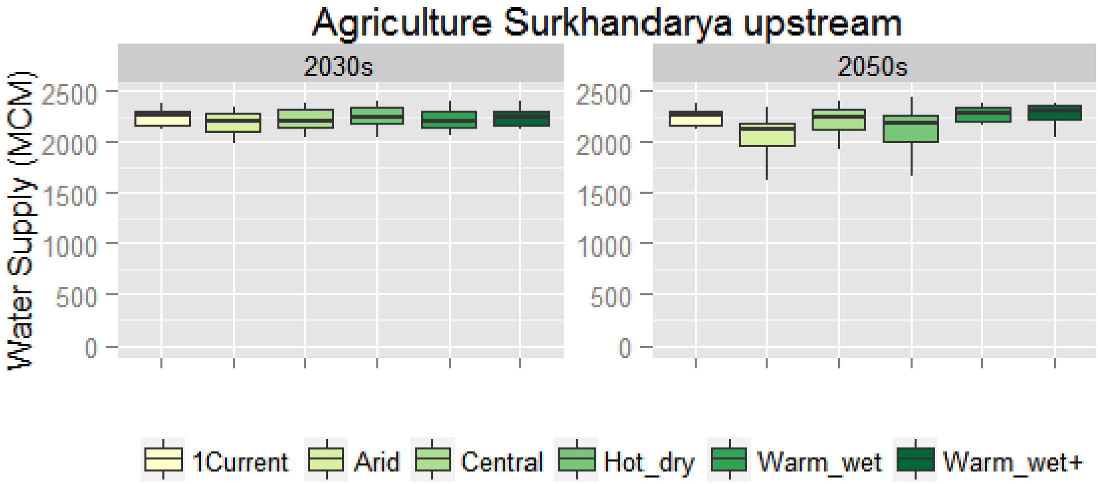
Agriculture Surkhandarya upstream
2030s
2050s
Water Supply (MCM)
0
500
1000
1500
2000
2500
1Current
Arid
Central
Hot_dry
Warm_wet
Warm_wet+

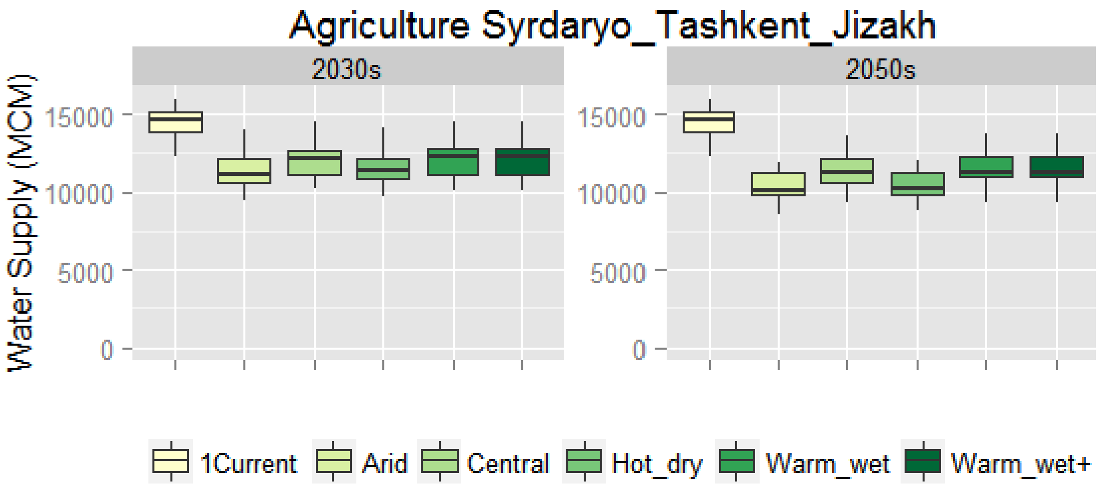
Agriculture Syrdaryo_Tashkent_Jizakh
2030s
2050s
Water Supply (MCM)
0
5000
10000
15000
1Current
Arid
Central
Hot_dry
Warm_wet
Warm_wet+

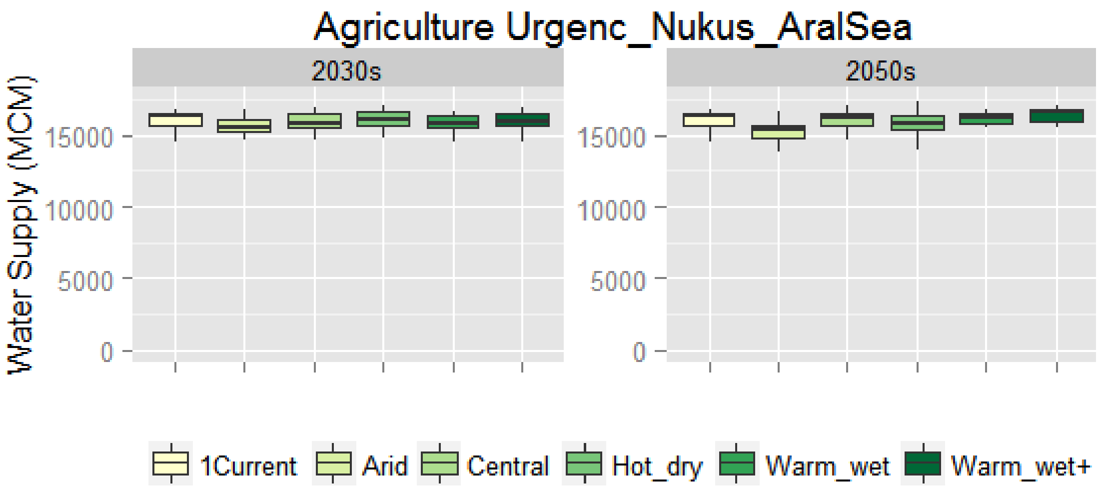
Agriculture Urgenc_Nukus_AralSea
2030s
2050s
Water Supply (MCM)
0
5000
10000
15000
1Current
Arid
Central
Hot_dry
Warm_wet
Warm_wet+

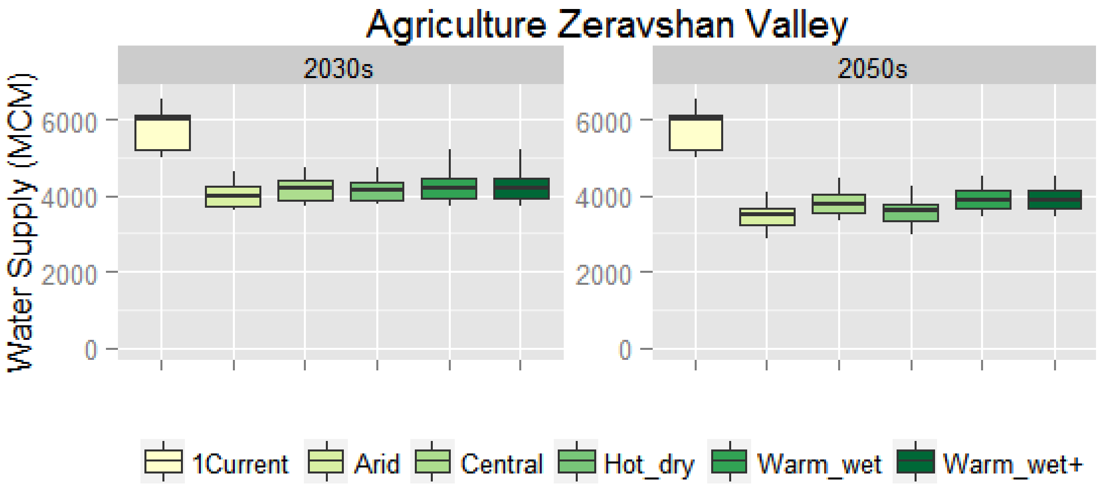

V.2 With planned infrastructure

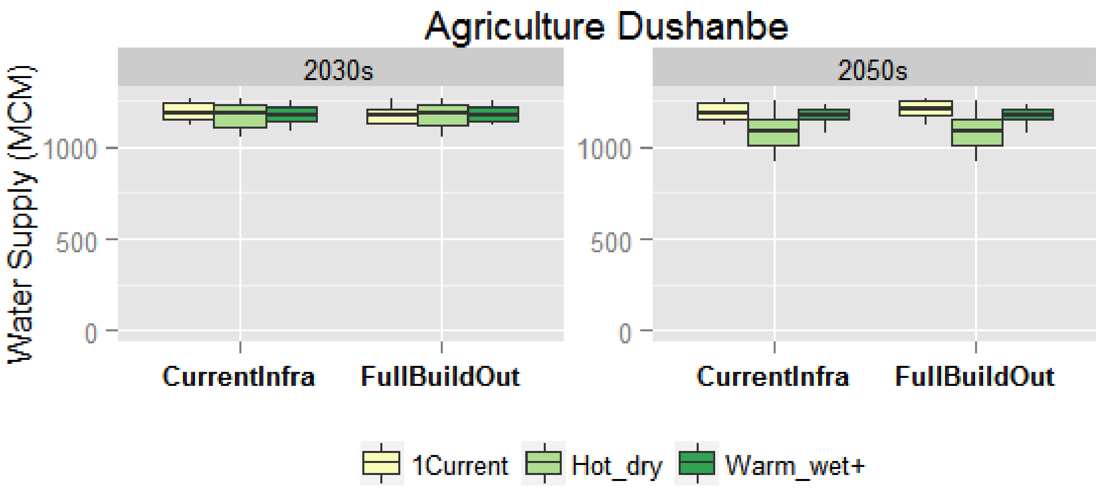

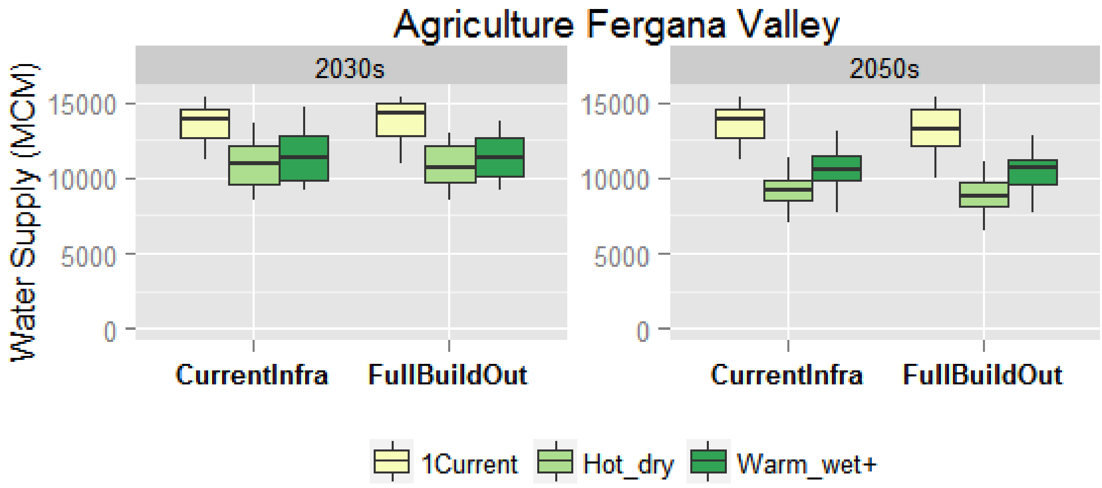
Agriculture Fergana Valley
2030s
2050s
Water Supply (MCM)
0
5000
10000
15000
CurrentInfra
FullBuildOut
1Current
Hot_dry
Warm_wet+

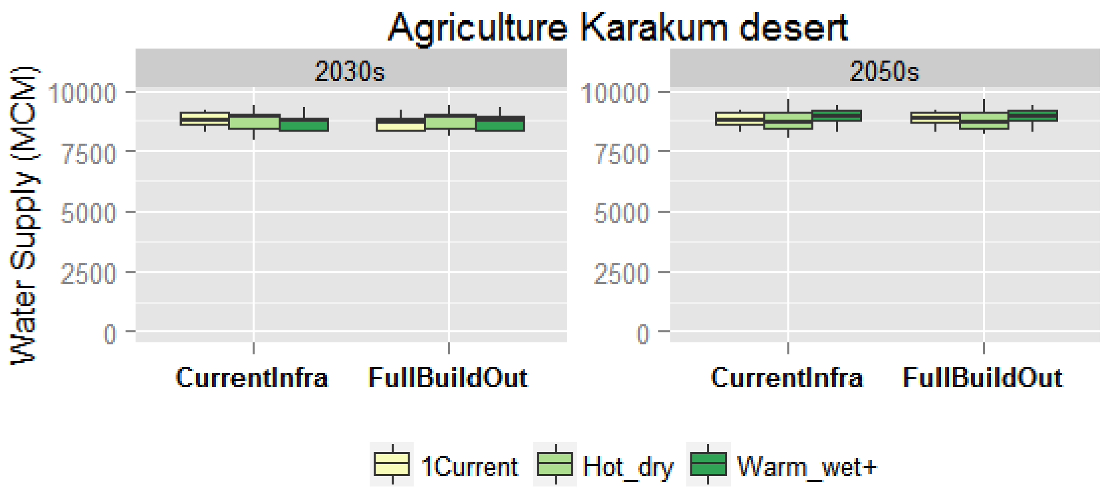
Agriculture Karakum desert
2030s
2050s
Water Supply (MCM)
0
2500
5000
7500
10000
CurrentInfra
FullBuildOut
1Current
Hot_dry
Warm_wet+

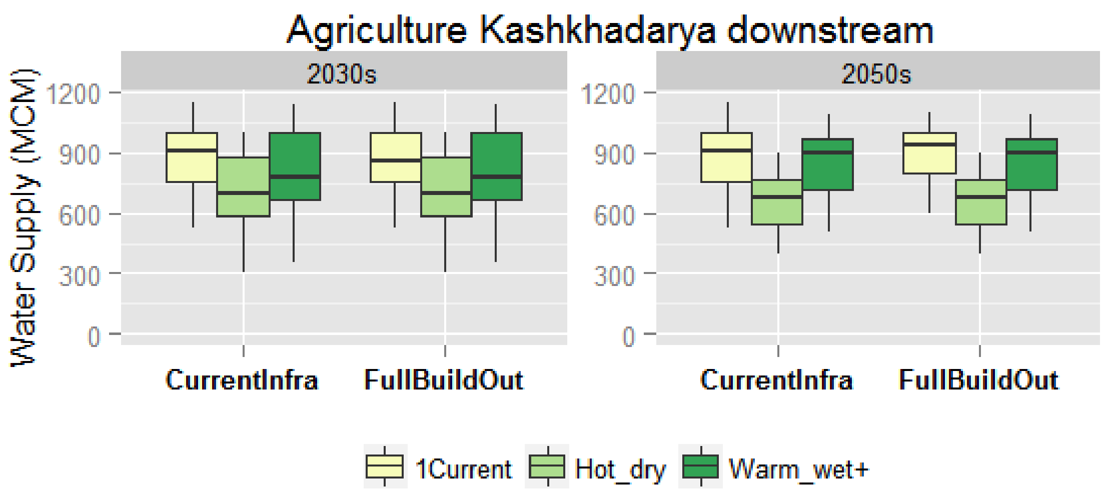
Agriculture Kashkhadarya downstream
2030s
2050s
Water Supply (MCM)
0
300
600
900
1200
CurrentInfra
FullBuildOut
1Current
Hot_dry
Warm_wet+

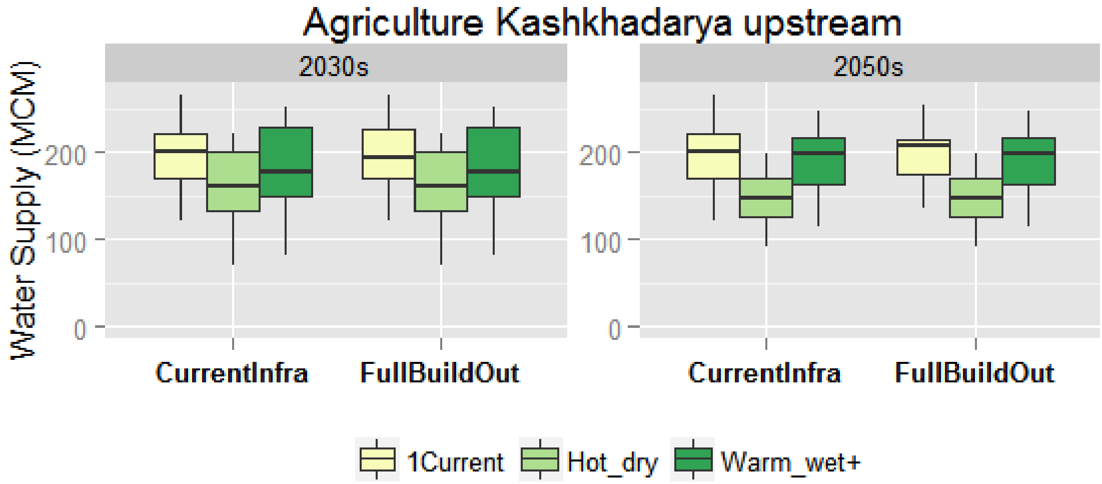
Agriculture Kashkhadarya upstream
2030s
2050s
Water Supply (MCM)
0
100
200
CurrentInfra
FullBuildOut
1Current
Hot_dry
Warm_wet+

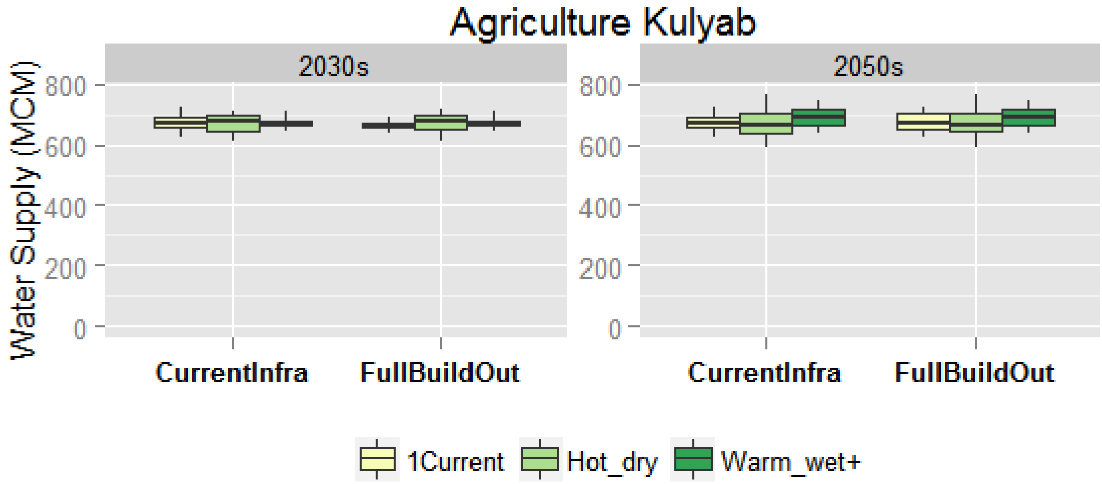
Agriculture Kulyab
2030s
2050s
Water Supply (MCM)
0
200
400
600
800
CurrentInfra
FullBuildOut
1Current
Hot_dry
Warm_wet+

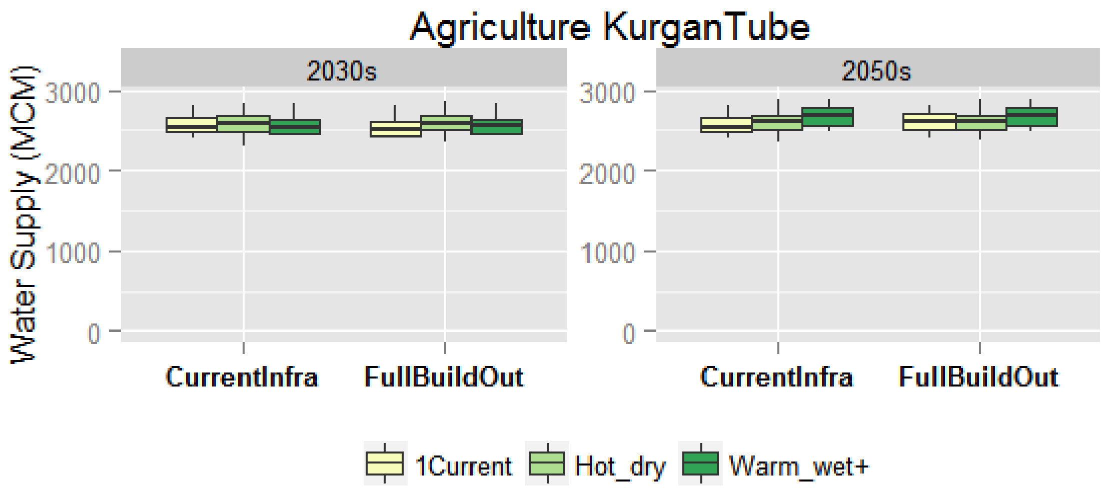
Agriculture KurganTube
2030s
2050s
Water Supply (MCM)
0
1000
2000
3000
CurrentInfra
FullBuildOut
1Current
Hot_dry
Warm_wet+

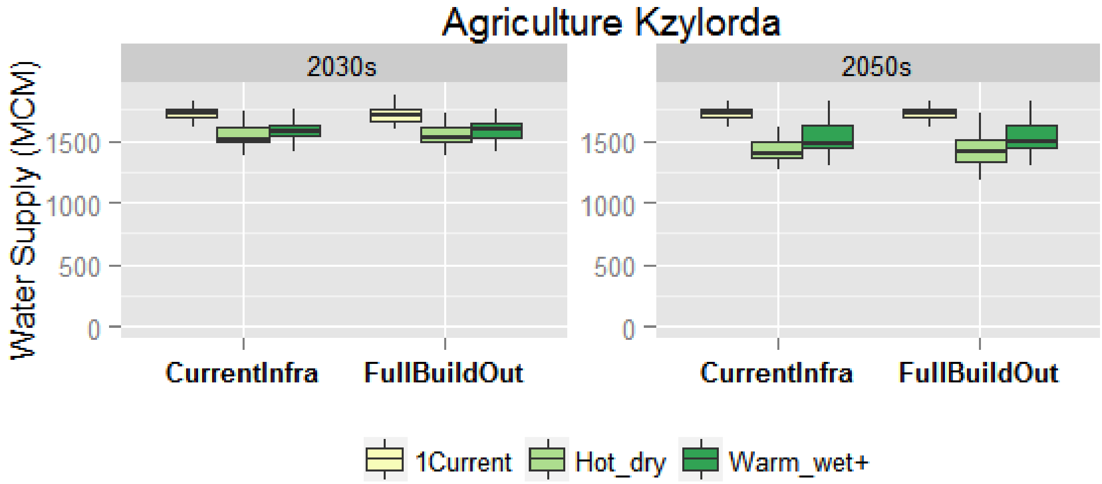
Agriculture Kzylorda
2030s
2050s
Water Supply (MCM)
0
500
1000
1500
CurrentInfra
FullBuildOut
1Current
Hot_dry
Warm_wet+

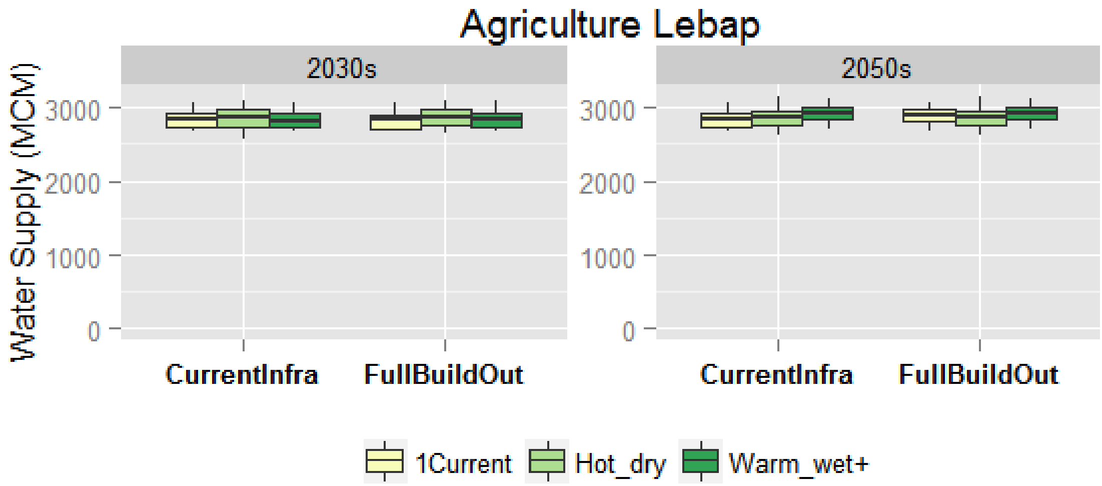
Agriculture Lebap
2030s
2050s
Water Supply (MCM)
0
1000
2000
3000
CurrentInfra
FullBuildOut
1Current
Hot_dry
Warm_wet+

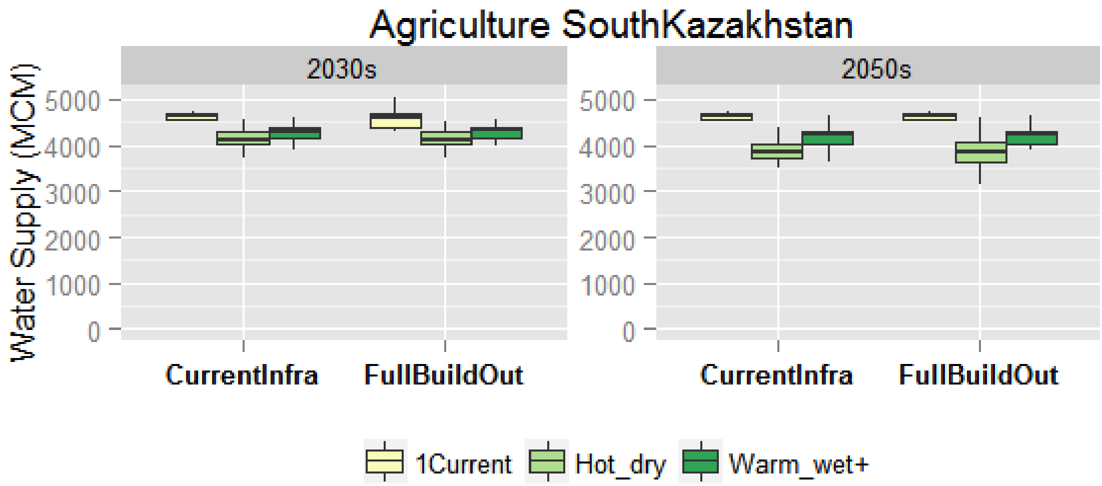
Agriculture SouthKazakhstan
2030s
2050s
Water Supply (MCM)
0
1000
2000
3000
4000
5000
CurrentInfra
FullBuildOut
1Current
Hot_dry
Warm_wet+

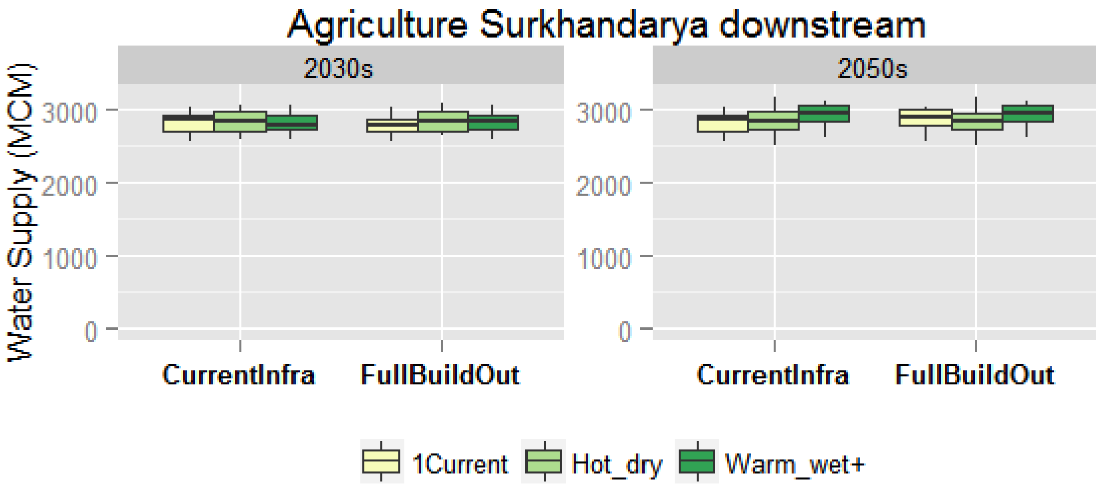
Agriculture Surkhandarya downstream
2030s
2050s
Water Supply (MCM)
3000
2000
1000
0
CurrentInfra
FullBuildOut
1Current
Hot_dry
Warm_wet+

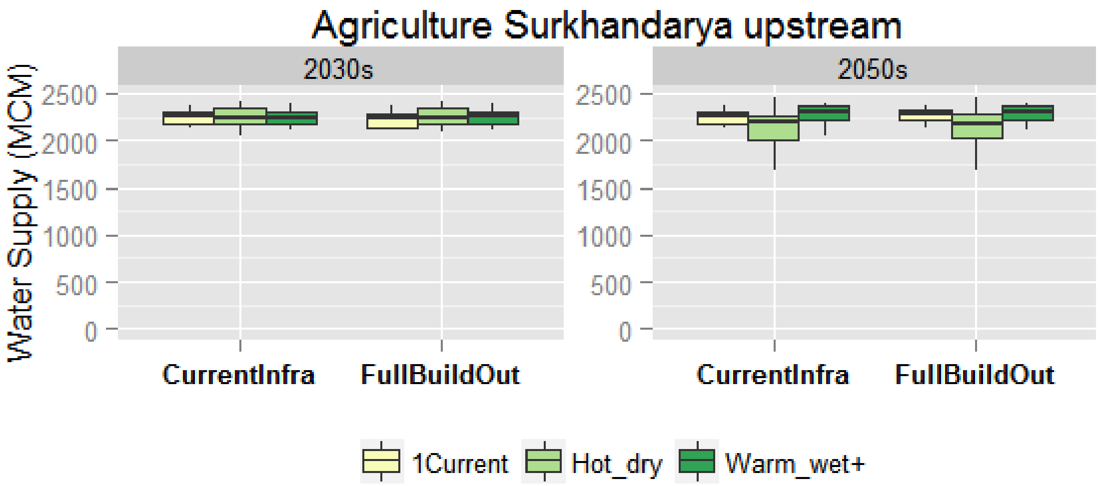
Agriculture Surkhandarya upstream
2030s
2050s
Water Supply (MCM)
2500
2000
1500
1000
500
0
CurrentInfra
FullBuildOut
1Current
Hot_dry
Warm_wet+

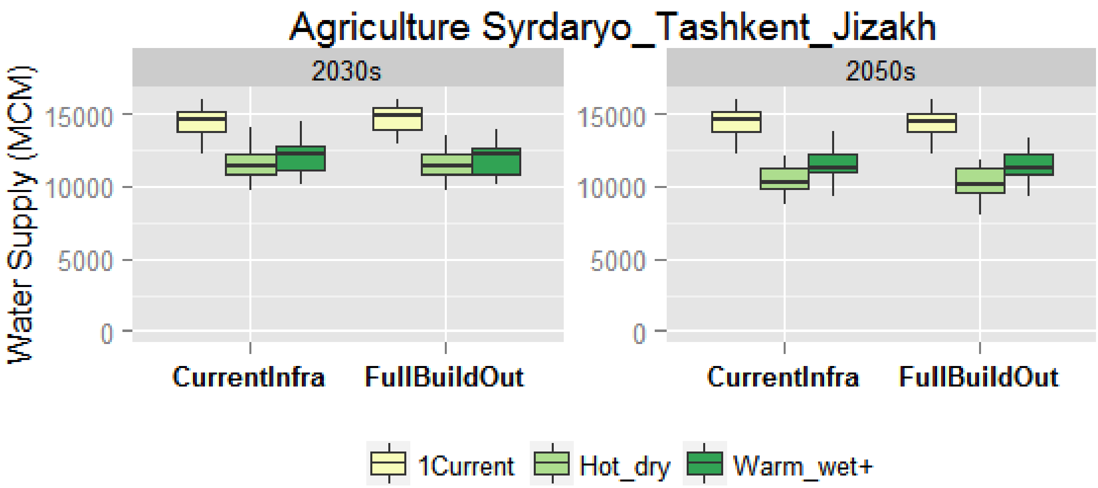
Agriculture Syrdaryo_Tashkent_Jizakh
2030s
2050s
Water Supply (MCM)
15000
10000
5000
0
CurrentInfra
FullBuildOut
1Current
Hot_dry
Warm_wet+

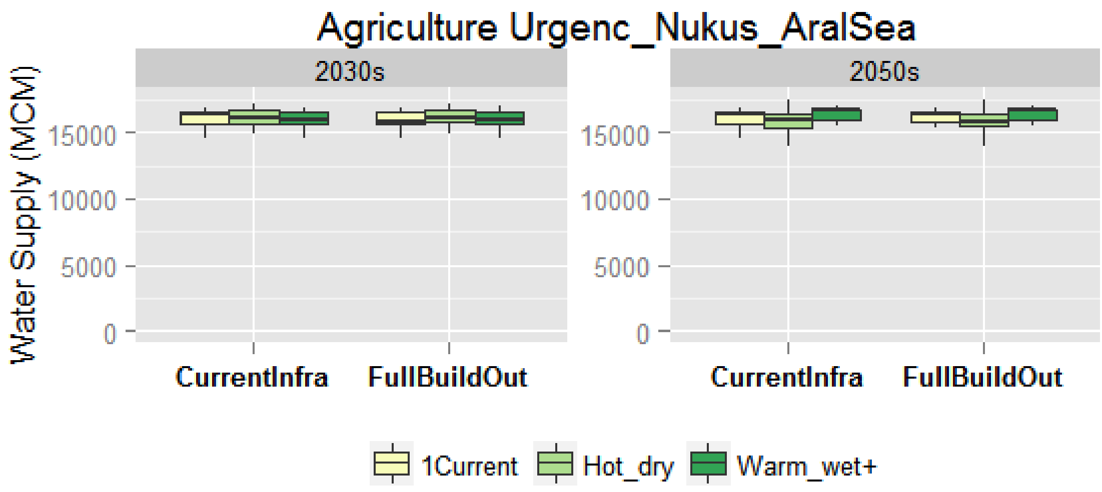

Agriculture Urgenc_Nukus_AralSea
2030s
2050s
Water Supply (MCM)
15000
10000
5000
0
CurrentInfra
FullBuildOut
1Current
Hot_dry
Warm_wet+

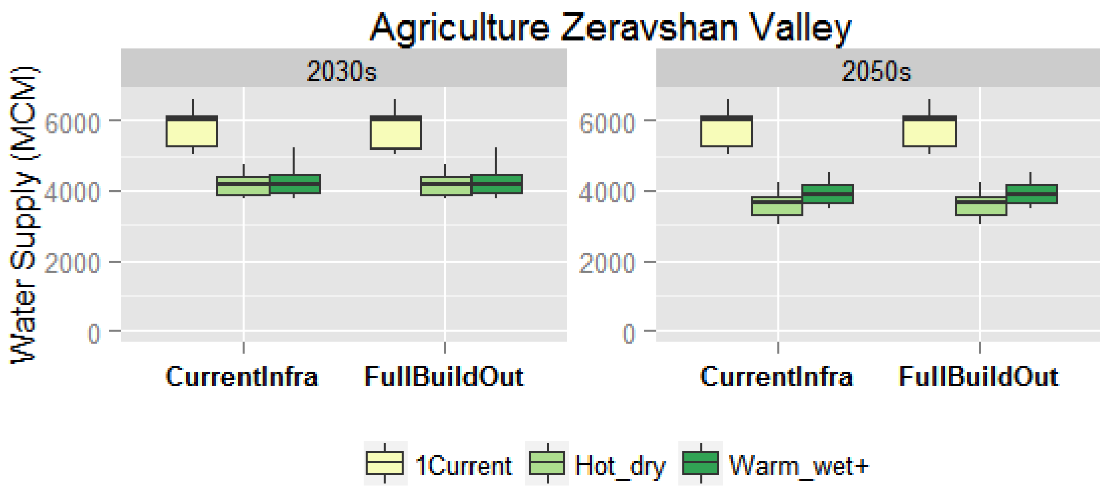

Agriculture Zeravshan Valley
2030s
2050s
Water Supply (MCM)
6000
4000
2000
0
CurrentInfra
FullBuildOut
1Current
Hot_dry
Warm_wet+